CATALYSIS BY MODIFIED PILLARED CLAYS AND POROUS CLAY HETEROSTRUCTURES

Thesis submitted to

Cochin University of Science and Technology

in partial fulfillment of the requirements for the degree of

Doctor of Philosophy

in

Chemistry

Under the Faculty of Science

By

NISSAM E

Under the Supervision of

Dr. S. SUGUNAN

DEPARTMENT OF APPLIED CHEMISTRY
COCHIN UNIVERSITY OF SCIENCE AND TECHNOLOGY
COCHIN-682 022, KERALA, INDIA

October 2014

Catalysis by Modified Pillared Clays and Porous Clay Heterostructures

Ph.D. Thesis under the Faculty of Science

Author:

Nissam E
Research Fellow,
Department of Applied Chemistry,
Cochin University of Science and Technology,
Cochin - 682 022, Kerala, India.
Email: nsmkummil@gmail.com

Supervisor:
Dr. S. Sugunan
Emeritus Professor,
Department of Applied Chemistry,
Cochin University of Science and Technology,
Cochin - 682 022, Kerala, India.
Email: ssg@cusat.ac.in

October 2014

Department of Applied Chemistry
Cochin University of Science and Technology
Kochi - 682 022, India.

Dr. S. Sugunan
Emeritus Professor

Date: *-10-2014*

Certificate

Certified that the thesis work entitled "**Catalysis by Modified Pillared Clays and Porous Clay Heterostructures**" submitted by **Mr. Nissam E** is an authentic record of research work carried out by him under my supervision at the Department of Applied Chemistry in partial fulfillment of the requirements for the degree of Doctor of Philosophy in Chemistry of Cochin University of Science and Technology and has not been included in any other thesis previously for the award of any other degree. All the relevant corrections and modifications suggested by the audience and recommended by the Doctoral committee of the candidate during the presynopsis seminar have been incorporated in the thesis.

Dr. S. Sugunan
(Supervising Guide)

Declaration

I hereby declare that the work presented in the thesis entitled "**Catalysis by Modified Pillared Clays and Porous Clay Heterostructures**" is my own unaided work under the supervision of **Dr. S. Sugunan**, Emeritus Professor in Department of Applied Chemistry, Cochin University of Science and Technology, Kochi-22, and not included in any other thesis submitted previously for the award of any other degree.

Kochi-22
-10-2014

Nissam E

To My Mother…….

Acknowledgement

I express my deep gratitude and respect to my guide Dr. S. Sugunan for his valuable guidance, strong motivation, keen interest and constant encouragement during the entire period of my work. I thank him for constructive criticism and useful suggestions.

I am grateful to Dr. N. Manoj, Head of the Department and Dr. K Sreekumar former Head of the Department for providing the necessary facilities for my research. I also express gratitude to Dr. S. Prathapan, Doctoral committee member for his help and suggestions.

I take this opportunity to thank all the teaching and non teaching staff of the Department of Applied chemistry for their help and good will. I take this opportunity to convey my regards to all the teachers from my school time who opened the door of knowledge to me.

I would like to record my sincere thanks to my senior lab mates Dr. Bolie Therattil, Dr. Reshmi, Dr. Rajesh K.M, Dr. Ambili.V.K and Dr. Dhanya for their advices and comments. I also express thanks to my lab mates Rose Miss, Mothi, Reni, Cimi, Soumini , Sandhya ,Honey and Soumya for their affection ,valuable suggestions and joyful company. I am also grateful to the warm friendship of Anoop, Jomon, Mahesh, Shan and friends of other labs.

My vocabulary fails short to express gratitude to my parents who allowed me to focus on research even though they greatly needed my presence. I am indebted to my sisters and their family members for their constant support throughout my life.

My special thank to staff of STIC CUSAT, IIT Madras, IIT Mumbai, NCL Pune, Sud Cheme Cochin for their help during various analysis.

I also take this opportunity to thank Head, Department Of Chemistry, MES College Mampad and other colleagues for their support and encouragement.

The financial support from CSIR and KSCSTE are acknowledged with great pleasure.

Nissam E

Preface

Catalysts can be simple or complex, synthetic or natural chemicals, which are capable of making an otherwise impracticable reaction to occur under the mildest possible conditions. An important family of catalysts that has received considerable attention of the synthetic chemist in recent times is "clays" by virtue of their low cost and natural abundance and inherent sorptive, swelling, ion exchange, acidic and textural properties. Both in their native state and in numerous modified forms, clays are versatile materials that catalyze a variety of chemical reactions such as alkylation, acylation, isomerisation, oxidation, etc. As aluminosilicate of layer structure the interlayer gallery can be effectively used for hosting guest molecule of potential interest for various applications. Just as they can be molded into any shape, their microstructure can be changed to suit chemist's needs to promote diverse chemical reactions.

The propping apart of natural clay layers by intercalation of bulky inorganic cationic species followed by calcination result in materials known as **Pillared Clays (PILCs).** These materials have increased surface area, pore volume, acidity, catalytic activity and thermal stability than parent clay**.** The development of nanotechnology and template mechanism led to the invention of new clay based materials with mesoporous structures called **Porous Clay Heterostructures (PCHs).** PCHs overcame the traditional pore size limitations of clays with pore size in mesoporous range and having narrow pore size distribution. They have mesostructured silica in the intergallery region which can be functionalized for incorporating various active groups for various potential applications.

The present work involves the preparation of pillared clays (Zr, Al, Fe-Al), porous clay heterostructures (Si, Zr-Si), their transition metal (Cu, Ni,V,Co) loaded analogues. Dodeca tungstophosphoric acid (DTP) is supported on porous clay heterostructures by three different methods. The catalysts were

characterized by various physico chemical methods and catalytic activities were comparatively evaluated for industrially important alkylation, acetalization and oxidation reactions. Efforts are made to correlate activity with textural and acidic properties of catalysts.

The thesis organized in to nine chapters. The first three chapters deals with the introduction, materials, methods and physicochemical characterization respectively. Then the following four chapters deals with the activity studies of prepared PILCs and PCHs for industrially important reaction such as tertiary butylation of phenol, oxidation of phenol, hydroxylation of benzene, and oxidation of benzyl alcohol. The eighth chapter deals with the preparation of DTP supported porous clay heterostructues, their characterization and activity studies for acetalization reaction. Last chapter summarizes and concludes the present work with a brief future outlook.

Contents

.....ꕥ.....

Chapter 1

INTRODUCTION AND LITERATURE SURVEY

One of the greatest challenges before synthetic chemist and material scientist is to develop material from cheap natural resources and produce chemicals by adopting greener technologies. Among the viable alternatives available for green synthetic methods, clays and clay-based catalysts in particular have attracted significant attention due to their high abundance and low cost. The sorptive, swelling, ion exchange, acidic and textural properties make clays attractive for various applications like adsorption and catalysis. As aluminosilicates of layer structure, the interlayer space can be effectively used for hosting guest molecule for various applications. The interest level in clays among the scientific community has increased dramatically in recent years due to their intercalation chemistry and various modification possibilities. This chapter includes a brief introduction to clay minerals, their structure, different modification procedures such as pillaring, template assisted modifications process like porous clay heterostructures etc. A brief review of modified clays and catalytic applications of modified clays for various organic transformations are presented. Scope and objectives of present work are also given in this chapter.

1.1 Introduction

Geologists, mineralogists, chemists and soil scientists all approach the term "clay" in a quite different manner. Historically the term clay has been referred to the small inorganic particles with less than 2μ size of a soil fraction without regard to composition or crystallinity and clay minerals has been referred to the specific phyllosilicates of layered, hydrous magnesium or aluminium silicates in such a soil fraction. In 1995 Joint Nomenclature Committie of AIPEA **(Association Internationale Pour lEtude Des Argiles)** defined clays as a ''Material composed primarily of fine-grained particles which is generally plastic at appropriate water contents and will harden when dried or fired '' [1-2]. The term clay generally refers to aluminosilicates with layer structure where the particle size is in the micron range and exhibit cation exchange capacity. This broad term encompasses zeolites but the term is normally used in connection with sheet silicate only. Clays and zeolites both are aluminosilicates, but in zeolites both silicon and aluminium forms tetrahedra and zeolites have well defined three dimensional structures. Clay minerals are produced as a result of weathering, hydrothermal alteration or diagenesis. Two broad class of clays are identified, cationic clays (clay minerals) which are wide spread in nature and anionic clays (LDHs materials) which are rare in nature and usually synthesized in laboratories and industries in an easy and inexpensive way.

Clays have been used from the very beginning of civilization for making cooking pots, potteries, bricks and drainage pipe. Ancient people realized the plastic nature of clay i.e., when mixed with sufficient amount of water it is plastic and can be molded in to any desired shape and when it is heated it changed in to dry solid mass. Fireclays are used for more refractory purposes

such as heat-resistant tiles or bricks. The major use of clay is for the manufacture of cement. Hundred million tons of clays find commercial applications in fields as diverse as ceramics, building materials, paper coatings, fillers, drilling muds, foundry molds, pharmaceuticals, skin care products, kitty litter and laundry detergents. Organoclay gels are added to paints to improve its rheological properties. The performance of cosmetics is enhanced by the use of organo clays and they allow good colour retention and coverage.

1.1.1 Structure of Clays

Clays have two structural units, silica tetrahedra and alumina or magnesia octahedra, both form layer structure, silica tetrahedra by corner sharing alumina octahedra by edge sharing. By sharing three oxygen atoms silica tetrahedra are polymerized to form a hexagonal mesh in one dimension and the fourth oxygen (apical) lie perpendicular to it and it is cornerly shared with aluminium or magnesium octahedral sheets [3].

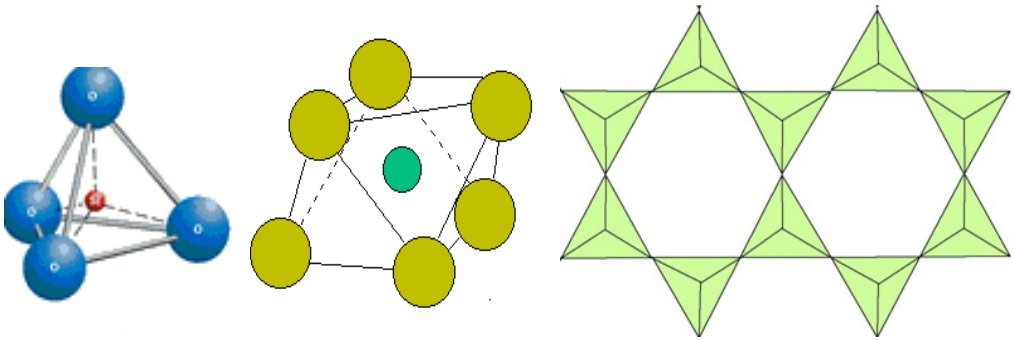

Figure 1.1. structural units of clays

Different combination of tetrahedral and octahedral sheets forms different clay minerals. In 1:1 clay mineral such as in kaolinite, one tetrahedral sheet combines with one octahedral sheet.

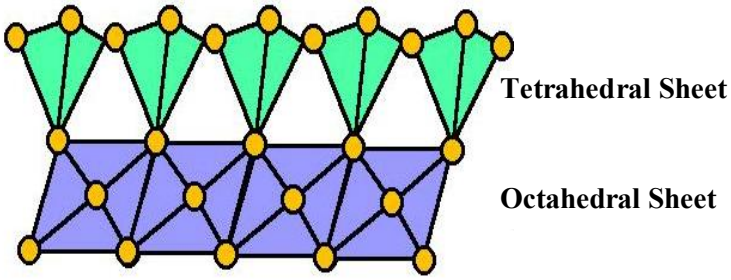

Figure 1.2. Structure of 1:1 clay

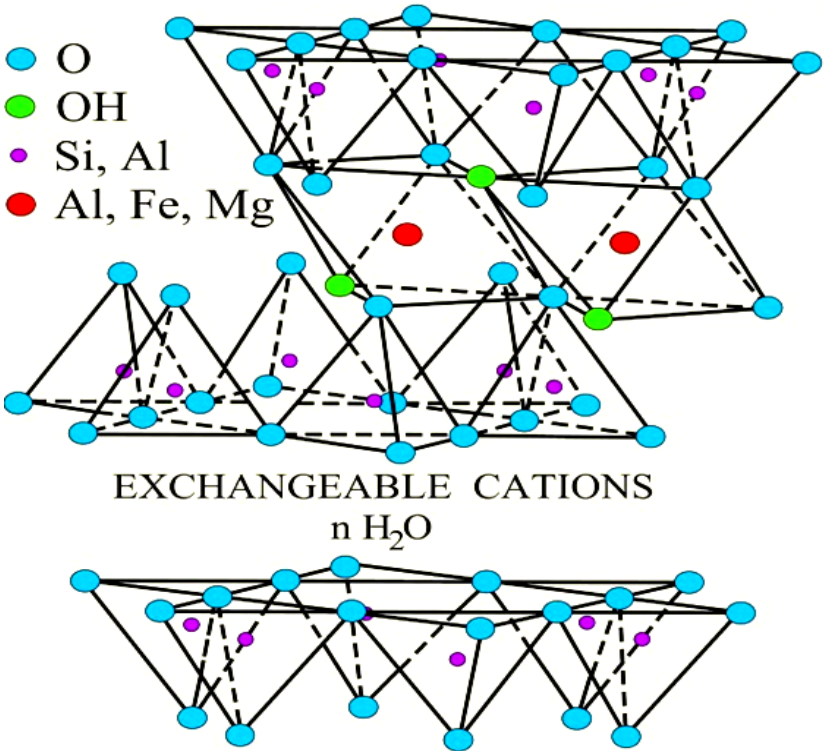

Figure 1.3. Structure of montmorillonite clay

In 2:1 clays such as in montmorillonite the octahedral sheet is sandwiched between two tetrahedral sheets facing to each other to form a three sheet complex called a lamella (1nm thickness). The interlayer and the T-O-T layers

are bound together by both electrostatic and hydrogen-bonding force. Octahedral aluminium may sometimes isomorphously substituted by low valence Mg^{2+}or Fe^{2+} creating -ve charge [4]. The tetrahedral silicon may also be substituted by low valance Al creating -ve charges and the net negative charge is balanced by cations like H^{+}, $Na^{+,}$ K^{+} Ca^{2+} etc or water between the layers. Thus naturally occurring clays have -vely charged layer structures balanced by exchangeable interlayer cations and they are usually called cationic clays since they have cation exchange capacity. Thus, the primary structure of clay is lamellar with parallel layers of tetrahedral silicate and octahedral aluminate sheets. Secondary structure stems from valence deficiencies in primary structure. The tertiary structure is a consequence of secondary structure in which interstitial cations that are trapped as freely moving ions between negatively charged layers [5]. If the trivalent aluminium is the dominant cation in the octahedral layer, then only 2/3 of the octahedral sites are occupied. Such a structure is described as "dioctahedral", since there are two octahedral cations per unit cell. When a divalent cation such as Mg^{2+} is dominant in the octahedral layer, all the available sites are filled. They have three octahedral cations per half unit cell and the structure is described as "trioctahedral".

According to AIPEA recommendation, clays can be classified in to different types based on their layer type, layer charge and chemical composition. Their classification is summarized in Table 1.1 [2].

Table 1.1 Classification of clays

Structure Type	Layer charge	Group	Composition	Examples	Remarks
1 : 1 (TO)	0	Kaolin-Serpentine	$Al_4Si_4O_{10}(OH)_8$	Kaolinite,dickite, nacrite	Kaolin subgroup, dioctahedral, nonswelling
			$Al_4Si_4O_{10}(OH)_8 \cdot 4H_2O$	Halloysite,	Kaolin subgroup, dioctahedral, swelling
			$Mg_6Si_4O_{10}(OH)_8$	Chrysotile,antigorite, lizardite	Serpentine subgroup, trioctahedral, nonswelling
2 : 1 (TOT)	0	Pyrophyllite–Talc	$Al_4Si_8O_{20}(OH)_4$	Pyrophyllite	Dioctahedral, nonswelling
			$Mg_6Si_8O_{20}(OH)_4$	Talc	Talc, Trioctahedral, nonswelling
2 : 1 (TOT)	0.5–1.2	Smectite	$[(Al_4)(Si_{7.5-6.8}Al_{0.5-1.2})O_{20}(OH)_4]\ X_{0.5-1.2}$	Beidellite	Dioctahedral, swelling
			$[(Al_{3.5-2.8}Mg_{0.5-1.2})(Si_8)O_{20}(OH)_4]\ X_{0.5-1.2}$	Montmorillonite	
			$[(Fe_{4.0})(Si_{7.5-6.8}Al_{0.5-1.2})O_{20}(OH)_4]\ X_{0.5-1.2}$	Nontronite	
			$[(Mg_6)(Si_{7.5-6.8}Al_{0.5-1.2})O_{20}(OH)_4]\ X_{0.5-1.2}$	Saponite	Trioctahedral, swelling
			$[(Mg_{5.5-4.8}Li_{0.5-1.2})(Si_8)O_{20}(OH)_4]\ X_{0.5-1.2}$	Hectorite	
2 : 1 (TOT	1.2–1.8	Vermiculite	$[(Al_4)(Si_{6.8-6.2}Al_{1.2-1.8})O_{20}(OH)_4]\ x_{1.2-1.8}$	Vermiculite	Dioctahedral, swelling
			$[(Mg_6)(Si_{6.8-6.2}Al_{1.2-1.8})O_{20}(OH)_4]\ X_{1.2-1.8}$	Vermiculite	Trioctahedral, swelling
2 : 1 (TOT	2	Illite	$Al_4)(Si_{7.5-6.5}Al_{0.5-.5})O_{20}(OH)_4]K_{0.5-1.}$	Illite	Dioctahedral, nonswelling
			Glauconite	Illite rih in Fe	
2 : 1	2	Mica	$[(Al_4)(Si_6Al_2)\ O_{20}(OH,F)_4]K_2$	Muscovite	Dioctahedral, nonswelling
			$[(Fe_2Mg_2)(Si8)\ O_{20}(OH,F)_4]K_2$	Celadonite	
			$[(Mg_6)(Si_6Al_2)\ O_{20}(OH,F)_4]K_2$	Phlogopite	Trioctahedral, nonswelling
			$[(Li_2Mg_4)(Si_8)\ O_{20}(OH,F)_4]K_2$	Taenolite	Trioctahedral, lithium mica
			$[(Al_4)(Si_4Al_4)\ O_{20}(OH,F)4]Ca_2$	Margarite	Dioctahedral, nonswelling
2 : 1 channels or inverted ribbons	Variable	Palygorskite	$[(Mg,Al)_4(Si_{7.5-7.75}Al_{0.5-0.25})\ O_{20}(OH)_2(OH_2)_4]X$	Palygorskite	Dioctahedral, nonswelling
			$[(Mg,M)_8(Si,M^*)_{12}O_{30}(OH)_4(OH)_2)_4]X$	Sepiolite	Trioctahedral (M - Al, Fe(III); M*-Fe(III), Mn(II)
2 : 1:1	Variable			Clinochlor	[TOT]O[TOT] structure

The interest level in clays among the scientific community has increased dramatically in recent years due to their intercalation chemistry and various modification possibilities. The interlayer gallery can be effectively used for hosting guest molecule for various applications. The sorptive, swelling, ion exchange, acidic and textural properties make clays attractive for various applications like adsorption and catalysis [6-7]. Clay based sensors were reported in literature owing to its large surface area and layer structure [8]. These cheap natural materials can be used as support for the immobilization of enzymes [9]. These natural nanomaterials can be successfully used as template for the synthesis of nano materials and the properties of the nano materials depend on nature, basal spacing and cation exchange capacity of the clays [10]. S. J George et al. prepared an aminoclay which can act as scaffold for dangling donor and acceptor dye molecules on clay by a non covalent interaction and at a particular composition of clay to dye, a gel is formed which can be used as light harvesting material in solar cell [11]. Graphene oxide and polymer dendrimer intercalated clays can be used for the storage of hydrogen owing to its high storage efficiency [12]. High surface area and biocompatibility make clays suitable candidate as drug carrier for the controlled release of drugs [13]. Because of high aspect ratio, in-plane strength and low cost, clays are added to polymers as a fillers and the clay polymer nanocomposites have enhanced mechanical strength, thermal stability, barrier properties and flame retardance [14].

1.2 Properties of clays

1.2.1 Swelling capacity

The smectite clays have the capacity to expand beyond a single molecular layer of intercalant. Swelling is a reversible processes that occur

essentially from extra hydration of inter lamellar cations. The extent of swelling depends on layer charge, location of charge and nature of swelling agent [2]. Talc and phyrophyllite have very low capacity to swell as they have nearly zero charge. Clays with very large charges such as mica swell most readily with divalent, trivalent and polyvalent cations and swelling decreases according to that order. Thus Li and Na exchanged form of minerals are particularly susceptible to swelling by water [15]. Several models were recommended for explaining swelling mechanism of smectites [16]. A macroscopic energy balance model for crystalline swelling of 2:1 phyllosilicates was suggested by Laird [17].

1.2.2 Cation Exchange Capacity

Cation exchange capacity (CEC) is defined as the amount of exchangeable cations that a clay mineral can absorb at a specific pH. This is a measurement of the net negative charge of clay layers. The negative charges are produced in clay layers as a result of the following process [2].

(a) Isomorphous substitution within the lattice,
(b) Broken bonds at edges and external surfaces,
(c) The dissociation of assessable hydroxyl groups

Since exchangeable cations compensate the unbalanced charge in the interior of layer due to isomorpous substitution, CEC is a measure of the degree of substitution [18].

1.2.3 Acidity of clays

Clays have both Lewis and Bronsted acidity. Protons and polarizing cations in the interlayer contribute to Bronsted acidity. H_3O^+ ions associated with negatively charged clay layers contribute to Bronsted acidity. Brosted

acidity also arises from terminal hydroxyl groups and from bridging oxygen atoms. The strong dependence of Bronsted acidity on structural OH groups has been evidenced from many reports [19]. Al^{3+} occurring at edge or arising from Si-O-Al bond rupturing contributes to Lewis acidity. Dehydroxylation of Bronsted site would also lead to Lewis acidity. Obviously water will convert the Lewis sites in to Bronsted sites, a fact that limits the study of Lewis sites to relatively anhydrous systems [20].

1.2.4 Clays as catalyst

In 1865, Von Leibeg noticed the unusual property of china clay that could catalyze the formation of water from oxygen and hydrogen at temperature and pressure they were usually unreactive. It was one of the earliest catalysts used for cracking petroleum. Eugenehoundry found that acid modified smectite gave gasoline in high yield when used as petroleum cracking catalysts [21] and were used extensively as commercial catalysts until the mid 60s. There is theory that prebiotic life is originated with the formation of biomolecules catalyzed by natural clay minerals[22]. Experimental results suggested that certain montmorillonite minerals have a tendency to bind and catalyze small molecules to form larger molecules and oligomers like RNA [23] and they could facilitate the transformation of RNA into vesicles [24]. Although "life-from-clay" is still under debate, it is obvious that raw clay minerals inherently possess super-selective adsorption [25] and excellent catalytic activity. The catalytic role of clays have been recognized in several natural process like chemical transformation in soils [26] petroleum forming reactions [27] and the reactions related to evolution [28].

1.3 Modification in clays

Natural clays may not be efficient for acid catalyzed reactions especially if the unit cell composition is neutral or balanced with alkali or alkaline earth metals. Further strategic modifications are needed with the clear objective of improving the acidity, porosity, thermal stability, mechanical strength etc for variety of applications. Among the various clay minerals smectites are usually modified for catalytic purpose as they have layer charge and have swelling capacity. Among smectites, montmorillonite is most studied because of its high abundance, cation exchange capacity, swelling capacity, intrinsic acidity and relatively high surface area. Montmorillonite is commercially available in two forms as Montmorillonite KSF and K10, having different surface area but almost same acidity. Their Hammett acidity (H_0) is -8 which is similar to that of Conc. HNO_3. The important modification strategies include acid activation, ion exchange, intercalation, pillaring, grafting etc.

1.3.1 Acid activation

In this modification procedure, clays are treated with mineral acid like HCl, H_2SO_4 etc which replaces the inter lamellar cations with protons. Acid activation causes little damage to the silicate layer where the structures for the centre of platelet remain intact. However there may be dissolution of some Al^{3+} and Mg^{2+} of octahedral layer leading to to more broken edge M-O^- bonds and those ions then occupy the interlayer sites. The rate of dissolution increases with the concentration of acid, temperature, contact time and increasing Mg content in the octahedral sheets [29]. Surface area may increase due to the dealumination which contributes to mesoporosity. The acidity may be enhanced due to exchanged protons in the interlayer and leached hydrated

alumina occupying the cation exchange sites. However prolonged acid activation may result complete dealumination which will lead to the collapse of clay layer. Among acid activated clays K-10 is representative of a commodity product that has immense applications in organic synthesis [30]. The use of concentrated inorganic acids, however leads to environmental issues owing to the generation of a great deal of acidic wastewater, in addition to equipment corrosion and operational dangers. Instead of inorganic acids organic acids such as carboxylic acids and sulfonic acids, can provide an alternative route to activate clay minerals. In addition, organic acid could lead to different degrees of changes in the layer, interlayer, and the edges compared with those attacked by mineral acids [31].

1.3.2 Cation exchange

In this method interlamellar cations are exchanged with cations by treatment with metal salt solution. Such a principle affords a facile way to prepare a clay based catalyst with the desired ions as catalytically active species. The monovalent (Na^+) and divalent (Ca^{2+}) cations which commonly occupy the interlayer region in natural clay can be readily replaced by other ions. In this way, either homoionic or heteroionic montmorillonite in principle can be produced. Furthermore, hydrophilic clays can be changed into hydrophobic clays by exchange with organic cations such as quaternary ammonium cations NR_4^+ [32].

1.3.3 Intercalation

Intercalation is the insertion of guest molecules in interlamellar space of the clays with the preservation of layer structure. Organic compounds or inorganic complexes can be intercalated in to the interlamellar region. On the

basis of CEC of clay more than 95 % of guest ions can be incorporated in to the clay layers [33-34]. Non ionic guests with large dipole moments such as ketones and nitriles can be adsorbed in to the exchangeable metallic ions within the layer according to their coordination with ionic sites in the interlayers. A large variety of organic molecules are intercalated by so called displacement method [35]. The intercalation of polymers in to the clay layer is an important growing area of research. Hybridization with polymer molecule may result material with high mechanical and flame retardant properties. Intercalation of bulky metal organic compounds or chiral complexes into clay minerals gives an alternative pathway to biomimetic catalyst systems [36]. The immobilizations of complex catalyst in clay structure makes it possible to conduct reactions in heterogeneous way to minimize many of the technical and economical barriers associated with the use of homogeneous catalysts. The advantages of catalyst intercalation go beyond mere immobilization as the chemical and physical forces acting interlayers, can affect catalytic specificity relative to homogeneous solution [37].

1.3.4 Grafting

Organic molecules can be covalently bonded to silanol (Si-OH) or aluminol (Al-OH) group of clay layers. An example for such modification is given in Figure1.4. A fluorescent dye dansyl was grafted in to kaolinite clay by two step process. The authors claim that this is the first example for grafting of a fluorescent dye which will have tremendous application in future [38]. Functionalization with APTES is another example for grafting.

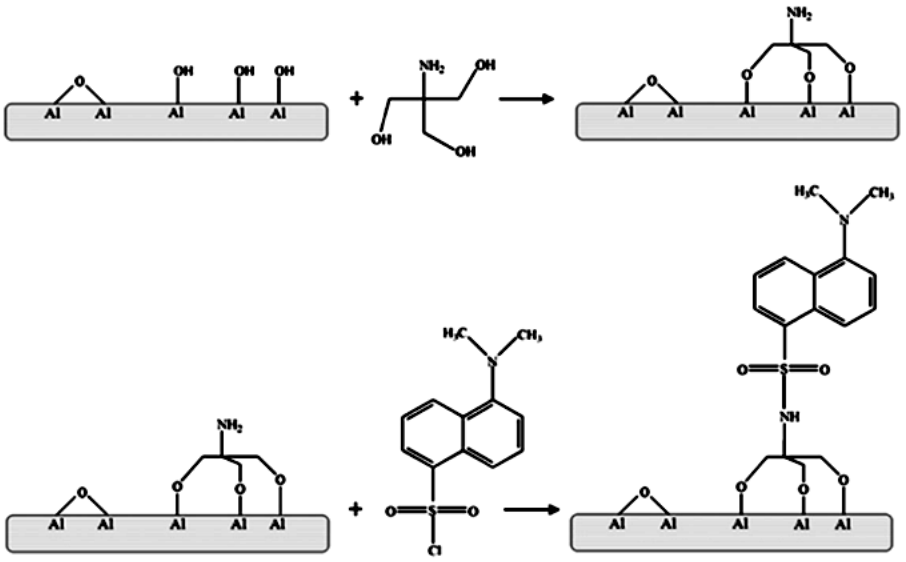

Figure 1.4. Two step grafting on clays

1.4 Pillared clays

The concept of using intercalation chemistry to transform the lamellar solid in to a porous structure by inserting molecular props between the layers of clays was introduced by Barrer and Macleod in 1965 [39]. They used organic compound tetra alkyl ammonium ions to open up lamellae and develop porosity. However the organic pillaring agent collapsed at relatively modest temperature. Oil price hike in the mid seventies spurred research for materials having large surface area than that of zeolites and could be used as cracking catalyst and having good thermal stability led to the development of material called "Pillared Inter Layered Clays (PILCs)" or simply pillared clays [40]. The term "Pillaring and Pillared" originates from the work of Brindley, Semples [41] and Vaughan ,Lussier in 1973 [42]. They found that thermally stable robust inorganic metal oxide species could be intercalated between the clay layers.

Pillaring is the process in which metal oxide pillars are inserted between the clay layers to prop apart the natural clay layers. They are prepared by the intercalation of bulky inorganic poly oxo- hydroxo cationic species followed by calcination.The robust metal oxide pillars formed between the clay layers prevent the collapse of the expanded layers and lead to the formation of large pores depending upon the extent of pillaring. Consequently, a bi-dimensional zeolite-like material with high thermal stability and high surface area was produced. The micropore structure is tailored by the nature of the host material and nature of the pillaring species and the resulting material may have pore sizes larger than those of zeolites and zeolite-related materials. Furthermore, intrinsic catalytic activity is induced in the pillared interlayered solids according to the nature of the pillar. Thus, the pillared derivatives have received widespread interest as a new type of microporous solid that can serve as shape selective catalysts, separating agents, supports, sorbents, etc. By varying the size, charge and shape of entering ion, a homogenous network of micropores obtained with pore opening ranging from 16-30 A^0.

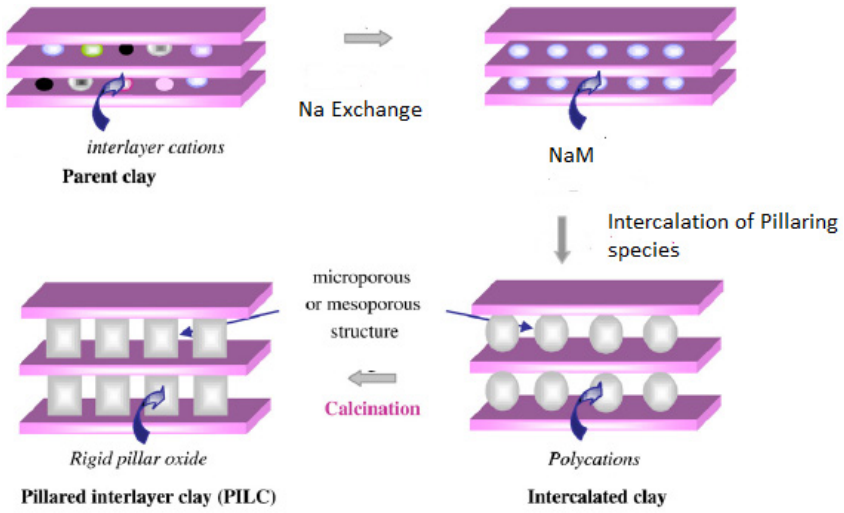

Figure 1.5. Scheme of pillaring process

Pillaring mechanism consists of the exchange reaction between interlamellar charge balancing cations (preferably Na^+) by cationic oligomers/polymers (Pn^{v+}) of pillaring solution. If M is the symbol representing clay, then pillaring process can be represented as

$$MNa_v + P_n{}^{v+} \rightarrow MP_n + v\,Na^+$$

The gallery height or spacing increases by a length somewhat lower than the radius of oligomer. The oligomer itself is produced from condensation reaction such as

$$nP^{z+} \rightarrow Pn^{v+} + n\,(Z\text{-}v\,)H^+ + X\,H_2O$$

The careful processing of the intercalated solid transforms the clay structure into a thermally stable porous structure. Dehydration and dehydroxylation of the polycation occurs in calcinations step to get stable oxide cluster as a pillar between the layers. Calcination shifts the bonding between interlayer species and clay layers from ionic to covalent. The nature and extent of crosslinking action of Pn^{V+} on adjacent microcrystals depends on the nature of surface of clay and that of pillar. Since the pillaring oligomers are cationic, they will be distributed on the surface as far as possible to reduce mutual electrostatic repulsion. The microporous structures of pillared clays are characterized by the distance between intercalated metal oxide pillars (inter pillar distance) and interlayer distances. The interlayer spacing depends on the chemical nature and height of intercalating species and the inter pillar distance is related to the density of pillars which in turn depends on the extent of distribution of charge density on clay layers and also on size of pillars.

1.4.1 Pillaring agents

In general, preparation of porous pillared materials consists of a direct exchange of the interlayer cations of smectite clays by cationic precursors to form intercalated clays. In the preparation of intercalated clays, the preparation of metal precursors is a crucial step. Cationic precursors can be categorized into four different groups, such as

1) polynuclear metal oxo or hydroxo cations,
2) metal chelate complex ions,
3) metal cluster complex ions
4) positively charged colloidal sols

On heating, these intercalated species are converted to metal oxide pillars, expanding the smectite layers.

1.4.2 Polynuclear metal oxo–hydroxo cations

These are the most commonly used pillaring agents that are usually obtained by the partial hydrolysis of metal salts at specific pH. Mostly the M_{13} oligomeric species formed by the base hydrolysis at specific OH/M ratio proved to be the better pillaring species. The formation of poly nuclear cations was first recognized by Bjerrum [43] in his study on the hydrolysis of Cr^{3+} and later for metal ions such as Al^{3+}, Be^{2+}, Zr^{4+}, Hf^{4+},Ti^{4+}, Fe^{3+}, Ga^{3+} and Ce^{4+} by other workers [44-61].

Until now most of the research on pillared clays has been focused on the Al_{13} polyoxocation as a pillaring agent since the solution chemistry of aluminium was well known. Solutions containing this complex are prepared through forced partial hydrolysis by the addition of a base (hydroxide,

carbonate, etc.) to $AlCl_3$ or $Al(NO_3)_3$ solutions up to an OH/Al molar ratio of 2.5. From ^{27}Al NMR and small angle X-ray scattering it has been proven that the pillaring species is most probably the tridecamer $[AlO_4Al_{12}(OH)_{24}(H_2O)_{12}]^{7+}$ with a Keggin structure composed of one aluminium tetrahedron surrounded by 12 aluminium octahedra [62]. Upon calcination the Al_{13} polycation yield Al_2O_3 pillars.

$$[Al_{13}O_4(OH)_{24}(H_2O)_{12}]^{7+} \rightarrow 6.5Al_2O_3 + 7H^+ + 20.5H_2O$$

This equation only suffices the idea of what is actually happening in the solid during heating. This is a very simple approximation because the pillars are not simple metal oxides and during the calcination process the cross-linking reaction can also take place, which involves the formation of true bonds between the pillars and clay mineral layers [31].

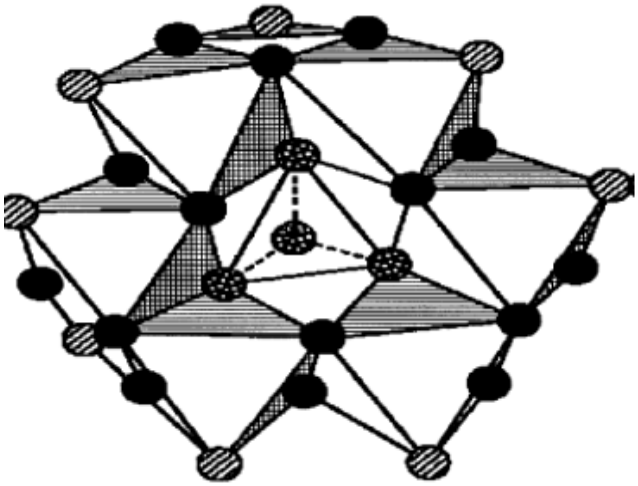

Figure 1.6. Keggin structure of aluminium pillaring species

Plee et al. used ^{27}Al and ^{29}Si solid state nuclear magnetic resonance (MAS NMR) techniques to study the thermal transformation of the pillars and

their linkage with the clay sheets [63]. Their ^{27}Al MAS NMR spectra of beidellite (which have Al/Si substitution in tetrahedral layers) revealed two separate Al (IV) resonances, one due to the tetrahedral Al present in the clay structure and the other one in the center of the Al_{13} pillar. They proposed a model in which linking of the pillar to the tetrahedral sheet induced an inversion of an Al tetrahedron of the tetrahedral sheet. This would lead to new Si-O- Al linkages, in which the negative charge is exposed in the interlayer space. Such a linkage should induce a larger number of stronger, Bronsted acid sites, observed for pillared beidellite. Alternative linkages between the pillar and the tetrahedral sheet can be formed by the inversion of a Si tetrahedron of the tetrahedral sheet or by inversion of the Si -O- Al bond in a tetrahedron.

1.4.3 Zirconium pillaring agent

In the case of Zr pillaring species the solution chemistry is fairly complex and zirconyl ion is mainly found as tetramer. Zirconium poly oxo-hydroxo cations of the type $[Zr_4(OH)_8(H_2O)_{16}]^{8+}$ or $[Zr_4(OH)_8(H_2O)_{16}(Cl,Br)_x]^{(8-x)+}$ can be used to prepare zirconium pillared clays [64-65]. Zirconium poly oxocation can be prepared by dissolution and aging of zirconyl chloride $ZrOCl_2\ H_2O$. In zirconium tetramer, four zirconium ions are located in the four corners of slightly distorted square linked OH bridges placed above and below the plane of that square [66]. Controlled polymerization offers the possibility to prepare pillared clays with different interlayer distances and surface areas [67]. The degree of polymerization depends on the concentration of pillaring species, pH and aging of intercalated clay suspension. Depending on exact preparation method a rather variation in basal spacing and surface area were observed.

Addition of bases like NaOH accelerates the polymerization and increases the stability of the Zr pillared clays due to a higher pillar density [67].

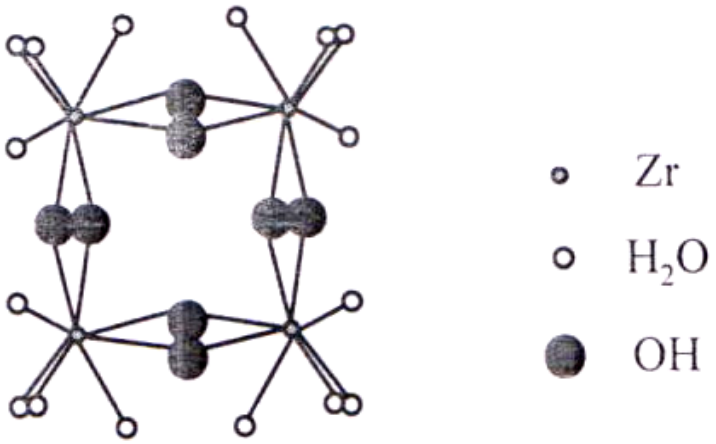

Figure 1.7. Structure of zirconium pillaring species

Ohtsuka et al. observed two different phases in intercalated clays [69]. Clays pillared with a solution containing less than 1 M zirconyl chloride exhibited a basal spacing of 23.3 Å, whereas pillaring with a solution containing a higher zirconyl chloride concentration had a basal spacing of 21.3 Å Insertion of single zirconium tetramers parallel to the clay layers surface form the low basal spacing of approximately 13–14 Å[70]. This is in contrast to observations of Yamanaka and Brindley. They observed a basal spacing around 19.6 Å which was interpreted as formed by either the same tetramers standing perpendicular to the clay layer surface or by stacking of two tetramers on top of each other [71]. However, there is no clear evidence for this type of pillar positioning. The larger basal spacing between 19 and 24 Å in some of the zirconium pillared clays are interpreted as being due to either the formation of larger polymeric cations or by overlap due to mismatch between cations adsorbed on opposite clay layers [72]. FT-IR studies on pyridine adsorption on Zr pillared clays showed that the Lewis acid sites were

only located on the pillars, while the Bronsted acid sites were associated with the exposed clay surface and the pillar clay bonding [73].

1.4.5 Cationic metal complexes as pillaring agent

Incorporation of metal chelate cations $[M(chel)_3]^{3+}$ in to smectite clays and subsequent calcination provide metal oxide pillared materials. The first successful preparation of Mn pillared clay was by the intercalation of trimeric $[Mn_3O(COOCH_3)_6(H_2O)_3]CH_3COO$ complexes [74]. Similarly chromium pillared clays were reported in the literature by the intercalation of trimeric chromium oxyformate $[Cr_3O(HCO_2)_6(H_2O)_3]$ as pillaring agent [75]. Similarly magnetic iron oxide pillared clays were prepared by the intercalation of $[Fe_3O(OCOCH_3)_6.\ CH_3COOH.\ 2H_2O]^+$ as pillaring agent [76].

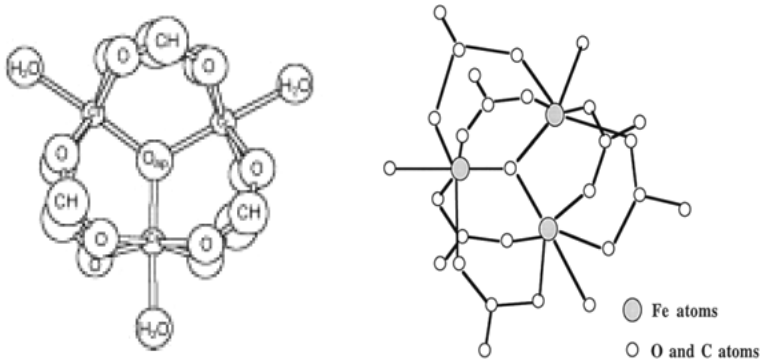

Figure 1.7 Structure of cationic complex pillaring species

1.4.6 From positively charged sol

Positively charged metal oxide sols can be intercalated into the interlayer of clays by cation-exchange reactions, providing pillared materials after calcinations. Although pillared materials with super galleries were made, the pore structure is not homogeneous and the pore size distribution occurs over a

broad range because the interlamellar region is stuffed with flocculated sol particles of different sizes. Titanium pillared clays can be prepared by this approach. Titanium sol prepared by the hydrolysis of titanium alkoxide by HCl can be used as pillaring agent for the preparation of titanium pillared clays [77].

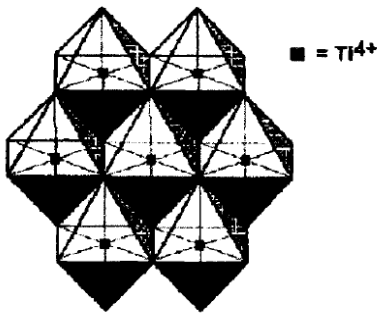

Figure 1.8 Structure of titanium pillaring species

1.4.7 From metal cluster cations

This is a new approach of intercalating rare transition metal oxide pillars inside the clay layer. Pillaring of smectite with niobium and tantalum oxides was achieved with the cation exchange and subsequent oxidation of niobium and tantalum cluster cations of the type $M_6Cl_{12}^{n+}$ (n = 2,3; M = Nb, Ta, Mo). The niobium oxide and tantalum pillared clays after calcination at 325 ^oC exhibited an interlayer spacing around 9 Å and BET surface area of 60–70 m^2/g only [78].

1.4.8 Factors affecting the pillaring process

The structural textural and acidic properties of pillared clays depend on recipe of preparation process. The various factors influencing are

- The source and type of clay

- Cation Exchange Capacity of clays
- Concentration of pillaring agent
- pH
- Temperature of intercalation and intercalation time
- Aging
- Washing
- Drying
- Calcination

Several host clays which have appreciable layer charge and swelling capacity can be used as parent materials. The intercalation of montmorillonite is, by far, the most documented process. The pillaring of saponite, beidellite, vermiculite, hectorite, mica, laponite and synthetic clays were also been reported [79–93]. The effects of the reaction time and other conditions (temperature, shaking/stirring speed) have been also studied by several authors [94-95]. The washing, drying, and calcination processes have a great influence on the properties of the final solids, especially in the development of the porosity.

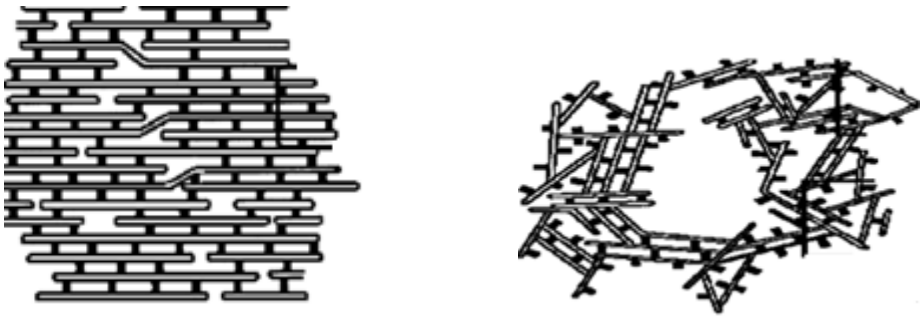

Face to face ordered aggregation in pillared clays

House of card like structure

Figure 1.9 Aggregation of layers in pillared clays

Drying have dramatic influence as air drying predominantly leads to face-face association while freeze drying leads edge to face or edge to edge aggregation leading to structure referred as "house of cards" [96]. Finally, calcination of the solids can also be carried out in different ways (in air or in inert atmosphere) in order to best stabilize the metallic polycations. The effect of calcination temperatures and heating rates were also reported by many researchers. In conclusion, the final properties of the pillared clays strongly depend on the thermal history of each sample.

1.4.9 Characteristics of Pillared Clays

A broad spectrum of pillared clays can be formed by control of experimental variables prior to the addition of clay, during clay addition and post pillaring reactions. The structural evolution of pillars does not involve clay lattice reconstruction, i.e., the basic structure of clay remain intact. Comparison of model isotherms based on cylindrical pore geometry with the help of DFT and experimentally observed pore volume distribution showed that nature of clay surface was nearly unaffected by pillaring reaction [97-98]. It has been proved that thermal stability of clays is improved after the pillaring process. Up on dehydroxylation during calcination step, the bond between the pillar and clay is thought to shift from ionic to near covalent which results in stabilization of porous network.

1.4.10 Acidity of pillared clays

Pillaring the clay will modify the surface acidity in at least two ways. 1) the polycationic pillars displaces the cation originally present on the surface of clay. 2) Pillar's own acidity may create Si-OH-Al bridges in smectites with aluminium substitution in the tetrahedral layer. These OH may provide an

anchoring point to the pillar. There is a general agreement on the presence of higher proportion of Lewis sites than Bronsted sites in pillared clays [99-100]. In calcined forms the pillar being usually metal oxide clusters contribute mainly to Lewis acidity. However unavoidable contribution to Bronsted acidity by pillar has also been evidenced [101,102]. The structural hydroxyl groups are major source of Bronsted acidity in dried samples which slowly disappear during thermal activation due to the migration of protons in to clay lattice sites where the –ve charge originates.

1.4.11 Advantages of pillaring

The main advantage of pillaring process includes

- Increase in basal spacing of clay
- Increase in pore size and surface area
- Enhancement of acidity
- Enhancement of thermal stability
- The active species are immobilized as "pillars" which do not leach in liquid reactions in polar solvents in comparison with ion exchanged clay catalysts.
- Enhancement in catalytic activity

1.4.12 Mixed pillaring

The thermal stability, surface area, surface acidity, porosity etc of single oxide PILCS can be improved by incorporating a second component to pillars**.** Various metals have been reported in combination with the AI polyoxocation, the most important of them being Fe, Ga, Si, and Zr. A large number of mixed pillared clays such as Ga-Al, Al-Fe, Al-Zr, Al-Cr, Fe-Cr, Fe-Zr etc. were reported in literature [105-111]. The second pillaring species may form

discrete or mixed pillars depending on metal combination and preparation conditions. For example Ga forms mixed pillars in which the pillaring species $[GaO_4Al_{12}(OH)_{24}H_2O_{12}]^{7+}$ is a tridecamer with central gallium tetrahedron surrounded by twelve aluminium octahedra.

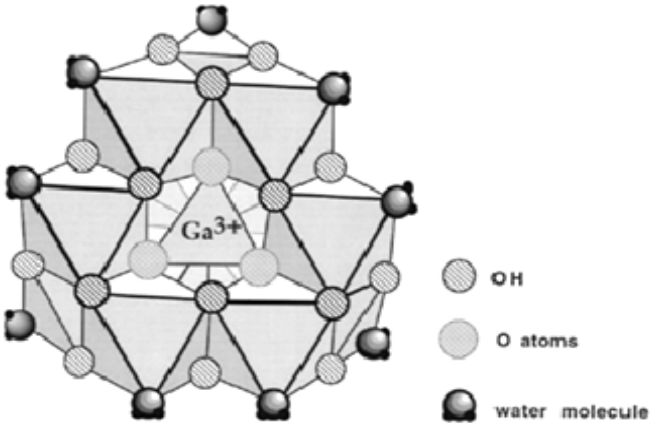

Figure 1.10 Structure of Mixed Al-Ga pillaring species

Bradley et al. [105] carried out a complete study on Ga–Al-pillared solids, by hydrolysis of $GaCl_3$ or a mixture of $GaCl_3$ and $AlCl_3$ respectively. They compared the thermal stability of montmorillonite pillared with Al_{13}, Ga_{13}, and $GaAl_{12}$ oligomers. The study of the changes in basal spacing upon calcination showed that the stability increased in the order $Ga_{13} < Al_{13} < GaAl_{12}$. Lewis acid site concentration was very high in the Ga-Al pillared clays and the Bronsted acidity decreased in the order $GaAl_{12} > Al_{13} > Ga_{13}$.

In Fe- Al mixed Pillared clays both mixed and discrete species were reported in literature. Lee et al. presented a detailed study of Fe –Al mixed pillared clays and their intercalating solutions [112]. These materials were studied by Mossbauer spectroscopy. It was found that iron preferentially decorated the surface of the alumina pillars and at least one monolayer of Fe(III) was accommodated at the surface of the pillars. Even though the

formation of $[Al_{12.5}Fe_{0.5}O_4(OH)_{24}]^{7+}$ polycations was postulated, the authors did not find any evidence of mixed species containing iron and aluminum in the same complex, but rather with discrete alumina and iron oxide pillars. Bergaya et al. proposed the formation of mixed $Al_{13-x}Fe_x$ pillars in Al-Fe pillared laponite, based on the Fe content of the pillared solids [93]. Chemical analysis and H_2 TPR experiments showed the presence of two iron species, in the mixed pillars and discrete iron pillars. Al–Fe pillars in alumina rich samples were particularly active for a syngas conversion reaction, showing high selectivity to light olefins probably due to the presence of $FeAl_xO_y$ mixed oxides.

1.4.13 Post pillaring modifications

The suphate or phosphate groups can be anchored in to the metal oxide pillars by adsorption method to improve the acidity. Phosphoric acid anchored on the metal oxide pillars of aluminium exhibit an increased Bronsted acidity which was ascribed to the formation of monodentate or bidendate complexes [113]. The pillared clays can be used as suitable support for dispersing transition metals whose presence may help as catalysts in reactions that requires redox nature or multifunctionality.

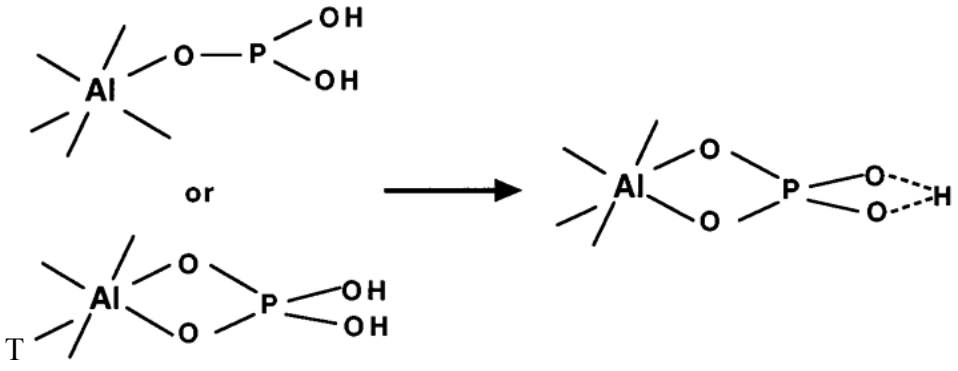

Figure 1.11 Anchoring of phosphate group on metal oxide pillars

Applications of pillared clays

The relevance of PILCs is evident from the extensive reviews [7,98] of scientific literature and books [6,21] being published in last few years. An important aspect of their relevance is that PILCs can be prepared in large scale without much cost and can provide commercial PILCs with low price. Many natural clays from the different part of the world is often evaluated to develop PILCs. Thus natural resources of the country can be valorized to get value added products. The major interests of pillared clays are related to heterogeneous catalysis but other uses are also reported in the field of environmental uses, thermal insulators, pigments, electrodes and membranes.

1.5 Porous clay heterostructures (PCHs)

Since the discovery of Mobil Catalytic Material (MCM) in 1992 [114], a lot of research has been conducted on mesoporous materials. In 1995 Galarneau et al. [115] applied the MCM technology on natural fluorohectorite clay, obtaining a large pore clay derivative, designated as Porous Clay Heterostructures (PCHs). PCH materials are relatively new class of modified clays in which mesoporous silica network is incorporated between the gallery of smectite clays by a template assisted route. These new derivatives are formed by surfactant-directed assembly of open-framework silica in the galleries of smectite clays with high charge density. In the synthesis of a PCH material, clay is firstly opened up by the introduction of an ionic surfactant via a cation exchange reaction (usually by long chain alkyl ammonium cations). Neutral amine co-surfactant molecules are then intercalated along with silica precursor (such as TEOS) and its insitu hydrolysis and polymerization around micellar template of surfactant and co-surfactant give rise to a templated

heterostructure. After calcination for the removal of organic surfactants the porous network of silica within interlayer region is being formed [115-108].

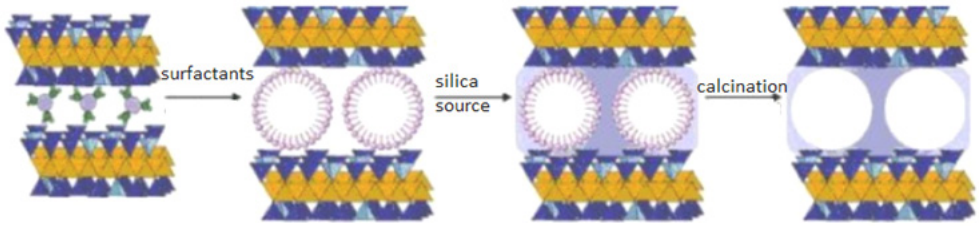

Figure 1.12. Mechanism of PCH formation

PCHs attracted particular attention due to its high surface area (250- 1000 m^2/g), ion exchange capacity, surface acidity, mesoporosity with narrow pore size distribution, good thermal stability and mechanical strength. In contrast to pillared clays whose pore sizes are typically in the microporous range with wide pore size distribution, PCH materials exhibit regular porosity in the super micropore to mesoporous range. In that sense porous clay heterostuructures transcend the pore size limitation of pillared clays [115]. PCH materials have properties inherent to both components, the properties of clays (e.g; CEC and acidity) and properties of silica network (e.g; ability to be functionalized).

In fact PCH materials are pillared clays with silica pillars inserted between clay layers. The difference in the preparation process and the difference in mechanism of process lead to the new terminology called porous clay heterostructures. In some respects the approach is similar to conventional pillaring process, where pillared clays are formed by the insertion of dense nanosclale aggregates in to the galleries of layered host. The pillaring process is mostly governed by CEC of clay, nature of pillaring species and recipe of pillaring process, where as in PCH materials intergallery templating process

involves the insitu assembly of surfactants and inorganic precursor nanostructures, the morphology of which will be determined by the collective energetic of inorganic organic species as they assemble together. The choice of surfactant, its alkyl chain length and surfactant to precursor ratio all plays a crucial role in preparation process [115-116].

The preparation process of PCH materials has some analogy with the preparation of MCM type materials. Synthesis makes use of the micellar ordering of silicate species and the supra molecular ordering of surfactants as in the synthesis of mesoporous MCM-41 molecular sieves. However PCH assembly differs from MCM-41 chemistry in so far as framework organization occurs in the restricted two-dimensional gallery region of the clay rather than in the three-dimensional bulk phase [115]. Since PCH design combines the open framework structure of the gallery silica with the chemistry of the clay layer, new properties for selective heterogeneous catalysis may be anticipated. Surfactant removal from synthesized PCHs by calcination results in the formation of protons which migrate in to interlayers to balance clay layer charges. Consequently silica in interlayer PCHs are intrinsically acidic, where pure silica meso structures possess little or no acidity. In PCH materials new Bronsted acid sites are created along with the retention of intrinsic acidity of clays. More over PCH materials are stable indefinitely while it has been reported that MCM-41 material degrades after two months of preparation at ambient conditions [118].

The major acidic sites related to PCH material are Bronsted acid sites. This is due to the formation of protons during the calcination step by the decomposition of surfactants [118]. The silanol group of newly formed silica pillars also contributes to Bronsted acidity. In addition, the silicate layers can undergo local restructuring upon calcination at elevated temperatures, giving

rise to Lewis acid sites in the gallery region [119-120]. Lewis acidity of PCHs materials can be improved by addition of transition metals. Metals can be incorporated in to intragallery silica frame work of porous clay heterostructures by the addition of corresponding metal alkoxide along with silica source in preparation process by the direct synthesis approach.

The preparation procedure was extended by various researchers to prepare PCHs materials involving species other than silica which introduce novel synthetic aims. Thus Ti or Zr can be incorporated in to the wall of intragallery silica by the addition of precursor of titanium alkoxides or zirconium alkoxide along with silica source in preparation process [121-122]. But huge amount of metals could not be added in this fashion as that will lead to structural collapse. The generation of alumina/silica PCHs has been achieved by Ahenach et al. using a molecular designed dispersion method [123]. The irreversible adsorption of the aluminium acetylacetonate complex followed by its thermal decomposition yielded aluminium oxide PCHs. In this way, AlO_x species can be grafted on to the surface of previously formed PCHs leading to the formation of Si-(OH)-Al bonds by anchoring with surface silanol of PCHs. Zhou et al. prepared Al/SiPCHs by the in situ assembly of TEOS and aluminium isopropoxide precursors. Although aluminium was incorporated with in pillars by Si-O-Al bonds providing lewis acid sites, textural properties are not improved so much compared to other Al incorporation methods [124]. Recently F. Kooli et al. prepared aluminium incorporated PCH materials by the use of aluminium intercalated clay, aluminium pillared clay, dodecylamine and a silica source [125]. This method allowed them to reduce the use of the organic template and to incorporate the aluminum species directly into the silica framework intercalated between the

clay sheets in one step. The PCH material prepared from the Al_{13}-intercalated clay exhibited higher surface area, mesopore volume, Bronsted and Lewis acid sites. However, the use of pillared clays did not lead to the formation of PCH material due to the strong interaction between the alumina species and the clay sheets, which hindered their exchange with dodecylamine, as indicated by XRD and ^{29}Si and ^{27}Al solid-state NMR results.

Aminopropylsilane has been employed to functionalise PCHs material for further immoblisation of copper and vanadium complexes creating effective catalyst for epoxidation reactions [126]. In the same way PCH modified with APTES were used for immobilizing Mn(III) salen complexes to develop heterogeneous catalysts for asymmetric epoxidation of alkenes [127].

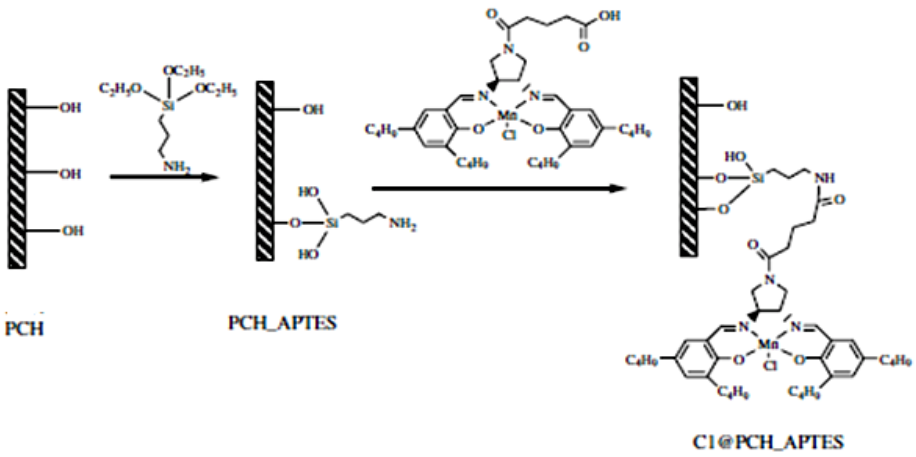

Figure 1.13. Mn salen complex immobilised on PCHs

PCHs modified with APTES can be used as adsorbing subtrate for cabon dioxide. 3-mercapto propyltrimethoxysilane functionalized PCHs were used as heavy metal absorbent (Cd, Cu, Mn, Ni, Pb and Hg) useful for water treatment and modified electrodes [126-127]. Recent advances in PCH material include the development of more efficient and functional materials exploring different

type of clays, modifying the synthetic methodology described by Pinnavaia et al. and using the known precursors. For example PCHs prepared from several smectites such as saponite, montmorillonite and vermiculite have been modified by ion exchange method to incorporate metal active phases (Fe, Cu etc.) to develop optimum catalyst for $DeNO_X$ reactions with ammonia [130-131].

Another new type of porous material related to clay is delaminated porous clay heterostructures (DPCHs). Letaief and R.Hitzky described a controlled route for the formation of delaminated silica porous clay heterostructures [132]. Pre swelled organoclay in polar solvent such as alcohols is treated with alkoxide followed by the addition of water give rise to hetero coagulation of expanded organoclay suspension with alkoxide being hydrolyzed to give nano particles assembled to the clay derivative network.

1.6 Catalysis by modified pillared clays

The use of metal exchanged /supported and intercalated clay based materials in organic synthesis has a rather extensive history. The pillaring of clays increases the accessibility of the reactant molecules to the interlayer catalytic sites, resulting in a possibly high catalytic activity. Simultaneously, the interlayer and interpillar distances exert shape selective effect, which control diffusion rates of reactant, reaction intermediates and products. Most catalytic reactions using pillared clays as catalysts are based on the acidic properties of the catalyst. PILCs have been investigated as acid catalysts for various reactions like alkylation, acylation, isomerisation, cracking, dispropanation and methanol conversion [6,133,134].

The suitability of pillared clays as a catalyst support has been explored because of their textural acidic properties. Transition metal can be deposited in to pillared clays by ion exchange or wet impregnation methods. Potential application of pillared clays in catalytic process of redox or bifunctional nature would require pillared clays to accommodate transition metals as active species. Literature reviews show that copper and vanadium have been vastly explored as active species and to lesser extent nickel, cobalt and other elements. Aluminium pillared clay is greatly explored as catalytic support compared to other pillared clays. Since the present work mainly focus on catalysis by metal supported pillared clays, catalytic application of those materials for various organic transformations is summarized in Table 1.2.

Table 1.2. Transition metal supported pillared clays for various organic transformations

Catalyst	Reaction	Reference
Cu/Al Pillared clay	Xylene and toluene oxidation	135
Cu/ Al Pillared clay	Hydroxylation of benzene	136
Cu/Al Pillared clay	Oxidation of phenol	137
Cu or Ce /Al Pillared clay	Preferential oxidation Of CO	138
Cu/Fe-Al Pillared Clay (FAZA)	SCR of NO with C_3H_6	139
Rh/Ni/Pd ce/AlPC	Dry reforming of methane	140
Pd or Ce/ Al Pillared clay	Deep oxidation of benzene	141
CoMo/ Al Pillared clay	Ethyl benzene to styrene	142
NiMo/ Al Pillared clay	Hydrotreating of crude oil	143
Ce/Zr or Al pillared clay	Cyclohexanone transformation	144
Cu/Pd Aluminium pillared clay	Nitrate Reduction	145
Ce or Fe/Al pillared clay	2 propanol oxidation	146
Co/ Al Pillared clay	Ethyl benzene to Styrene	147
Fe, Ce, or Ag/Ti Pillared clay	SCR Of NO	148
Cu/Ti pillared clay	Catalytic combustion of methane	149
Neobium /Al pillared clay	Synthesis of β hydroxyl ether	150
V/ZrPC	Oxidative dehydrogenation of propane	151
V/FePILC	Catalytic oxidation of H_2S	152
V/TiPILC	Selective catalytic reduction of NO	153

1.7 Objectives of the present work

Transition metals can be deposited in to pillared clays and porous clay heterostructures by ion exchange or impregnation method. Acidic properties of pillared clay together with the redox properties of transition metals make them interesting material for organic transformations. In Pillared clays transition metals mainly reside on pillars rather than on silicate layers, uniformly distributed when loaded in small quantities showing promising catalytic activities. The hydrophobicity of porous clay heterostructures may be reduced by incorporating metals like Ti or Zr by direct method which may also contribute to overall acidity. However huge amount of metal cannot be added in that fashion as it leads to the structural collapse. The hydrophilicity, acidity, redox property etc may be improved by incorporating transition metals by ion exchange or wet impregnation methods.

Catalysis by heteropoly acids (HPAs) has attracted increasing attention in both academic and industrial fields because of their unique strong Bronsted acidity and structure alterability. The bulk heteropoly acids have some disadvantages like extremely small surface area and high solubility in polar solvents. Hence, to improve catalytic applications of HPAs, it has to be dispersed on high surface area of carriers such as silica, active carbon, molecular sieves, Al_2O_3 and so on. Owing to relatively large pore size and surface area of PCHS, heteropoly acids can be successfully anchored on the mesoporous channels of silicon pillars of PCHs.

The main objectives of the work are

- Prepare single and mixed pillared clays like zirconium, iron-aluminium pillared clays by ion exchange method.
- Prepare porous clay heterostructures like silicon and zirconium silicon PCHs by template assisted method.
- Modify PILCs and PCHs by loading transition metals like Cu, Ni, Co, V etc. by wet impregnation method.
- Characterize the prepared catalysts using different physico chemical techniques like X-ray Diffraction, Surface area measurement, FTIR, UV-Vis DRS, ICP-AES, ^{29}Si NMR, TPR, XPS, Acidity measurements using TPD of ammonia, SEM, TEM etc.
- Evaluate the catalytic activity of the prepared catalysts for organic transformations like liquid phase oxidation of phenol, hydroxylation benzene, oxidation of benzyl alcohol and vapour phase tertiary butylation of phenol.
- Immobilize heteropoly acid dodeca tungstophosphoric acid on porous clay heterostructures and characterize the supported catalysts using different characterization techniques and evaluate the catalytic activity for acetalization of cyclohexanone reaction.

References

[1] S. Guggenheim, R.T. Martin, Clays Clay Miner., 43 (1995) 255.

[2] S. M. Averbach, Hand book of Layered materials, Marcel Dekker Inc (2004).

[3] R. E. Grim, Clay mineralogy, 2nd edition, MCGraw Hill, Newyork (1968).

[4] J. P. Rupert, W.T. Granquist, T.J. Pinnavia, Chemistry of clays and clay minerals, A.C.D Newman (ed) (1987).

[5] P. Laszlo, Science, 235 (1987)1473.

[6] A. Gil, S. A.Korilli, R. Trujillano, M. A. Vincente, Pillared clays and related catalysis, Springer (2010).

[7] A. Gil, L. M. Gandia, M. A. Vicente Catal.Rev-Sci., 42 (1&2) (2000) 145.

[8] D. Brondani, C.W. Schreeren, J. Dupont, I.C. Vieira, Analyst. 137 (2012) 3732

[9] G. Sanjay, S. Sugunan, Catalysis Communications, 6 (2005) 525.

[10] T. Tsoufis, J .F. Colomer, E. Macallini, L. Jankovic, P. Rudolf, D.Gournis, Chem. Eur J., 18 (2012) 9305.

[11] K. V. Rao, K. K. R Dutta, M. Eswaramoorthy, S. J. George, Angew. Chem., 123 (2011)1211.

[12] A. Abdelkrim, Int. J. Hydrogen Energy, 37 (2012) 5032.

[13] R. Suresh, S. N Borkar, V. A Sawant, V. S. Shinde, S. K Dimble, International Journal of pharmaceutical sciences and nanotechnology 3 (2010) 901.

[14] T. D. Fornes, D. R. Paul, Polymer, 44 (2003) 4993.

[15] R. Glaeser, J. Mering, C. R. Acod, Sci, Cer. D, 267 (1968) 463.

[16] P. A. Politowicz, J. J. Kozak, J. Phy. Chem., 92 (1981) 6078.

[17] D. A. Laird, Clays clay Miner., 44 (1986) 553.

[18] D. Barthomenf, Characterizations of Heterogeneous Catalyts, Elsevier, Amsterdam, 311(1985).

[19] E. Booij, J. T. Kloprogge, Appl. Clay Sci. II, (1996) 155.

[20] W. J. Wilson, Clay minerlogy: Spectroscopic and chemical determinative methods, Chapman & Hall (1994).

[21] F. Bergaya, B. K. G. Theng, G. Lagaly, Handbook of clay science, Elsevier (2006).

[22] N. W. Gabel, C. Ponnamperuma, Nature, 216 (1967) 453.

[23] J. P. Ferris, A. R. Hill, R. Liu, L. E. Orgel, Nature, 381 (1996) 59.

[24] J. W. Szostak, Angew. Chem. Int. Ed., 49 (41) (2010) 7386.

[25] S. Komarneni, N. Kozai, W. J. Paulus, Nature, 410 (2001) 771.

[26] S. W. Baily, J. L. White, Residue Rev., 32 (1970) 19.

[27] A. Shimoyama, W. D. Johns, Nature, 232 (1971) 140.

[28] H. Lahav, D. White, S. Chang, Science, 201 (1978) 67.

[29] D. A. Morgen, D.B. Shaw, M. J. Sidebottom, T. C. Soon, R. E. Taylor, J. Am. Oil Chem. Soc., 62 (1985) 292.

[30] D. N. Milind, P. Pradeep, S. Arumugam, Organic preparations and procedures int., 32 (1) (2000) 1.

[31] A. Steudel, L. F. Batenburg, H. R. Fischer, P. G. Weidler, K. Emmerich, Appl. Clay.Sci., 44 (1–2) (2009) 105.

[32] D. S. Tong, C. H. Zhou, M. Y. L i, W. H. Y u, J. Beltramini, C. X. Lin, Z. P. Xu, Appl. Clay Sci., 48 (4) (2010) 569.

[33] I. Sissoko, E. T. Iyagba, R. Sahai, J. Biloen, Solid State Chem., 60 (1985) 283.

[34] R. Thevenot, R. Szymanski, P. Chaumette, Clays Clay Miner., 37 (1989) 396.

[35] G. Lagaly, Phil Trans. Roy. Soc. Lond., A 311 (1984) 315.

[36] F. Bedioui, Coordin. Chem. Rev., 144 (1995) 39.

[37] G. J. Churchman, Appl. Clay Sci., 21 (1995) 177.

[38] E. Moretti, L. Storaro, G. Chessa, A. Talon, E. Callone, K. J. Mueller, F. Enrichi , M. Lenarda , J. Colloid. Interface Sci., 375 (2012)112.

[39] R. M. Barrer, D. M. McLeod, Trans Faraday Soc., 51 (1955) 1290.

[40] C. B. Molina , J. A. Casas, A. H. Pizarro, Clay ; Types properties and uses, Nova Science publishers. Inc (2011)

[41] G.W. Brindley, R. E. Sempels, Clay Minerals, 12 (1977) 229.

[42] D. E. W. Vaughan, R. J. Lussier, in Proc. 5th International Conference on Zeo1ites, Naples, L.V.C. Rees (ed), Hyeden, London (1980) 94.

[43] N. Bjerrum, Phys. Chem., 59 (1907) 349

[44] R. Burch, C. I. Warburton, J. Catal., 97 (1986) 503.

[45] F. Figueras, A. Mattrod-Bashi, G. Fetter, A. Thrierr, J. V. Zanchetta, J. Catal., 119 (1989) 91.

[46] E. M. Farfan-Torres, E. Sham, P. Grange, Catal. Today, 15 (1992) 515.

[47] J. P. Sterte, Clays Clay Miner., 34 (1986) 658.

[48] S. Yamanaka, T. Nishihara, M. Hattori, Mater. Chem. Phys., 17 (1987) 87.

[49] A. Bernier, L. F. Admaiai, P. Grange, Appl. Catal., 77 (1991) 269.

[50] H. L. Del Castillo, P. Grange, Appl. Catal. A: Gen., 103 (1993) 23.

[51] F. Kooli, J. Bovey, W. Jones, J. Mater. Chem., 7 (1997) 153.

[52] T. J. Pinnavaia, S. D. Landau, M. S. Tzou, I. D. Johnson, M. Lipsicas, J. Am. Chem. Soc., 107 (1985) 4783.

[53] A. Drljaca, J. R. Anderson, L. Spiccia, T. W. Turney, Inorg. Chem., 31 (1992) 4894.

[54] B. M. Choudary, A. D. Prasad, V. Swapna, V. L. K. Valli, V. Bhuma, Tetrahedron, 48 (1992) 953.

[55] R. Toranzo, M. A. Vicente, M. A. Banares-Munoz, Chem. Mater., 9 (1997) 1829.

[56] M. Sychev, V. H. J. de Beer, A. Kodentsov, E. M. van Oers, R. A. van Santen, J. Catal., 168 (1997) 245.

[57] E. G. Rightor, M. S. Tzou, T. J. Pinnavaia, J. Catal., 130 (1991) 29.

[58] W. Y. Lee, R. H. Raythatha, B. J. Tatarchuk, J. Catal., 115 (1989) 159.

[59] S. Yamanaka, T. Doi, S. Sako, M. Hattori, Mater. Res. Bull., 19 (1984) 161.

[60] M. A. Martin-Luengo, H. Martins-Carvalho, J. Ladriere, P. Grange, Clay Miner., 24 (1989) 495.

[61] A. Bellaloui, D. Plee, P. Meriaudeau, Appl. Catal., 63 (1990) L7.

[62] G. Johansson, Acta Chem. Scand., 14 (1960) 771.

[63] D. Plee, F. Borg, L. Gatineau, J. J. Fripiat, J. Amer. Chem.Soc**.** 107 (1985) 2362.

[64] M. L. Occelli, J. Mol. Catal., 35 (1986) 377.

[65] D. Zhao, Y. Yang, X. Guo, Inorg. Chem., 31, (1992) 4727.

[66] J. S. Johnson, K. A. Kraus, J. Amer. Chem. Soc., 78 (1956) 3937.

[67] G. J. J. Bartley, Catal. Today, 2 (1988) 233.

[68] E. M. Fanfan-Torres, O. Dedeycker, P. Grange, in Scientific Bases for the Preparation of Heterogeneous Catalysts, 5th Int.Symp., Louvain-La-Neuve, Belgium, (1990).

[69] K. Ohtsuka, Y. Hayashi, M. Suda, Chem. Mater., 5 (1993) 1823.

[70] R. Burch, C. I. Warburton, J. Catal., 97 (1986) 511.

[71] S. Yamanaka, G. W. Brindley, Clays and Clay Minerals, 27 (1979) 119.

[72] J. T. Kloprogge, J. Poro. Mater., 5 (1998) 5.

[73] S. A. Bagshaw, R. P. Cooney, Chem. Mater., 5 (1993) 1101.

[74] T. Mishra, K. M. Parida, Mater. Chem., 7 (1997) 147.

[75] J. B. Yoon, S. H. Hwang, J. H. Choy, Bull. Korean Chem. Soc., 21 (2000) 989.

[76] K. M. Parida, T. Mishra, D. Das, S. N. Chintalpudi, Appl, Clay Sci., 15 (1999) 463.

[77] S. Yamanaka, T. Nishihara, M. Hattori, Y. Suzuki, Mater. Chem. Phys., 17 (1987) 87.

[78] S. P. Christiano, J. Wang, T. J. Pinnavaia, Inorg. Chem. 249 (1985) 1222.

[79] S. Chevalier, R. Franck, H. Suquet, J. F. Lambert, D. Barthomeuf, J. Chem. Soc. Faraday Trans., 90 (1994) 667.

[80] L. Bergaoui, J. F. Lambert, M. A. Vicente, L. J. Michot, F. Villieras, Langmuir, 11 (1995) 2849.

[81] M. A. Vicente, M. A. Banares-Munoz, M. Suarez, J. M. Pozas, J. D. Lopez-Gonza lez, J. Santamarıia, A. Jimenez-Lopez, Langmuir, 12 (1996) 5143.

[82] M. A. Vicente, M. Suarez, M. A. Banares-Munoz, J. M. Martın Pozas, Clays Clay Miner., 45 (1997) 761.

[83] J. T. Kloprogge, E. Booy, J. B. H. Jansen, J. W. Geus, Clay Miner., 29 (1994) 153.

[84] J. Miehe-Brendle, L. Khouchaf, J. Baron, R. Le Dred, M. H. Tuilier, Microporo.Mater., 11 (1997) 171.

[85] R. Swarnakar, K. B. Brandt, R. A. Kydd, Appl. Catal. A: Gen., 142 (1996) 61.

[86] L. J. Michot, D. Tracas, B. S. Lartiges, F. Lhote, C. H. Pons, Clay Miner., 29 (1994) 133.

[87] J. Sterte, J. Shabtai, Clays Clay Miner., 35 (1987) 429.

[88] M. de Bock, N. Maes, P. Cool, I. Heylen, E. F. Vansant, J. Porous Mater., 3 (1996) 207.

[89] P. Cool, E. F. Vansant, Microporous Mater., 6 (1996) 27.

[90] R. Butruille, L. J. Michot, O. Barres, T. J. Pinnavaia, J. Catal., 139 (1993) 664.

[91] J. Gaaf, R. A. van Santen, A. Knoester, B. van Wingerden, J. Chem. Soc., Chem. Commun., (1983) 655.

[92] P. Cool, N. Maes, I. Heylen, M. de Bock, E. F. Vansant, J. Porous Mater., 3 (1996) 157.

[93] F. Bergaya, N. Hassoun, J. Barrault, L. Gatineau, Clay Miner., 28 (1993)109.

[94] A. Gil, M. Montes, J. Mater. Chem., 4 (1994) 1491.

[95] N. D. Hutson, M. J. Hoekstra, R. T. Yang, Micropor.Mesopor. Mater., 28 (1999) 447.

[96] O. H. Van, "An Introduction to Clay colloidal chemistry", Wiley N.Y (1977)

[97] A. Gil, M. Montes, Langmuir, 10 (1994) 291.

[98] A. Gil, S. A. Korili, M. A. Vicente, Catal. Rev., 50:2 (2008)153.

[99] D. Plee, A. S. Chutz, G. Poncelot, J. J. Fripiat, "Catalysis by acids and bases", Elsevier Amsterdam (1985).

[100] J. M. Lambert, G. Poncelot, Topics Catal., 4 (1997) 43.

[101] M. L. Occelli, R.M. Tindwa, Clays clay Miner., 31 (1983)22.

[102] J. Kijenski, A. Baiker, Catal. Today, 5 (1989) 12.

[103] S. M. Bradley, R.A. Kydd, J. Catal., 141 (1993) 239.

[104] F. Gonzalez, C. Pesquera, C. Blanco, I. Benito, S. Mendioroz, Inorg. Chem.,31 (1992) 727.

[105] S. M. Bradley, R. A. Kydd, J. Catal., 142 (1993) 448.

[106] M. L. Occelli, J. Mol. Catal., 35 (1986) 377.

[107] C. Catrinescu, D. Arsene, P . Apopei, C. Teodosiu, Appl. Clay Sci., 58 (2012) 96

[108] N. Ksontini, W. Najjar, A. Ghorbel, J. Phy. Chem. Solids, 69 (2008) 1112.

[109] S. Nancy, A. L. Andrea, M. Rafael, M. Sonia, Catal. Today, 133 (2008) 530.

[110] C. Cezar, A. Daniela, A. Petru, T. Carmen, Appl. Clay Sci., 58 (2012) 96.

[111] K. Manju , S. Sugunan, Chem. Eng. J., 115 (2006) 139.

[112] W.Y. Lee, R.H. Raythatha, B. J. Tatarchuk, J. Catal. 115 (1989) 159.

[113] Y. F. Shen, A. N. Ko, P. Grage, Appl.Catal., 67 (1990) 93.

[114] J. B. Higgins, J. L. Schlenker, J. Am. Chem. Soc., 114 (1992) 10834.

[115] A. Galarneau, A. Barodawalla, T. J. Pinnavaia, Nature, 374 (1995) 529.

[116] P. Cool, J. Ahenach, O. Collart, E. F. Vansant, Stud. Surf. Sci. Catal., 129 (2000) 409.

[117] M. Pichowicz, R. Mokaya, Chem. Commun., (2001) 2100.

[118] M. Polverejan, Y. Liu, T.J. Pinnavaia, Chem. Mater., 14 (2002) 2283.

[119] J. Ahenach, P. Cool, E. F. Vansant, Phys. Chem. Chem. Phys., 2 (2000) 5750.

[120] M. Polverejan, T. R. Pauly, T. J. Pinnavaia, Chem. Mater., 12 (2000) 2698.

[121] L. Chmielarz, B. Gil, P. Kustrowski, Z. Piwowarska, B. Dudek, M. Michalik, J. Solid State Chem., 182 (2009) 1094.

[122] J. A. Cecilia, C. Garcia-Sancho, F. Franco, Micropor.and Mesopor. Mater.,176 (2013) 95.

[123] J. Ahenach, P. Cool, E. F. Vansant, Phys. Chem. Chem. Phys., 2 (2000) 5750.

[124] C. Zhou, X. Li, Z. Ge, Q. Li, D. Tong, Catal. Today, 607 (2004) 93.

[125] F. Kooli , Micropor. and Mesopor. Mater., 184 (2014) 184.

[126] C. Pereira, K. Biernacki, S.L.H. Rebelo, C. Freire, J.Mol. Catal. A: Chem., 312 (2009) 53.

[127] I. K. Biernacka, A. R. Silva, A. P. Carvalho, J. Pires, C. Freire, Catal. Lett.,134 (2010) 63.

[128] J. Aurelien, Tchinda, N. Emmanuel, W. Alain, Sensors and Actuators B: Chem.,121 (2007) 113.

[129] R. Tassannapayak, R. Magaraphan, H. Manuspiya, Adv. Mat. Research 55-57 (2008) 617.

[130] L. Chielarz, P. Kustrowski, R. Dziembaj, P. Cool, E.F. Vasant, Catal. Today,119 (2007) 181.

[131] L. Chmielarz, P. Kustroswki, Z. Piwowarska, B. Dudek, B. Gil, M. Michalik, Appl. Catal. B, 88 (2009) 331.

[132] S. Letaief, M. A. Martin-Luengo, P. Aranda, E. Ruiz-Hitzky, Advance Functional materials, 16 (2006) 401.

[133] C. H Zhou, Appl.Clay Sci., 53 (2011) 87.

[134] G. Nagendrappa, Appl.Clay Sci., 53 (2011) 106.

[135] K. Bahranoski, M. Gasior, A. Kieleski, J. Podobinski, K. Wodnika, Clay miner., 34 (1999) 79.

[136] J. Pan, C. Wang, S. Guo, J. Li, Z. Yang , Catal. Commun., 9 (2008) 176.

[137] K. Bahranoski, M. Gasior, A. Kieleski, J. Podobinski, K. Wodnika, Clay miner., 46 (1998) 98-102.

[138] V Ramaswamy, S. Sachin, C. Satyanarayana, Appl. Catal. B: Environ., 84 (2008) 21.

[139] S. Perathoner, A.Vaccari, Clay Miner., 32 (1997) 123.

[140] S. Barama, C. Dupeyrat-Batiot, M. Capron, E. Bordes-Richard, O. Bakhti-Mohammedi, Catal. Today, 141 (2008) 385.

[141] Z. Shufeng, Z. Renxian, Appl. Surf. Sci., 253 (2006) 2508.

[142] A. Moronta, M. Troconis, E. Gonzalez, C. Moran, J. Sanchez, A. Gonza lez, J. Quinon, Appl. Catal. A:Gen., 310 (2006) 199.

[143] P. Salerno S. Mendioroz, A. L. Agudo, Appl. Clay Sci., 23 (2003) 287.

[144] B. G. Mishra, G. Ranga Rao, J. Porous Mater.,10 (2003) 93.

[145] G. Ranga Rao, B. G. Mishra, J. Porous Mater., 14 (2007) 205.

[146] J. G. Carriazo, M. A. Centeno, J. A. Odriozola, S. Moreno, R. Molina, Appl. Catal.A: Gen., 317(2007) 120.

[147] E. Gonzalez, A. Moronta , Appl.Catal.A: Gen., 258 (2004) 99.

[148] J. Arfaoui, L. Khalfallah Boudali , A. Ghorbel , G. Delahay, Catal. Today. , 142 (2009) 234

[149] X Xu, Y Pan, X Cui, S. Zhanghuai, J. Natural Gas Chem.,13 (2004) 204.

[150] J Marcel, R. Gallo, S Teixeira, U Schuchardt, Appl. Catal. A: Gen., 311 (2006) 199.

[151] K. Bahranowski, R. Grabowski, B. Grzybowska, A. Kielski, E.M. Serwicka, K. W. Walsh, K. Wodnicka, Topics in Catalysis, 11 (2000) 255.

[152] K. V. Bineesh, M. Ilkim, M. S. Park, K. Y. Lee, D.W. Parka, Catal. Today, (2011)

[153] J. Arfaoui, L. K.Boudali, A. Ghorbel, G. Delaha, J. Phy. Chem. Solids, 69 (2008) 1121.

.....ooo.....

Chapter 2

MATERIALS AND METHODS

The preparation of catalyst is usually regarded as an art considered more as alchemy than science with the predominance of trial and error methods. A mixture of inspiration, science, technology and empirism is used in their design and development. A Minor deviation in preparation conditions results in marked variation in physical chemical as well as catalytic properties of the ultimate material. Hence the methodological preparation and the characterization is a central aspect of catalyst development. The establishment of empirical relationships between the factors that govern catalyst composition, particle size and shape and pore dimensions on the one hand, and catalytic performance on the other hand, are extremely useful in the process of catalyst development. In the present chapter detailed description of the methodology adopted for the catalysts preparation, different characterization techniques and activity studies are given.

2.1 Introduction

Catalysis is a complex phenomenon involves the interaction of reactant molecules with the active site of the catalysts. The performance of the catalysts depends on the recipe of the preparation process. A minute change in the preparation condition can lead to a marked change in properties of catalysts. A complete knowledge on the exact location, structure and electronic ground state of the active site in the catalysts is essential to establish a basic understanding about the structure- activity correlations and to improve the efficiency of the catalyst for higher selectivity and stability. Thus a methodological preparation and characterization is highly essential. Pillared clays such as aluminium, iron-aluminium and zirconium pillared clays were prepared by ion exchange method. Porous clay heterostructures such as zirconium silicon porous clay hetero structures were prepared by template assisted route. Transition metals such as copper, nickel, cobalt, vanadium, cerium etc were loaded in pillared clays and porous clay heterostructures by wet impregnation method. The prepared catalysts were characterized by various physicochemical methods such as ICP-AES analysis, XRD, Surface area and pore volume measurements, Thermo gravimetric analysis, FT- IR spectroscopy, UV-Vis DRS, X-ray Photoelectron Spectroscopy, Temperature Programmed Reduction analysis, Scanning electron microscopy and Transition Electron Microscopy and surface Acidity measurements like TPD of Ammonia. The methodology adopted for the preparations of catalysts and various experimental techniques adopted for the characterization of catalysts are discussed in detail.

2.2 Catalyst preparation

Chemicals used for the preparation of catalyst were given in Table 2.1

Table 2.1 Chemicals used for the preparation of catalysts

Materials	Suppliers
Montmorillonite (KSF)	Sigma Aldrich
Sodium nitrate	SD fine Chemicals
Aluminium nitrate	SD fine Chemicals
Ferric nitrate	Qualigens
Zirconium OxyChloride	Lobbe
TEOS	Sigma Aldrich
Zirconium (iv)isopropoxide (70%)	Sigma Aldrich
Hexadecyl amine	Sigma Aldrich
Cetyl trimethylammonium bromide (CTAB)	Sigma Aldrich
Cerium nitrate	Indian Rare Earth limited
Cobalt nitrate	SD fine chemicals
Copper nitrate	Qualigens
Nickel nitrate	Lobbe
Ammonium meta vanadate	SD fine chemicals
Ethanol	Merck
Oxalic acid	Merck

2.2.1 Preparation of Pillared Clays (PILCs)

Pillared clays were prepared from Montmorillonite (KSF) clay by ion exchange method. Montmorillonite clay (M) was exchanged with 0.2M $NaNO_3$ solution to produce Na-Montmorillonite (NaM). The pillaring agents of aluminium and iron were prepared by the partial hydrolysis of 0.2M $Al(NO_3)_3$ and $Fe(NO_3)_3$ solution respectively by the dropwise addition of 0.4 M NaOH solution under vigorous stirring (OH/M ratio is maintained as 2). For the preparation of aluminium pillared clay, the intercalation of pillaring species was done by refluxing aluminium polyoxocation solution to the pre swelled 1% Na-montmorillonite clay suspension maintained at 80^oC keeping Al/clay ratio 10mmol/g. The suspension was aged for 24 hours and then filtered, washed and dried at 110^oC for six hours followed by calcinations at 450^oC for 4 hours to get the aluminium pillared clay (AlPC). For the preparation of iron-

aluminium mixed pillared Clay (FeAlPC), aluminium and iron pillaring agents were taken in the molar ratio 3:1 and pillaring agents were added to the clay suspension maintained at 90^{o}C and the remaining procedure was done as same above.

For the preparation of zirconium pillared clay, freshly prepared 0.2 M $ZrOCl_2$ solution was used. The intercalation was done at 50^{o}C and it was then aged for four days followed by filtering and washing. It was dried at 110^{o}C for 6 hours and calcined at 500^{o}C for 4 hours to get zirconium pillared clay (ZrPC).

2.2.2 Preparation of Porous Clay Hetero Structures (PCHs)

NaM was exchanged with 0.1M CTAB at 50^{o}C for 24 hour. Hexadecylamine (HDA) was melted and dissolved in ethanol and stirred with silica source of tetraethyl orthosilicate (TEOS) (CTAB:HDA:TEOS-1:2:10). It was then intercalated with exchanged clay and the gel was stirred for 4 hour. For the preparation of zirconium silicon porous clay hetero structures, along with silicon precursor TEOS, zirconium tetra isopropoxide was used (Zr/Si =1:10). The intercalated clay was washed with 1:1 ethanol water solution, dried at 110 ^{o}C for 6 hours and calcined at 550^{o}C to get Porous Clay Heterostructures (PCHs)

2.2.3 Preparation of transition metal incorporated PILCs/ PCHs

Transition metal incorporated catalysts were prepared by the Wet Impregnation method. Required amount of metal nitrate was dissolved in minimum quantity of distilled water. For the preparation of vanadium loaded catalyst ammonium meta vanadate dissolved in oxalic acid was used. It was then added to the calcined PILCs/ PCHs and stirred for six hours. The water was then evaporated off by maintaining the mixture at 70^{o}C. The samples were then dried at 110^{o}C for 6 hours and finally calcined at 400^{o}C for 4 hours.

The metal incorporated pillared clays were denoted as T(x)MPC, where T is the transition metal , 'x' denotes the % weight of transition metal added and M is the pillaring cation. The transition metal loaded analogues of porous clay heterostructures are denoted by TZrSiPCH Where T is the transition metal added. 3% metal loaded zirconium silicon porous clay heterostructures were prepared. The following catalysts were prepared and characterized.

Table 2.2 Notation of catalysts

Catalyst notation	Description
ZrPC	Zirconium Pillared Clay
Cu(1)ZrPC	1% (Wt)Cu incorporated Zirconium Pillared Clay
Cu(3)ZrPC	3% (Wt)Cu incorporated Zirconium Pillared Clay
Cu(5)ZrPC	5% (Wt)Cu incorporated Zirconium Pillared Clay
Cu(7)ZrPC	7% (Wt)Cu incorporated Zirconium Pillared Clay
Ni(1)ZrPC	1% (Wt)Ni incorporated Zirconium Pillared Clay
Ni (3)ZrPC	3% (Wt)Ni incorporated Zirconium Pillared Clay
Ni(5)ZrPC	5% (Wt)Ni incorporated Zirconium pillared Clay
Co(1)ZrPC	1% (Wt)Co incorporated Zirconium pillared Clay
Co(3)ZrPC	3% (Wt)Co incorporated Zirconium pillared Clay
Co(5)ZrPC	5% (Wt)Co incorporated Zirconium pillared Clay
V(1)ZrPC	1% (Wt)V incorporated Zirconium pillared Clay
V(3)ZrPC	3% (Wt)V incorporated Zirconium pillared Clay
V(5)ZrPC	5% (Wt)V incorporated Zirconium pillared Clay
V(7)ZrPC	7% (Wt)V incorporated Zirconium pillared Clay
AlPC	Aluminium Pillared Clay
FeAlPC	Iron -Aluminium Pillared Clay
Ce(3)FeAlPC	3 % (Wt) Ce incorporated Iron -Aluminium Pillared Clay
SiPCH	Silicon Porous Clay Heterostructure
ZrSiPCH	Zirconium- Silicon Porous Clay Heterostructure
CuZrSiPCH	Cu incorporated Zirconium- Silicon Porous Clay Heterostructure
NiZrSiPCH	Ni Incorporated Zirconium- Silicon Porous Clay Heterostructure
CoZrSiPCH	Co incorporated Zirconium- Silicon Porous Clay Heterostructure
VZrSiPCH	Vanadium incorporated Zirconium- Silicon Porous Clay Heterostructure

2.3 Characterization of catalysts

2.3.1 Inductively Coupled Plasma Atomic Emission Spectroscopy (ICP-AES)

The elemental analyses of the materials were done using Inductively Coupled Plasma- Atomic Emission Spectrometer. Inductively Coupled Plasma - Atomic Emission Spectrometry (ICP-AES) is an emission spectrophotometric technique, exploiting the fact that excited electrons emit energy at a given wavelength as they return to ground state after excitation in high temperature argon plasma. The fundamental characteristic of this process is that each element emits energy at specific wavelengths peculiar to its atomic character. The advantage of ICP-AES analysis lies in its greater sensitivity and the possibility of multi element analysis which offers a tremendous saving in analysis time. When heated to temperatures above 6000^{o}C, gases such as argon form plasma containing a high proportion of electrons and ions. The plasma may be produced by an EC arc discharge or by inductive heating in an inductively coupled plasma

Discharge of a high voltage from a Tesla coil through flowing argon will provide free electrons, which will 'ignite' the gas to plasma. If the conducting plasma is enclosed in a high frequency electromagnetic field, then it will accelerate the ions and electrons and cause collisions with the support gas, argon, and the analyte. The temperature rises to around 10,000^{o}C. At such temperature, energy transfer is efficient and the plasma becomes self sustaining. It is held in place by magnetic field in the form of a fireball. The same aerosol enters the fireball at high speed and is pushed through it, becoming heated and emerging as a plumb, which contains the sample elements as atoms or ions, free of molecular association. As they cool to around 6000-7000^{o}C, they relax to their ground state and emit their characterstic spectral lines [1].

With ICP- AES there is little interference with ionization, since there is an excess of electrons present. The high temperature ensures that there is less interference from molecular species or from the matrix. Since a large number of elemental emission lines are excited, lines may overlap. By this technique up to 70 elements, both metals and non metals can be determined

Clay samples for analysis were prepared after removing silica, which was estimated. A known weight (W_1) of the sample was taken in a beaker, treated with concentrated sulphuric acid (95%, 30 mL) and was heated until SO_2 fumes were evolved. It was cooled, diluted with water and filtered with ashless filter paper. Filtrate was collected; the residue was heated in a platinum crucible and was weighed (W_2). To the weighed temperature treated sample, 40% HF was added in drops, warmed and strongly heated to dryness. This was repeated 5-6 times until no fumes of H_2SiF_6 were evolved. It was again incinerated to 800^oC for 1h, cooled and weighed (W_3). From the loss in weight, the amount of silica present can be estimated using the equation

$$\%SiO_2=(W_2-W_3)X100/W_1$$

Filtrate was diluted to a known volume and a small portion is taken for quantitative ICP- AES analysis. Analysis was done using 'GBC' Plasmalab 8440M instrument.

2.3.2 Cation Exchange Capacity (CEC)

It is the measure of exchangeable cations between the clay layers. It is also the measure of net -ve charge of clay layers. Compositional variation through ionic or isomorphous substituent within the clay mineral crystal lattice can leave the structural unit a net negative charge. The presence of this net negative charge means the soluble cations can be attracted or adsorbed on the

surface of clay mineral structural units without altering the basic structure of clay mineral. The ability of clay mineral to hold cations are termed as Cation Exchange Capacity (CEC). During pillaring process polyoxocations enters in the intergallery by ion exchange with exchangeable cations and remains as non exchangable metal oxide pillars after the calcination process. The decrese in CEC is a measure of the extent of pillaring [2]. For pillared clays it has been proposed that interpillar rather than interlayer distance controls pore size distribution [3]. This distance depends on the number of pillars introduced in to the clay layer which in turn is related to the amount of exchangable cations. Therefore CEC can be a key factor for the synthesis of pillared clays with desired pillar population[4]. There are several methods available for CEC determinations like exchange with ammonium, sodium and barium ions [5] or potentiometric titration [6] or employing triethylene tetramine and tetraethylene pentamine copper(II) complexes [7].

The CEC was determined by stirring 1 g of sample with 60 ml of 3M ammonium acetate solution for 8 hour at room temperature and it was then filtered. The resulting solid was washed with isopropyl alcohol and dried at 110 ^{o}C for 4 hour and then it was heated with 60% NaOH in KJeldahl flask. Ammonia released was collected in 0.025 M HCl solution and titrated against 0.025 M NaOH solution.

2.3.3 X-RAY DIFFRACTION (XRD)

In heterogeneous catalysis X-ray analysis is widely employed as it is a useful method for determining the three dimensional structure of solid substances. Recording the X-ray diffraction pattern of powdered crystalline samples by powder diffractometry has been applied for determining phase purity, to calculate the unit cell parameters, study of preferred orientation and

determination of particle size. It is also employed to identify allotropic transformation, transition to different phases, and the presence of foreign atoms in the crystal lattice. The principle of XRD is based on the interaction of X-rays with the periodic structure of a crystalline material which acts as a diffraction grating. A fixed wavelength is chosen for the incident radiation and the diffraction pattern is obtained by observing the intensity of the scattered radiation as a function of scattering angle of 2θ. The relationship between the wavelength of X ray beam λ, the angle of diffraction θ and the interplanar distance d is given by Bragg's equation.

$$n\lambda = 2d \sin\theta$$

where n is an integer called the order of diffraction.

Although the use of X-rays is very simple in its structure determination, it is very complicated in its fine details. Every crystalline structure has a unique X ray powder pattern since the line positions depend on size and line intensity depends on the type of atoms present and their arrangements in the crystals. In pillared clays XRD analysis is used to determine the basal spacing of the clay. It provides immediate information about the success of the intercalation/ pillaring process, as evidenced by the shifting of the basal spacing to higher values; i.e. lower angles in the diffractograms. Moreover, such intercalation can be observed even faster by carrying out the diffraction of oriented films obtained by a single drop of suspension during synthesis [8].

XRD patterns of the prepared catalysts were recorded in Bruker AXS D8 Advance X-Ray Diffractometer using Ni filtered CuKα radiation (λ=1.5406 Å) in the range 2θ from 0 to 80.

2.3.4 BET Surface Area Measurements

Most of the catalysts with practical importance are highly porous and possess large specific surface area. Hence it is necessary to specify the nature of pore structure as it controls the transport of reactants and products in catalytic reaction. Gas adsorption is the prominent method to obtain the comprehensive data with respect to surface area, porosity and pore size distribution**.**

Nitrogen adsorption is a commonly applied technique to characterise the porous and nonporous materials. The amount of adsorbed/desorbed gas is measured as a function of relative pressure, the corresponding plots give rise to isotherms. The shape of the isotherm depends on the porous texture of the measured solids. Nitrogen physisorption measurements are often done in liquid nitrogen temperature (-195.8^{o}C) to obtain accurate measurements at constant temperature. In this technique the amount of gas adsorbed on to the solid surface is directly correlated to material surface area and pore structure

Adsorption/desorption isotherms

IUPAC classified the isotherms in to six types (Fig 2.1) and the shape of isotherm depends on the porous texure of solid materials [9].

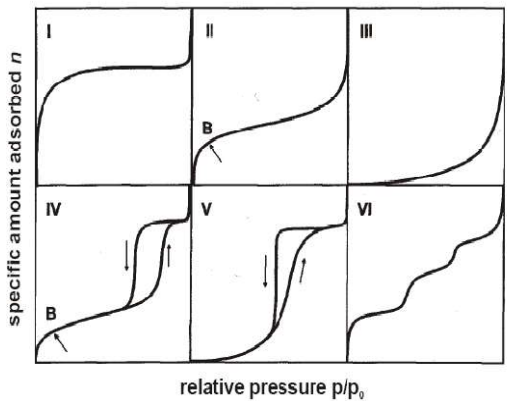

Type I - *microporous material,*

Type II - *macro- or non-porous material*

Type III - *macro- or non-porous material with weak adsorbate-solid interactions,*

Type IV - *mesoporous material,*

Type V - *mesoporous material with weak adsorbate - solid interaction*

Type VI - *stepwise adsorption at very weak adsorbate- solid interactions*

Figure 2.1 adsorption isotherms

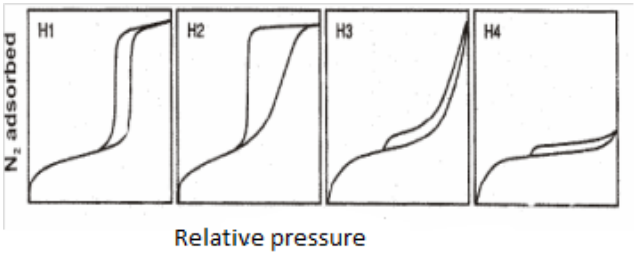

H1- typical for type IV isotherms,

H2- characteristic for "ink-bottle" pores,

H3 and H4 - slit pores

Figure 2.2 Hysterisis loop of porous materials

BET method is the widely adopted procedure for the determination of the surface area of the porous materials [10-11]. This method is based on the extension of the Langmuir theory to multilayer adsorption, it assumes that the heat of adsorption on the bare surface is different from the heats of adsorption of all successive layers.

The general form of BET equation can be written as

$$\frac{P}{V(P_0-P)} = \frac{1}{V_m C} + \left[\frac{C-1}{V_m C}\right]\frac{P}{P_0}$$, where

p - Adsorption equilibrium pressure

p_0 - Saturated vapour pressure of the adsorbate

V - Volume occupied by molecules adsorbed at equilibrium pressure

V_m - Volume of the adsorbate required for monolayer coverage

C - Constant related to the heat of adsorption

The BET plot is linear as long as only multilayer adsorption occurs. Plot of $\frac{P}{V(P_0-P)}$ against p/p_0 is a straight line with slope $C-1/CV_m$. From the slope and intercept, V_m can be calculated and the specific surface area of the sample can be calculated using the relation,

$$A=V_m N_0 A_m/W \times 22.414, \text{ where}$$

N_0 - Avogadro number

A_m - Molecular cross sectional area of the adsorbate

W - Weight of the catalyst sample

The pore volumes of samples were calculated by the t plot method [12-13]. In this method the adsorbed N_2 volume is plotted against statistical thickness of adsorbed N_2 layer to yield micropore volume on the basis of the relation

$$V = V_{micro} + 10^{-4} S_0 t$$

Where Vmicro is the volume of N_2 gas adsorbed in micropore and S_0 is the external surface area. A universal t curve of N_2 has been established which gives

$$t= [13.99 / 0.034 - \log(p/p_0)]^{0.5}$$

Where t is in Å

Pore diameter distributions and average pore diameters

Pore diameter and pore size distributions were calculated by the BJH method developed by Barret, Joyner and Halenda model based on Kelvin equation corrected for multilayer adsorption [14]. In this approach the filled pores are taken as a starting point. The emptying of the filled pores with decreasing relative pressure is incrementally evaluated to obtain a pore diameter distribution. For each increment the diameter of pores emptied is calculated according to the Kelvin equation

$$p/p_0 = \exp (- 2\gamma v/ r_k RT)$$

Where (p/p_0) is the relative vapour pressure over a curved surface, γ is the surface tension, V is the molar volume of the liquid, and r_k is the radius of curvature.

The mesopore size distribution is usually expressed as a plot of Vp/rp versus rp where Vp = mesopore volume

The simultaneous determination of surface area and pore volume of the catalysts were done at liquid nitrogen temperature with a Micromeritics Tristar 3000 surface area and porosity analyzer. Prior to the measurements the samples were degassed for 1h at 90^0C followed by degassing at 300^0C for 6 hours

2.3.5 Fourier Transform Infrared Spectroscopy (FT-IR)

FT-IR spectroscopy is one of the techniques capable of exploring the catalyst both in bulk and its surface. It has been extensively used for identifying the various functional groups on the catalyst itself, as well as for identifying adsorbed species and reaction intermediates on catalyst surface [15]. The technique works on the fact that bonds and group of bonds vibrate at characteristic frequencies. A molecule that is exposed to IR rays absorbs IR energy at frequencies which are characteristic to that molecule. The analysis of the spectrum was done by comparing with reported values. The most commonly used region for this purpose is the finger print region (1450-600 cm^{-1}). The Infrared induced vibrations of the samples were recorded using Thermo NICOLET 380 FT-IR Spectrometer by means of KBr pellet procedure. Spectra were taken in the transmission mode at atmospheric pressure and room temperature. The changes in the absorption bands were investigated in the 400-4000 cm^{-1} range. The resolution and acquisition applied were 4 cm^{-1} and 60 scans respectively.

2.3.6 UV –Visible Diffuse Reflectance Spectroscopy

UV-Visible diffuse reflectance spectroscopy is a non-destructive technique used for the identification and characterization of metal ion co-ordination. In this method, the samples interact with light energy, absorption and scattering takes place, producing a reflecting spectrum. It gives information regarding electronic transition between orbitals or bands in the case of atoms, ions and molecules in gaseous, liquid or solid state. Electronic excitations are of various types, namely, d-d transition and charger transfer (CT) transition etc. The d-d transition gives the information about the oxidation state and the co-ordination environment of the samples, where as CT transition is intense and is sensitive to the nature of donor and acceptor atoms. In catalysis, the information given by DRS mainly includes the active phase-support interactions. Metal centered transitions and charge transfer transitions can be clearly differentiated by UV-DRS and assignment of these gives a picture about the oxidation state and co-ordination environment of the transition metals [16]. It can also provide the electronic structure of dispersed metal oxides.

The UV Vis reflectance spectra were obtained in the range of 200-900 nm on Labomed UV-VIS Double Beam UVD-500 spectrophotometer equipped with an integrating sphere assembly, using $BaSO_4$ as reflectance standard.

2.3.7 Temperature Programmed Reduction (TPR)

Temperature programmed reduction is unique technique to study temperature dependence reduction behavior of metal oxides, mixed metal oxides, and metal oxides dispersed on a support. It also provides information on the phases present after impregnation, and on the eventual degree of

reduction. For metal oxide dispersed on a support systems, it provides information of the nature of dispersed species, ie whether the species is isolated, cluster or polymer. It provides information about the oxidation state of dispersed species as well as its interactions with support. For bimetallic catalysts, TPR patterns often indicate whether the two components are mixed, or not. In favorable cases where the catalyst particles are uniform, TPR yields activation energies for the reduction, as well as information on the mechanism of reduction [15].

TPR was carried out in a Micromeritics instrument: Chemi Soft TPx / TPR. 200 mg of the sample was used for each experiment. Prior to the reduction, the sample was preheated in He for an hour at 200^{o}C. After that 5% H_2-Ar mixture was switched on and the temperature was increased linearly at the rate of 10^{o}C /minute. A TCD detector cell detects the consumption of hydrogen in the reactant stream.

2.3.8 X-ray Photo Electron Spectroscopy (XPS)

XPS also known as electron spectroscopy for chemical analysis (ESCA) is one of the most powerful chemical technique that provides information on surface elemental composition, the oxidation state of the elements and, in favorable cases, on the dispersion of one phase over another [17]. XPS is based on the photoelectric effect in which binding energy (E_B) of core electron is overcome by the energy (hv) of an impinging soft Xray photon, the core level electron is excited and ejected from the analyte. The kinetic energy of ejected photoelectrons E_K are measured by an electron spectrometer whose work function is φ. Invoking conservation of energy the following relationship is obtained

$$E_B = hv - E_K - \varphi$$

The binding energy of the photoelectron is characteristic of the orbital from which electrons originate. The binding energy of the ejected photoelectrons depends on the final state configuration after photoemission. The final state is characterized by full relaxation of all atomic orbital's towards core level. There is usually some variation in core energy level for a given element in different chemical forms. This can be thought of as being caused by variations in the oxidation state and the local chemical or structural environment resulting in a variation in the net electrical charge on a given atom. The change in the electrical charge affects the energy of the photoelectron and so manifests as a slight shift in the measured core level binding energy. Such chemical shifts can be resolved in XPS spectra and this is a key aspect of the technique for catalyst characterization.

Shakeup peaks may occur when the outgoing photoelectron simultaneously interact with a valence electron and excite it (shake it up) to high energy level. The kinetic energy of the core electron is then slightly reduced giving a satellite structure a few eV below the core level position. Discrete shake-up losses are prominently present in the spectra of several oxides of nickel, iron, and cobalt, and of many other compounds. Such losses have diagnostic value as the precise loss structure depends on the environment of the atom. Today, XPS is becoming an increasingly important tool for studying the dispersion of supported catalysts, especially in systems where the usual methods for determining particle size are not applicable. Angle-dependent XPS measurements on single crystals provide structural information, such as layer thickness and adsorption geometry [15].

XPS data were recorded in an indigenously developed photoelectron spectrometer equipped with dual Al-Mg anodes interfaced with necessary data handling software. For all the catalysts, the spectra were recorded under high vaccum conditions using Al- Kα primary radiation operated at 150 W. A thin wafer of 12 mm diameter material was used for the studies. For Each analysis survey scan is done from 0 to 1200 eV. The spectra were corrected using the carbon 1s signal at 284.6 eV.

2.3.9 Solid state NMR

Solid state NMR spectroscopy has become a powerful tool for investigation of the solid surface of various heterogeneous catalysts such as zeolite, metal oxide, and solid heteropolyacids, which are widely used in petrochemical industry. Identification and characterization of the active centers, reaction intermediates, and products are essential for understanding reaction mechanisms occurring on the surface of heterogeneous catalysts. Compared to X-ray diffraction (XRD) which is determined by long-range orderings and periodicities, solid state NMR is more sensitive to local ordering and geometries, thus providing a more detailed description of the local structure, especially for powder samples. Multinuclear magic angle spinning (MAS) NMR especially ^{1}H MAS NMR, probe molecule techniques, double-resonance techniques and two dimension correlation techniques have been employed to reveal the detailed structure of the active sites on heterogeneous catalysts.

Solid state NMR studies of heterogeneous catalysts are usually carried out by Magic Angle Spinning (MAS) ie, rapid rotation of sample about an axis subtended at an angle of $54^{0}44'$ with respect to magnetic field. This technique removes line broadening from dipolar interactions, chemical shift anisotropy and quadrupolar interactions, since all interactions contain the term $(3\cos^{2}\theta-1)$

which is zero for magic angle. The number of signals in solid state NMR spectrum corresponds to number of different structural environment of observed nucleus in the sample while relative intensities corresponds to relative occupancies of different environment [18]. High resolution solid state NMR provides information about bonding situation, symmetry properties and dynamic behavior of solid state structures. ^{27} Al and ^{29} Si NMR measurements are usually done for the structure elucidation of clays.

Solid State MAS NMR experiments were carried out over a Bruker DSX-300 spectrometer at a resonance frequency of 75.4MHz. For all measurements a standard 4 mm double- bearing Bruker MAS probe was used. The number of scans collected was 1024. XWIN NMR software was employed to acquire and retrieve data. The standard used for ^{29}Si MAS NMR is tetra methylsilane (TMS) whose chemical shift is 0 ppm

2.3.10 Thermogravimetric Analsis (TG)

In heterogeneous catalysis thermo gravimetry is a well established technique in which the catalyst sample is subjected to high temperature at a specified heating rate. It provides the analyst with a quantitative measurement of any weight change associated with a transition. It finds well applications in the determination of drying range, calcination temperature, phase composition, percentage weight loss and stability limits of a catalyst. TG directly records the loss in weight of a sample with time while its temperature is raised through a temperature programme. In TG, the loss of weight of a sample is plotted against temperature. The plot is known as the thermogram. Changes in weight are due to the rupture of various physical and chemical bonds at elevated temperatures, which lead to the evolution of volatile products or the formation of heavier reaction products. The method requires a crucible in which the

sample is placed and it is attached to an automatic recording balance. The accessories associated with the balance enable to detect the mass change as a result of thermal treatment. The TG data were computer processed to get the thermograms. These dips correspond to the weight loss due to decomposition and hence provide an idea about the species lost during the heating step.

Dried samples were analyzed by Perkin Elmer Pyris Diamond TGA-DTA analyzer in nitrogen atmosphere with a heating rate of 10^{o}C /min from room temperature to 900 ^{o}C.

2.3.11 Scanning Electron Microscopy (SEM)

Scanning Electron Microscopy allows the imaging of the topography of a solid surface by using back scattered or secondary electrons with good resolution of about 5nm. These bombarding electrons also referred to as primary electrons dislodge electrons from the specimen itself. The dislodged electrons, also known as secondary electrons are attracted and collected by a positively biased grid or detector, and then translated in to a signal. To produce the SEM image, the electron beam is swept across the area being inspected, producing many such signals. These signals are then amplified, analyzed, and translated in to images of the topography being inspected. Finally, the image is shown on a cathode ray tube.

SEM analysis of the samples were done using JEOL JSM-840 A model 16211 scanning electron microscope analyzer with a resolution of 13 eV.

2.3.12 Transmission Electron Microscopy (TEM)

Transmission electron microscopy (TEM) is an imaging technique whereby a beam of electrons is transmitted through a specimen, then an image

is formed, magnified and directed to appear either on a fluorescent screen or layer of photographic film or to be detected by a sensor such as a CCD camera (charge couple device)[19]. The transmission electron microscope is based on the fact that electrons can be ascribed a wavelength but at the same time interact with magnetic fields as a point charge. A beam of electrons is applied instead of light, and the glass lenses are replaced by magnetic lenses. The lateral resolution of the best microscopes is down to atomic resolution. Like SEM, TEM uses an electron gun to produce the primary beam of electrons that will be focused by lenses and apertures into a very thin, coherent beam. This beam is then controlled to strike the specimen. A portion of this beam gets transmitted to the other side of the specimen, is collected, and processed to form the image. TEM of the samples was carried out in Philips CM 200 with resolution of 2.4 Å. Bulk materials have to be thinned to make them electron transparent. The typical column vacuum in the machine is $< 1x10^{-5}$ Pa.

2.3.13 Surface Acidity Measurements

Quantification and characterization of surface acid sites forms an important aspect of characterization of catalysts [20]. The concentration and strength of acid sites in solids cannot readily be measured using the types of basic molecular indicators used in the study of acid solutions because the sites in solids may be inaccessible to these molecules. Consequently, alternative techniques have been developed that are more applicable to solids and that enable their acidity to be compared with that of liquid acids. These include the thermal desorption of basic probe molecules (such as pyridine) coupled with IR spectroscopy, catalytic test reactions such as alkane cracking, adsorption techniques such as Temperature Programmed Desorption (TPD) of ammonia etc. Temperature Programmed Desorption (TPD) of ammonia and cumene

cracking reaction was used for the determination of acidity of prepared catalysts.

2.3.13.1 Temperature Programmed Desorption (TPD) of Ammonia

Temperature programmed desorption of ammonia (TPDA) is widely used for the direct determination of cumulative acidity and acid site distribution. It was first introduced by Amenomiya and Cvetanovic [21]. The probe molecule used is ammonia which can titrate acid sites of any strength and is accessible to even micropores due to its small size. NH_3 chemisorbs on a surface having acidic protons, electron acceptor sites and hydrogen from weakly acidic hydroxyls and thus can detect most types of acid sites.

In this technique a definite weight of pelletized activated sample was placed in a specially designed reactor and was heated at a linear rate. The sample was preheated at 300^{o}C for 30 minutes under nitrogen flow. After that, the sample was cooled to room temperature. A definite amount of ammonia was injected in to the system and was allowed to attain equilibrium. Then excess physisorbed ammonia was flushed out of the reactor by a current of nitrogen. The temperature was gradually increased and ammonia desorbed at an interval of 100^{o}C is passed in to dilute sulphuric acid. The ammonia desorbed at each stage was determined by titrating the unreacted sulphuric acid against standard sodium hydroxide using phenolphthalein as indicator. The amount of ammonia desorbed at 40-200^{o}C, 200-400^{o}C and 400-600^{o}C were assigned as weak, medium and strong acid sites respectively.

2.3.13.2 Cumene Cracking Reaction

The vapour phase cumene cracking reaction can be used as a model reaction for identifying the Lewis and Bronsted acid sites of heterogeneous

catalysts. Cumene undergo different reactions on different type of acid sites [22-24]. Cumene can be cracked to benzene and propene over Bronsted acid sites through dealkylation reactions and dehydrogenated to α-methyl styrene over Lewis acid sites. An idea about the Bronsted and Lewis acid sites possessed by the catalysts can be derived by comparing the amount of benzene and α-methyl styrene produced during the reaction.

The vapour phase cumene conversion reaction was carried out at atmospheric pressure in a fixed bed down flow glass reactor at a temperature of 400^{o}C. The previously activated catalyst was packed between silica beads in the reactor with glass wool. The liquid reactant was fed into the reactor with the help of a syringe pump at a flow rate of 4ml/h. The products were analyzed by Chemito GC 1000 gas chromatograph with FID detector using BP-1 capillary column. Analysis conditions are specified in Table 2.3

2.4 Catalytic Activity Measurements

2.4.1 Tertiary butylation of phenol

Tertiary butylation of phenol was done in vapour phase. Prior to the reaction the catalysts were activated for 1hr at 300^{o}C. The catalyst was packed in between quartz wool pack and sandwiched between silica beads. The reactor was placed inside a temperature controlled furnace with a thermocouple to measure the reaction temperature. In a typical reaction, a mixture of phenol and tertiary butanol in an optimized ratio was fed into the reactor at a specific flow rate using a syringe pump at a preset reaction temperature. The products were condensed and collected in an ice trap and analyzed by a Chemito 8610 GC with an FID detector and an OV-17 column. The products were confirmed by GC-MS analysis. The conversion was expressed in terms of phenol reacted and the product selectivity was expressed as the ratio of amount of particular product to

total amount of products multiplied by 100. Analysis conditions are specified in Table 2.3

2.4.2 Procedure for oxidation reactions

Hydroxylations of benzene, oxidation of phenol and benzyl alcohol were done in liquid phase in 50mL Round bottom flask equipped with a condenser. The flask was immersed in an oil bath in order to make the working temperature constant. In a typical run substrate and catalyst were added to the solvent. Then the oxidant was added to the reaction mixture after attaining the required temperature. For hydroxylation of benzene and oxidation of phenol, 30% H_2O_2 is used as oxidant. The reaction mixture was stirred with magnetic stirrer for the specific reaction time. The reaction mixture was withdrawn at specific intervals and the products were identified by GCMS and quantitatively analyzed using gas chromatograph with analysis conditions specified in Table 2.3

2.4.3 Acetalization of cyclohexanone

One-pot acetalization reactions of carbonyl compounds were carried out in a 50 mL double neck RB flask equipped with a magnetic stirrer, thermometer, water condenser and temperature controller. In a typical run, cyclohexanone and methanol in a specific ratio was added to catalyst in to the R.B. flask and magnetically stirred. The products were withdrawn at the end of the reaction and were analyzed with a Chemito GC1000 gas chromatograph equipped with a BP-1 capillary column under the analysis conditions specified in the Table 2.3.

Table 2.3 Analysis conditions of GC.

Reaction	GC/Column/ detector	Injection Temp (^oC)	Detection Temp (^oC)	Temperature programme
Cumene cracking	Chemito 1000, BP-1 capillary,FID	200	200	60^{o}C-2 min-10^{o}C/min-100^{o}C-2min-10^{0}C/min-200^{0}C-2min
Tertiary Butylation of phenol	Chemito 8610, OV-17, FID	230	250	120^{o}C-2min-8^{o}C/min-250^{o}C-1min
Oxidation of phenol	Chemito 8610, OV-17, FID	250	270	140^{o}C-2min-80^{o}C/min-250^{o}C-1min
Hydroxylation of benzene	Chemito 8610, OV-17, FID	230	270	60^{o}C-2min-3^{o}C/min-70^{o}C-10^{o}C/min-250^{o}C-1^{o}min
Oxidation of benzyl alcohol	Chemito 8610, OV-17, FID	230	250	70^{o}C-1min-10^{o}C/min-100^{o}C-1min-10^{o}C/min-250^{o}C-1min
Acetalization of cyclohexanone	Chemito 1000,BP-1 capillary , FID	100	100	70^{o}C-1min-5^{o}C/min-125^{o}C-1min-100C/min-200^{o}C-1min

Quantification was done after considering the response factors of reactants and products using standard mixtures and the conversion and selectivity values are reported with error limit of ± 2%.

References

[1]. A. Montaser, D. W. Golightly, Inductively Coupled Plasmas in Analytical tomic Spectromety. 2nd ed. VCH Publishers, Newyork (1992).

[2]. R. Keren, Clays. Clay Miner.,34 (1986) 534.

[3]. M. Horio, K. Suzuki, H. Masuda,T. Mori, Appl. Catal. A :Gen, 72 (1999)109.

[4]. K. Suzuki, M. Horio, T. Mori , Bull. Chem. Soc. Jpn, 64 (1991) 732.

[5]. H. Laudelout. In: ACD Newman, ed. Chemistry of Clays and Clay Minerals. NewYork: Wiley-Interscience, (1987)

[6]. C. R. Eggleton, Clays ,Clay Miner., 47 (1999) 174.

[7]. L. P. Meir, G. Kahr ,Clays , Clay Miner.,47 (1999) 386.

[8]. A. Gil, S. A. Korili, R. Trujillano, M. A. Vicente, Appl. Clay Sci., 53 (2011) 97

[9]. K. S. W. Sing, D. H. Everett, R. A. W. Haul, L. Moscou, R. A. Pierotti, J. Rouquerol, T. Siemieniewska, Pure Appl. Chem., 57 (1985) 603.

[10]. B. C Lippens, J.H de Boer , J.catal., 4 (1965) 19.

[11]. S. Bruauer, P. H. Emmet, E. Teller , J.Am. Chem. Soc., 309 (1938) 60.

[12]. J. M . de Boer, R. C. Lippens, B. G. Linsen, J.C. P. Broekhoff, Van Der Heuvel, T. Singa, J. Colloid Inter. Sci., 21 (1966) 405.

[13]. D. W. Rutherford, C. T. Chiou, D.D Eberl, Clays Clay Miner., 45 (1997) 534.

[14]. M. Kruk, M. Jaroniec, A. Sayari, Langmuir, 13 (1997) 6267.

[15]. J. W. Newmansverdritet, Spectroscopy in Catalysis , Wiley-VCH (2007)

[16]. M. A. Larrubia, G. Busca, Mater. Chem. Phys., 72 (2001) 337.

[17]. D. Briggs, M. P. Seah, Practical Surface Analysis: Auger and X- Ray Photoelectron Spectroscopy. Wiley, New York, 1996.

[18]. A. Howie, "Characterisation of Catalyts" J Thomas, RM Lambert(eds) John Wiley, Newyork (1989).

[19]. B. Fultz, J. Howe, Transmission Electron Microscopy and Diffractometry of Materials, Springer, 2nd edn. (2002).

[20]. D. Srinivas, Appl. Catal. A, 246 (2003) 323.

[21]. Y. Amenomiya, R.J. Cvetanovic, J. Phys. Chem., 67 (1963) 144.

[22]. S. M. Bradley, R. A. Kydd, J. Catal., 141 (1993) 239.

[23]. T. Mishra, K. M. Parida, S. B. Rao, Appl. Catal. A., 166 (1998) 115.

[24]. M. Hino, M. Kurashige, K. Arata, Catal. Commun., 5 (2004) 107.

.....ꕥ.....

Chapter 3

PHYSICO CHEMICAL CHARACTERIZATION

Characterization of the prepared catalyst is the central aspect of catalyst development. The elucidation of the composition, structure, chemical as well as the physical properties of catalysts, adsorbate and intermediate on the catalyst surface is vital for understanding the relationship between catalyst property and performance. The basic information on structure-catalytic activity relationship will lie ultimately of great value in designing new catalysts. In the case of supported catalysts it is crucial to know the active ingredient on catalyst surface. The investigation on surface composition as well as local structure of catalyst at atomic level and its correlation with catalytic activity is the goal of the fundamental catalytic research. Spectroscopy, microscopy, diffraction, adsorption/desorption methods, thermal analysis or bulk reaction such as oxidation or reduction all offer tools to investigate the nature of an active catalyst. This chapter deals with the result and discussion pertaining to structural, acidic and textural characteristics of prepared catalysts by various spectroscopic or nonspectroscopic methods.

3.1 Introduction

The aim of characterization of catalysis is to obtain information concerning the active surface in atomic level under reaction conditions. A heterogeneous catalytic reaction begins with the adsorption of the reacting species onto the surface of the catalyst, where intramolecular bonds are broken or weakened. Then the adsorbed species react on the surface, often in several consecutive steps to produce products. Finally, the products desorbs from the surface, thereby regenerating the active sites on the surface. The function of the catalyst is to provide an energetically favorable pathway for the desired reaction in which the activation barriers of all intermediate steps are low compared to the activation energy of the gas phase reaction. A complete knowledge on the exact location, structure and electronic ground state of the active sites on the catalyst structure is essential to establish a basic understanding about the structure- activity correlations and to improve the efficiency of the catalyst for higher selectivity and stability. Establishing empirical relationship between catalyst property and catalyst activity is very useful in catalyst development

3.2 Elemental Analysis

The Elemental analyses of the pillared clays were done by ICP-AES and the results are given in Table 3.1. Clays are aluminium or magnesium silicates which contain 56.5 % silica, 20.7 % alumina, 2.6 % magnesium etc. as their constituents. The parent clay also contains considerable amount of exchangeable cations like Na^+, K^+, Ca^{2+} etc. The amount of these elements is reduced as a result of pillaring as insertion of pillaring species occurs at the expense these of cations by exchange process [1]. The decreases in CEC of clay after the pillaring process support this view. It can be seen that

appreciable amount of metal was incorporated during the pillaring process. After the aluminium pillaring the amount of aluminium is increased from 20.7 to 35.8 Wt. %. In iron-aluminium pillared clay the weight % of aluminium and iron are 30.5 and 16.5 respectively. In zirconium pillared clay, 28.5 weight % of Zr was incorporated after the pillaring process.

In porous clay heterostructures the amount of silica increased from 55.4 to 74.4 Wt. %. In ZrSiPCH the amount of Zr incorporated was 4.2 Wt.%. The exchangeable cation like Na, K and Ca persist in PCHs even after their formation indicating that the formation mechanism is a template assisted self assembling rather than an exchange type [2].

Table 3.1 Elemental analysis of PILCs and PCHs.

Catalyst	Si	Al	Fe	Na	K	Mg	Ca	Zr
M	56.5	20.7	12.1	2.7	2.8	2.6	2.6	
NaM	55.4	19.5	11.9	7.6	2.5	2.6	0.5	
AlPC	47.9	35.8	11.2	0.4	1.7	2.1	0.9	
FeAlPC	47.6	30.5	16.5	0.4	2.0	2.2	0.8	
ZrPC	46.0	17.1	4.2	0.3	1.4	2.1	0.4	28.5
SiPCH	74.4	12.7	4.4	4.5	1.8	1.9	0.3	
ZrSiPCH	71.2	11.3	4.9	4.5	1.8	1.7	0.4	4.2

(The values are in wt. % with the error limit of ± 2%)

The amount of transition metals in transition metal loaded PILCs and PCHs were also estimated and the results are given in Table 3.2. In all cases the metals detected were less than theoretical loading. The weight percent of cerium and cobalt were calculated from EDAX analysis. The EDAX spectrum of Ce(3)Fe-AlPC and CoZrSiPCH are given in Fig. 3.1 and 3.2 respectively.

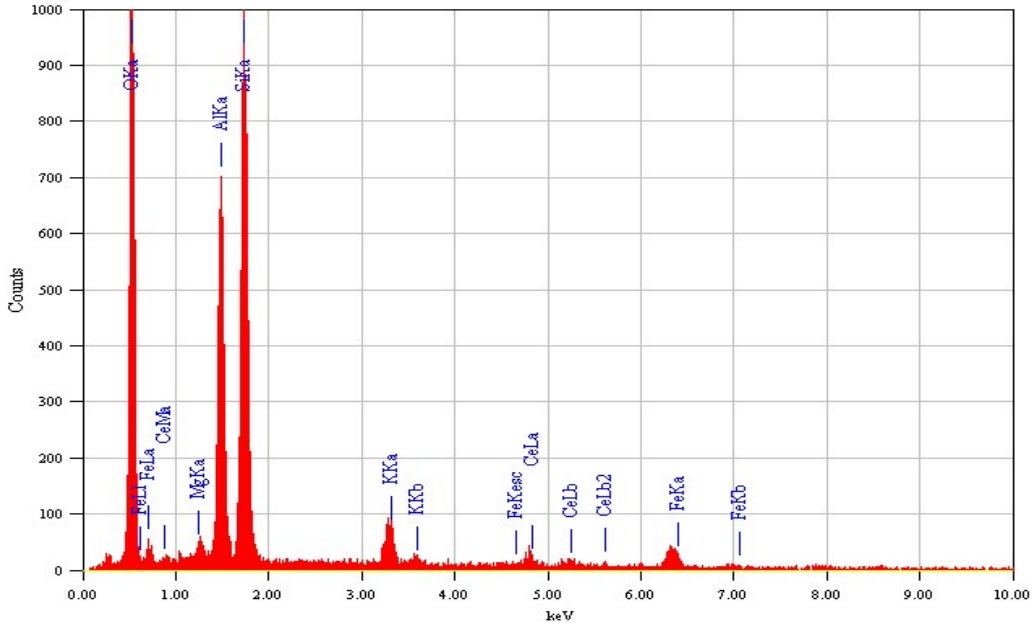

Fig.3.1 EDAX spectrum Of Ce(3)FeAlPC

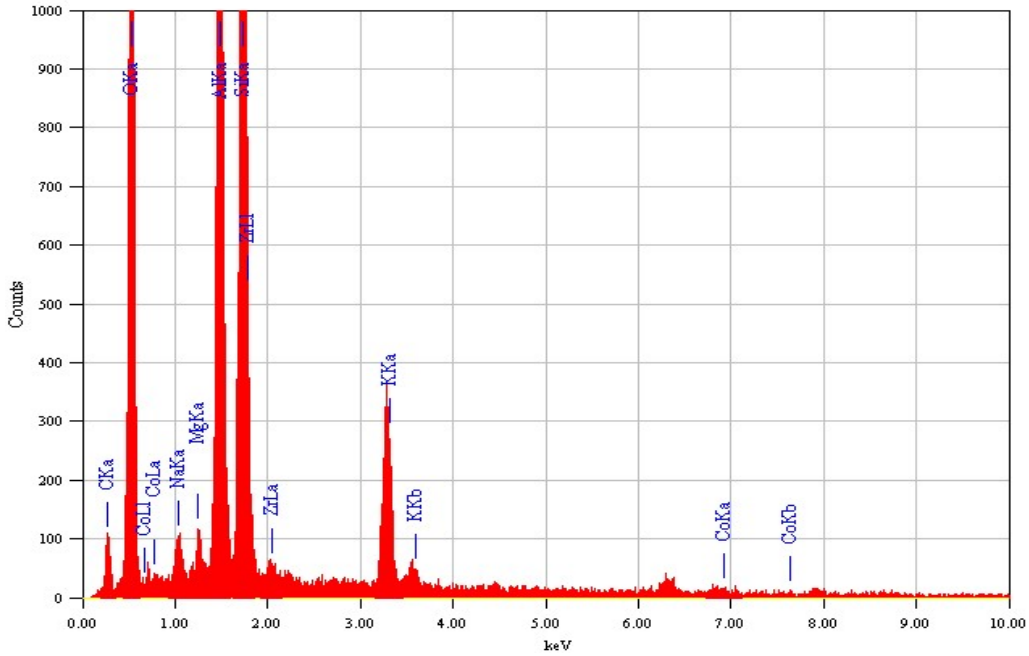

Fig.3.2 EDAX spectrum Of CoZrSiPCH

Table 3.2. Elemental analysis of metal loaded PILCs and PCHs

Catalysts	Wt. % of transition metal detected	Catalysts	Wt. % of transition metal detected
Cu (1)ZrPC	0.6	V1)ZrPC	0.7
Cu(3)ZrPC	1.6	V(3)ZrPC	1.9
Cu(5)ZrPC	3.7	V(5)ZrPC	4.0
Ni(1)ZrPc	0.6	Ce(3) AlFe	1.7
Ni (3)ZrPC	2.4	Ce (3)AlPC	1.8
Ni(5)ZrPC	4.2	CuZrSiPCH	2.3
Co(3)ZrPC	2.1	Ni ZrSiPCH	2.9
Co(5)ZrPC	3.8	Co ZrSiPCH	2.8
		VZrSiPCH	2.1

3.3 Cation Exchange Capacity

Cation Exchange Capacity of catalysts were estimated by ammonium acetate extraction method by the procedure given section 2.3.2. CEC is a measure of exchangeable cations in the interlamellar region and the estimation of residual CEC is measure of effectiveness of pillaring [3]. The CEC of clays are reduced as a result of pillaring as pillaring is eventually an exchange process. Even after pillaring process a part of exchangeable cations remains in interlayer regions and this residual CEC provides an estimation of fraction of layer charge, which is not compensated by pillaring species. The protons that are formed in final calcination step of pillaring process also restore the CEC of clay.

Since pillaring were done on NaM, the residual CEC of NaM is taken as 100 %. After the pillaring process, CEC and residual CEC decreased to a grater extent. The residual CEC for pillared clays are in the order FeAlPC <

ZrPC < AlPC and the effectiveness of pillaring is in the reverse order. The high residual value of AlPC indicates that aluminium polyoxocation is least effective in pillaring process. The presence of residual CEC even after pillaring process implies that there is further scope for incorporation of transition metals by exchange process.

It can be seen that porous clay heterostructures have higher residual CEC than that of pillared clays. This may be due to the fact that in porous clays heterostructure formation mechanism is not an exchange type but a template assisted self assembling mechanism. Various researchers studied the cation exchange capacity of porous clay heterostructures and its high CEC was utilized for the removal of heavy metals in waste water [4-5].

Table 3.3 CEC of PILCs and PCHs

Catalyst	CEC (mmol/g)	Residual CEC (%)
NaM	0.86	100
ZrPC	0.32	37.2
AlPC	0.37	43
FeAlPC	0.24	27.9
SiPCH	0.48	55.8
ZrSiPCH	0.42	48.8

3.4 XRD

XRD pattern of clays consist of broad peaks instead of sharp peaks. It is attributed to the semi crystalline nature of clays. The success of pillaring process can be readily understood from XRD analysis by the indication of increase in d (001) spacing which results from the incorporation of metal oxide clusters between the layers. The XRD patterns of pillared clays are

shown in Fig 3.3. The parent clay shows peak at 2θ value 8.9^0 corresponding to the basal (001 plane) spacing of 9.8 Å. After the pillaring process this value shifted to lower 2θ values which indicate the increase in basal spacing of clays due to the propping apart of clay layers by the insertion of metal oxide pillars [6]. In all cases high intensity for pillaring peak were observed compared to the peak at 8.9^0. Aluminium pillared clays have the d spacing value of 19.2 Å.. The d spacing was increased to 21.5 Å for iron aluminium pillared clays. It is reported that mixed oxide pillared clays have larger d spacing compared to single metal oxide pillared clays [7-8]. The existence of peaks of small intensity at 8.9^0 even after pillaring process in aluminium and iron aluminium pillared clays is attributed to the presence of small amount of unexpanded clays in the samples [9].

Zirconium pillared clays have d spacing of 20.2 Å. This value is greater than the d spacing of zirconium pillared clays reported in which single tetramer of zirconium pillaring species is aligned parallel to the clay sheets. It is also greater than that of Zr pillared clay in which two tetramers are aligned on top of each other perpendicular to the clay sheets [10]. This value of d spacing can be interpreted as the result of insertion of polymer of zirconium tetramers of large size [11]. For porous clay heterostructures there is a large shift in basal spacing and d spacing of 44.5Å for SiPCH and 42.4 Å for ZrSiPCH respectively are observed.

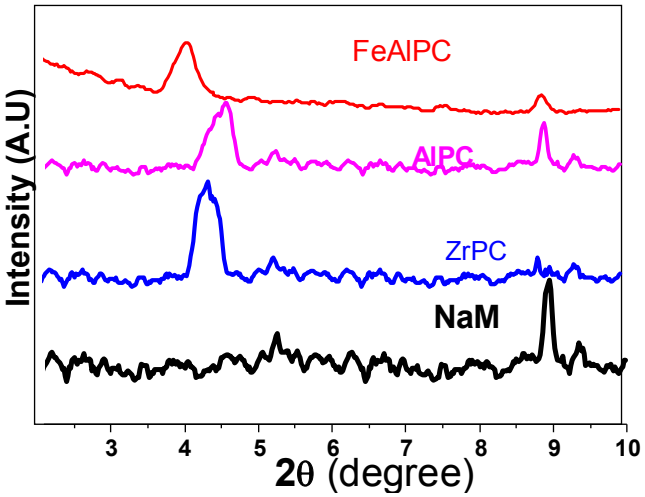

Figure 3.3. XRD patterns of pillared clays

Table 3.4 XRD results of PILCs and PCHs

Catalysts	2θ (degree)	$d_{(001)}$ (Å)
Na-M	8.94	9.8
Zr PC	4.36	20.2
AlPC	4.59	19.2
FeAlPC	4.10	21.5
ZrSiPCH	2.08	42.4
SiPCH	1.98	44.5

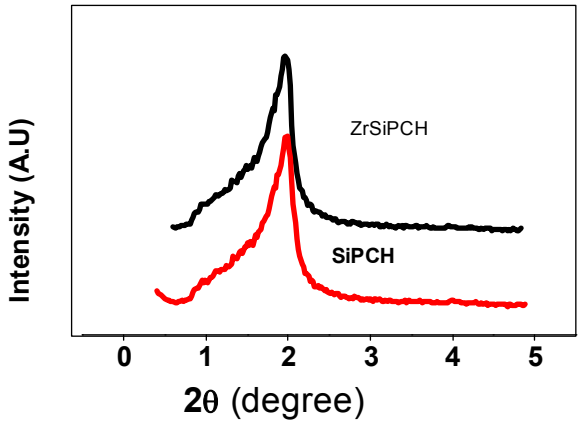

Figure 3.5 XRD pattern of PCHs

The wide angle XRD patterns of metal incorporated pillared clays are given in Fig 3.6. Peaks at 2θ values of 19.6^0 and 35.1^0 correspond to the reflection from (110) and (130) planes respectively of 2:1 phyllosilicate clay [12-13]. The peak at 2θ value of 26.7^0 corresponds to quartz impurity [8,14]. For metal loaded pillared clays, up 5 % of metal loading, peaks corresponding to metals were not found (with the exception of nickel) which indicate that the metals were uniformly distributed over the catalyst surface. The XRD patterns of copper loaded zirconium pillared clays are given in Figure 3.6.

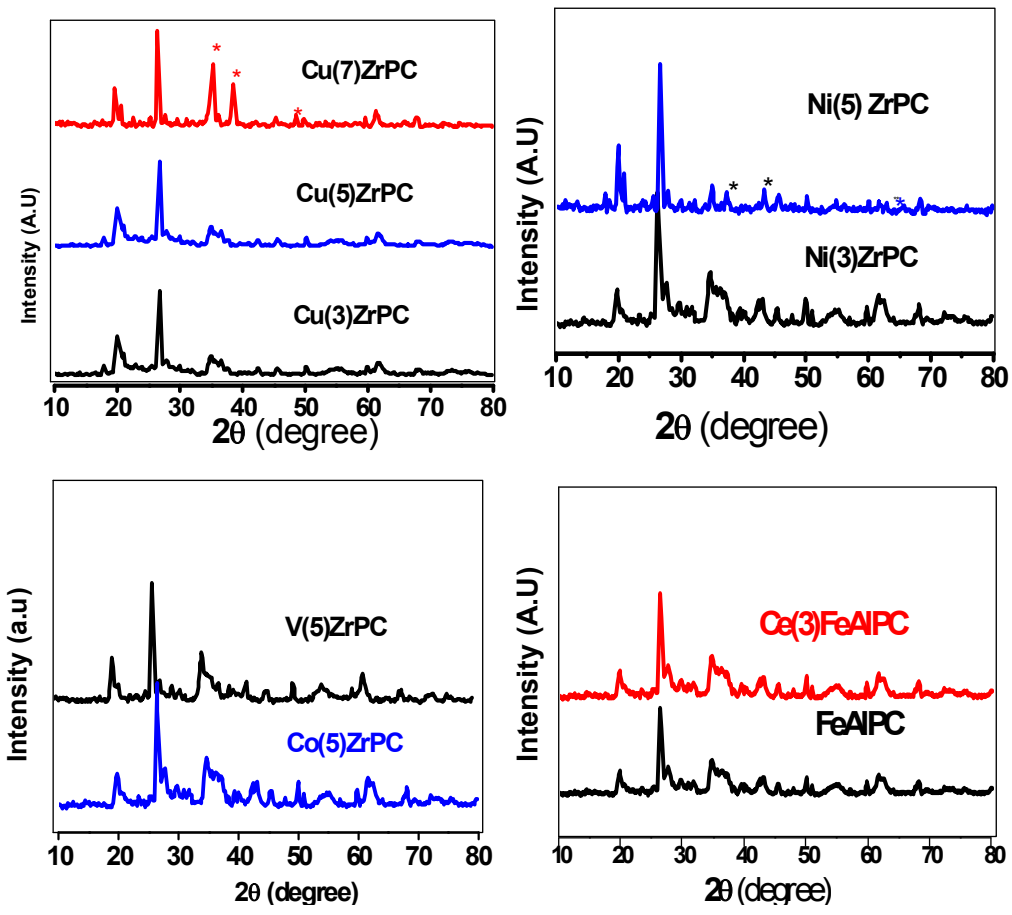

Figure 3.6 XRD pattern of metal loaded zirconium pillared clays

Up to 5%, copper is uniformly distributed. In 7% copper loaded zirconium pillared clays peaks at 2θ values of 35.5^0 and 38.8^0 corresponds to CuO clusters [15]. For nickel loaded zirconium pillared clays even 5 % nickel loaded catalyst showed peaks at 2θ values of 37.2^0,43.3^0, 64.4^0 correspond to NiO [16]. XRD pattern of cobalt and vanadium loaded zirconium pillared clays are devoid of peaks corresponding to metal oxides indicating that they were dispersed uniformly over catalyst surface.

XRD patterns of metal loaded porous clay heterstructure are given in Figure 3.7. The characteristics peaks corresponding to higher reflection plane of 2:1 phyllosilicate clays are retained in PCHs which indicate that laminar structure of clays are preserved even after modification. The XRD patterns of metal incorporated porous clay heterostructures are also devoid of peaks corresponding to metal oxides indicating that the active metal species is uniformly distributed over the surface.

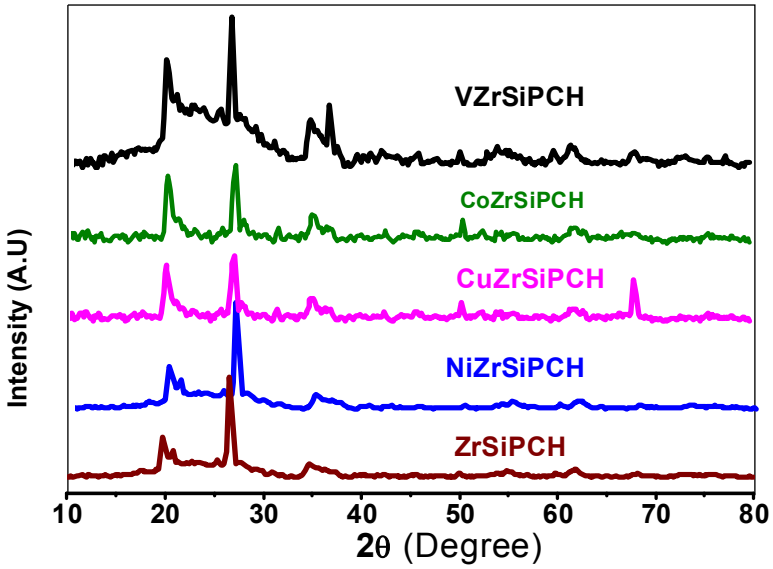

Figure 3.7 XRD pattern of metal loaded porous clay heterostructures

3.5 Surface area measurements

The textural properties of pillared clays are given in the Table 3.5. The parent clay has a BET surface area of 17 m^2/g only. After exchange with sodium the surface area was increased to 70 m^2/g. The increase in surface area of sodium montmorillonite is attributed to the dealumination of octahedral aluminium during exchange process which may be present in interlayer region. After the pillaring process, surface area and pore volume increased drastically since metal oxide pillars are inserted in between the two dimensional gallery of clay layers to produce a three dimensional porous network [17-18].

Table 3.5 Surface area and pore volume of PILCs

Catalyst	Surface area S_{BET} (m^2/g)	Pore volume cm^3/g
M	17	-
NaM	70	0.0253
ZrPC	152	0.1952
Cu(1)ZrPC	144	0.1719
Cu(3)ZrPC	114	0.1445
Cu(5)ZrPC	113	0.1411
Ni(1)ZrPc	137	0.1485
Ni (3)ZrPC	121	0.1263
Ni(5)ZrPC	98	0.0895
Co(3)ZrPC	117	0.1382
Co(5)ZrPC	108	-
V1)ZrPC	139	-
V(3)ZrPC	118	0.1358
V(5)ZrPC	102	-
FeAlPC	132	0.1713
Ce(3)FeAlPC	143	0.1728

The active surfaces of clays are now more accessible due to the expansion of clay layers. In metal loaded pillared clays the surface area and pore volume

decrease with metal loading. This is due to the filling of pores with metal species. But in the case of Ce loaded Fe-AlPC, the surface area is higher than that of Fe-AlPC. This may be due to the additional surface area provided by ceria mesopores. R. Zhou et al. reported similar results in the case of cerium loaded aluminium pillared clays [19].

The textural properties of porous clay heterostructures are given in Table 3.6. Porous clay heterostructures have higher surface area, pore diameter and pore volume than that of pillared clays. After the incorporation of metals surface area, pore volume and pore diameter of zirconium silicon porous clay heterostructures decreased due to occupancy of metal species in pores.

The adsorption isotherms of pillared clays are shown in Fig. 3.8. The adsorption isotherm of pillared clays are blends of type I and type IV isotherms with hysteresis loop H4 characteristics of mesoporous materials with some micropores [20]. At lower p/p_0 value the adsorption isotherms have the shape of type I isotherm characteristic of micro porous material according to Brunauer, Deming, Deming and Teller (BDDT) classification [21]. But at higher p/p_0 values it shows hysteresis loop of H4 type charcteristics of slit like pores according to IUPAC classification [22].

Table 3.6. Textural properties of porous clay heterostructures

Catalyst	S_{BET} (m^2/g)	Pore diameter (Å)	Pore volume (cm^3/g)
SiPCH	441	42.2	0.7319
ZrSiPCH	414	41.5	0.7266
CuZrSiPCH	319	38.5	0.5043
NiZrSiPCH	256	40.4	0.4291
CoZrSiPCH	365	38.8	0.4954
VZrSiPCH	324	37.8	0.3938

The adsorption isotherms of porous clay hetero structures are shown in Figure 3.9. They are of type IV with hysteresis loop H3 characteristics of mesoporous materials with open cylindrical pores [23]. The ratio of micropore volume to total pore volume is high in pillared clays compared to porous clay heterostructures since pillared clays possess both micro and mesopores.

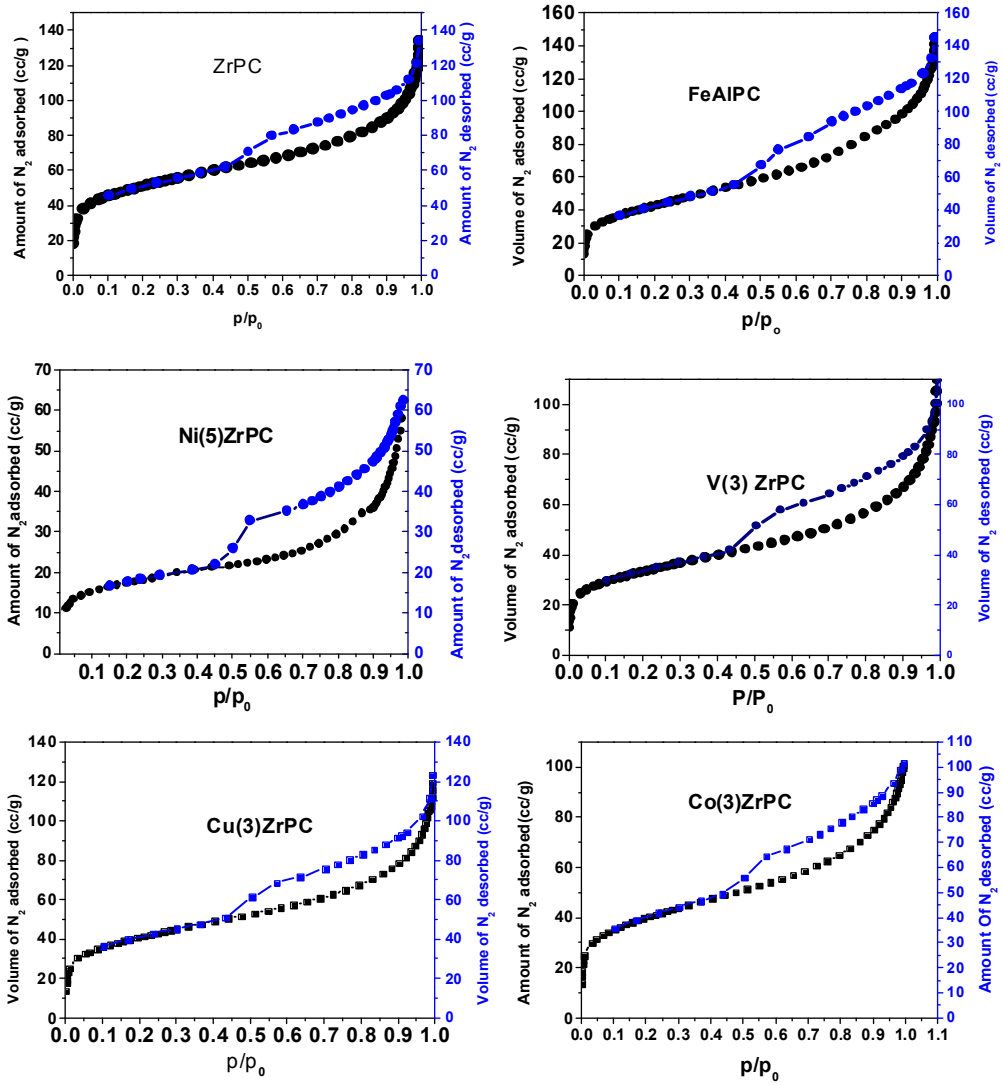

Figure 3.8 Adsorption isotherms of pillared clays

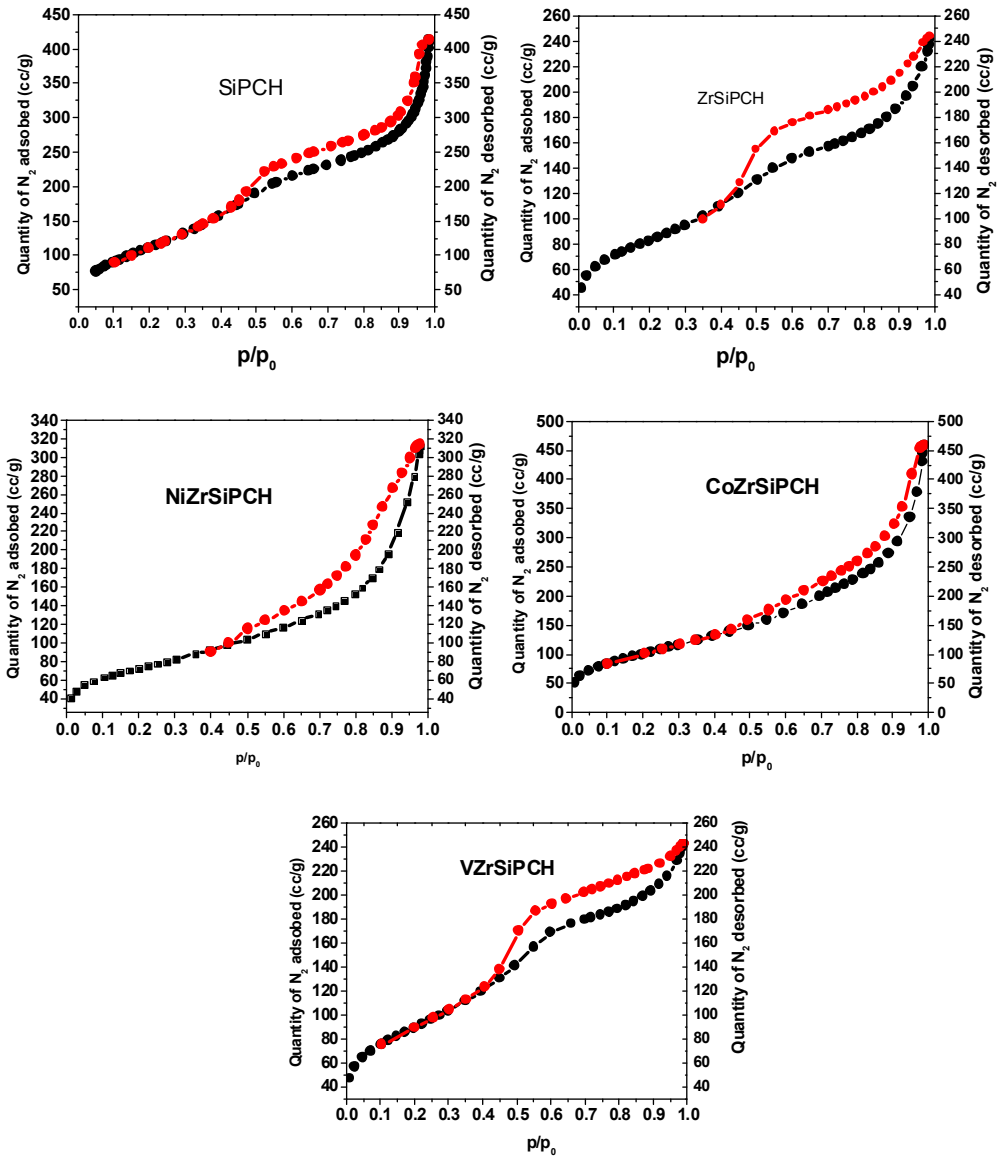

Figure 3.9 Adsorption isotherms of PCHs

The pore size distribution has been determined by referring BJH model as applied to the desorption branch of isotherm (desorption branch better meets the requirements of ideal wetting inherent in the model) [24]. The

average pore size distributions of representative catalysts are given in Figure 3.10. The pore size of pillared clays can be varied from 5 Å to over 60 Å depending on the synthesis conditions, parent clays [25], CEC of clays [26], type of the metal oxide pillars [27] and thermal treatment temperature [28]. Generally PILCs exhibit bimodal pore size distribution with pore size bigger than zeolites, which show advantages in reactions with larger molecules. In the present case, pillared clays and its transition metal loaded analogues have average pore diameter in the range of 28-34 Å where as porous clay heterostructures and its transition metal loaded analogues have average pore diameter in the range of 38-42 Å with narrow pore size distribution.

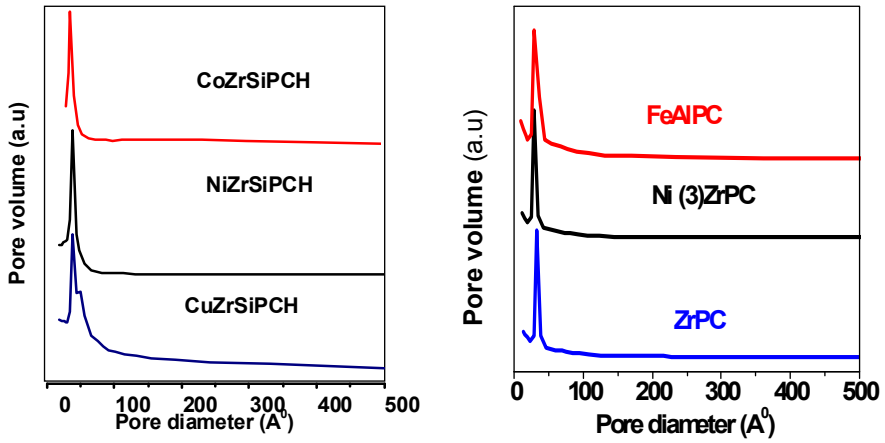

Figure 3.10 Pore size distribution of PILCs and PCHs

3.6 FT-IR Spectroscopy

FT-IR spectra of sodium montmorillonite and pillared clays in the range 400 to 4000cm^{-1} are shown in Figure 3.11**.** For NaM, a broad band near 3500 cm^{-1} corresponds to the stretching vibration of OH group. This peak is very intense for sodium montmorillonite. The intensity of this peak is considerably reduced for the pillared samples showing the loss of hydroxyl groups upon

pillaring during the calcinations step at higher temperature. For all the pillared samples there are two peaks around 3500 cm^{-1} corresponding to the hydroxyl groups. One may be assigned to the pillar OH group and the other assigned to layer hydroxyl groups [29-30]. Peak around 1600 cm^{-1} is due to bending vibrations of water. Pillaring process replaces a large amount of interlayer cations that generally exist as hydrated, which leads to the decreases the intensity of –OH peaks. The band around 1060 cm^{-1} is due to asymmetric stretching vibrations of SiO_2 tetrahedra. A band around 800 cm^{-1} is due to stretching vibrations of Al octahedral and absorption in the range 526-471cm^{-1} is due to bending vibration of Si-O.

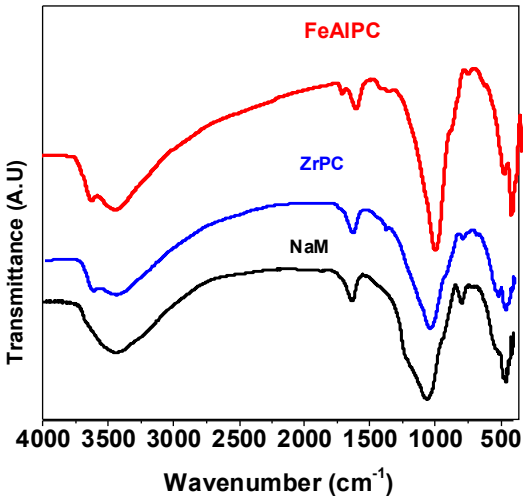

Figure 3.11 FT-IR spectra of pillared clays

The retention of all the peaks in pillared clays reveals that the basic clay structure is preserved after the pillaring process. In metal loaded zirconium pillared clays the intensity of OH stretching peak associated with pillars is reduced and is shifted to lower wave number due to the coordination of metal species to Pillar –OH [31-32].

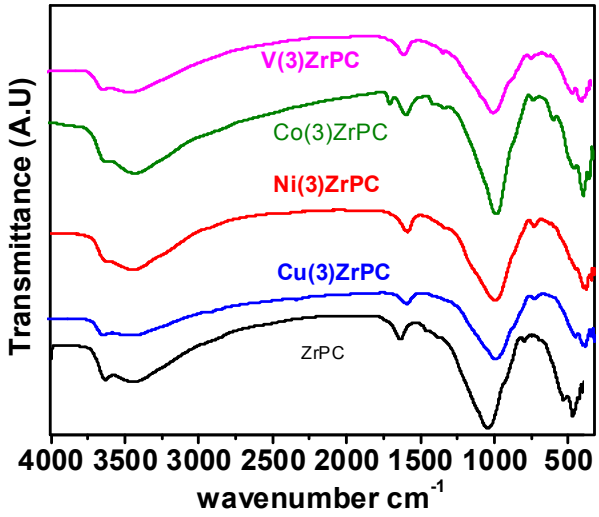

Figure 3.12. FT-IR spectrum of metal incorporated zirconium pillared clays

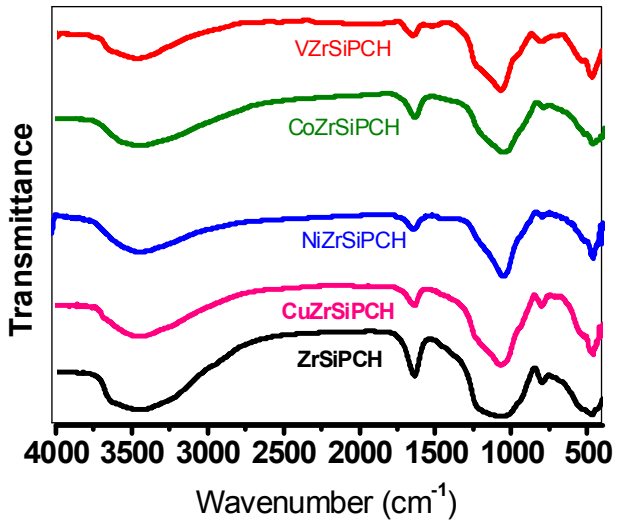

Figure 3.13. FT-IR spectra of metal incorporated porous clay heterostructures

FT–IR spectrum of porous clay heterostructures are given in Figure 3.12. All the peaks of clays are retained in porous clay heterostructures. The intensity of OH stretching peak and bending peak increased in porous clay

heterostructures due the formation of new silanols in the intergallery region. But after the incorporation of metals the Si-O asymmetric stretching and Si-O bending peaks were shifted to lower wave number in PCH material due to the coordination of metals to silica framework [33].

3.7 ^{29}Si NMR

Silicon NMR spectrum provides information about different chemical environment to which the silicon nucleus belongs. For silicon nucleus (Spin =1/2) the chemical shift is affected mainly by the electron density on oxygen atom of silicon tetrahedron. Therefore the nature of neighboring atoms coordinated to these atoms can influence the chemical shift of silicon nucleus. The connectivity of Si nuclei in silicate species is described by usual Q^n notation, Q represents a silicon nucleus connected to four oxygen atoms forming a tetrahedron. The superscript n is the number of Q units attached to central SiO_4. Thus Q^0 denotes monomeric orthosilicate, Q^1 denotes end group of chains where Si atoms are liked through oxygen atoms to one silicon and three atoms other than silicon atom, Q^2 denotes middle groups in chains or cycle in which silicon is linked through oxygen to two silica atoms and two other atoms, Q^3 denotes chain branching sites in which Si ^{IV} atoms are linked through oxygen atoms to three other Si atoms and an atom other than silicon. Q^4 represents three dimensionally cross linked silica groups in which all Si atoms are linked through oxygen atoms to silicon atoms.

Figure 3.13 shows the Si NMR spectra of pure montmorillonite and pillared clays. The parent clay consists of two peaks. The resonance near -93.8 ppm corresponds to Q^3 environment in which Si ^{IV} atoms are linked to three other Si atoms and one aluminium or other metal atoms through oxygen

atom ie T(3Si, 1Al). The other peak near -110 ppm corresponds to Q^4 environment in which Si ^{IV} atoms are linked to four other Si atoms through oxygen atom [34-36]. This is due to quartz impurity in the parent clay which is in line with observation in XRD. The intensity of Q^3 peak is greater than Q^4 peak indicating that majorities of silicon atoms are linked to three silicon atoms and one other atom. On pillaring the T resonance shifts and broadens considerably. For zirconium pillared clay it is shifted to -94.4 ppm and for iron-aluminium pillared clay it is shifted to -94.5 ppm respectively. These shifts even though small indicate the strain in local environment of silicon atoms and it is proportional to the size of intercalated species. The presence of Si-O-M pillar site may be responsible for the broadened resonance observed in the spectrum of PILCs [36].

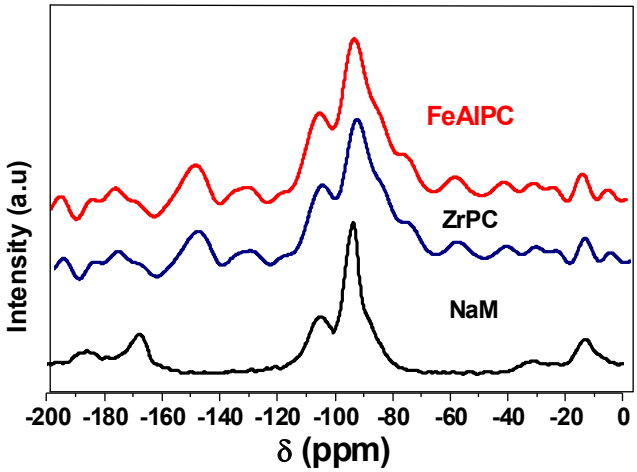

Figure 3.13 Si NMR of PILCs

Si NMR spectrum of porous clay heterostructures is given in Fig. 3.14. For silicon porous clay heterostructures the Q^4 peak which is at -108 ppm is more intense than Q^3 which indicate the successful incorporation of mesoporous silica in the intergallery of clay layers [37]. For zirconium silicon

porous clay heterostructures and their cobalt loaded analogous an additional peak around -88.6 and -88.8 ppm respectively were observed which indicate the presence of Q^2 environment in which silicon atom is liked to two other atoms than silicon through oxygen atoms. This also indicates the successful incorporation of zirconium in intergallery region of silica.

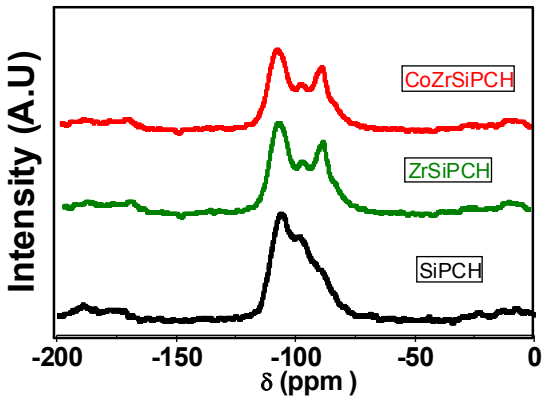

Figure 3.14 Si NMR of PCHs

3.8 UV-Vis Diffuse Reflectance Spectroscopy

UV-Vis DRS is a useful technique for studying the local coordination environment and electronic state of isolated as well as aggregated transition metal oxides in a support. The basic tetrahedral silicate layers in the clay lattice do not absorb light in the range of 200-800 nm except when the transition metal ions are incorporated in the silicate structure. Aluminium oxide is also a direct band gap insulator which does not absorb light in the UV-region of the spectrum. The UV-Vis DR spectra of metal loaded pillared clays are shown in Figure 3.15. For cerium impregnated Fe-Al pillared clay the broad adsorption peak detected in the range of 250–450 nm is related to

$Fe^{3+} \leftarrow O^{2-}$ charge transfer [38]. The bands in the region of 300–400 nm are characteristics of Fe^{3+} in octahedral coordination. The peak around 290 nm corresponds to $Ce^{4+} \leftarrow O^{2-}$ charge transfer transitions [39].

The UV DRS spectrum of copper incorporated zirconium pillared clay is given in Figure 3.15. Peak around 210 nm, attributed to $O^{2-} \rightarrow Zr^{4+}$ charge transfer is observed in all zirconium pillared clays [40]. For Cu(5)ZrPC peak in the range of 220 -300 corresponds to $Cu^{2+} \leftarrow O^{2-}$ charge transfer in isolated Cu^{2+} species [41-42]. No significant absorption peak above 300 nm is observed, suggesting that it is free of copper oxide oligomers or clustered copper species.

Cobalt incorporated zirconium pillared clays show peaks at 595 and 650 nm corresponding to electronic transitions of Co^{2+} [$^4A_2$ (F)$\rightarrow ^4T_1$(P)] [43]. Peak around 260 nm corresponds to oxygen to cobalt charge transfer [44]. The absence of peak at 410 nm indicates the absence of Co (III) species in the sample [45].

In V(5)ZrPC, peak around 260 nm can be assigned to isolated vanadium in tetrahedral coordination [46]. In the case of V(7)ZrPC catalyst presence of very broad peak around 300 nm can be deconvoluted to two absorption peaks, one at 260 nm, corresponding to isolated vanadium and other around 350 nm corresponding to polymeric V-O-V species respectively [47].

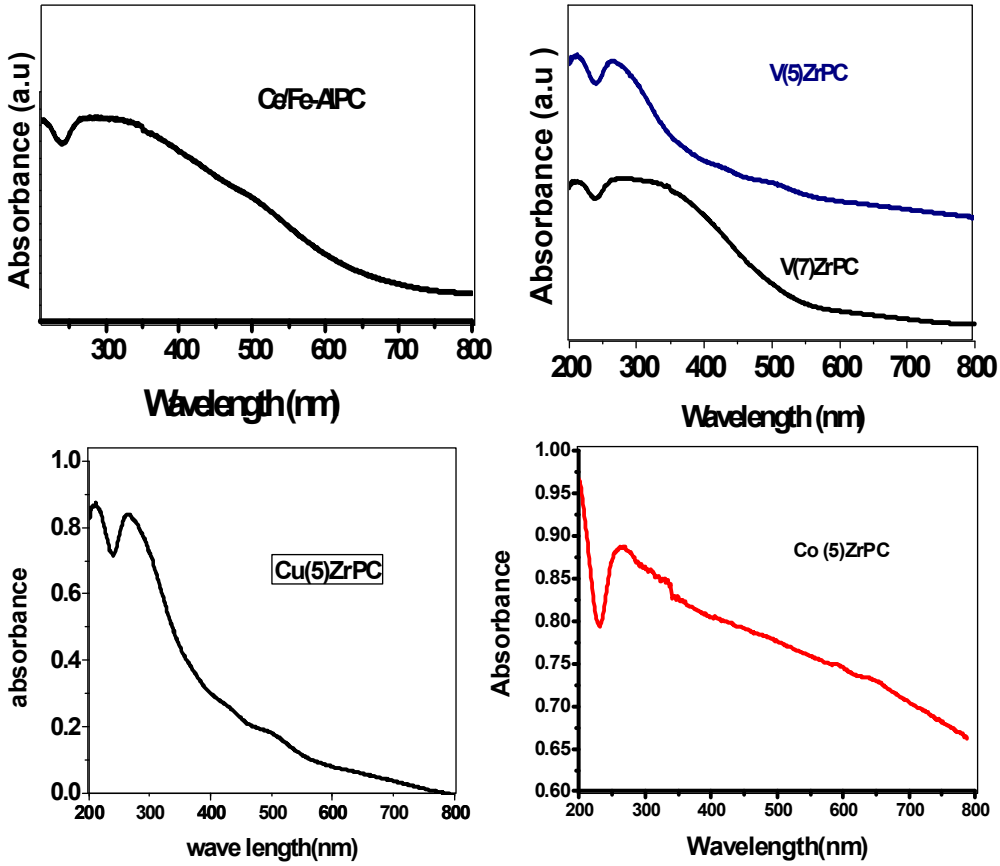

Figure 3.15 UV-vis DRS spectra of metal loaded PILCs

3.9 Temperature Programmed Reduction (TPR)

Temperature-programmed reduction (TPR) has been extensively applied to the characterization of reducible catalysts including metal and metal oxide system in suitable supports. It is especially suitable for studying highly dispersed supported catalyst systems with low loading. TPR profiles of catalysts are given in Figure 3.16. According to the literature the following reduction processes can be considered for supported copper systems [48-50].

$CuO + H_2 \rightarrow Cu^0 + H_2O$ (H_2-TPR peak in the 170-200^oC range)

$Cu^{2+} + 1/2H_2 \rightarrow Cu^+ + H^+$ (> 200^oC for isolated/ oligomeric /clustered species)

$Cu^+ + 1/2H_2 \rightarrow Cu^0 + H^+$ (> 420^oC)

For Cu(5)ZrPC catalyst, a peak at 280^oC corresponds to reduction of isolated Cu^{2+} species [44]. This indicates that active copper species are uniformly distributed over the support. With increasing amount of copper this peak broadens and is shifted towards higher temperature. In 7% Cu loaded zirconium pillared clay, in addition to this peak there is another peak around 400^oC corresponding to the reduction of agglomerated copper clusters [46]. A small peak at 500^oC is observed in all catalysts corresponding to the reduction of Fe^{3+} isomorphously substituted or present in interlayer of clay.

For nickel loaded zirconium pillared clays and porous clay heterostructures, a peak at 390^0C corresponds to reduction of isolated Ni^{2+} species [50-51]. For NiZrSiPCH, the peak around 600^oC corresponds to the reduction of NiO which has strong interaction with silica support [48]. In Ni(5)ZrPC, peak at 210 ^oC can be assigned as the reduction of bulk type NiO which is easily reducible than supported nickel oxides [52]. The reduction peaks at 730^oC is assigned as the reduction peak of amorphous nickel silicate/zirconate [53].

V(5)ZrPC and VZrSiPCH catalyst show reduction peak at 515^oC and 535^oC respectively. Peak around 500^oC corresponds to the reduction of V^{5+} in tetrahedral coordination [54-55]. The difference in temperature may be due to the varying amount of vanadium content or due to varying degree of interaction with support.

In Cobalt loaded silicon zirconium porous clay heterostructures, the broad peak centered on 470^{0}C corresponds to the reduction of CoO to metallic cobalt. The absence of reduction peak of Co^{3+} to Co^{2+} around 280^{o}C indicates the absence of Co_3O_4 type oxides in the catalyst [56-57]. The higher temperature reduction peaks can be assigned to the reduction of barely reducible cobalt silicate species(Co_2SiO_4) which might have formed during high temperature calcinations [58].

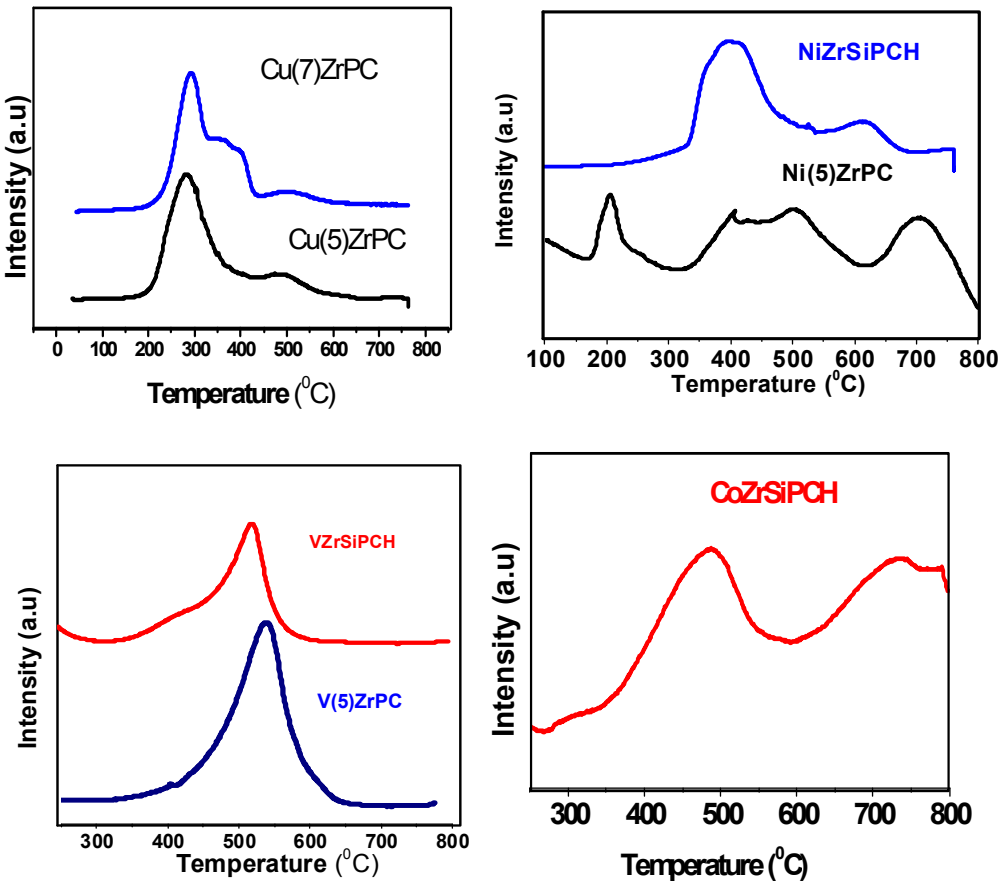

Figure 3.16 TPR profiles of catalysts

3.10 XPS (X-Ray Photo Electron Spectroscopy)

XPS has long been recognized as a primary tool for the detection of chemical species at the surface of solids. In heteroatom substituted mesostructured silica frame work prepared by direct method, there is always question of true incorporation of the hetero atom in the frame work, as opposed to its presence as a segregated oxide phase. The nature and oxidation state of zirconium in zirconium- silicon porous clay heterostructure can be understood from XPS analysis. The XPS survey scan for the representative catalyst CoZrSiPCH is shown in Figure 3.17. The survey scan consists of peaks corresponding to the B. E value of Co2p, Zr 3d, Si 2p and O 1s as expected.

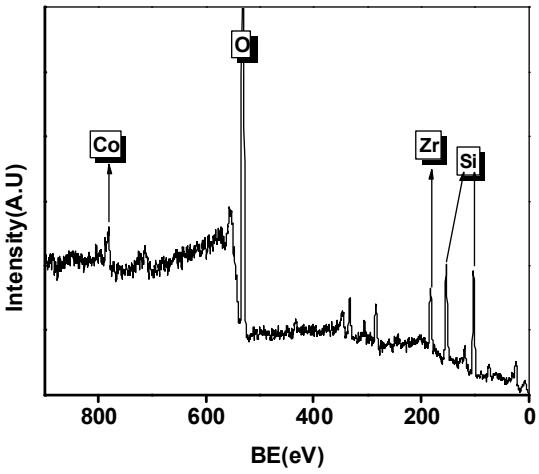

Figure 3. 17 Survey scan XPS of CoZrSiPCH catalysts

The binding energy of Zr 3d $_{5/2}$ at 182.9 eV corresponds to Zr^{4+} attached to oxygen atom and peak at 185.4 eV corresponds to Zr^{4+} attached to OH group. The binding energy of Zr 3d5/2 is higher than that of ZrO_2 (182.2 eV) indicating that the local structure of zirconium is different from that of pure

ZrO_2 and the formation of segregate oxide phase is ruled out [59]. Zirconium exists as Zr^{4+} and it can isomorphously substitute silicon atom in intergallery silica pillars or it can anchor to oxygen atom of intergallery silica frame work.

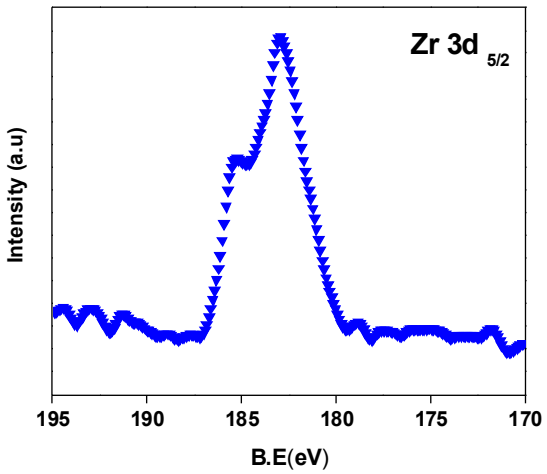

Figure 3.18 core level XPS spectra of Zr in CoZrSiPCH catalysts

The binding energy values of cobalt at 781.4 eV and 796.8 eV are assigned to Co $2p_{3/2}$ and Co $2p_{1/2}$ states respectively with the energy gap of 15.6 eV corresponding to cobalt in +2 oxidation state [60]. The peaks at 786.1eV and 803.4eV are assigned as shake up peaks. The concomitant energy difference (15.0 eV for Co_3O_4, 15.6 eV for CoO) and the line shape make it possible to distinguish between $Co^{2+}$and Co^{3+}[61]. In addition, a shoulder at the high energy side, which can be traced back to a shake-up process, can only be observed with Co^{2+} compounds in the high spin state whereas the diamagnetic low-spin Co^{3+} does not show any shake up peaks [62].

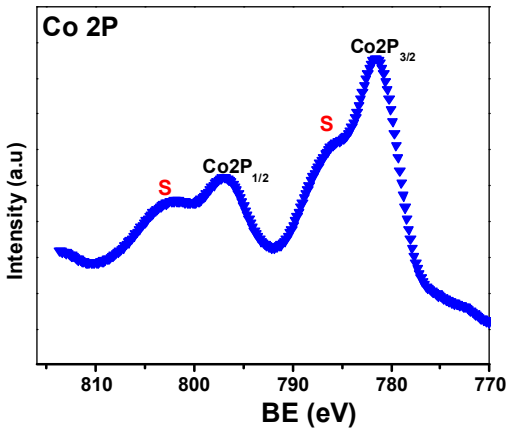

Figure 3.19 Core level XPS spectra of cobalt in CoZrSiPCH catalysts

3.11 Thermo gravimetric Analysis

The heat changes associated with the preparation process and the thermal stability of the prepared catalysts can be understood from thermo gravimetric analysis. Figure 3.20 depicts the TG profile of NaM and uncalcined intercalated clays. The weight loss up to 200°C corresponds to the loss of physisorbed water. The weight loss above 200°C in sodium montmorillonite is as a result of removal of water originating from dehydration of the layers. This structural collapse continues up to 800°C.

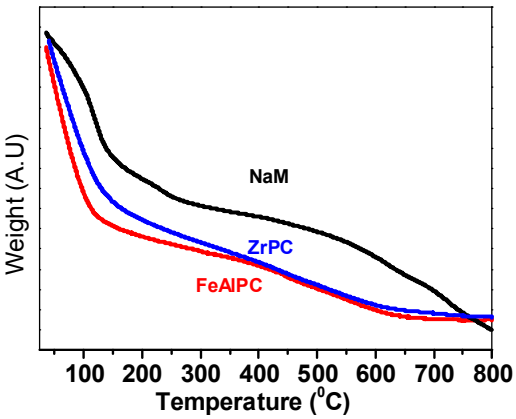

Figure 3.20 TG of PILCs

In intercalated samples the weight loss from 200°C to 400 °C is due to the removal of water from the surface, micro pores and the dehydroxylation of hydroxy metal oligomer or polymers. The new deflection at 400°C is due to the transformation of metal hydroxide in to metal oxide pillars [63]. Not much weight loss above 550°C is observed which indicates the additional stability due to the pillaring process.

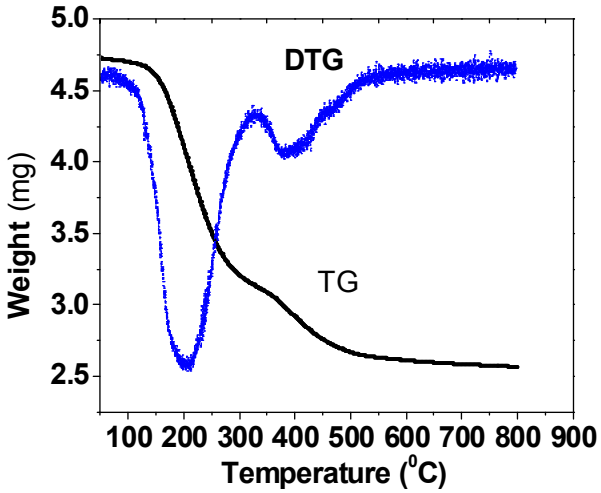

Figure 3.21 TG/DTG of ZrSiPCH

The TG and DTG profiles of uncalcined porous clay heterostructures are shown in Figure 3.21. The weight loss above 200^{0}C is due to the loss of physisorbed water. The weight loss from 200 to 300^{0}C is due to the loss of co- surfactant hexadecyl amine and weight loss in the range 300-500^{0}C may be due to the loss of cationic surfactant CTAB. The weight loss above 500^{0}C is absent in porous clay heterostructure indicating the extra stability of these materials. They have higher thermal stability than pillared clays as reported in literature [64].

3.12 Scanning Electron Microscopy (SEM)

Scanning Electron Microscopic analysis gives idea about the surface topology of the catalysts. The layer structure of clay is evident from SEM pictures. The retention of this structure in the pillared clay suggests that the basic clay layer is unaffected on pillaring. The parent montmorillonite is composed of small flaky particles. Pillaring transforms it in to large discrete particles [65]. Aggregates of silica can be seen in the SEM image of zirconium silicon porous clay heterostructures.

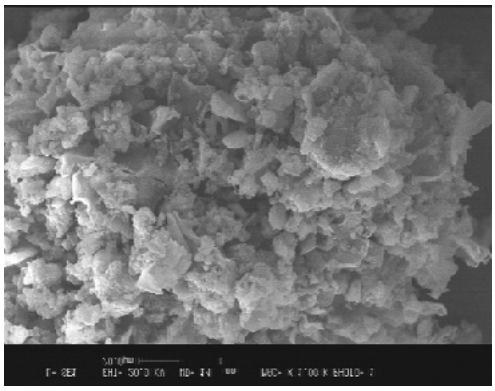

SEM image of NaM

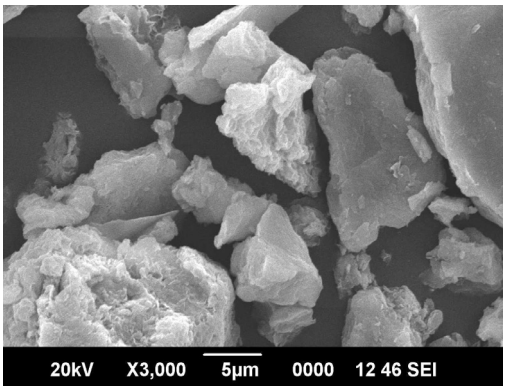

SEM image of ZrPC

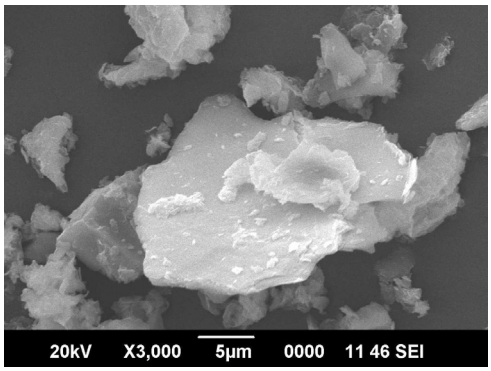

SEM image of Cu(5)ZrPC

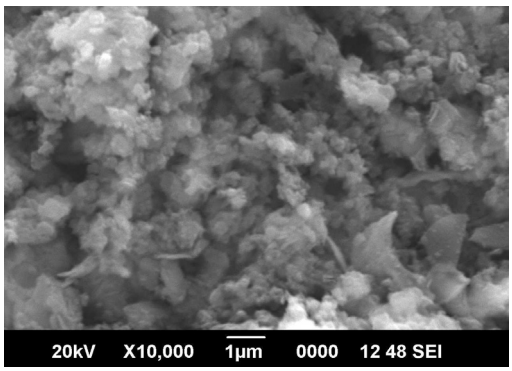

SEM image of ZrSiPCH

Figure 3.22 SEM images of catalysts

3.13 Transmission Electron Microscopy (TEM)

The morphological analysis was also carried out using TEM. Efforts to obtain good resolved TEM images of PCH materials are usually met with limited success [37,66]. The low magnification image shows that the larger particles consist of aggregated domains of several layers oriented in all directions. Although the clay layers have been easily observed, resolving the intragallery pore structure has been more difficult due to the turbostratic nature of clay materials [37]. It can also be seen that the clay layers are discernible as solid dark lines and the pores appear in lighter contrast between the layers.

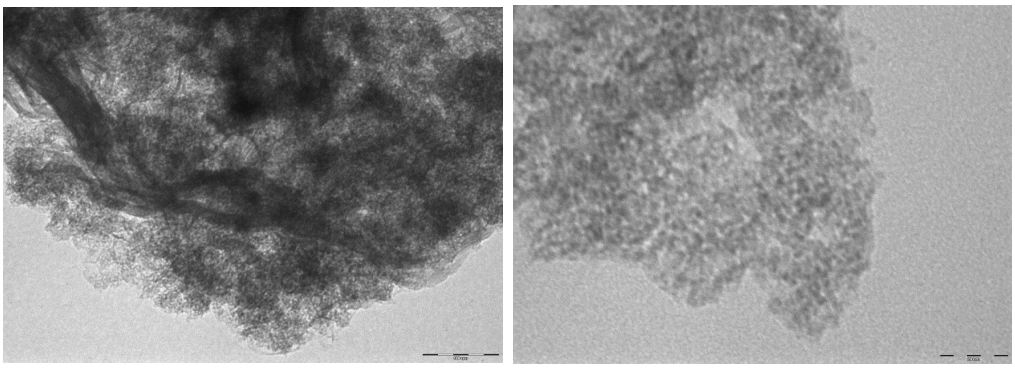

CoZrSiPCH

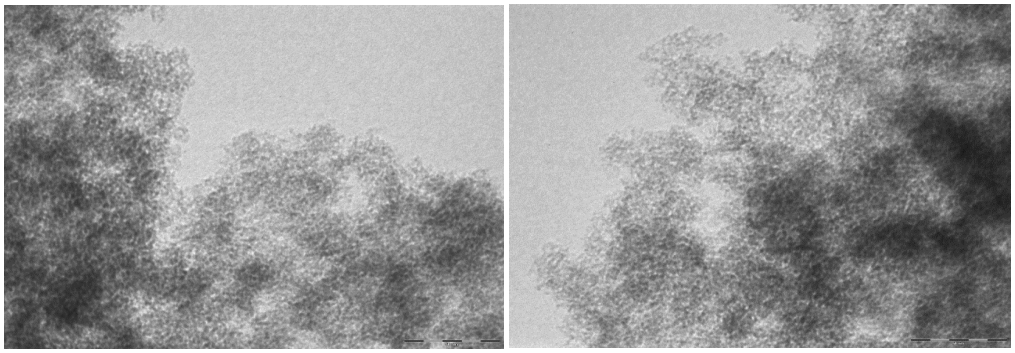

CuZrSiPCH **NiZrSiPCH**

Figure 3.23 TEM image of PCHs

The framework pore orientation is not persistent, indicating a significant degree of disorder within the gallery. Other orientations of the planes reveal wormhole-like morphology at the external surfaces of the clay plates

3.14 Acidity measurements

The nature and strength of various acid sites possessed by heterogeneous catalysts have important role in determining their catalytic properties. The acidic properties of the catalysts were investigated with the help of techniques such as TPD of ammonia and cumene cracking reactions which indicated the existence of both Lewis and Bronsted acid sites on the catalysts.

3.14.1 TPD of Ammonia

TPD of ammonia is widely used for the direct determination of cumulative acidity as well as acid site distribution in solid acids. The small molecular size and strong basicity allow ammonia molecules to adsorb on acid sites located to even very narrow pores. The acidity measurements using TPD of ammonia were done following the procedure described in the section 2.3.13.1. The results of acidity measurements using TPD of ammonia are given in Table 3.7.

Previously, acidity in pillared materials was thought to be of the Lewis acid type resulting mainly from dehydroxylation of the hydrated large interlayer cations [67]. However, when heated, these polyoxycations form oxide clusters and protons, which are retained as charge compensating cations and possibly enhance the Bronsted acidity also [68]. The parent clay has substantial acidity in weak and medium region. As a result of pillaring a drastic increase in acidity in weak, medium and strong acidic region is observed. During the pillaring process the desegregation of clay layer helps in exposing more number of acidic sites and the expansion of layer structure in

pillared clays increases the accessibility of interlayer protons which otherwise obscure to reactant molecules in parent clay due to smaller interlayer distance. In addition metal oxide pillars formed in the interlayer can contribute to the overall acidity of pillared material. In metal loaded pillared clays after the introduction of transition metals the strong acidic sites increases at the expense of weak and medium acid sites. Even though in copper and vanadium loaded zirconium pillared clays, a small increase in acidic sites in the stronger region is observed but their cumulative acidity is decreased. This may be due to the fact that transition metals are coordinated to surface hydroxyl groups in PILCs. This may also be due to the large reduction in surface area of Cu and V loaded catalysts which restrict the accessibility of acidic sites for NH_3 adsorption.

Table 3.7 TPD of ammonia results of catalysts

Catalysts	Weak (mmol/g)	Medium (mmol/g)	Strong (mmol/g)	Cumulative (mmol/g)
NaM	0.249	0.137	0.034	0.420
ZrPC	0.544	0.253	0.126	0.923
Cu(3)ZrPC	0.526	0.236	0.135	0.897
Ni(3)ZrPC	0.567	0.250	0.168	0.985
Co(3)ZrPC	0.528	0.258	0.154	0.940
V(3)ZrPC	0.518	0.248	0.138	0.904
AlPC	0.443	0.308	0.132	0.883
FeAlPC	0.383	0.265	0.103	0.751
Ce(3)FeAlPC	0.368	0.293	0.108	0.769
SiPCH	0.628	0.347	0.038	1.013
ZrSiPCH	0.729	0.365	0.105	1.199
CuZrSiPCH	0.616	0.317	0.132	1.065
NiZrSiPCH	0.749	0.342	0.163	1.254
CoZrSiPCH	0.768	0.358	0.166	1.298
VZrSiPCH	0.738	0.332	0.145	1.215

In the case of porous clay heterostructures the majority of acidic sites are in weak and medium region which can be correlated to Bronsted sites. In porous clay heterostructures, protons are liberated by the decomposition of surfactant molecules during the calcination step and are migrated to layers and contributed to Bronsted acidity [69]. Lewis acid sites are also created in porous clay heterostructures in the gallery region due to the restructuring of silicate layers during calcination at elevated temperatures [70]. Incorporation of zirconium in porous clay heterostructures resulted in improvement in acidic sites in weak, medium and strong acid regions. Incorporation of transition metals improved the acidity in strongly acidic region at the expense of medium acidic sites. This may be due to the consumption of surface hydroxyl groups (Bronsted sites) for anchoring active metal species or masking of surface hydroxyl groups by active metal species. Their cumulative acidity values are greater than that of pillared clays. The cumulative acidity of porous clay heterostructures are in the order SiPCH < CuZrSiPCH < ZrSiPCH < VZrSIPCH < NiZrSiPCH < CoZrSiPCH.

3.14.2 Cumene Cracking Reaction

The cumene cracking reaction was performed over the prepared catalysts as the model reaction for characterizing the acid sites present in the catalysts. Cumene is cracked to benzene and propene over Bronsted acid sites through dealkylation reaction by a mechanism involving cabonium ion intermediate. During cumene cracking, the dehydrogenation leads to the formation of α-methyl styrene which has been ascribed to Lewis acid sites [71]. Dealkylation and side chain cracking also result in the formation of ethyl benzene, toluene and styrene as minor products. Comparisons of the relative amounts of dealkylated and dehydrogenated products provide information

about the relative amount of Bronsted and Lewis acid sites on the catalysts surface [72]. The mechanisms of the cumene cracking reaction over Bronsted and Lewis sites are given in Scheme 3.2a and 3.2b respectively.

Scheme 3.1 Cumene cracking reaction

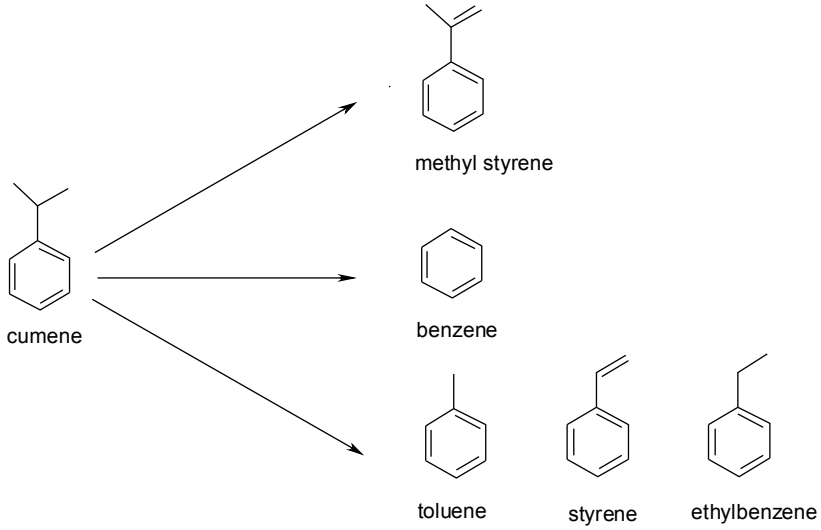

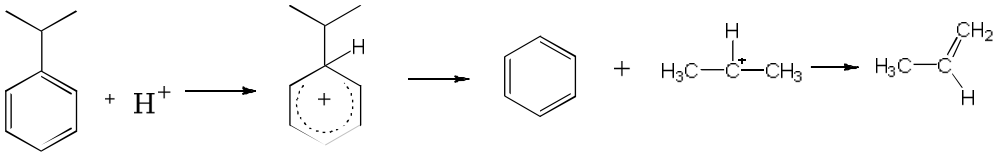

Scheme 3.2a. Dealkylation over Bronsted sites

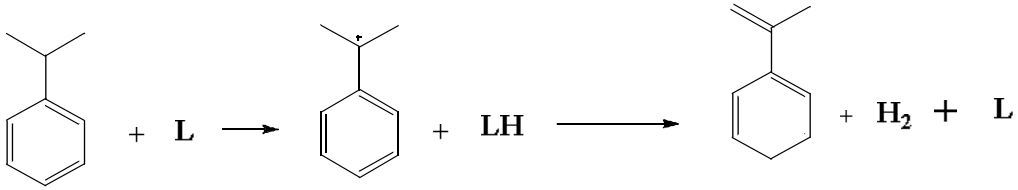

Scheme 3.2b. Dehydrogenation over Lewis sites

Cumene cracking reactions were done in vapour phase mode as the procedure described in section 2.3.13.2 and the results are tabulated in the Table 3.8. From the Table it can be seen that pillared clays predominantly yielded α- methyl styrene as the major product indicating that they possess substantial amount of Lewis acid sites. The conversion of cumene is higher in nickel and cobalt loaded zirconium pillared clays than zirconium pillared clays due to their higher amount of acid sites as evident from TPD of ammonia. But the selectivity for α-methyl styrene is reduced probably due to its lower surface area and pore volume which in turn led to the reduced availability of Lewis sites.

Table 3.8 Results of cumene cracking reaction, Temperature-400°C, Flow rate-4mL/hour, Catalyst amount-250mg, Time on stream-2 hour

Catalysts	Conversion (%)	Selectivity (%)		Lewis/Bronsted acidity Ratio
		α -Methyl styrene	Dealkylated products	
ZrPC	29	63	37	1.70
Cu(3)ZrPC	27	63	37	1.70
Ni(3)ZrPC	43	53	47	1.12
Co(3)ZrPC	38	50	50	1.0
V(3)ZrPC	27	63	37	1.70
FeAlPC	25	65	35	1.85
Ce(3)FeAlPC	26	60	40	1.50
SiPCH	37	30	70	0.42
ZrSiPCH	44	35	65	0.53
CuZrSiPCH	37	40	60	0.66
NiZrSiPCH	54	37	63	0.58
CoZrSiPCH	52	38	62	0.61
VZrSiPCH	46	45	55	0.81

Porous clay hetrostructures showed higher conversion than pillared clays due to their higher surface area and cumulative acidity. Porous clay heterostructures mainly produced dealkylated products indicating that the major acid sites are Bronsted sites. In ZrSiPCH, incorporation of zirconium into intergallery silica frame work led to the enhancement in activity and an increase in conversion and selectivity of α-methyl styrene is noted. This shows that zirconium mainly contribute to Lewis sites. The α-methyl styrene selectivity of zirconium silicon porous clay heterostructures improved up on metal incorporation validating the improvement of Lewis acidity up on transition metal incorporation.

3.15 Conclusions

- Textural and acidic properties of the clays were tuned by pillaring and post pillaring modifications.
- The shift in 2θ value to lower range and increase in d(001) spacing indicate the success of the pillaring process.
- Surface area, pore volume etc increased dramatically as a result of pillaring process.
- Porous clay heterostructures have higher surface area, average pore diameter and narrow pore size distribution than that of pillared clays.
- The adsorption isotherm of PILCs is a blend of type I and IV which corresponds to slit like pores.
- The adsorption isotherm of PCHs material is that of type IV with hysteresis loop H3 corresponding to open cylindrical pores.

- The IR spectrum of PILCs and PCHs are in accordance with literature without much variation compared to parent montmorillonite indicating that basic clay structure is retained even after modification
- The silicon NMR of PCHs materials have intense peak at 108 ppm corresponding to Q^4 environment which indicates that mesoporous silica is incorporated between clay layers
- Thermo gravimetric analysis showed that thermal stability is improved after the pillaring process. PCH materials have higher thermal stability than PILCs
- In metal loaded pillared clays, up to 5% metal species were uniformly dispersed (with the exception of Ni) as evident from XRD and TPR analysis
- Impregnation of transition metals in PILCs and PCHs enhanced acidity of catalyst as evident from TPD of ammonia and cumene cracking reactions.
- For porous clay heterostructures the acidic sites have major contribution from weak and medium sites as evident from TPD of ammonia which can be related to the Bronsted sites.
- Pillared clays got more Lewis acidity than PCHs as inferred from α-methyl styrene selectivity in cumene cracking reaction.
- SEM images show that layer structure is preserved even after modification. Worm hole like morphology is observed in TEM image of PCHs materials

- In ZrSiPCHS, Zr exists as Zr^{4+} and incorporated to silica frame work in the intergallary of clay layers as evident from XPS analysis
- At lower loading in copper loaded zirconium pillared clays, copper exists as isolated species with +2 oxidation state. At higher loading, Cu exists as clusters as evident from reduction peak at higher temperatures in TPR.
- In vanadium incorporated PILCs and PCHs, vanadium exist as isolated V^{5+} in tetrahedral coordination confirmed from TPR and UV-Vis DRS analysis
- In cobalt loaded PCHs, cobalt exists as CoO with 2+ oxidation state as confirmed from XPS.

Reference

[1] D. T. B. Tennakoon, W. Jones, J. M. Thomas, Solid State lonics, 24 (1987) 205.

[2] A. Galarneau, A. Barodawalla, T. J. Pinnavaia, Nature, 374 (1995) 529.

[3] R. Keren, Clays and Clay Miner., 34 (1986) 534.

[4] M. Bejenlloun, P. Cool, T. Linssen, E.F. Vansant, Micropor. Mesopor. Mater., 49 (2001) 83.

[5] R. Tassanapayak, R. Magaraphan, H. Manuspiya, Adv. Mater. Res., 55 (2008) 617.

[6] E. G. Rightor, M. S. Tzou, T. J. Pinnavaia, J. Catal., 130 (1991) 29.

[7] J. Sterte, Preparation of Catalysts, V. G. Poncelet, P. A. Jacobs, P. Grange, B. Delmon (eds), Elsevier Science, Amsterdam, (1991) 301.

[8] E. Booij, J. T. Kloprogge, J. A. R. van. Veen, Appl. Clay Sci., II (1996)155.

[9] A. Gil, L. M. Gandia, M. A. Vicente Catal. Rev-Sci., 42 (1&2) (2000) 145.

[10] S. Yamanaka, G.W. Brindley, Clays and Clay Miner., 27 (1979) 119.

[11] J. T. Kloprogge, J. Por. Mater., 5 (1998) 5.

[12] H. H. Mao, B. S. Li, X. Li, L. W. Yue, Micropor. Mesopor. Mater.,130 (2010) 314.

[13] S. Bracco, P. Valsesia, L. Ferretti, P. Sozzani, M. Mauri, A. Comotti, Micropor. Mesopor. Mater., 107 (2008) 102.

[14] M. Hitipogu, C. Helvaci, S. C Chamberlain, H. Babalik, J. Afr. Earth Sci., 57 (2010) 525.

[15] Y. Hu, L. Dong, J. Wang, Y. Chen, J. Mol. Catal. A: Chem.,162 (2000) 307.

[16] Y. Li, Q. Fu, M. F. Stephalopolous, Appl. Catal. B., 27 (2000) 179.

[17] M. Averbach, Hand book of Layered materials, Marcel Dekker Inc (2004).

[18] F. Bergaya, B. K. G. Theng, G. lagaly, Handbook of clay science, Elsevier (2006).

[19] S. Zuo, R. Zhou, Appl. Surf. Sci., 253 (2006) 2508.

[20] A. Gil, M. Montes, Langmuir, 10 (1994) 291.

[21] S. J Gregg, K. S. W Sing, Adsorption, Surface Area and Porosity; Academic Press: London (1991).

[22] K. S. W. Sing, D. H Everett, R. A. W. Haul, L. Moscou, R. A Pierotti, J. Rouquerol, T. Siemienieweka, J. Pure Appl. Chem., 57 (1985) 803.

[23] F. Rojas, I. Kornhauser, C. Felipe, J. M. Esparza, S. Cordero, A. Dominguez, J. L. Riccardo, Phys. Chem. Chem. Phys., 4 (2002) 2346.

[24] G. P Barrett, L.G Joyner, R. H Halenda, J. Am. Chem. Soc., 73 (1950) 373.

[25] M. L. Occelli, J.V. Senders, J. Lynch, J. Catal.,107 (1987) 557.

[26] L. S. Cheng, R. T. Yang, Micropor. Mater., 8 (1997) 177.

[27] A. Gil, A. Massinon, P. Grange, Micropor. Mater., 4 (1995) 369.

[28] A. Gil, M. Montes, J. Mater. Chem., 4 (1994) 1491.

[29] S. Bodoardo, R. Chiappetta, B. Onida, F. Figueras, E. Garrone, Micropor. Mater., 20 (1998)187.

[30] L. Poppl, E. Toth, I. Paszli, V. Izvekov, M. Gabor, J. Thermal Anal., 53 (1998) 585.

[31] C. Mosser, L. J. Michot, F. Villieras, M. Romeo, Clays Clay Miner., 45 (1997) 789.

[32] J. T. Kloprogge, E. Mahmutagic, R. L. Frost, J. Colloid. Interf. Sci., 296 (2006) 640.

[33] F. Gao, Y. Zhang, H. Wan, Y. Kong, X. Wu, L. Dong, B. Li, Y. Chen, Micropor. Mesopor. Mater., 110 (2008) 508.

[34] D. Plee, F. Borg, L. Gatineau, J. L. Fripiat, J. Am. Chem. Soc., 107 (l985) 2362.

[35] D. T. B. Tennakoon, W. Jones, J.M. Thomas, J. Chem. Soc., Faraday Trans., 182 (1986) 3081.

[36] J. F. Lambert, S. Chevalier, R. Frank, H. Suquet, D. Barthomeof, J. Chem. Soc., Faraday Trans., 190 (1994) 67.

[37] M. Polverejan, T. R. Pauly, T. J. Pinnavaia, Chem. Mater., 12 (2000) 2698.

[38] A. Vinu, D. P. Sawant, K. Ariga, K. Z. Hossain, S.B. Halligudi, M. Hartmann, M. Nomura, J.Chem. Mater., 1*7 (*2005) 5339.

[39] M. Selvaraj, D. W. Park, Micropor. Mesopor. Mater., 138 (2011)101.

[40] E. Gianotti, M. E. Raimondi, L. Marchese, G. Martra, T. Maschmeyer, J. M. Seddon, S. Coluccia, Catal. Lett., 76 (2001)1.

[41] W.G. Su, S.G. Wang, P.L Ying PL, Z.C Feng, C. Li, J. Catal., 268 (2009) 165.

[42] R. A. Schoonheydt, Catal. Rev. Sci. Eng., 35 (1993)129.

[43] P. Katsoulidis, D. E. Petrakis, G. S. Armatas, P. N. Trikalitis, P. J. Pomonis, Micropor. Mesopor. Mater., 92 (2006) 71.

[44] F. E. Trigueiro, C. M. Ferreira, J. C. Volta, W. A. Gonzalez, P. G. P. Oliveria, Catal.Today, 118 (2006) 425.

[45] W. A. Carvalho, P. B. Varaldo, M. Wallau, U. Schuchardt, Zeolites, 18 (1997) 408.

[46] B. Solsona, T. Blasco, J. M. L Neito, M.L Pena, F. Rey, A. V. Moya, J. Catal., 203 (2001) 443.

[47] J. L. Male, H. G. Neisser, A. T. Bell, T. D. Tilley, J. Catal., 194 (2000) 431.

[48] G. V. Shanbhag, T. Joseph, S.B. Halligudi, J. Catal., 250 (2007) 274.

[49] M. Richter, M. J. G Fait, R. Eckelt, E. Schreier, M. Schneider, M. M. Pohl, R, Fricke, Appl. Catal. B, 73(2007) 269.

[50] Y. Dong, X.Niu, Y. Zhu, F. Yuan, H. Fu, Catal Lett., 141 (2011) 242.

[51] W. Tian, S. Guo, L. Shi, Bull. Korean Chem. Soc., 33(2012) 5.

[52] B. Mile, D. Stirling, M. Zammitt, A. Lovell, M. Webb, J. Catal., 114 (1988) 217.

[53] J. Zielinski, Catalysis Lett., 31 (1995) 47.

[54] M. L Pena, A.Dejoz, V Forner, E. Rey, J. M Lopez Niolo, Appl. Catal. A, 209 (2001)155.

[55] Y. M. Liu, Y. Cao, N. Yi, W. L. Feng, W. L. Dai, S. R. Yan, H. Y. He, K. N. Fan, J Catal., 224 (2004) 417

[56] N. Ahmad, S. T. Hussain, B. Muhammad, T. Mahmood, Z. Ali, N. Ali, S. M. Abbas, R. Hussain, S. M. Aslam, Digest Journal of Nanomaterials and Biostructures, 8 (2013) 347.

[57] C. K. Ling, N. A. M. Zabidi, C. Mohan, J. Appl. Sci., 11 (2011)1436.

[58] E. van Steen, G. S. Sewell, R. A. Makhothe, C. Micklethwaite, H. Manstein, M. de Lange and C. T. OConnor, J. Catal., 162 (1996) 220.

[59] D. J. Jones, J. J. Jimenez, A. J. Lopez, P. M. Torres, P. O. Pastor, E. R. Castellon, J. Roziere, Chem. Commun., (1997) 431.

[60] J. B. Li, Z. Q. Jiang, K. Qian, W. Huang, Chinese J. Chem. Phys., 25 (2012) 103.

[61] P. Konova, M. Stoyanova, A. Naydenov, S. Chris-toskova, D. Mehandjiev, Appl. Catal. A., 298 (2006) 109.

[62] M. Vob, D. Borgmann, G. Wedler, J. Catal., 212 (2002) 10.

[63] M. I. Avena, R. Cabrol, C. P. De Pauli, Clays Clay Miner., 38 (1990) 356.

[64] L. Chmielarz, B. Gil, P. Kustrowski, Z. Piwowarska, B. Dudek, M. Michalik, J. Solid State Chem., 182 (2009) 1094.

[65] N. Binitha, Structural tuning of montmorillonite clays by pillaring: designing of shape selective solid acid catalysts, PhD thesis (2006) Cochin University of Science and Technology (2006).

[66] A. J. Tchinda, E. Ngameni, I. T. Kenfack, A. Walcarius, Chem. Mater., 21 (2009) 4111.

[67] M. L. Occelli, 1. Mol. Cat., 35 (1986) 377.

[68] J. M. Lambert, G. Poncelot, Topics Catal., 4 (1997) 43.

[69] A. Galarneau, A. Barodawalla, T. J Pinnavaia, Nature, 374 (1995) 529.

[70] J. Ahenach, P.Cool, E. F. Vansant. Phys. Chem. Chem. Phys.,2 (2000) 5750.

[71] T. Mishra, K. M. Parida, Appl. Catal. A Gen., 166 (1998) 123.

[72] A. Gil, L. M. Gandia, M. A. Vicente, Catal. Rev. Sci. Eng., 42 (2000) 145.

.....ooo.....

Chapter 4

TERTIARY BUTYLATION OF PHENOL

Friedel Craft alkylation is one of the most widely used synthetic tools for the introduction of alkyl groups in aromatics. Generally alkylation reaction is carried out by homogeneous Lewis acid catalysts such as aluminium chloride or Bronsted acid catalyst such as sulphuric acid which pose serious environmental issues. The corrosive nature of traditional liquid phase Friedel Craft catalysts directed major search for green eco-friendly heterogeneous catalysts with high catalytic efficiency. Natural aluminosilicates such as zeolites and clays are solid acids that are particularly promising candidates owing to their intrinsic acidity to substitute liquid acids in chemical transformations. Tertiary butylation of phenol is an industrially important reaction as the alkylated product found profound application in industry. Butylation of phenol reaction is regarded as a model test reaction in order to understand the behavior of solid acid catalysts. Furthermore, the mechanistic aspects developed by several researchers facilitate to understand the reaction pathways which will be helpful to choose the nature of catalysts depending on the kind of product one can look for. Vapour phase alkylation of phenol is done over transition metal impregnated pillared clays and porous clay heterostructures. Reaction parameters are optimized to get maximum conversion. Kinetics of the reaction was studied and kinetic parameters were evaluated.

4.1 Introduction

The alkylation of phenol and substituted phenols is one of the fundamental and industrially important reaction due to the usage of alkylated products in large amounts in the manufacture of antioxidants and phenolic resins [1-2]. Their derivatives found application ranging from pharmaceuticals to pesticides. Aklylation of phenol mainly yield mono alkylated products 2-tertiary butylphenol (2-TBP), 4-teriary butylphenol (4-TBP) and disubstituted product 2, 4 di tertiary butylphenol (2, 4 di-TBP). 4- tertiary butyl phenol is used as raw materials in the production of phenolic resins, synthetic lubricants, antioxidants, polymerization inhibitors, wire enamels, printing inks, lube additives, phosphate ester and fragrances. 2-TBP is an intermediate for pesticides, fragrances and other products. 2, 4-Di-TBP is an intermediate for antioxidants and pharmaceuticals. Numerous attempts have been made to prepare both homogeneous and heterogeneous catalysts for the alkylation of phenols and substituted phenols due to the numerous applications of aklylated phenols.

Alkylated phenols are commercially prepared by reacting phenol with pure isobutylene gas or C4 fraction of naphtha using a liquid acid catalyst, which gives wide product distribution. Both C- and O-alkylations are possible depending on reaction conditions such as temperature, source of isobutylene and type of catalyst. The direct alkylation of phenol with short-chain alcohols and olefins is widely reported for the preparation of these intermediates. In general, tert-butylation of phenols is carried out in a homogeneous medium using sulphuric acid, phosphoric acid, aluminium chloride, boric acid or boron trifluoride as the catalyst [3-5]. The uses of the homogeneous mineral acids are restricted owing to its hazardous nature in addition to the tedious work-up for

the separation of catalyst from the products. Therefore, considerable efforts have been made for the development of suitable heterogeneous solid acid catalysts. Various solid acid catalysts such as zeolite materials, modified mesoporous silica materials, ionic liquids, supported heteropolyacids, polymer resins have been reported for tertiary butylation of phenols in liquid phase as well as in vapour phase with alkyting agent tertiary butanol or methyl tertiary butyl ether (MTBE) [6-8]. Most of the solid acid catalysts reported are active and the most important problem is the selectivity for the desired product. Recently P Selvam et al. reviewed various solid acids used for this title reaction and their reaction conditions and their product selectivity [6].

Depending on the nature of catalyst, alkylation of phenol can take place at oxygen of phenol to produce phenyl ethers (O- alkylation) and /or at ring carbon atoms to produce alkylated phenols(C- alkylation) (Scheme 8.1).

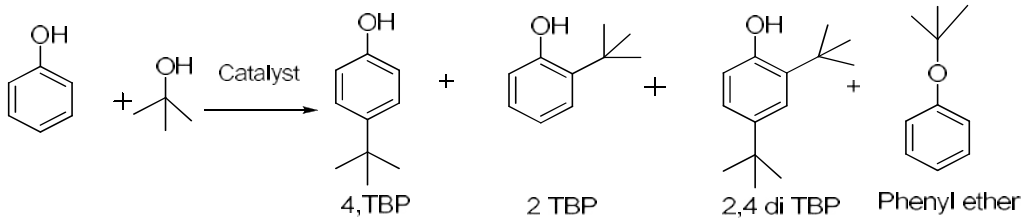

Scheme 8.1- Products of Tertiary butyaltion of phenol

In general, C- alkylation requires strong acid sites than those responsible for O-alkylation. The catalyst react with alkylating agent to form a carbocation which attack on phenol ring preferentially in ortho and /or para position of –OH group according to the rule of electrophilic substitution. Since the monoalkylated products are more reactive than phenol, they get further alkylated if there is no steric hindrance. Although the electrophilic aromatic

substitutions of phenol produce thermodynamically favorable m isomer (3-TBP) the o- and/or p-isomers are kinetically more favored. Though o-isomer is kinetically more favorable than the p-isomer, steric hindrance at o-position leads to easy isomerization of o-isomer to more stable p-isomer. However the selectivity of the products strongly depends on the nature of the acidic sites as well as the reaction temperatures [6].

The use of solid catalysts came in practice as early as 1956 by Kolka et al. by the use of aluminium phenoxide for the liquid-phase alkylation of phenol which yielded 2-TBP is the major product [7]. Since the reaction is acid catalyzed, solid acids such as zeolite H Beta and zeolite Y with high intrinsic acidity and thermal stability were employed for the reaction [8-10]. Corma et al. have first employed zeolite H-Y as a potential catalyst for this reaction and showed that at low temperature, O-alkylated product tertiary butyl phenyl ether (TBPE) and at higher temperature, C-alkylated products were obtained as the major products [8]. However the selectivity of bulky 2, 4 di TBP was very poor due to the small pore diameter in the microporous region (<2 nm). However, the use of large pore zeolites such as H-Y and H-BEA provided more phenol conversion with appreciable 2, 4-di-TBP selectivity [11-14]. Recently hierarchical zeolites were also evaluated for the tertiary butylation of phenol [15-17]. Hierarchical H-ZSM-15 showed very high activity for phenol conversion (85%) with 40% 2, 4-di-TBP selectivity due the presence of hierarchical pore facilitating the formation of 2, 4-diTBP converting *2*-TBP and 4-TBP in to 2, 4 di-TBP [17].

A huge volume of literature is devoted to the vapour phase butylation of phenol over mesoporous silca materials such as MCM-41[18-26], MCM-48 [27-29] and SBA-15 [30-32]. Sakthivel et al. for the first time, studied

vapor-phase tertiary butylation of phenol over H-AlMCM-41[18]. The conversion of phenol varied depending on the reaction conditions with greater than 80% 4-TBPselectivity. At higher reaction temperatures, an increase in thermodynamically favorable 2-TBP product was noticed. Various transition metal ions (Zn, Fe, Co) containing H-AlMCM-41 were also executed for this reaction [19-21]. The main products were found to be 2-TBP. The presence of cobalt in the extra framework of mesoporous materials brings both phenol and isobutyl cation in close proximity and favours the formation of 2-TBP. Studies were also conducted in various trivalent metal ions such as B, Al, Ga, Fe substituted MCM-41 catalysts for tertiary butylation of phenol [22-24]. Tertiary butylation of phenol is also used as model test reaction to understand the nature of acid sites as well acidic strength of various catalysts. A series of H-AlMCM-41 catalyts using various aluminium sources and different aluminium content were evaluated for the title reaction [25-26]. The reaction was executed over trivalent metal substituted Me-MCM-48 (where Me - B, Al, Ga, Fe) catalysts [27-29]. Me-MCM-48 catalysts were found to be superior in activity and selectivity for dialkylated products compared to the corresponding MCM-41 analogues due to three-dimensional pore openings which reduces the deactivation considerably. Recently T. Jiang et al. evaluated sulphated zirconium incorporated MCM-48 for the alkylation of phenol which showed more than 90% conversion [30].

Tertiary butylation of phenol was also reported over various metal modified SBA-15 by various researchers [31-33]. Phenol conversion and 2, 4-di-TBP selectivity is more in these catalysts compared to their MCM-41 analogues owing to their large three dimensional mesopores and strong Bronsted acidity. Various researchers studied vapor phase alkylation of phenol

and substituted phenols over AlSBA-15 [32-33]. They have reported a good phenol conversion with considerable amount of diTBP and 4-TBP selectivity. They also observed decreased conversion at very high temperature due to considerable dealkylation process. Several other mesostructured and disordered metallosilicates were also screened for the title reaction [34-37].

Tertiary butylation of phenol was also reported over sulphated zirconia and sulfated titania which showed good 4-TBP selectivity [38]. Various heteropoly acids loaded on various supports such as ZrO_2 [39-40], alumina [41], APO [42], SBA-15 [43] also were evaluated for the title reaction owing to their high Bronsted acidity. Devassy et al. have studied heteropolyacids silicotungstic acid (STA) and phosphomolybdic acid (PMA) supported on zirconia catalysts for tertiary butylation of phenol [39-40]. STA/$ZrO_2$was found to be more reactive since STA stabilizes the tetragonal phase of ZrO_2. Tertiary butylation of phenol was carried out over MCM-41 supported PTA and rare earth metal triflates in supercritical carbon dioxide showed excellent conversion [45]. Their high reactivity was attributed to the very good solubility of reactants, products and minimal coke formation as coke gets dissolved in supercritical CO_2.

Ionic liquids [46-51] such as 1-butyl-3-methylimidazolium hexa fluorophosphate ([bmim]PF_6)$_3$ and 2-methyl pyridinium trifluoro acetate were appeared to be most promising for tertiary butylation of phenol with high conversion and dialkylated product selectivity. The observed high selectivity of 2, 4-diTBP is attributed to strong acidic nature (Hammett constant around 1.5) of the catalysts [51].

Various cation exchanged resins such as Amberlyst-15, Nafion NR-50, Engelhard F-24, monodispersed K-2661 and p- toluene sulfonic acid (p-TSA)

were used for liquid phase tertiary butylation using MTBE as alkylating agent [52-53]. Alkylation of phenol was done using various other alkylating agents such as mono tertiary butyl ether of mono ethyl glycol (MEG-MTBE), TBA and isobutylene (i-BT) over Amberlyst-15 catalysts [52]. It was found that the overall rate of the reactions depend on the different alkylating agent in the following order i-BT > MEG-MTBE >MTBE > TBA. Density functional theory (DFT) [53-54] studies on the phenol alkylation over Amberlyst-15 catalyst showed that the energy barrier for the C-alkylation is 5-10 kcal/mol higher than that of O-alkylation and it was reduced significantly by protonation. It was also demonstrated that the acidity of the catalyst can control the reaction pathway significantly and the ortho/para ratio could be well controlled by this way.

Clay based catalysts were also reported for the title reaction. G. D. Yadav et al. [55] have employed several phosphotungstic acid loaded montmorillonite (K-10) clay based catalysts for liquid phase tertiary butylation of phenol using MTBE and TBA as alkylating agents. Among them, 20% PTA/K-10 showed better phenol conversion with good 4 -TBP selectivity than K-10 and unsupported PTA owing to easy availability of protons and its blocked pores which induce shape selectivity. Scinde et al. studied liquid phase alkylation of phenol with TBA with $FeCl_3$/K-10 calayst [56]. Sugunan et al. studied tertiary butylation of phenol over ion exchanged pillared clays and showed that incorporation of transition metal in pillared clays resulted improvements in conversion of the phenol [57].

From the above discussion it is clear that the conversion and selectivity of the reaction depends on nature of catalysts, its acidity, textural properties and reaction conditions. Tertiary butylation of phenol was done in vapour phase. The reactor tube was charged with active catalyst sandwiched between

silica beads. The liquid reactants were fed in to reactor by syringe pump and desired temperature is maintained. The products of the reaction were collected downstream from the reactor at specified intervals. The major products of reactions are 2-TBP, 4-TBP and 2, 4-DTBP.Phenyl ether was not detected at all since the reaction was done at high temperature. The reaction conditions are optimized to get maximum conversion.

4.2 Effect of Reaction Parameters

4.2.1 Effect of phenol to tertiary butanol ratio

Reactions were done at different phenol to tertiary butanol ratio and the result is shown in Figure 4.1. The phenol conversion increases with increase in phenol to TBA ratio and maximum conversion is obtained at 1:3 ratio. Further increases in mole ratio do not increase the conversion as it will only dilute phenol. More over there may be competitive adsorption of TBA over phenol

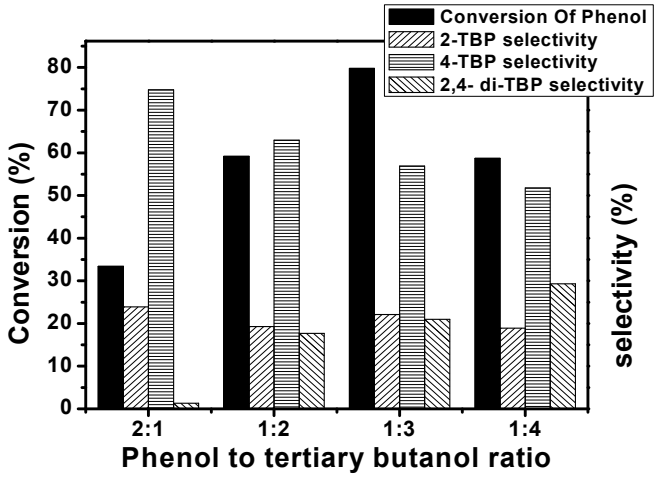

Figure 4.1 Effect of phenol to TBA mole ratio, Temperature - 190^{o}C, WHSV-10.08, Time -2hour, Catalyst-CoZrSiPCH

and only few sites are available for phenol molecule to adsorb and hence conversion decreases [12]. The dialkylated product selectivity increases with increase in TBA ratio in the feed. This may be due to the higher availability of tertiary butanol which results further alkylation of monoalkylated products. Similar results have been found in mono and bimetal substituted MCM-41 molecular sieves [18-24].

4.2.2 Effect of temperature

Reactions were done at different temperature from 160 ^{o}C to 200 ^{o}C and results are shown in Figure 4.2. Reaction temperature has profound influence on conversion and product selectivity. A steady increase in conversion is noted with increase in temperature and conversion reaches maximum at 190^{o}C and then falls. The decrese in conversion at higher temperature may be due to the predominant dealkylation over alkylation and the diminishing availability of TBA. At higher reaction temperatures the formation of undesired products are prominent and they consumes reactants (TBA) without producing the desired products leading to lower phenol conversion. The 4-TBP selectivity increases with temperature. The observed selectivity of 4-TBP is due to the different diffusion kinetics as compared to other products and the absence of secondary alkylation products. Similar trends have been reported for other catalysts also [22-24, 58]. Song et al. explained the preferential formation of 4-TBP as due to different diffusion kinetics with the help of computational modeling [59].The selectivity of 2.4 di- TBP is maximum at lower temperature which may be due to the higher availability and stability of tertiary butyl cation. The 2, 4- di-TBP selectivity decreases with increase in temperature. For further studies 190 ^{o}C is taken as the optimum temperature.

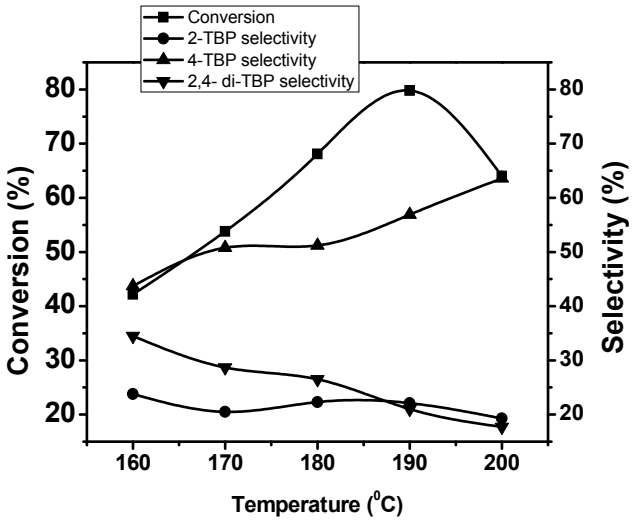

Figure 4.2 Effect of Temperature, Phenol to TBA mole ratio-1:3, WHSV-10.08, Time -2hour, Catalyst-CoZrSiPCH

4.2.3 Effect of flow rate (WHSV)

The flow rate of the reactants greatly influences the reaction rate. Very low contact time (high flow rate) may result in poor reaction as little time is available for the adsorption of the reactants on the catalysts surface, where as high contact time mostly results in undesired products. Hence in order to get maximum conversion and selectivity an optimum flow rate is essential. The reactions were done at various WHSV (Weight Hourly Space Velocity) and result is shown in Figure 8.3. As expected, phenol conversion decreases with increase in WHSV due to shorter contact time with catalysts. Maximum conversion is obtained for WHSV, 10.08. The selectivity of 2-TBP increases with increase in WHSV. The increase of the 2-TBP yield with increasing space velocity has been ascribed to the elimination of inter particle diffusional resistances at higher space velocities [21]. The dialkylated product selectivity decreases with increase in WHSV.

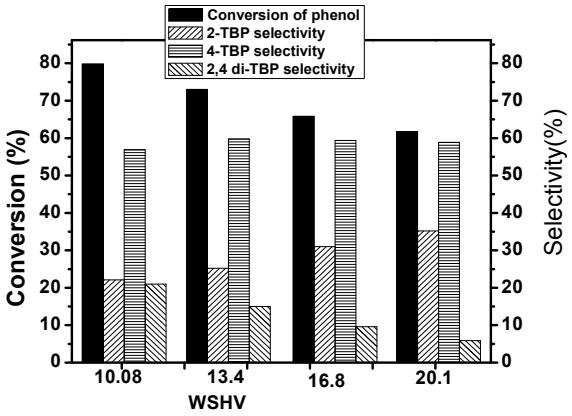

Figure 4.3 Effect of WHSV, Phenol to TBA mole ratio-1:3, Temperature -190^{o}C, Time -2hour,Catalyst-CoZrSiPCH

4.2.4 Effect of time on stream

Maximum conversion is obtained after 2nd hour and the catalysts retain its appreciable activity after several hours. The selectivity of di substituted products increases with progress of the reaction time and then a slight decrease is noted.

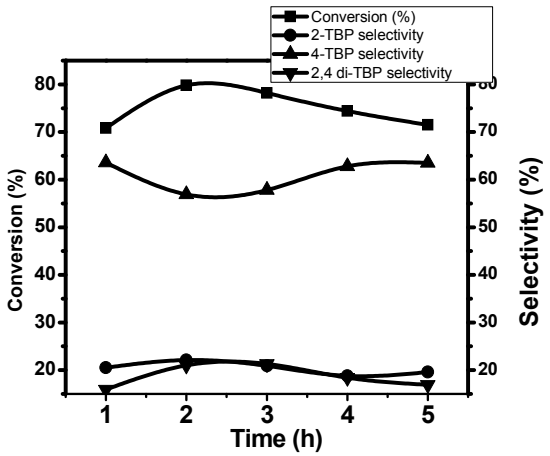

Figure 4.4 Effect of time, Phenol to TBA mole ratio – 1:3, Temperature -190^{o}C, WHSV-10.08, Catalyst-CoZrSiPCH

This may be due to the following reasons. Dialkylated product selectivity is usually correlated with Lewis acidity. The water molecules formed during the reaction convert some of Lewis acid sites into Bronsted sites. Pore blocking due to the formation of coke may also result in reduction in dialkylated product selectivity. From the above experiments it is clear that reaction conditions play a crucial role for obtaining good conversion and selectivity for the products. Vapour phase tertiary butylation of phenol was done over all the prepared catalysts with optimized conditions given in the Table 4.1. The results are given in Table 4.2.

Table. 4.1. Optimized reaction conditions

Parameters	Optimized conditions
Temperature	190^{o}C
WHSV	10.08
Phenol to TBA ratio	1: 3
Time on stream	2 hour

Table 4.2 Performance of different catalysts for tertiary butylation of phenol,

Catalyst	Conversion of phenol (%)	Rate constant ($mol^{-1}l\ min^{-1}m^{-2}$)x 10^3	Selectivity(%)		
			2 -TBP	4- TBP	2, 4- di -TBP
NaM	11	0.291	21	78	1
ZrPC	46	0.852	31	59	10
Cu(3)ZrPC	39	0.905	31	63.	6
Ni(3)ZrPC	56	1.48	32	57.	11
Co(3)ZrPC	55	1.40	28	57	15
V(3)ZrPC	50	1.24	25	65	10
FeAlPC	42	1.21	11	85	4
SiPCH	59	0.452	32	53	15
ZrSiPCH	68	0.628	25	59	16
CuZrPCH	66	0.757	20	63	17
NiZrSiPCH	74.	1.22	26	55	19
CoZrSiPCH	80	0.99	22	57	21
VZrSiPCH	72	0.89	24	59	17

From the results it can be seen that negligible conversion is obtained for unmodified clay with very small dialkylated product selectivity. This lower conversion may be due to lower surface area and pore volume of parent clay. Reasonable conversion of phenol is observed for zirconium pillared clays and its transition metal impregnated analogues. In nickel, vanadium and cobalt loaded zirconium pillared clays conversion of phenol is greater than that of bare zirconium pillared clay probably due to the higher acidity of those catalysts than that of zirconium pillared clay.

In copper impregnated samples conversion of phenol and selectivity of dialkylated product is lower than that of zirconium pillared clay due to its lower surface area and lower acidity than that of zirconium pillared clay. Almost similar dialkylated product selectivity is observed for transition metal loaded zirconium pillared clays with the exception of copper.

The conversion of phenol for the porous clay heterostructures and its transition metal loaded analogues are greater than that of pillared clays and its transition metal loaded analogues. This may be due to the higher total acidity, higher surface area and larger pore size of PCHs than that of pillared clays. The dialkyalted product selectivity is also greater than that of pillared clays. The maximum conversion is obtained for CoZrSPCH catalyst by virtue of its higher total acidity. For the conversion of phenol, PCHs follows the same trend of the conversion of cumene in cumene cracking reaction. The dialkylated product selectivity usually depends on the strong acid sites (Lewis sites). In PCHs the dialkylated product selectivity can be correlated with strong acidity obtained from TPD of ammonia. Such correlation cannot be made in PILCs as pore size limitation play a crucial role for the production of dialkylated products even though PILCs contain sufficient amount of strong acid sites.

4.2.5 Effect of substrates

Alkylation of phenol was done with different alkylating agents and the result is given in Table 4.3. Tertiary butyl bromide shows greater conversion than tertiary butanol probably due to greater polarizing and leaving power of bromide ions compared to -OH. In alcohols tertiary butanol showed higher conversion due to higher stability of its carbocation intermediate.

Figure 4.3 Effect of substrate, phenol to alkylating agent mole ratio-3:1, Temperature -190^{o}C, Flow rate -4ml/hr, Time -2hour

Substrates		Conversion/ selectivity (%)	
Phenol	T- butyl bromide	Conversion of phenol	83
		2- TBP	33
		4- TBP	43
		2, 4- di-TBP	24
Phenol	Isopropanol	Conversion of phenol	64
		2, 4 Di Isopropyl phenol	34
		Isopropyl phenols	66
Phenol	Methanol	Conversion of phenol	58
		Cresols	97
		Anisole	3

4.2.6 Correlation between activity and acidity

Corma et al. found in zeolites that strong acid sites are required for the selectivity of 2, 4 di-TBP and medium sites are helpful in 4-TBP selectivity [8]. In both pillared clays and porous clay heterostructures, the phenol conversion can be correlated with total acidity due to medium and strong acid sites obtained from TPD of ammonia. The dialkylated product selectivity in PCHs can be correlated with strong acid sites obtained from the TPD of ammonia. The conversion of phenol in PCHs can be correlated with the conversion of cumene cracking reaction.

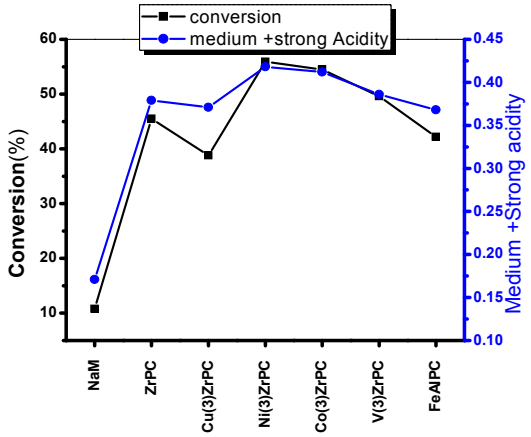

Figure 4.5 Correlation between activity and acidity in pillared clays

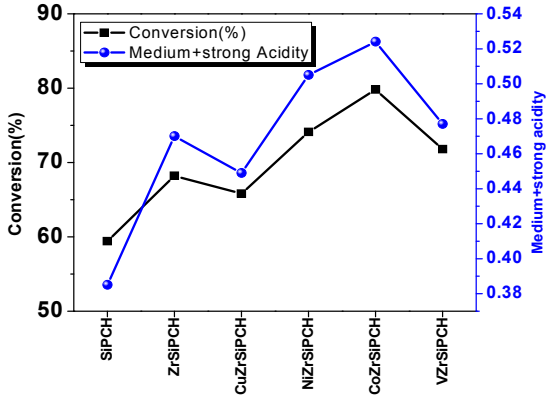

Figure 4.6 Correlation between activity and acidity in porous clay heterostructures

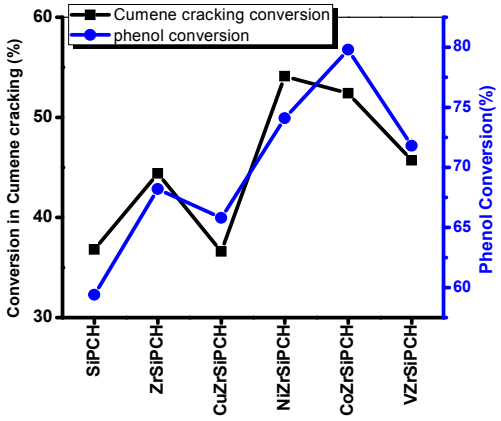

Figure 4.7 Correlation between activity and acidity in porous clay heterostructures

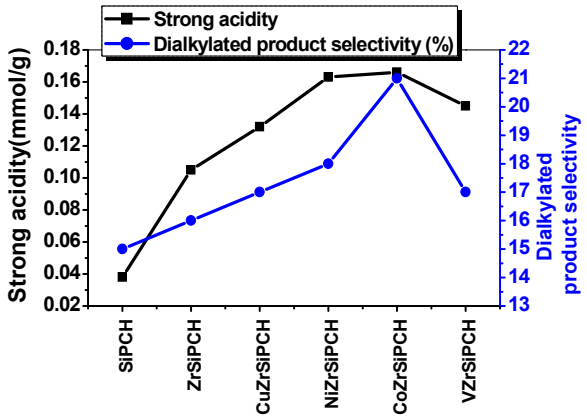

Figure 4.8 Correlation between dialkylated product selectivity and strong acidity in PCHs

4.2.7 Discussion

Generally for alkylation reaction by solid acids, the catalytic activity is controlled by acidity where as the selectivity of the products are controlled by pore structure and acid strength of catalyst. In the present reaction, alkylation of phenol predominantly give para substituted product, 4-TBP.The accepted mechanism for the aromatic alkylation is that both phenol and tertiary carbocation adsorb on acidic sites of catalysts. Then tertiary carbocation interact with adsorbed phenol forming a π- complex by electrophilic substitution which rearranges to give σ –complex. The complex on proton elimination gives tertiary butyl phenol. It has been suggested that the phenol is adsorbed in such a manner that π-electron cloud of aromatic ring is parallel to surface of acid sites. It allows the alkylation at the para position easier compared to ortho positions. In a kinetically controlled heterogeneous catalyzed reactions, both electronic and steric factor play major roles. It is also reported that there is steric hindrance in transition state by the introduction of bulkier tertiary group at ortho positions and isomerization take place to give para selective product.

By carefully choosing reaction conditions one can manipulate the selectivity of the particular product over others. High temperature and low phenol to TBA ratio favor monoalkylated product selectively where as low reaction temperature and high TBA ratio favours dialkyl product. Pore structures of catalyst also have tremendous influence on selectivity. The selectivity of 2, 4 diTBP is high in porous clay heterostructures due to their large pore size.

The activities of catalysts were compared with other catalysts reported in literature and data are given in Table 4.4.

Table 4.4. Tertiary Butylation of Phenol over different reported catalysts

Catalysts	Temp (^{0}C)	Alkylating agent and ratio	Conversion (%)	Selectivity (%)				Ref
				2-TBP	4-TBP	2,4-di-TBP	others	
20%PTA/K10	150	2:1(MTBE)	68	38	38	23	2	55
K10	150	2:1 (MTBE)	52	33	39	25	3	55
$FeCl_3$/K10	150	2:1(TBA)	10	30.5	66.8	2.7		56
Zn/FeAlPC	200	3:1(TBA	51	70.1		29.1		57
H-AlMCM-41	175	1:4(TBA)	47.5	12.8	81	3.7		21
AlMCM -41	175	1;2(TBA)	35.9	8.1	83.4	3.9		60
FeAlMCM-41	200	1:3(TBA	50.1	10.4	75.2	14.4		18
HAlSBA-15	150	4:1(TBA)	86.3	7.0	47	43.9		32
HGaFSM	160	2:1(TBA)	80.3	3.8	49	45.8		62
DTP/SBA-15	150	1:3(TBA)	70.1	6.6	79.2	14.2		43
CoZrSiPCH	190	1:3(TBA)	80	22	57	21		This work

As far as phenol conversion is concerned, the catalyst CoZrSiPCH is best among clay based catalysts with appreciable dialkylated product selectivity. Its conversion is reasonable and promising. Its activity and

selectivity for dialkylated products is comparable or even better than that of metal modified MCM systems. Comparing with modified SBA -15 systems its selectivity for dialkylated products is inferior to them.

4.3 Kinetic studies

Computational studies reveal that both phenol and tertiary butanol adsorb weakly on acid sites of catalyst [61]. Since both reactants are weakly adsorbed on the catalyst surface a second order power law may be formulated [56]. The rate of the reaction can be written as,

$\frac{-dCp}{dt} = k_2.Cp.C_m.W$, where Cp is the concentration of phenol, W- weight of the catalyst, C_m- concentration of alkylating agent.

This is a typical second order equation which on integration gives

$$\ln\frac{(M_R - X_P)}{M_R(1 - X_P)} = Cp_0(M_R - 1)k_2.t.W$$

where Cp_0 - intial concentration of phenol. M_R- the molar ratio of alkylating agent, X_p- conversion of phenol, W- weight of the catalyst, t-time of reaction in minutes.

Thus a plot of LHS against time or 1/WHSV gives a straight line which pass through the origin. The validity of this equation can be checked by plotting $\ln\frac{(M_R - X_P)}{M_R(1 - X_P)}$ against $\frac{1}{WHSV}$ which gives stright line passing through the origin.

The apparent rate constant of the reaction is calculated by the equation and is given in the Table 8.4

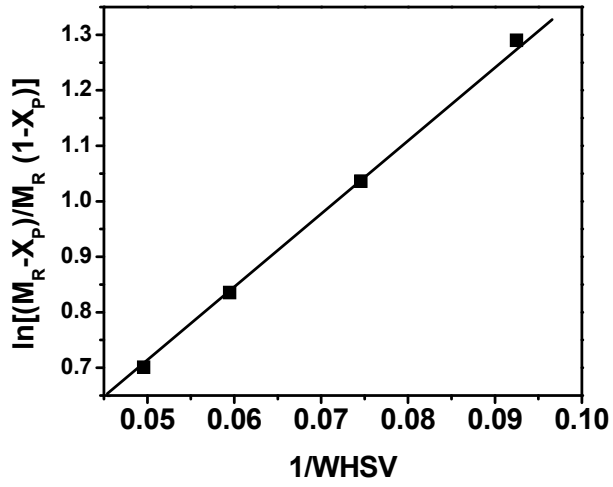

Figure 4.9 Validation of second order kinetics for tertiary butylation of phenol over CoZrSiPCH catalyst

$$\text{Apparent rate constant } k_2 = \frac{2.303}{Cp_0(M_R - 1)t.S.A.W} \log \frac{(M_R - X_P)}{M_R(1 - X_P)}$$

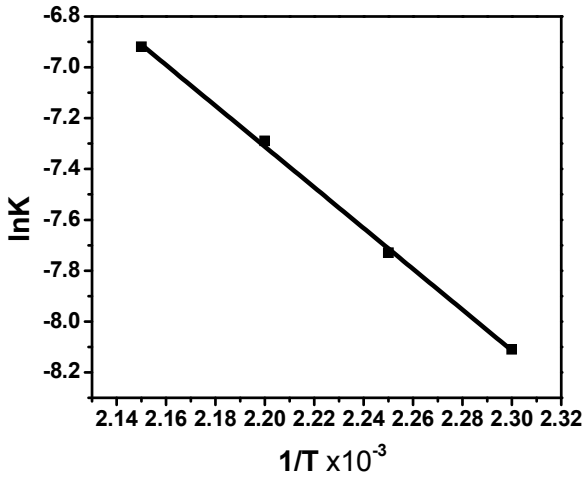

Figure 4.10 Arrhenius plot for tertiary butylation of phenol over CoZrSiPCH catalyst

Arrhenius plot was made as shown Figure 4.10. Kinetic parameters Ea and A were evaluated in the temperature range assuming the diffusion and

mass transfer effects were insignificant. The Enthalpy of activation and Entropy of activation were calculated by the equation.

$$\Delta H^{\dagger} = E_a - n\,RT$$

$$\Delta S^{\dagger} = R\,[\ln A - \ln(kT/h) - n]$$

The kinetic parameters were calculated and are given in Table 8.5

Table 8.5 Kinetic parameters

Kinetic parameters	
Activation energy E_a	66.67 kJ/mol
Frequency factor A	3.06×10^8 (kg of catalyst)$^{-1}$ min^{-1}
Enthalpy of activation $\Delta H^{\dagger}$	61.72kJ /mol
Entropy of activation $\Delta S^{\dagger}$	- 175.57 J/Mol /K

The high value of activation energy indicates that reaction is intrinsically kinetically controlled. The activation energy is within the limit (30-130 kJ/mol) of phenol alkylation reactions reported in literature. The negative value of entropy implies that the reactant molecules are more ordered on the catalyst surface than in vapour phase.

4.5 Conclusions

- Zirconium pillared clays and zirconium silicon porous clay heterostructures effectively catalyze the tertiary butylation of phenol reaction.
- Incorporation of transition metals improves the catalytic efficiency of both pillared clays and porous clay heterostructures except in the case of copper.
- Conversion increases with increase in temperature and maximum conversion is obtained at 190^{o}C. The dialkylated product selectivity decrease with increase in temperature.

- Conversion and dialkylated product selectivity increases with increase in phenol to TBA ratio.
- Conversion decreases with increase in flow rate and maximum conversion is obtained at WHSV 10.08.
- Porous clay heterostructures and its transition metal loaded analogues show higher conversion and dialkylated product selectivity than pillared clays and its transition metal loaded analogues by virtue of their higher surface area, pore size and acidity.
- CoZrSiPCH shows highest conversion with appreciable dialkylated product selectivity. This result is comparable to that of metal modified mesoporous silica materials.
- A good correlation is obtained between conversion of phenol and acidity due to medium and strong acid sites obtained from TPD of ammonia
- Kinetics studies show that the reaction follows second order kinetics. The high value of activation energy implies that reaction is intrinsically kinetically controlled.

References

[1] N. J. L. Megson, Phenolic Resins Chemistry, Academic Press Inc. New York (1958).

[2] J. H. Clark, J. D. Macquarrie, Org. Process Res. Develop., 1 (1997) 149.

[3] A. Knop, L. A. Pilato, Phenolic Resins: Chemistry, Application and Performance-Future Directions, Springer-Verlag, Berlin, Heidelberg (1985).

[4] M. E. Putnam, E. C. Britton, and R. P. Perkins, Method of making tertiary alkyl phenols, U.S. Patent 2039344 (1936).

[5] R. J. Laufer, M. D. Kulik, U.S.Patent 3408 (1968).

[6] P. Selvam, N. V. Krishna, A. Sakthivel, Adva. Poro. Mater., 1(2013)239.

[7] A. J. Kolka, J. P. Napolitano, G. G. Elike, J. Org. Chem. 21., (1956) 712.

[8] A. Corma, H. Garcia, J. Primo, J. Chem. Res., (S) 40 (1988) 1.

[9] K. Zhang, H. Zhang, G. Xu, S. Xiang, D. Xu, S. Liu and H. Li, Appl.Catal. A, 201 (2001) 83.

[10] R. Anand, R. Maheswari, K. Gore, B. Tope, J. Mol. Catal. A., 218(2) (2004) 241.

[11] C. D. Chang, S. D. Hellring, U.S. Patent 5288 (2003).

[12] S. Subramanian, A. Mitra, C. V. V. Satyanarayana, D. K.Chakrabarty, Appl. Catal. A: Gen., 159 (1997) 229.

[13] K. Zhang, C. Huang, H. Zhang, S. Xiang, S. Liu, D. Xu, H. Li, Appl. Catal. A: Gen. 166 (1998) 89.

[14] K. Zhang, H. Zhang, G. Xu, S. Xiang, D. Xu, S. Liu, H. Li, Appl. Catal. A: Gen., 207 (2001)183.

[15] L. Xu, S. Wu, J. Guan, H. Wang, Y. Ma, K. Song, H. Xu, H. Xing, C. Xu, Z. Wang, Q. Kan, Catal. Commun., 9 (2008) 1272.

[16] L. Xu, Y. Ma, W. Ding, J. Guan, S. Wu, Q. Kan, Mater. Res. Bull., 45 (2010) 1293.

[17] Y. Song, Z. Hua, Y. Zhu, J. Zhou, X. Zhou, Z. Liu, J. Shi, J. Mater. Chem., 22 (2012) 3327.

[18] A. Sakthivel, N. Saritha, P. Selvam, Catal. Lett., 72 (2001) 225.

[19] M. Karthik, A. K. Tripathi, N. M. Gupta, A. Vinu, M. Hartmann, M. Palanichamy, V. Murugesan, Appl. Catal. A: Gen., 268 (2004) 139.

[20] R. Savidha, A. Pandurangan, M. Palanichamy V. Murugesan, J. Mol. Catal. A: Chem., 211 (2004)165.

[21] A. Vinu, K. U. Nandhini, V. Murugesan, W. Bohlmann, V. Umamaheswari, A. Poppl, M. Hartmann, Appl. Catal. A: Gen., 265 (2004) 1.

[22] S. K. Badamali, A. Sakthivel, P. Selvam, Catal. Lett., 65 (2000) 153.

[23] A. Sakthivel, P. Selvam, Bull. Catal. Soc. India, 1 (2002) 43.

[24] A. Sakthivel, P. Selvam, Catal. Lett., 84 (2002) 37.

[25] S. K. Badamali, A. Sakthivel P. Selvam, Catal. Today, 63 (2000) 291.

[26] A. Sakthivel, S. E. Dapurkar, N. M. Gupta, S. K. Klushreshtha, P. Selvam, Micropor. Mesopor. Mater., 65 (2003) 177.

[27] S. E. Dapurkar, P. Selvam, Appl. Catal. A: Gen., 254 (2003) 239.

[28] S. E. Dapurkar, P. Selvam, J. Catal., 244 (2004) 178.

[29] S. E. Dapurkar, P. Selvam, Catal. Today, 96 (2004) 135.

[30] T. Jiang, Y. Ma, J. Cheng, W. Liu, X. Zhou, Q. Zhao, H. Yin, Journal of the Association of Arab Universities for Basic and Applied Sciences (2014).

[31] A. Ungureanu, B. Dragoi, V. Hulea, T. Cacciaguerra, D. Meloni, V. Solinas, E. Dumitriu, Micropor. Mesopor. Mater., 163 (2012) 51.

[32] A. Vinu, B. M. Devassy, S. B. Halligudi, W. Bhlmann, M. Hartmann, Appl. Catal. A: Gen., 281 (2005) 207.

[33] W. Shujie, H. Jiahui, W. Tonghao, S. Ke, W. Hongsu, X. Lihong, X. Haiyan, X. Ling, G. Jingqi, and K. Qiubin, Chin. J. Catal., 27 (2006) 9.

[34] R. Anand, R. Maheswari, U. Hanefeld, J. Catal. 242 (2006) 82.

[35] K. Bachari, A. Touileb, M. Touati, O. Cherifi, J. Mol. Catal. A: Chem. 294 (2008) 61.

[36] K. Bachari, R. M. Guerroudj, M. Lamouchi, Reac. Kinet. Mech. Cat. 102 (2011) 219.

[37] P. Srinivasu, A. Vinu, Chem. Eur. J., 14 (2008) 3553.

[38] R. Sunajadevi, S. Sugunan, Catal. Lette., 99 (2005) 3.

[39] B. M. Devassy, G. V. Shanbhag, S. P. Mirajkar, W. Bohringer, J. Fletcher, and S. B. Halligudi, J. Mol. Catal. A: Chem., 233 (2005) 141.

[40] B. M. Devassy, G. V. Shanbhag, S. B. Halligudi, J. Mol. Catal. A: Chem., 247 (2006) 162.

[41] N. Bhatt, A. Patel, J. Taiwan Institute of Chem. Eng., 42 (2011) 356.

[42] K. U. Nandhini, J. H. Mabel, B. Arabindoo, M. Palanichamy, V. Murugesan, Micropor. Mesopor. Mater., 96 (2006) 21.

[43] G. Satishkumar, M. Vishnuvarthan, M. Palanichamy, V. Murugesan, J. Mol. Catal. A. Chem., 260 (2006) 49.

[44] K. U. Nandhini, B. Arabindoo, M. Palanichamy, V. Murugesan, J. Mol. Catal. A: Chem., 223 (2004) 201.

[45] G. Kamalakar, K. Komura, Y. Sugi, Ind. Eng. Chem. Res., 45 (2006) 6118.

[46] H. Y. Shen, Z. M. A. Judeh, C. B. Ching, Tetrahedron Lett., 44 (2003) 981.

[47] H. Y. Shen, Z. A. Judeh, C. B. Ching, Q. H. Xia, J. Mol. Catal. A: Chem., 212 (2004) 301.

[48] P. Elavarasan, K. Kondamudi, S. Upadhyayula, Chem. Eng. J., 166 (2011) 340.

[49] Z. Duan, Y. Gu, J. Zhang, L. Zhu, Y. Deng, J. Mol. Catal. A: Chem., 250 (2006) 163.

[50] M. Hajek, M. T. Radoiu, J. Mol. Catal. A: Chem., 160 (2000) 383.

[51] F. Bigi, M. L. Conforti, R. Maggi, A. Mazzacani, G. Sartori, Tetrahedron Lett., 42 (2001) 6543.

[52] K. G. Chandra, M. M. Sharma, Catal. Lett., 19 (1993) 309.

[53] F. Adam, K. M. Hello, T. H. Ali, Appl. Catal. A: Gen., 399 (2011) 42.

[54] Q. Ma, Deb. Chakraborty, F. Faglioni, R. P. Muller, W. A.Goddard, J. Phys. Chem. A, 110 (2006) 2246.

[55] G. D. Yadav, N. S. Doshi, Appl. Catal. A: Gen., 236 (2002) 129.

[56] A. B. Scinde, N. B. Shrigadi, S. D. Samant, Appl. Catal. A: Gen., 276 (2004) 5.

[57] M. Kurian, S. Sugunan, Catal. Commun., 7 (2006) 417.

[58] R. C. Deka, R. Vetrivel, J. Catal., 174(1998) 88.

[59] C. Song, X. Ma, A. D. Schmitz, H. H. Schobert, Appl. Catal. A, 182 (1999) 175

[60] A. Sakthivel, S. K. Badamali, P. Selvam, Micropor. Mesopor. Mater., 9 (2000) 457.

[61] X. Nie, M. J. Janik, X. Guo, X. Liu, C. Song, Catal. Today., 165 (2011) 120.

[62] K. Bachari, R. M. Guerroudj, M. Lamouchi, Reac. Kinet. Mech. Cat., 102 (2011) 219.

.....ooo.....

Chapter 5

OXIDATION OF PHENOL

Effluents originating from agro industries and food-processing activities usually contain several classes of phenolic compounds that exhibit low biodegradability and increased toxicity. Wastewater effluents which are too dilute to incinerate and yet too toxic to biotreat can be suitably dealt with catalyzed wet oxidation(CWO).The resources with solid catalysts offers a suitable technological alternatives to conventional homogeneously catalyzed or non catalytic routes because the treatments takes place at milder conditions and the catalyst can be easily recovered and reused. Among the catalysed wet oxidations, Wet Peroxide Oxidation (WPO) is the preferred advance oxidation process because the active oxygen content of hydrogen peroxide is higher than other oxidants. Water is the only byproduct formed and the oxidant is inexpensive and aqueous hydrogen peroxide is a stable reagent to handle. Removal of phenol from effluent can be brought about by Wet Peroxide Oxidation at ambient conditions. An added advantage is that the oxidation of phenol produces catechol and hydroquinone, two important intermediate in agrochemical and fine chemical industries. Wet peroxide oxidation of phenol is done over various transition metal loaded pillared clays. Influence of various reaction conditions were thoroughly studied.

5.1 Introduction

Hydroxylation of phenol to dihydroxy products is an industrially important reaction as the products found immense application in various fields. The products, hydroquinone and catechol have been used in large scale as photographic film developer, antioxidant, polymerization inhibitor and used as synthetic intermediate for the production of medicines, perfumes, pesticides etc [1]. The quinone derivatives play an important role in bio-systems and find many miscellaneous industrial applications. More over phenol is considered as one of the most toxic water pollutants, harmful to human health and to water life [2,6]. It is classified as a teratogenic and carcinogenic agent listed in water hazard class two in several countries. Hydroxyl radicals have been effectively applied in the field of environmental remediation of pollutants because of their strong oxidation potential capable of degrading wide range of products. Different Advanced Oxidation Processes (AOPs) have been used to generate the •OH radicals. Among them, the classic Fenton and Fenton-like reagents which contain Fe(II) or Fe (III) in combination with H_2O_2 remain attractive alternatives for the treatment of non biodegradable contaminants such as phenol [3-6]. However, these systems are seriously affected by the typical drawback of homogeneous catalysis such as separation, regeneration and also by ineffective consumption of oxidant H_2O_2. Fenton reaction uses a high concentration (normally >10 mg/L) of iron that must subsequently be removed and can result in sludges. Additionally, it requires acidic conditions, typically below pH 3.0, which is unfavorable in practice because of the costs of acidification during processing and neutralization after treatment.

Thus, different Fenton-like heterogeneous catalysts which can operate under less acidic conditions have been developed by immobilizing transition

metal cations such as copper, iron, titanium, vanadium etc on adequate supports such as silica, zeolites, pillared clays, activated carbon, polymers, resins etc. However, depending on the chemical composition and preparation method, these catalysts often show considerable difference in phenol conversion or in product selectivity due to the heterogeneous distribution of the metal species both inside and outside the framework of molecular sieves. They can be dispersed inside the framework as isolated and clustered metal-oxygen units or on the surface as the metal-oxygen clusters with different nuclearity.

A series of heterogeneous catalysts such as TS-1, Ti-MWW, metal oxides, heteropoly compounds have been reported for the hydroxylation of phenol from both fundamental and industrial standpoints [7–11]. Titanium Silicate (TS-1), a titanium containing zeolite was found to be superior to other catalyst for phenol hydroxylation due to the decreased formation of tar and polluting bye products and subsequently the method was commercialized. The extent of phenol hydroxylation over TS-1 is determined by pore geometry, external surface Ti sites and the nature of solvent. Phenol hydroxylation is found to be diffusion limited as hydroquinone was formed inside the zeolite channels where as catechol was formed out in external surface. Though TS-1 is an excellent catalyst, their industrial applications were limited by lack of thermal stability, complex preparation procedure and higher cost.

Fe-containing molecular sieves, such as Fe-containing zeolite, Fe-ZSM-5 [12] ferrisilicate [13], Fe-containing mesoporous silica such as Fe-MCM-41 [14], Fe-MCM-48 [15], Fe-SBA-15 [16], Fe_2O_3 supported alumina [17] and FeALPO [18] were recently reported in literature which showed high catalytic performance for the oxidation of phenol using H_2O_2 as oxidant. Iron immobilized

on supports such as activated carbon [19-23], carbon aerogels [23-24] and carbon nanotubes [25] were also reported for phenol oxidation. Recently a core shell catalyst Pd/SiO_2@Fe-MS in which Pd/SiO_2 core covered with iron containing mesoporous silica shell (Fe-MS) was successfully employed for insitu generation of H_2O_2 form H_2 and O_2 and one pot hydroxylation of phenol [26]. Pillared clay containing iron oxide pillars such as iron pillared clay [27] iron containing silicon pillared clay (Fe-SPC) [28] and mixed pillared clay such as Fe-Al pillared clays [29-32] were successfully employed for the removal of phenolic compounds in water combining good catalytic activity with high stability against iron leaching.

In the recent decade, the copper-modified molecular sieves, such as CuAPO-11 [33], Cu/Y[34], Cu/ZSM-5[35], CuO/MCM-48 [36] , Cu/MCM-41 [37-38] , Cu/HMS[39], CuSBA-15 [40], Cu containing LDHs etc. have also been showed to be excellent catalysts for the hydroxylation of phenol. A novel Cu-Bi-V-O complex was found to be very active for phenol hydroxylation in which the active species is Cu^{2+} investigated by ESR spin trapping technique [41]. Santos et.al explored the reaction using for copper bearing commercial catalyst and found that hydroxyl radicals are major reaction intermediates [42]. Wang et al. reported that not only the isolated Cu^{2+}species but also a small amount of clustered Cu^{2+}species is necessary to improve the product selectivity while the clustered copper ions are thought to be inactive in the oxidation of the aromatic ring, but accelerate the nonproductive decomposition of hydrogen peroxide[40]. In copper doped aluminium pillared clays, Cu exists either as isolated Cu^{2+} ions anchored in to aluminium pillars or as patches of amorphous CuO and the yield of diphenols was almost near to commercial TS-1 catalyst [43]. Barrault et al. employed mixed Al-Cu pillared clay for the

title reaction in milder reaction conditions and found a complete heterogeneous reaction rather than homogeneous Fenton like oxidation [44]. Wide range of other catalysts such as molybdovanadophosphoric acid modified zirconia [45], vanadium silicate with MEL structure [46], VS-2[47] etc. have also been employed for phenol hydroxylation.

Pillared clays like titanium [48,51], zirconium [49], iron [27] and mixed pillared like Fe-Zr [50], Fe-Al [28-32], Al-Cu [44] were successfully employed for phenol hydroxylation. Boundali et al. proposed the availability of Bronsted sites for better performance of the catalyst [51]. Metal loaded pillared clays by virtue of redox properties of metals were found to be very good catalyst for oxidation reaction especially for phenol hydroxylation reaction [32,44]. An extensive literature can be found regarding the use of pillared clays in CWPO since this type of solids are among the favorite catalysts to promote Fenton oxidation of organic compounds. Recently several authors have reviewed the use of pillared clays for heterogeneous Fenton [52], photo-Fenton [53], Fenton like reactions [54]. Most of the work focused on the complete oxidation of phenol in long hours (usually very low concentration of phenol in the range of 10^{-4} or 10^{-3} M) where phenol removal was estimated in terms of TOC. Here hydroxylation of phenol was done over various metal loaded pillared clays and porous clay heterostructures in aqueous media. Our interest was to convert phenol in to useful product than complete oxidation.

The liquid phase hydroxylation of phenol was carried out over prepared catalysts as the procedure described in section 2.4.2. Quantitative estimation of tarry products was not pursued and conversion of phenol refers conversion to dihydroxy phenols. Thus the percent conversion (wt%) of phenol is the total

percentage of phenol transformed in to diphenols. The effect of various reaction parameters were studied and optimized to get maximum conversion.

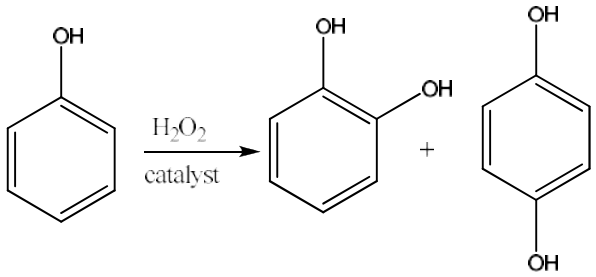

Scheme 5.1 Oxidation of Phenol

5.2 Effect of Reaction Parameters

5.2.1 Effect of reaction time

The effect of time on reaction rate was studied and result is given in Figure 5.1. For iron containing pillared clays such as Ce(3)FeAlPC, after an induction period of about 5 minutes reaction occurs violently and a good conversion is obtained even after ten minutes. The induction period may be as the result of the time required for surface activation of the condensed phase [55]. Some researchers relate it to the time required for the adsorption of reactant onto the catalyst surface [56]. Conversion increases with time and maximum conversion was observed at 45 minutes and then conversion drops. For transition metal loaded zirconium pillared clays and porous clay heterostrutures conversion increases steadily with reaction time and maximum conversion was obtained after 75 minutes and then conversion falls. This change in activity pattern may be attributed to poisoning of surface sites by reaction products. Tar produced by over oxidation of diphenol is a major poison for active sites.

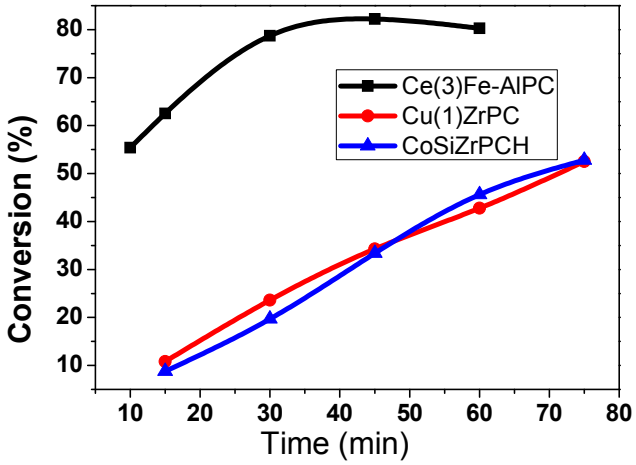

Figure 5.1 Effect of time on conversion, Temperature -70°C, phenol-1 mL,phenol: water: H_2O_2 =1:5:5 (volume ratio), catalyst-100 mg

The selectivity of hydroquinone improves with time. It has been reported in zeolites and molecular sieves that hydroquinone is formed inside the pores [7]. As time goes by more reactant molecules diffuse in and out of the pores leading to increased hydroquinone selectivity.

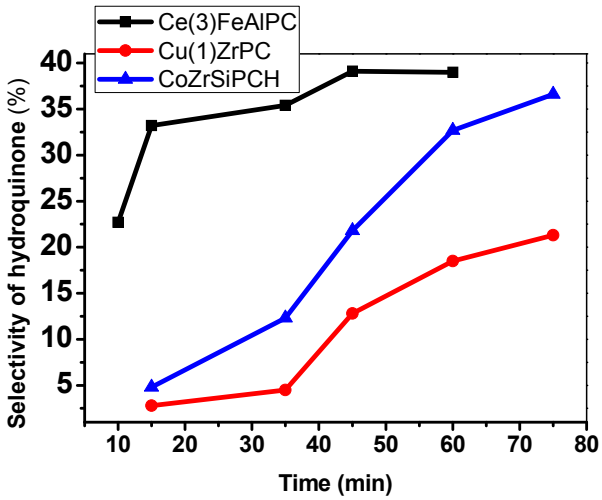

Figure 5.2 Effect of time on selectivity, Temperature -70°C, phenol-1 mL, phenol: water: H_2O_2 =1:5:5 (volume ratio), catalyst-100 mg

5.2.2 Effect of temperature

The effect of temperature on reaction rate was studied in the temperature range from 50°C to 80°C and the result is given in Figure 5.3. The reaction rate increase with increase in temperature. Maximum conversion is observed at 70°C. Partially miscible phenol and water mixture forms a homogeneous solution above its Critical Solution Temperature. Above 70°C the conversion falls due to decomposition of hydrogen peroxide as reported by many researchers [45,57-58]. As in the case of earlier reports, low temperature favors high yield of hydroquinone but its selectivity suffers with raise in temperature [32].

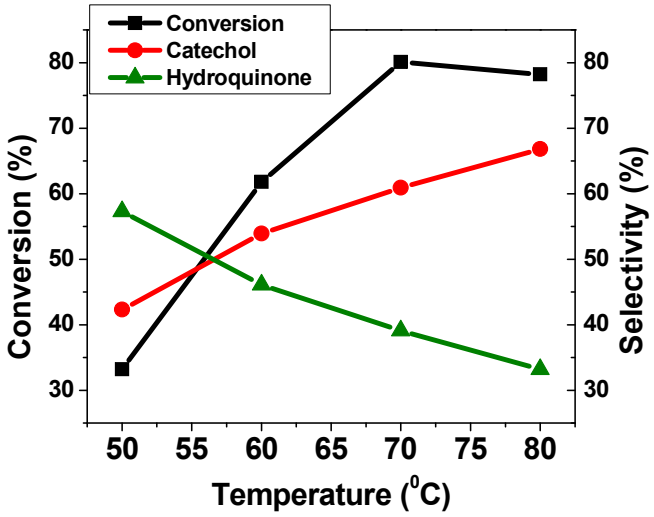

Figure 5.3 Effect of temperature on conversion, Time -45 minutes, Catalyst-100 mg, Catalyst-Ce(3)FeAlPC, phenol-1 mL phenol :water: H_2O_2 -1:5:5 (volume ratio)

5.2.3 Effect of catalyst amount

A minimum catalyst amount is required for an easy occurrence of reaction. From the Figure 5.4, it can be seen that phenol oxidation increases with increase in catalyst amount up to an optimum level and then it drops. The

increase in number of active sites in concurrence with increase in catalyst amount accelerates the decomposition of hydrogen peroxide. At higher catalyst loading, there is also chance for the adsorption of products to the active sites which also leads to lower conversion. It is reported that the excess of catalyst has no benefit on phenol hydroxylation and large excess of catalyst may reduce the yield to great extent [59].

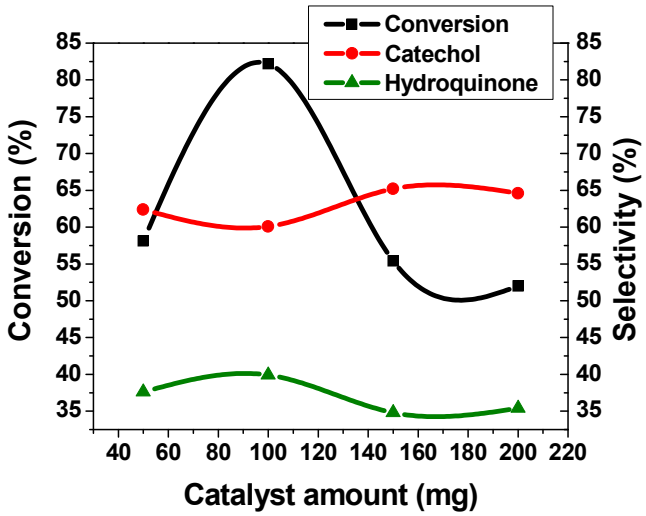

Figure 5.4 Effect of catalyst amount, Temperature-70°C, phenol-1 mL, phenol: water: H_2O_2 =1:5:5 (volume ratio), Time-45 minutes, Catalyst-Ce(3)FeAlPC

5.2.4 Effect of solvent

Hydroxylation of phenol is carried out in various solvents such as isopropanol, dioxane, acetonitrile and water and the result is given in Figure 5.5. The conversion was very low for organic solvents. However, high selectivity of hydroquinone was observed for the solvent dioxane.

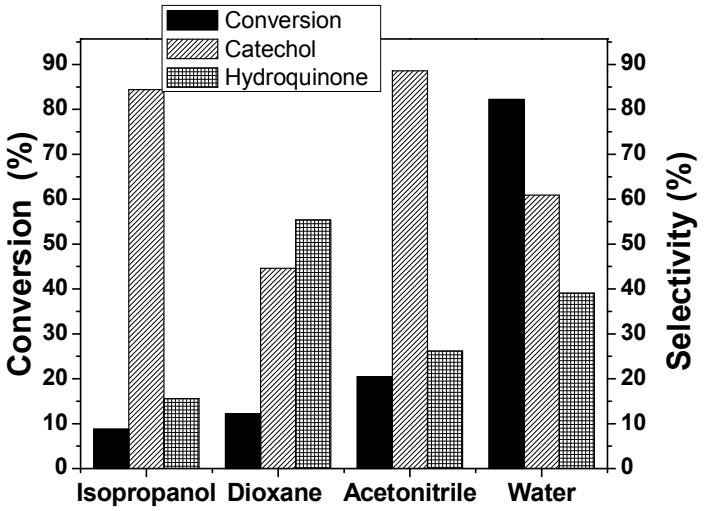

Figure 5.5 Effect of solvent on conversion, Temperature-70°C, catalyst-100 mg, phenol-1 mL, phenol : solvent : H_2O_2 = 1:5:5 (volume ratio), Catalyst-Ce(3)FeAlPC

A change from organic solvents to water led to a significant increase in phenol conversion which indicates that water is the best solvent for phenol hydroxylation. This may be attributed to the fact that phenol and H_2O_2 reach the active sites more easily in water than other organic solvents. At the same mole fraction, the activity coefficient of phenol is much higher in water than other solvents [60]. More over heterogeneous Fenton type mechanism is operated well in aqueous medium than organic solvents. One of the most interesting aspect for water as solvent is that it is safe, cheap, green and environmental friendly. So the reaction can be extended for the removal of phenolic compounds in waste water stream.

5.2.5 Effect of phenol concentration

The influence of the amount of phenol on reaction was studied by varying the amount of phenol and keeping the amount of water and H_2O_2 as constant. The observations are given in Figure 5.6

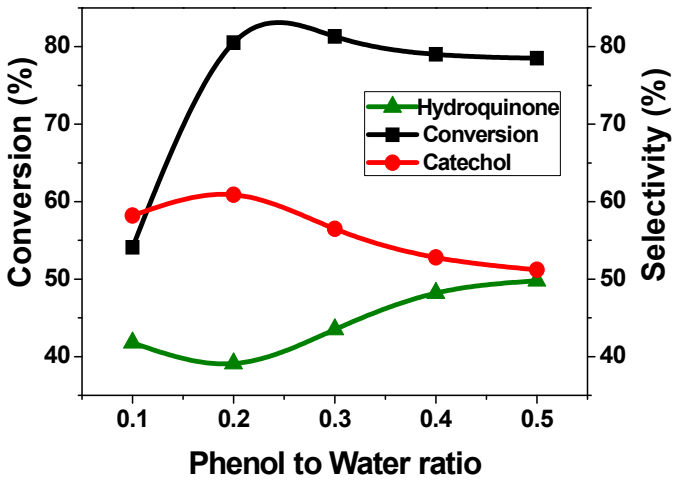

Figure 5.6 Effect of phenol concentration, Temperature-70°C, Time-45 minutes, H_2O_2-5 mL, Water-5 mL, Catalyst-100 mg, Catalyst-Ce(3)FeAlPC

From the Figure it can be inferred that a minimum phenol concentration is required for the good conversion. The reaction rate increases with increase in phenol concentration and after an optimum level rate falls. At low concentration of phenol, due to the flooding of solvent molecules, phenol molecules cannot approach active sites which leads to reduced conversion. At higher concentration of phenol, there may not be sufficient number of active sites for all the molecules to react and the decrease in conversion is observed due to the fact that conversion is calculated as weight % of phenol reacted. Hydroquinone selectivity increases steadily with increase in amount of phenol. Increase in concentration of phenol increase the rate of diffusion of reactants in to the pores and the selectivity of hydroquinone increases.

5.2.6 Effect of oxidant ratio

The effect of oxidant amount on phenol hydroxylation reaction was studied by varying the phenol to oxidant (30 % H_2O_2) ratio from 1:3 to 1: 8 (volume ratio). Phenol oxidation increases with increase in oxidant concentration and reaches maximum at phenol to oxidant ratio of 1:6 after that conversion decreases. The rate of deep oxidation of diphenols to tar is prominent in higher concentration of H_2O_2.The self decomposition of H_2O_2 is also high at high concentration of oxidant which also leads to low conversion. Catechol selectivity decreases and hydroquinone selectivity increases with increase in oxidant amount.

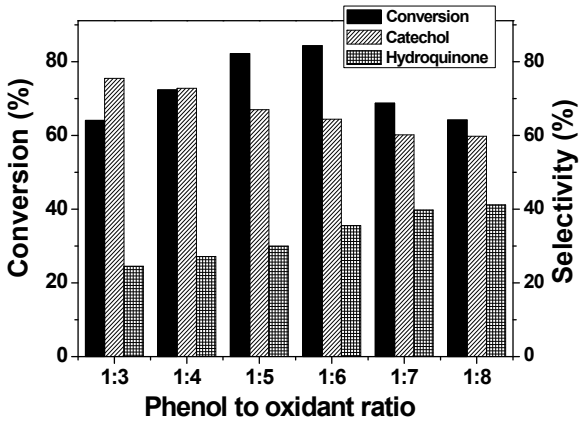

Figure 5.7 Effect of phenol to oxidant ratio, Temperature-70^{o}C, Time-45 minutes, catalyst-100mg, phenol-1 mL, Water-5 mL, Catalyst-Ce(3)FeAlPC

5.2.7 Effect of catalysts

The hydroxylation of phenol was done over prepared catalysts in aqueous media and the results are given in Table 5.1 and Table 5.2

Table 5.1 Oxidation of phenol, Temperature -70°C, Phenol-1 mL, phenol:water: H_2O_2 -1:5:5 (volume ratio), Catalyst-100 mg, Time-45 min

Catalysts	Conversion of phenol (%)	Selectivity	
		Catechol	Hydroquinone
NaM	36	79	21
AlPC	63	67	33
FeAlPC	69	67	33
Ce(3)FeAlPC	82	61	39

Table 5.2 Oxidation of phenol, Temperature -70°C, phenol -1 mL, phenol: water: H_2O_2 -1:5:5 (volume ratio), Catalyst-100 mg, Time-75 min

Catalyst	Conversion of phenol (%)	Selectivity (%)	
		Catechol	Hydroquinone
ZrPC	47	72	28
Cu(1)ZrPC	53	79	21
Cu(3)ZrPC	50	83	17
Cu(5)ZrPC	45	82	18
Ni(1)ZrPC	59	73	27
Ni(3)ZrPC	61	74	26
Ni(5)ZrPC	47	79	21
Co(3)ZrPC	57	75	25
Co(5)ZrPC	55	76.	24
V(3)ZrPC	57	82	18
V(5)ZrPC	65	85	15
SiPCH	25	61	39
ZrSiPCH	43	65	35
CuZrSiPCH	48	68	32
NiZrSiPCH	50	71	29
CoZrSiPCH	53	63	37
VZrSiPCH	51	73	27
Nil	4	82	18

Sodium montmorillonite itself shows some activity due its iron content and intrinsic acidity. It can be seen that conversion increased to more than two times in aluminium pillared clays due its high surface area, acidity and more accessibility of active iron species than that of sodium montmorillonite. Phenol hydroxylation is strongly diffusion limited and it was believed that hydroquinone is formed inside the pores and catechol and other products were formed in external surface [7]. FeAlPC showed higher conversion than AlPC due to higher iron content and higher surface area and pore volume. The incorporation of cerium in pillared clays led to enhancement in conversion of phenol and selectivity of hydroquinone. Cerium impregnated iron aluminium pillared clay got more than 80 % conversion of phenol within 45 minutes. This may be due to the promoting effect of ceria, its redox property and additional surface area provided by the ceria mesopores. The Fenton type behavior of ceria and the promoting role of cerium in iron based catalysts systems were studied by various researchers [61]. Cerium species played two roles in this model reaction. First, as a widely used promoter in redox reactions, the introduction of ceria could efficiently improve the diphenol distribution. Hydroquinone selectivity is slightly raised after the incorporation of cerium. Cerium forms a metaloxo peroxide species [62] which react with phenol to form hydroquinone rather than catechol.

Even though zirconium pillared clays have higher surface area and total acidity than aluminium pillared clay, they showed lower phenol conversion than aluminium pillared clays. This may be due to the lower amount of active species iron. Conversion improved upon transition metal loading. Conversion increases with increase in metal content up to 3 % with the exception of copper and vanadium. In copper loaded zirconium pillared clays, 3% Cu loaded pillared

clays showed lower conversion than that of 1% Cu loaded zirconium pillared clay probably due to large decrease in surface area and nonproductive decomposition of H_2O_2 over active sites. The nature and dispersion of metal have tremendous effect on oxidation reaction and it was reported that isolated metal species rather than clusters have high potential for oxidation reaction. Huge amount of transition metal loading will not contribute significantly to conversion instead nonproductive decomposition of H_2O_2 is resulted over metal oxide clusters. Ni(5)ZrPC showed lower conversion than that of Ni(3)ZrPC due to lower surface area and probably due to the decomposition H_2O_2 over NiO clusters whose presence was confirmed from XRD and TPR analysis. V(5)ZrPC showed higher conversion since it contains only isolated vanadium species as confirmed from TPR analysis. The selectivity for hydroquinone in iron aluminium pillared clay is greater than that of transition metal loaded zirconium pillared clays due to higher surface area and pore volume. The selectivity of hydroquinone decreases with increase in metal content due to the increase in hindrance of reactant molecules to enter the pore due to pore blocking.

Silicon porous clay heterostructures showed less conversion than that of sodium montmorillonite due to its higher hydrophobicity [63]. Incorporation of zirconium and transition metals improved conversion due to the redox nature of metal species incorporated, increase in acidity and increase in hydrophilicity. Hydroquinone selectivity is higher in zirconium silicon porous clay heterostructures and its transition metal loaded analogues than zirconium pillared clays and its transition metal loaded catalysts owing to its higher pore size. Cobalt incorporated zirconium silicon porous clays showed maximum activity due to their higher surface area and higher strong acid sites.

5.2.8 Correlation between acidity and activity

Though acidity is not an important factor for oxidation reactions, several reports were available in literature suggesting the participation of acid sites in hydroxylation of phenol [48, 51]. In pillared clays the conversion is correlated with total acidity obtained from TPD of ammonia. Figure 5.8 shows the correlation of activity with acidity in pillared clays. In the case of transition metal incorporated zirconium pillared clays a good correlation was obtained. The amount of iron and its redox property play a crucial role rather than acidity in aluminium and iron aluminium pillared clays.

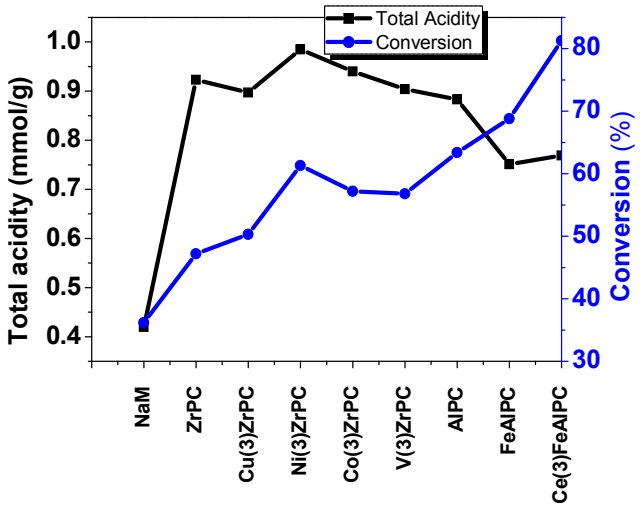

Figure 5.8 correlation between acidity and activity in pillared clays

In the case of porous clay heterostructures correlation can be made with conversion and strong acidity obtained from TPD of ammonia and is shown in Figure.5.9.

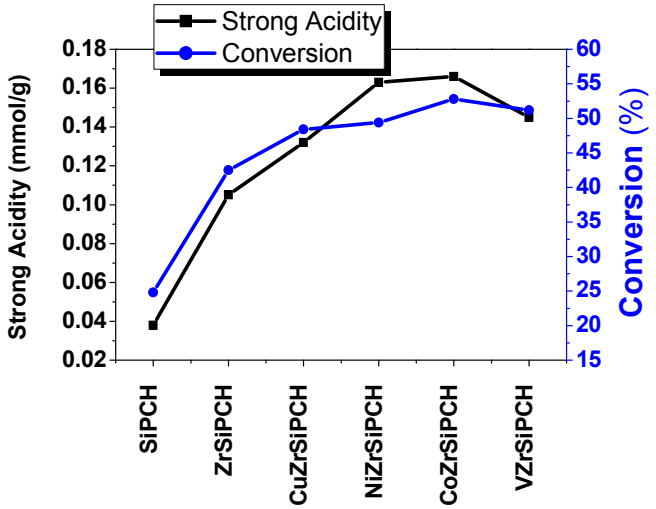

Figure 5.9 Correlation between acidity and activity in porous clay heterostructures

5.2.9 Reusability studies

The advantages of heterogeneous catalysis include the easy separation of catalysts from the final reaction mixture and subsequent reusage of the catalysts. To study the reusability, the catalysts were removed from the reaction mixture after the reaction by filtration. It was thoroughly washed with acetone and dried in an air oven and activated for 3 hours at 400^{o}C.The same catalyst was used again for carrying out another reaction under the same reaction conditions. It can be seen that the catalyst retains its activity even after 4th cycle. The selectivity of hydroquinone decreases after each cycle. This may be due to pore blockage by tary products.

Table 5.3 Reusability studies of oxidation of phenol over Ce(3)FeAlPC

Cycle	Conversion Of phenol (%)	Selectivity (%)	
		Catechol	hydroquinone
2	79	64	36
3	77	73	27
4	72	78	22

Temperature -70^{o}C, Phenol-1 mL, phenol: water: H_2O_2 -1:5:5 (volume ratio), Catalyst-100 mg, Time-45 min

5.2.10 Mechanism of reaction

Several mechanisms have been proposed for hydroxylation of phenol with H_2O_2. Most of them were based on free radical even though electrophilic mechanism has been postulated over commercial titano silicates. A heterogeneous homogeneous free radical mechanism has been suggested over solid acids according to which free radicals are formed on the surface of solid acids which subsequently involve in propagation and termination in solution [64]. For the phenol hydroxylation reaction with H_2O_2, the formations of CAT and HQ are thermodynamically parallel reactions; however, kinetically the ortho-displacement of phenol with hydroxyl is more preponderant than the para-displacement according to the quantum optimizing computation. So, the higher selectivity to CAT can result from the kinetic control [65]. Franco et al. proposed that kinetically ortho position is more favoured over para substitution due to steric effect on reaction, which can be explained in terms of transition state involving a complex with the OH of phenol and OH radical of the peroxide peroxide [37].

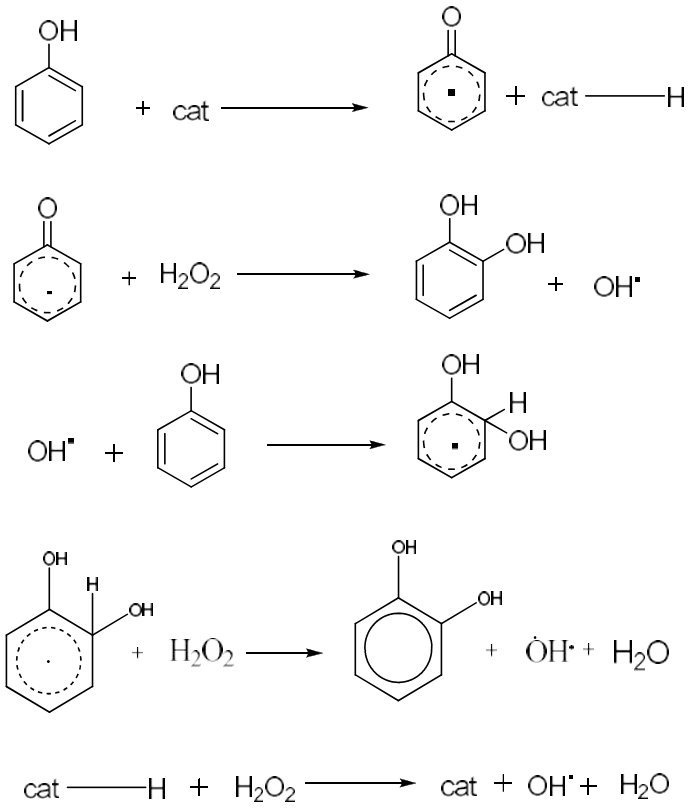

Scheme 5.2 Mechanism of oxidation of phenol over iron containing pillared clays

Even though we have not done any mechanistic studies the Initial induction period followed by bursting of reaction mixture in iron aluminium pillared clays suggest a free radical mechanism as in earlier reports [32]. The suggested mechanism involves the formation of phenoxy radical on catalyst surface, which then reacts with peroxide giving OH radical and biphenol. The produced free radical propagates the chain by attacking phenol molecule, forming diphenol.

The reaction mechanism for the hydroxylation of phenol employing copper ion has been previously proposed as free radical type on the basis of

the chemical similarity between copper and iron. However, in our experiment of phenol hydroxylation with metal loaded zirconium pillared clays no induction period was observed. Hence the free radical type mechanism can be ruled out as induction period is a unique feature of the radical-type mechanism [66-67]. Moreover, the phenol hydroxylation exclusively at the ortho and para positions suggests reaction to be an electrophilic substitution, probably involving HO^+ species. Two path ways can be suggested as in the case of earlier reports [38]. In first mechanism the interaction of H_2O_2 with metal oxo species has been reported to produce a metaloxo peroxide intermediate, as described in Scheme 5.3 [68-69]. The metal hydroperoxide species may be stabilized by hydrogen bonding between the hydroperoxide ion and the oxygen atom of support [70] or with solvent molecule like water [71].Phenol reacts with the M-O-OH intermediate to form products.

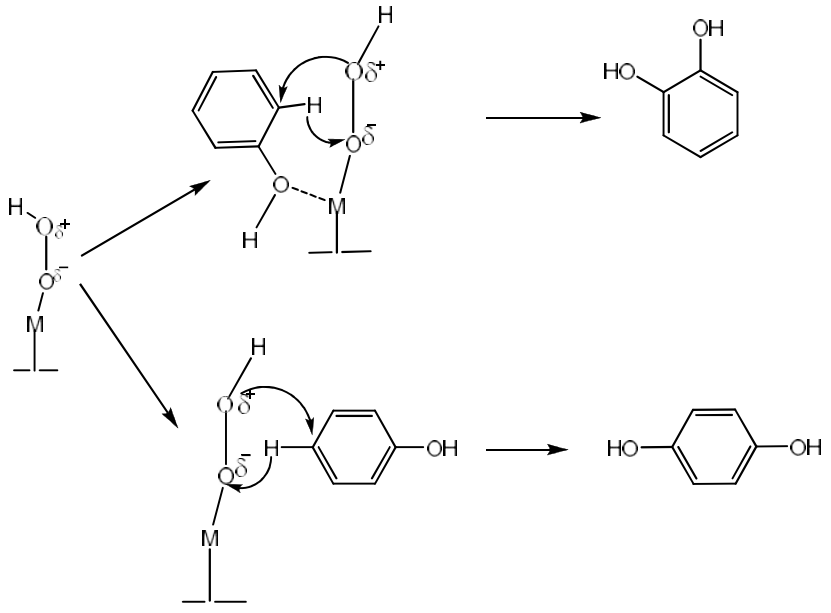

Scheme 5.3 Mechanism of phenol oxidation over metal incorporated zirconium pillared clays (pathway-1)

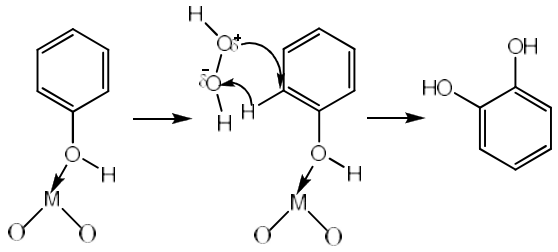

Path way -2

Scheme 5.4 Mechanism of reaction over metal incorporated zirconium pillared clays.

In second pathway phenol is adsorbed on active metal sites to form phenoxo-metal complex [72] and subsequently oxidized to produce CAT by activated H_2O_2. In alcohol medium atoms of solvents can be strongly coordinated to metal active sites to form stable alkoxo-metal complexes, which can destroy the reactive intermediate formation and thus reduce the rate of reaction [73].

5.3 Conclusions

- Aluminium pillared clays, iron aluminium pillared clays, metal loaded zirconium pillared clays and porous clay heterostructure were found to be effective catalysts for hydroxylation of phenol in aqueous media.
- Among various catalysts prepared, cerium impregnated iron- aluminium pillared clay was found to be the best catalyst with more than 80% conversion in 45 minutes owing to redox property and additional surface area provided by ceria mesopores.
- Effect of various parameters were studied and optimized for maximum conversion.

- Reaction rate increases with temperature and reaches a maximum at 70^{o}C. Hydroquinone selectivity decreases with temperature.
- The conversion and hydroquinone product selectivity increase with time. In iron pillared clays an induction period is noted suggesting a free radical type mechanism. In metal loaded zirconium pillared clays an electrophilic mechanism involving metalaxo-peroxide species is proposed.
- In metal loaded pillared clays activity can be correlated with total acidity obtained for TPD Of ammonia. In metal incorporated zirconium silicon porous clay heterostructures activity can be correlated with strong acidity obtained from TPD of ammonia. In iron aluminium pillared clays and cerium impregnated iron aluminium pillared clays high conversion is due its redox property rather than acidity.
- Among various solvents used, water is found to be the best solvent invoking the scope for utilization of these catalysts for the removal of phenolic compounds in waste water stream.

References

[1] K. Weissermel, H. J. Arpe, Industrial Organic Chemistry, VCH, Weinheim, (1993) 358

[2] ATSDR, ToxFAQs™ for Phenol. Agency for Toxic Substances and Disease Registry (ATSDR) (http://www.atsdr.cdc.gov/). (2008)

[3] H. J. H. Fenton, J. Chem. Soc., 65, 899

[4] G. A. Hamilton, J. P. Friedman, P. M. Campbell, J. Am. Chem. Soc., 88 (1966) 266.

[5] S. Esplugas, J. Jiménez, S. Contreras, E. Pascual, M. Rodriguez, Water Res., 36 (2002) 1034.

[6] G. Busca, S. Berardinelli, C. Resini, L. Arrigí, J. Hazard. Mater., 160 (2008) 265

[7] A. Tuel, S. Moussakhouzami, Y. Bentaarit, C. Naccache, J. Mol. Catal., 68 (1991) 45.

[8] D. A. Wang, Z. Q. Liu, F. Q. Liu, X. Ai, X. T. Zhang, Y. Cao, J. F. Yu, T. H. Wu, Y. B. Bai, T. J. Li, X. Y. Tang, Appl. Catal. A., 174 (1998) 25.

[9] H. P. Zhang, X. M. Zhang, Y. Ding, L. Yan, T. Ren, J. S. Suo, New J. Chem., 26 (2002) 376.

[10] A. Wroblewska, G. Wojtowicz, E. Makuch ,J. Adv. Oxid. Technol., 14 (2011) 267.

[11] A. Wroblewska, J. Adv. Oxid. Technol., 15 (2012) 418.

[12] A. L. Villa., C. A. Caro, C. M. Correa, J. Mol. Catal. A: Chem., 228 (2005) 233.

[13] B. Li, J. Xu, Liu, J. Zuo, S. Pan, Z. Wu, J. Colloid. Interface. Sci., 366 (2012) 114.

[14] J. Hoi, S. Yoon, S. Jang, W. Ahn, Catal. Today, 73 (2006) 280.

[15] W. Zhao, Y. Luo, P. Deng, Q. Li, Catal. Lett., 73 (2001) 199.

[16] M. I. Pariente, F. Martinez, J. A. Melero, J. A. Botas, Appl. Catal. B: Environ., 85 (2008) 24.

[17] C. Luca, F. Ivorra, P. Massa, R. Fenoglio, Ind. Eng. Chem. Res., 51 (2012) 8979.

[18] X. Zhao, Z. Sun, Z. Z. Li, G. Li, X. Wang, Catal. Lett., 143 (2013) 57.

[19] S. G. Huling, R. G. Arnold, R. A. Sierka, P. K. Jones, D. Dine, J. Environ. Eng., 126 (2000) 595.

[20] J. A. Zazo, J. A. Casas, A. F. Mohedano, J. J. Rodriguez, Appl. Catal. B: Environ., 65 (2006) 261.

[21] A. Quintanilla, A. F. Fraile, J. A. Casas, J. J. Rodriguez, J. Hazard. Mater., 146 (2007) 582.

[22] C. S. Castro, M. C. Gerreiro, L. C. A. Oliveira, M. Goncalves, A. S. Anastasio, M. Nazzarro, Appl. Catal. A: Gen., 367 (2009) 53.

[23] J. H. Ramirez, F. J. Maldonado-Hodar, A. F. Perez-Cadenas, C. Moreno-Castilla, C. A. Costa, L. M. Madeira, Appl. Catal. B Environ., 75 (2007) 312.

[24] F. Duarte, F. J. Maldonado-Hodar, A. F. Perez-Cadenas, L. M. Madeira, Appl. Catal.B: Environ., 85 (2009) 139.

[25] Q. Liao, J. Sun, L. Gao, Colloids Surf. A: Physicochem. Eng. Aspects, 345 (2009) 95.

[26] S. Ikurumi, S. Okada, K. Nakatsuka, T. Kamegawa, K. Mori, H. Yamashita, J. Phys. Chem. C, 118 (2014) 575.

[27] H. Bel, P. Da Costa, P. Beaunier, M. E. Galvez, M. B. Zina, Appl. Clay Scien., 46 (2014) 91.

[28] S. Yanga, G. Lianga, A. Gua, H. Mao, Appl. Surface Sci., 285 (2013) 721.

[29] N. Ksontini, W. Najjar, A. Ghorbel, J. Phys. Chem. Solids., 69 (2008).

[30] N. Sanabria, A. A. lvarez, R. Molina, S. Moreno, Catal. Today, 133 (2008) 530.

[31] C. Catrinescu, D. Arsene, P. Apopei, C. Teodosiu, Appl. Clay Sci., 58 (2012) 96.

[32] M. Kurian, S. Sugunan, Chem.Eng. J., 115 (2006) 139.

[33] X. Qi, L. Zhang, W. Xie, T. Ji, R. Li, Appl. Catal. A., 276 (2004) 89.

[34] J. Wang, J. N. Park, H. C. Jeong, K. S. Choi, X. Y. Wei, S.-I. Hong, C. W Lee., Energy Fuels, 18 (2004) 470.

[35] A. L. Villa, C. A. Caro, C. M. Correa, J. Mol. Catal: A., 228 (2005) 233.

[36] L. L. Lou, S. Liu., Catal. Commun, 6 (2005) 762.

[37] L. N. Franco, I. H. Perez, A. Pliego, A. M. Franco, Catal. Today, 75 (2002) 189.

[38] G. Zhang, J. Long, X. Wang, Z. Zhang, W. Dai, P. Liu, Z. L. Ling Wu, X. Fu, Langmuir, 26 (2010) 1362.

[39] Z. Fu, J. Chen, D. Yin, D. Yin, L. Zhang, Y. Zhang, Catal. Lett., 66 (2000) 105.

[40] L. Wang, A. Kong, B. Chen, H. Ding, Y. Shan, M. He, J. Mol. Catal. A., 230 (2005) 143.

[41] J. Sun, X. Meng,Y. Shi, R. Wang, S. Feng, D. Jiang, R. Xu, F. S. Xiao, J. Catal., 193 (2000) 199.

[42] A. Santos, P. Yustos, B. Durban, F. G. Ochoa, Catal. Today., 48 (1999) 109.

[43] K. Bahranowski, M. Gasior, A. Kielski, J. Podobinski, E. M. Serwicka, L. A. Vartikian, K. Wodnicka, Clays. Clay Miner., 46 (1998) 98.

[44] J. Barrault, M. Abdellaou, C. Bouchoule, M. Majeste, J. M. Tatibouet, A. Louloudi, N. H. Gangas, Appl. Catal: B, 27 (2000) 225.

[45] K. M. Parida, S. Mallick, J. Mol. Catal. A: Chem., 79 (2008) 104.

[46] P. H. P. Rao, A. V. Ramaswamy, P. Ratnaswamy, J. Catal., 137 (1992) 137.

[47] N. Vlagappan, V. Rishani, J. Chem. Soc. Commun., 374 (1995).

[48] H. L del Castillo, A. Gil, P. Grange, Clays Clay Miner., 44 (1996) 706.

[49] S.V. Awate, P. N. Joshi, Korean J. Chem. Eng., 18 (2001) 257.

[50] C. B. Molina, L. Calvol, J. Rodriguez, J. Appl. Clay Sci., 45 (2009) 206.

[51] L. K. Boudali, A. Ghorbel, D. Tichit, F. Figueras, Micropor. Mater., 2 (1994) 525.

[52] S. Navalon, M. Alvaro, H. Garcia, Appl. Catal B: Environ., 99 (2010) 1.

[53] H. J. Ramirez, M. A Vincente, L. M. Madeira, Appl. Catal. B., 98 (2010) 10.

[54] J. G. Ramirez, B. K. G Theng, M .L. Mora, Appl. Clay Sci., 47 (2010) 182.

[55] H. S. Lacheen, E. Iglesia, Phys. Chem. Chem. Phys., 7 (2005) 538.

[56] J. F. Dubreuil, J. Garcia-Serna, E. G. Verdugo, L. M. Dudd, G. R. Aird, W. B. Thomas, M. Poliakoff, J. Supercrit. Fluids., 39 (2006) 220.

[57] Z. L Hua, J. Zhou, J. L. Shi, Chem. Commun., 47 (2011) 10536.

[58] J. S. Choi, S. S. Yoon, S. H. Jang, W. S Ahn, Catal. Today., 111 (2006) 280.

[59] R. Yu, F. S. Xiao, D. Wang, G. Pang, R .Xu, Catal. Lett., 49 (1997) 49.

[60] S.I. Saudler "Chemical and Engineering Thermodynamics" 2nd ed,Elsevier (1982)

[61] F. Tomul, Appl. Surf. Sci., 258 (2011) 1836.

[62] Y. Zhang, F. Gao, H. Wana, C. Wu, Y. Kong, X. Wu, B. Zhao, Y. Chen, Micropor. Mesopor. Mater.,113 (2008) 393.

[63] A. Sampieri, G. Fetter, P. Bosch, S. Bulbulian, J. Porous Mater., 11 (2004) 157.

[64] C. Meyer, G. Clement, J. C. Balaceanu "Proc.3rd Int.Congress on catalysis" Vol I (1965)

[65] J. M. Zhang, H. S. Feng, Chem. React. Eng. Technol., 20 (2004) 239.

[66] J. S. Choi, S. S. Yoon, S. H. Jang, W. S. Ahn, Catal. Today, 111 (2006) 280.

[67] J. Long, X. Wang, Z. Ding, Z. Zhang, H. Lin, W. Dai, X. Fu, J. Catal., 264 (2009) 163.

[68] G. L. Elizarova, L. G. Matvienko, O. L. Ogorodnikova, V. N. Parmon., Kinet. Catal., 41 (2000) 332.

[69] K. Bahranowski, R. Dula, M. Gasior, M. Labanowska, A. Michalik, L. A. Artikian, E. M. Serwicka, Appl. Clay Sci., 18 (2001) 93.

[70] S. Ito, T. Okuno, H. Matsushima, T. Tokii, Y. Nishida, J. Chem. Soc. Dalton Trans., (1996) 4479.

[71] M. G. Clerici, P. Ingallina, J. Catal., 140 (1993) 71.

[72] U. Wilkenhconer, G. Langhendries, F. L. Baron, G. V. Gammon, D. W. Jacobs, P. A. Steen, J. Catal., 203 (2001) 201.

[73] M. Kubota, K. Yamamoto, Bull. Chem. Soc. Jpn., 51 (1978) 2909.

.....ൠ.....

Chapter 6

HYDROXYLATION OF BENZENE

Research is going on in full swing to develop new efficient oxygenation catalysts for functionalizing feedstock alkanes to raw oxygen-containing chemicals. New environment friendly catalytic processes using clean oxidants like molecular oxygen or hydrogen peroxide are being explored exhaustively recently. In this direction, H_2O_2 in presence of active metal oxide catalysts is extensively explored towards low temperature oxidation reactions. However, in presence of transition metal ions, applications of hydrogen peroxide as an oxidant has been limited due to the self-decomposition of the oxidant. But fine dispersion of transition metal ions on suitable supports overcomes this demerit by site isolation of redox metal ions, and has been proven as an excellent catalyst for a variety of oxidation reactions.

Phenol, one of the most important intermediate for organic synthesis is commercially prepared by multistep cumene process which has several serious disadvantages. The direct hydroxylation of benzene with hydrogen peroxide as oxidant is widely attempted green process at the mild conditions which would be one of the most useful processes in the future. Here in we report liquid phase hydroxylation of benzene with H_2O_2 over transition metal impregnated PILCs and PCHs under mild reaction conditions.

6.1 Introduction

Phenol is an important intermediate in the chemical industry used for the manufacturing of resins, caprolactam, adipic acid, fibers, antioxidants, agrochemicals and many other chemicals. Phenol is commercially produced via the multy step Hock process [1], where benzene is converted in to cumene by the alkylation of benzene with propene in presence of silica supported phosphoric acid and then cumene is non catalytically oxidized to cumene hydroperoxide in aqueous emulsion and it is followed by its subsequent cleavage in acidic media yield equimolar amounts of phenol and acetone (Scheme.6.1). The process has several disadvantages like low yield of phenol, high energy cost, an explosive intermediate (cumene hydroperoxide) and requirement to treat the by-product of acetone. More over the economy of this process is strongly dependent on the market price of the side product acetone. Thus, the direct hydroxylation of benzene to phenol with high atom efficiency and high selectivity becomes one of the most challenging task and has attracted much attention.

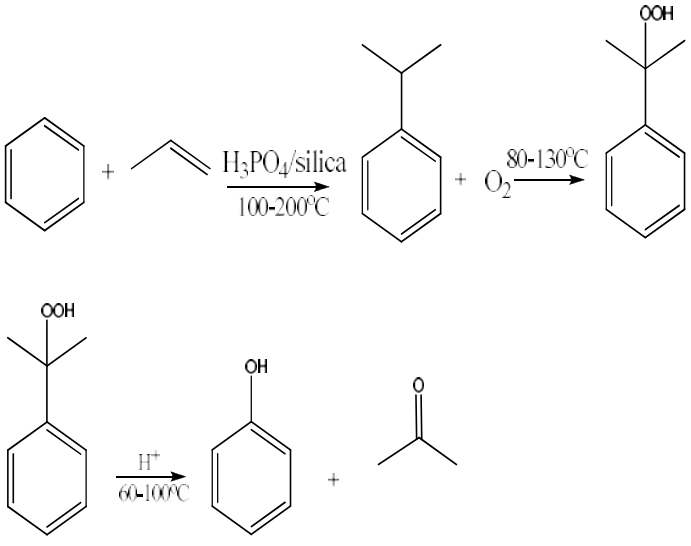

Scheme 6.1 Cumene Precess

To achieve direct hydroxylation of aromatic compounds, a neutral oxygen species or radical oxygen species might work as the active species. A variety of oxygen sources such as O_2 [2-3], H_2O_2 [4-7], N_2O [8-9] and a mixture of oxygen and hydrogen [10] have been utilized for the direct hydroxylation of benzene. When molecular oxygen is used as the oxidant for hydroxylation of benzene, sacrificial reductant such as hydrogen [10–14], carbon monoxide [15], ammonia [16-17], ascorbic acid etc. are usually required. High selectivity to phenol could be obtained with nitrous oxide as the oxidant at higher reaction temperature, but the source of raw material is limited. Benzene hydroxylation using oxygen requires the activation of C–H bonds in the aromatic ring and the subsequent insertion of oxygen. Most heterogeneous catalysts that contain transition metals, supply an oxygen species that has a negative charge, such as O^-, O^{2-} and O_2^-, all of which cause oxidation of benzene via the electrophilic reaction mechanism [18]. Air or oxygen is easily available. However, the efficiency of the catalysts is far from the level of industrial application. Amongst the oxidants, hydrogen peroxide has some obvious advantage due to the fact that water is the only byproduct and the process is simple, green, and economic. Hence direct hydroxylation of benzene in liquid phase with H_2O_2 in milder conditions is regarded as beneficial.

Hydroxylation of benzene to phenol was studied initially in the view of understanding the biological processes which showed the formation of biphenyl through cyclo hexadienyl radical and for understanding of Fenton's mechanism [19-22]. Friedel and Crafts studied the conversion of benzene to phenol using oxygen in gas phase in presence of aluminium chloride [23]. Later molybdenum, tungsten, copper, and vanadium oxides were explored for

hydroxylation of benzene using oxygen as oxidant [24-26]. However the practical application was limited as selectivity of phenol was very low. There were numerous investigations on liquid phase hydroxylation of benzene using homogeneous heteropolyacid catalysts such as iron and chromium containing phosphotungstic salts, vanadium substituted phosphotungstates and phosphomolybdates with hydrogen peroxide as an oxidant [27-32]. However, benzene conversion was very low over those catalysts.

Perego et al. evaluated the catalytic activity of titanium silicates for hydroxylation of benzene soon after its synthesis [33]. Bengoa et al. investigated the influence of structural properties of TS-1 on catalytic hydroxylation of benzene and indicated that synthesis conditions must be controlled carefully to get pure TS-1, as the presence of extra-framework titanium will inhibit benzene hydroxylation [34]. Balducci et al. observed a dramatic improvement of selectivity by using sulfolane as a cosolvent in a NH_4HF_2 modified TS-1 catalyst (TS-1B) due to the formation of complexes with phenolic compounds limiting the formation of over oxidation products [35].

Transition metal incorporated microporous or mesoporous materials were reported as active catalysts for direct hydroxylation of benzene to phenol. Ion-exchanged NaY zeolite with various cations (Cu^{2+}, Ni^{2+}, Zn^{2+}, Fe^{3+}, Cr^{3+}, Bi^{3+} and V^{4+}) were evaluated for hydroxylation of benzene with hydrogen peroxide [36]. The highest conversion of benzene (33.2%) was achieved using Cu-NaY with 100% selectivity to phenol. When 1:1 molar ratio of benzene/H_2O_2 was used, no over oxidation products were observed for all ion exchanged NaY zeolites. There were several reports about the hydroxylation of benzene over vanadium containing catalysts, such as VO_x species anchored

on amorphous siliceous material of MCM type catalysts such as MCM-41 [37-38], MCM-48) [39], VO_x species supported on SBA-15 [40], SBA-16 [41] and clay [42]. Vanadium containing microporous material VS-1 with different vanadium contents were evaluated for benzene hydroxylation and the leaching behavior were examined under different conditions. The results indicated that the mononuclear octahedral V^V, tetrahedral V^V and V^{IV} species in the framework showed good stability under the hydroxylation conditions [43]. V-HMS catalysts with isolated tetrahedral VO_4 species in the frame work were also studied for the title reaction in aqueous acetic acid as solvent [44]. Zhu et al. found in VO_x/SBA-16 that not only the highly dispersed isolated VO_4 species, but also the polymerized VO_4 units and the microcrystal of V_2O_5 on the surface of catalyst played key roles in the hydroxylation of benzene to phenol [41]. Vanadyl acetylacetonate complex grafted periodic mesoporous material prepared by the anchoring of vanadyl acetyl acetate group in to the amino functionalized MCM-41 showed better catalytic activities with higher stability than the framework substituted V-MCM-41 materials and the vanadium peroxo complex of V^{5+}-O-$O^{\bullet}$ radicals played an important role in the hydroxylation of benzene to phenol [45]. Tanarungsun et al. studied the hydroxylation of benzene with H_2O_2 using various transition metal catalysts (Cu, V, Fe) supported on TiO_2 support [46-47]. The addition of vanadium in the Fe/TiO_2 improved the activity of catalysts. A ternary metal catalyst composed of Cu, V and Fe showed good activity and ratio of Cu, V and Fe have tremendous effect on phenol yield and phenol selectivity [48]. Sugunan et al. studied the hydroxylation of benzene over chromium loaded mesoporous zirconium cerium mixed oxide and found to be promising.

Cu (II) substituted molecular sieves were found to be is active centre and efficient catalysts in liquid phase oxidation of aromatic compounds. Wang and coworkers studied the hydroxylation of benzene over Cu-MCM-41 prepared by sol-gel method with varying copper content [49]. The catalytic activity revealed that benzene conversion could reach 52.9%, but the phenol selectivity was greatly reduced due to the over oxidation. The selectivity to phenol was improved by the addition of acidic promoters such as B, Al to Cu-MCM-41 material [50]. X.Y. Qi et al. compared the activity of copper substituted aluminophosphate molecular sieves CuAPO-11having AEL topology with its redox analog CuAPO-5 having AFI topology [51]. The product distributions were governed by the nature of structure types of the copper-substituted materials. The peculiar porous structure related to AEL or AFI topology governed the product distributions in which phenol as a sole product was yielded over the AEL structure, whereas the formation of catechol and hydroquinone were favored over the AFI structure, particularly at higher benzene conversions. CuO supported hexagonal SBA-15[52], cubic KIT-6 [53], aluminium pillared clays [54] and Cu containing LDHs [55] were also reported for the title reaction.

Hydroxylation of benzene was also investigated over mesoporous Fe-MCM-41, Co-MCM-41 and Ni-MCM-41 catalysts with hexagonal and well-ordered structure [56]. The catalytic activity and selectivity of these catalysts were influenced by the quantity of the metal incorporated in the framework, adsorption capacity and stability of the catalyst against leaching. High benzene conversion (80.4%) was obtained with Co-MCM-41 (9.2% Co) in acetonitrile at 50^0C. It was revealed in Ti grafted MCM-41 that the surface hydrophobicity/hydrophilicity of the catalysts significantly affects the affinity

of the catalyst surface for reactant molecules with different polarity, thereby influencing the selectivity in the hydroxylation of benzene [57]. Iron oxide supported catalyst such as Fe/MgO [58], Fe^{3+}/Al_2O_3[59] were also proved to be effective for direct hydroxylation of benzene to phenol.

From the above discussion it was clear that amount, dispersion and nature of active metal oxide species in the metal supported catalysts have tremendous influence on benzene conversion and selectivity of phenol. Here in we report liquid phase hydroxylation of benzene with 30% H_2O_2 over transition metal impregnated PILCs and PCHs under mild reaction conditions. The reactions were done as the procedure described in section 2.4.2.The effect of various parameters were studied and optimized to get maximum conversion.

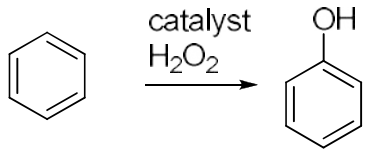

Scheme 6.2 Direct hydroxylation of benzene

6.2 Effect of Reaction Parameters

6.2.1 Effect of solvents

Solvents play a crucial role in benzene hydroxylation as keeping both benzene and hydrogen peroxide in one phase and facilitate an intimate contact between the reactants and the catalysts. Reactions were carried out in different solvents such as acetonitrile, dioxane and methanol and results are given in Figure 6.1. It was found that the benzene conversion was the highest for the acetonitrile solvent. This may be due to high dielectric constant of acetonitrile and low hydroxyl ion scavenging ability of acetonitrile. Probably the reaction

may be taking place through an ionic intermediate, which is most stabilized in a solvent of highest polarity. Some researchers have the opinion that acetonitrile does not behave as an inert solvent, but most likely forms a reactive intermediate with hydrogen peroxide, which by itself seems to be the active oxidant responsible for the phenol formation and thus leads to the highest benzene conversion [60].

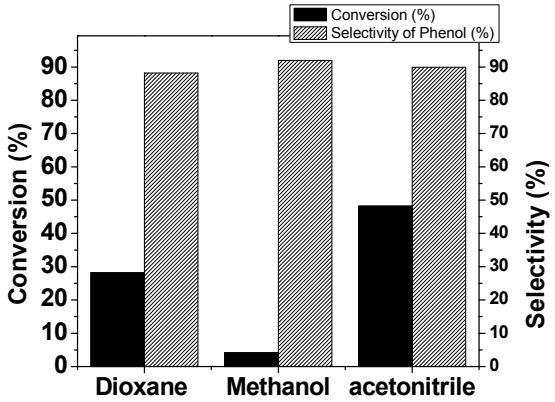

Figure 6.1 Effect of solvents, Catalyst- Cu(5)ZrPC, Temperature -60^{o}C, Time -3h, Benzene-10 mmol, Benzene to H_2O_2 ratio- 1:3, Solvent -5 mL, Catalyst -100mg

6.2.2 Effect of solvent amount

The effect of volume of acetonitrile was studied by varying the volume of acetonitrile from 5mL to 10mL. The volume of solvent is crucial as it may influence the polarity of reaction mixture and stabilize the reaction intermediates and keep benzene and H_2O_2 in one phase. The conversion increases with solvent amount and after an optimum amount conversion falls due to the competitive adsorption of solvent molecules over the active sites. The optimum acetonitrile amount is found to be 7.5 mL.

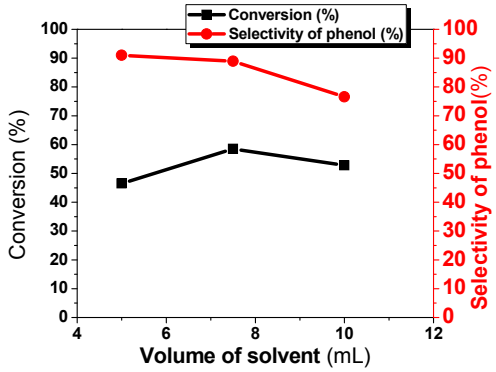

Figure 6.2 Effect of volume of acetonitrile, Catalyst- Cu(5)ZrPC, Temperature -60^{0}C, Time -3h, Benzene-10 mmol, Benzene to H_2O_2 ratio- 1:3, Catalyst -100mg

6.2.3 Effect of time

The Figure 6.3 depicts the progress of reaction with respect to time. A gradual increase in conversion was noted with increase in reaction time and maximum conversion was observed at 3rd hour and thereafter conversion remains the same. The selectivity of phenol decrease with time as the phenol formed is further hydroxylated and converted in to other byproducts. Hence 3 rd hour is taken as optimum time for further studies.

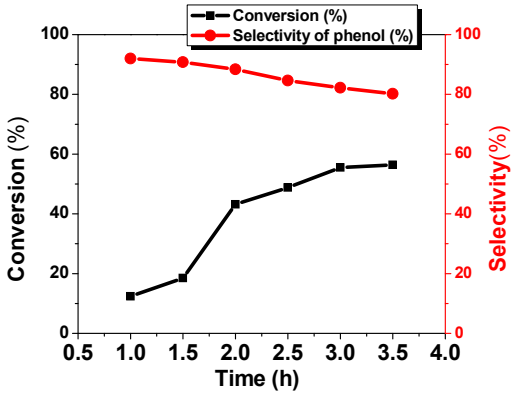

Figure 6.3 Effect of reaction time, Catalyst- Cu(5)ZrPC, Temperature -60^{o}C, Benzene-10 mmol, Benzene to H_2O_2 ratio- 1:3, Catalyst -100mg, Acetonitrile -7.5 mL

6.2.4 Effect of catalyst amount

The effect of catalyst amount was studied by varying catalyst amount from 80 mg to 140 mg. The conversion increases with increase in catalyst amount due to the proportional increase in active sites. Initially selectivity of phenol increases with catalyst amount and then selectivity of phenol decreases due to over oxidation of phenol to other byproducts.

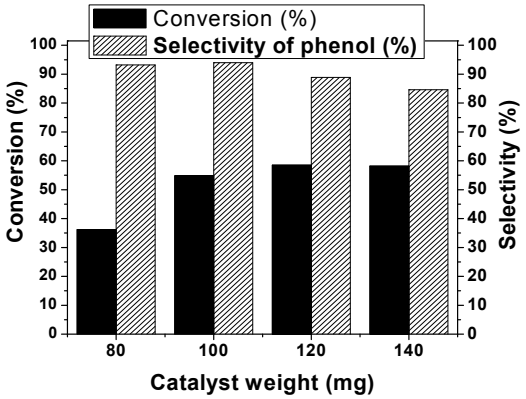

Figure 6.4 Effect of catalyst amount on hydroxylation benzene Catalyst- Cu(5)ZrPC, Temperature -60°C, Time -3h, Benzene-10 mmol, Benzene to H_2O_2 ratio- 1:3, Acetonitrile -7.5 mL

6.2.5 Effect of temperature

Hydroxylation reaction was performed in the temperature range of 30–70°C and the results are given in Figure 6.5. Conversion of benzene increases with increase in temperature and maximum conversion is obtained at 60°C. It can be seen that phenol selectivity gradually increases from 30 to 70°C. At low temperature, the lower phenol selectivity can be due to the fact that phenol is more active than benzene and phenol is further hydroxylated to diphenols and other by products. Above 60°C the conversion drops due to the competitive self decomposition of H_2O_2 without being involved in desired reaction. This

behavior is similar to other Cu-based materials like Cu-HMS [55] and Cu AlPC [54] catalysts reported in literature.

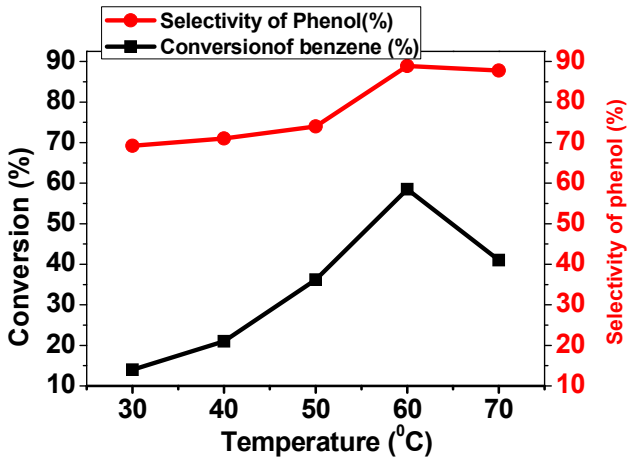

Figure 6.5 Effect of temperature, Catalyst- Cu(5)ZrPC, Time -3h, Benzene-10 mmol, Benzene to H_2O_2 ratio- 1:3, Catalyst -120mg,Acetonitrile -7.5 mL

6.2.6 Effect of oxidant ratio

The effect of benzene to oxidant (30% H_2O_2) ratio was studied from molar ratio 1 to 4 and the results are given in Figure 6.6.

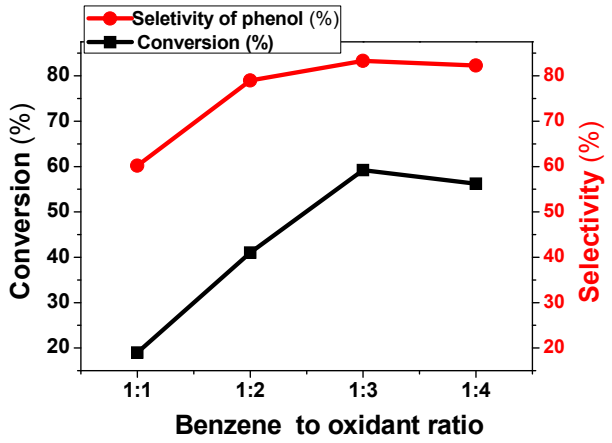

Figure 6.6 Effect of oxidant ratio, Catalyst- Cu(5)ZrPC, Temperature -60°C, Time -3h, Benzene-10 mmol, Acetonitrile -7.5 mL ,Catalyst -120mg

The conversion and selectivity of phenol increases with oxidant amount and maximum conversion is obtained at benzene to H_2O_2 ratio of 1: 3 and then conversion and selectivity falls. This may be ascribed to the self-catalytic decomposition of H_2O_2 and formation of deep oxidation products at higher oxidant amount.

6.2.7 Effect of different catalysts

The hydroxylation of benzene was performed over prepared catalysts with the optimized conditions and the results are summarized in the Table 6.1.

Table 6.1 Optimised reaction conditions

Parameters	Optimized conditions
Temperature (^{0}C)	60^{o}C
Time	3 hour
Solvent	Acetonitrile (7.5 mL)
Benzene	10 mmol
Benzene to H_2O_2 Ratio	1:3
Catalyst Amount	120 mg

It is clear from the Table 6.2 that Cu and V incorporated catalysts showed better activity compared to other metal incorporated catalysts. Cu incorporated catalysts showed the highest conversion which may prove that Cu is a highly active center of catalysts for the benzene hydroxylation. The bare zirconium pillared clay show low activity which substantiates the necessity of active redox metal species for benzene hydroxylation.

Table 6.2 Effect of catalyst on hydroxylation of benzene

Catalysts	Conversion of benzene (%)	TON	Selectivity (%)			
			Phenol	Catechol	Hydroquinone	Others
ZrPC	2		100			
Cu(1)ZrPC	37	47370	97	2	-	1
Cu(3)ZrPC	51	20939	93.	4	2	1
Cu(5)ZrPC	59	10264	89	7	3	1
V(1)ZrPC	11	8632	98	1	1	-
V(3)ZrPC	23	6087	92	3	3	2
V(5)ZrPC	38	4918	86	8	4	2
Ni(5)ZrPC	8	1181	95	3	1	1
Co (3)ZrPC	15	4159	89	7	4	-
Co(5)ZrPC	26	4038	79	13	6	2
FeAlPC	23	832	96	3	1	-
Ce(3)FeAlPC	25	646	94	4	2	-
CuZrSiPCH	32	8968	95	2	2	1
VZrSiPCH	28	6896	92	4	3	1
CoZrSiPCH	13	2746	90	5	3	2
Nil	0	-				

TON = (mmoles of reactant reacted / mmoles of active metal) x 100

The catalytic activity in terms of Turn Over Number (TON) was also calculated and is given in Table 6.2. The TON is maximum for Cu(1)ZrPC catalysts where the active Cu species is well dispersed as isolated copper oxide species. For the same metal species the conversion of benzene in zirconium pillared clay is higher than that of porous clay heterostructures probably due to the fact that benzene is more strongly adsorbed on the strong Lewis sites than on Bronsted sites. This is in accordance with earlier reports [50].

6.2.8 Effect of metal amount

Figure 6.7 depicts the influence of copper and vanadium content on the reaction. In copper and vanadium incorporated zirconium pillared clays, the

conversion of benzene increases with increase in metal content up to 5 % and then the conversion decreases. In the case of copper incorporated zirconium pillared clays, this may be due to the nonproductive self decomposition H_2O_2 over copper aggregates. From XRD and TPR data it was confirmed that copper was dispersed as isolated copper oxides species up to 5% Cu loading then clusters or aggregates of copper oxides are formed in zirconium pillared clays. Bahranowski et al. [61] have proved that isolated copper act as an active center for the oxidation of aromatic hydrocarbon and copper particularly in cluster form can catalyze the self decomposition of H_2O_2. It is also reported that isolated VO_x species of tetrahedral coordination in lower loading is more effective for the oxidation of aromatics than polymerized VOx species in higher vanadium loading [62]. In vanadium impregnated zirconium pillared clays conversion increases up to 5% due to the fact that vanadium exists as isolated VO_x species as evident from XRD and TPR analysis. The selectivity of phenol decreases with increase in metal content due to the over oxidation of phenol in to other by products over active sites.

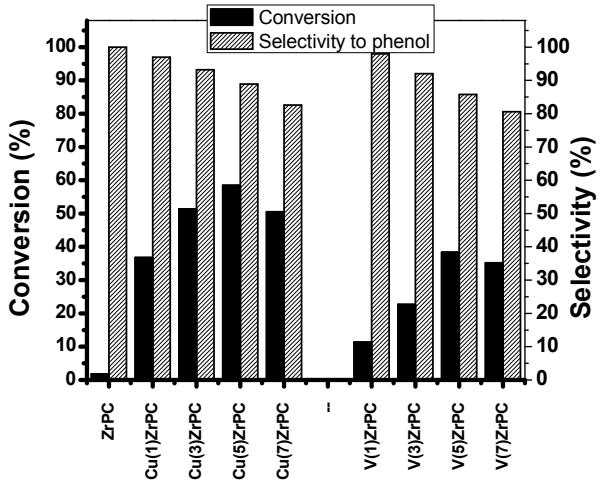

Figure 6.7 Effect of metal content

6.3 Mechanism of reaction

In oxidation reactions using hydrogen peroxide, the cleavage of the oxygen–oxygen bond in peroxides takes either of two distinct pathways homolitic cleavage leading to a radical pathway or heterolitic cleavage leading to ionic mechanism. For the oxidation of aromatics with hydrogen peroxide over transition metal oxide supported catalysts, it has been proposed that the hydroxylation of the aromatic ring occurs via the heterolytic mechanism, involving the formation of a metalloperoxide species [63-64]. The metaloxo hydroperoxide species may be stabilized by hydrogen bonding between the hydroperoxide ion and the oxygen atom of support [66] or polar solvent like acetonitrile. Even though no detailed mechanistic studies have been carried out in the present case hydroxylation of the ring indicates the possibility of heterolytic cleavage involving an ionic mechanism as depicted in the Scheme 6.3.

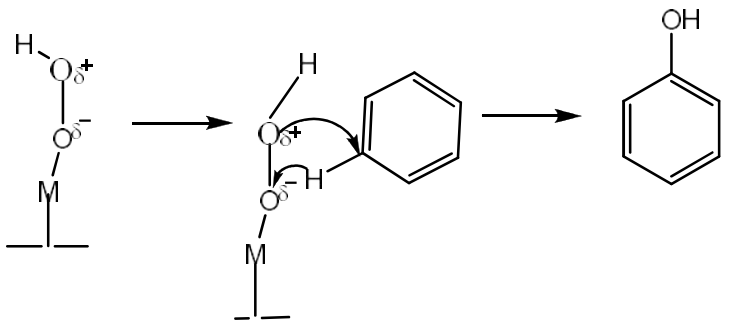

Scheme 6.3 Mechanism of reaction

6.4 Conclusions

- Copper and vanadium incorporated zirconium pillared clays were found to be effective catalyst for direct hydroxylation of benzene to phenol under milder reaction conditions.

- Nature and dispersion of metal species have tremendous effect on conversion and selectivity. Isolated Cu and vanadium oxide species were found to be active centres for hydroxylation of benzene. Selectivity of phenol decreases with metal content.
- Acetonitrile was found to be best solvent for the rection as it may stabilize the reaction intermediate.
- Conversion increases with temperature and maximum conversion is obtained at 60^{o}C. The phenol selectivity decreases with temperature.
- A mechanism involving ionic intermediate and metaloxo hydroperoxide species was proposed.

References

[1] W. L. Luyben, Ind. Eng. Chem. Res., 49 (2010) 719.

[2] V. I .G. Sobolev,I. Panov , A. S Khatitonov, V.N. Romannikov, V.M. Volodin, K.G Ione, (1993) 435.

[3] M. G. Clerici, Fine Chemicals through Heterogeneous Catalysis.Wiley-VCH, Weinheim, (2001) 538.

[4] K. Nomiya, H. Yanagibayashi, C. Nozaki, K. Kondoh, E. Hiramatsu, Y. Shimizu, J. Mol. Catal. A: Chem., 114 (1996) 181.

[5] L. Balducci, D. Bianchi, R. Bortolo, R. D. Aloisio, M. Ricci, R. Tassinari, R. Ungarelli, Angew. Chem., 115 (2003) 5087.

[6] D. Bianchi, L. Balducci, R. Bortolo, R. D. Aloisio, M. Ricci, G. Spano, R. Tassinari, C. Tonini, R. Ungarelli, Adv. Synth. Catal., 349 (2007) 979.

[7] D. Bianchi, R. Bortolo, R. Tassinari, M. Ricci, R. Vignola, Angew. Chem., 39 (2000) 4321.

[8] A. Ribera, I.W.C.E. Arends, S. de Vries, J. Perez-Ramirez, R.A. Sheldon, J. Catal., 195 (2000) 287.

[9] G. I. Panov , G. A Sheveleva, A.S. Kharitonov, V.N. Romannikov, Appl. Catal. A: Gen., 82(1992) 31.

[10] S. Niwa, M. Eswaramoorthy, J. Nair, A. Raj, N. Itoh, H. Shoji, T. Namba, F. Mizukami, Science 295 (2002) 105.

[11] T. Miyake, M. Hamada, H. Niwa, M. Nishizuka, M. Oguri, J. Mol. Catal.A., 178 (2002) 89.

[12] J. E. Remias, T. A. Pavlosky, A. Sen, J. Mol. Catal. A, 203 (2003) 179.

[13] K. Sato, S. Niwa, T. Hanaoka, K. Komura, T. Namba, F. Mizukami, Catal. Lett., 96 (2004) 107.

[14] N. I. Kuznetsovaa, L.I. Kuznetsova, V.A. Likholobovb, G.P. Pez, Catal. Today., 99 (2005) 193.

[15] M. Tani, T. Sakamoto, S. Mita, S. Sakaguchi, Y. Ishii, Angew. Chem., 44 (2005) 2.

[16] B. Liptakova, M. Bahidsky, M. Hronec, Appl. Catal. A ., 263 (2004) 33.

[17] M. Bahidsky, M. Hronec, Catal. Today, 91/92 (2004) 13.

[18] Y. Morooka, M. Akita, Catal. Today, 41(1998) 327.

[19] J. R. Lindsay Smith, R. O. C. Norman, J. Chem. Soc., (1963) 2897.

[20] N. Uri, Chem. Rev., 50 (1952) 375.

[21] J. H. Baxendale, J. Magee, Trans. Faraday Soc., 51 (1955) 205.

[22] C. Walling, S. Kato, J. Am. Chem. Soc., 93 (1971) 4275.

[23] C. Friedel, J. M. Crafts, Ann. Chim., (Paris) 14 (1888) 935.

[24] I. G. Farben, DE501467 (1927).

[25] Socony-Vacuum Oil Co.; US2456597 (1948).

[26] Chem. Abstr., (1949) 1805.

[27] N.I. Kuznetsovaa, L.I. Kuznetsova, V.A. Likholobovb, G.P. Pez, Catal. Today., 99 (2005) 193.

[28] M. Tani, T. Sakamoto, S. Mita, S. Sakaguchi, Y. Ishii, Angew. Chem., 44 (2005) 2.

[29] B. Liptakova, M. Bahidsky, M. Hronec, Appl. Catal. A., 263 (2004) 33.

[30] Y. Liu, K. Murata, M. Inaba, Catal. Commun., 6 (2005) 679.

[31] S. Yamaguchi, S. Sumimoto, Y. Ichihashi, S. Nishiyama, S. Tsuruya, Ind. Eng. Chem. Res., 44 (2005) 1.

[32] H. Kanzaki, T. Kitamura, R. Hamadab, S. Nishiyama, S. Tsuruya, J. Mol. Catal. A , 208 (2004) 203.

[33] G. Perego, Bellussi, C. Corno, M. Taramasso, F. Buonomo, A.Esposito, Stud. Surf. Sci. Catal., 48 (1989) 133.

[34] J. F. Bengoa, N. G. Gallegos, S. G. Marchetti, A. M. Alvarez, M. V.Cagnoli and A. A. Yeramián, Micropor. Mesopor. Mater., 24 **(**1998) 163.

[35] L. Balducci, D. Bianchi, R. Bortolo, R. D. Aloisio, M. Ricci, R.Tassinari , R. Ungarelli, Angew. Chem., 42 **(**2003) 4937.

[36] H. S. Abbo, S. J. J. Titinchi, Appl. Catal. A: Gen., 356(2009) 167.

[37] K. Lemke, H. Ehrich, U. Lohse, H. Berndt, K. Jahnisch, Appl. Catal. A: Gen., 243 (2003) 41.

[38] L. D. Nguyen, S. Loridant, H. Launay, A. Pigamo, J. L. Dubois, J. M. M. Millet, J. Catal., 237 (2006) 38.

[39] C. W. Lee, W. J. Lee, Y. K. Park , S. E. Park, Catal. Today., 61 (2000) 137.

[40] Y. Y. Gu, X. H. Zhao, G. R. Zhang, H. M. Ding, Y. K. Shan, Appl. Catal. A: Gen., 328 (2007) 150.

[41] Y. Zhu, Y. Dong, L. Zhao, F. Yuan, J. Catal. A: Chem., 315 (2010) 205.

[42] X. H. Gao, J. Xu, Appl. Clay Sci., 33 (2006) 1.

[43] B. Guo, L. F. Zhu, X. K. Hu, Q. Zhang, D. M. Tong, G. Y. Li , C.W. Hu, Catal. Sci.Technol., 1 (2011)1060.

[44] S. J. Feng, S. P. Pei, B. Yue, L. Ye, L. P. Qian, H. Y. He, Catal. Lett., 131 (2009) 458.

[45] C. H. Lee, T. S. Lin , C. Y. Mou, J. Phys. Chem. B., 107 (2003) 2543.

[46] G. Tanarungsun, W. Kiatkittipong, S. Assabumrungrat, H. Yamada, T. Tagawa, P. Praserthdam, J. Chem. Eng. Jpn., 40 (2007) 415.

[47] G. Tanarungsun, W. Kiatkittipong, S. Assabumrungrat, H. Yamada, T. Tagawa, P. Praserthdam, J. Ind. Eng. Chem., 13 (2007) 444.

[48] G. Tanarungsun, W. Kiatkittipong, P. Praserthdam, H. Yamada, T. Tagawa, S. Assabumrungrat, J. Ind. Eng. Chem., 14 (2008) 601.

[49] S. Y. Jiang, Y. Kong, C. Wu, Z. Xu, H. Y. Zhu, C. Y. Wang, J. Wangand Q. J. Yan, Chin, J. Catal., 27 (2006) 421.

[50] Y. Kong, X. J. Xu, Y. Wu, R. Zhang , J. Wang, Chin. J. Catal., 29 (2008) 385.

[51] X. Y. Qi, J. Y. Li, T. H. Ji, Y. J. Wang, L. L. Feng, Y. L. Zhu, X. T.Fan , C. Zhang, Micropor. Mesopor. Mater., 122 (2009) 36.

[52] K. M. Parida, D. Rath, Appl. Catal. A: Gen., 321 (2007)101.

[53] A. G. Kong, H. W. Wang, X. Yang, Y. W. Hou , Y. K. Shan, Micropor. Mesopor. Mater., 118 (2009) 348.

[54] J. Pan, C. Wang, S. Guo, J. Li, Z.Yang, Catal. Commun., 9 (2008) 176.

[55] A. Dubey, S. Kannan, Catal. Commun., 6 (2005) 394.

[56] V. Parvulescu , B. L. Su, Catal. Today., 69 (2001) 315.

[57] J. He, Z. Guo, H. Ma, D. G. Evans , X. Duan, J. Catal., 212 (2002) 22.

[58] N. K. Renuka, J. Catal. A: Chem., 316 (2010) 126.

[59] H. H. Monfared, Z. Amouei, J. Mol. Catal. A: Chem., 217 (2004) 161.

[60] M. Stockmann, F. Konietzni, J. U. Notheis, J. Voss, W. Keune, W. F. Maier, Appl. Catal. A: Gen., 208 (2001) 343.

[61] K. Bahranowski, R. Dula, M. Gasior, M. Labanowska, A. Michalik, L. A. Vartikian, E.M. Serwicka, Appl. Clay Sci., 18 (2001) 93.

[62] Y. Chen, Y. H. Lu, Ind. Eng. Chem. Res.38, (1999) 1893.

[63] R. Neumann, M. Levin-Elad, Appl. Catal. A .,122 (1995) 85.

[64] G. L. Elizarova, L. G. Matvienko, O. L Ogorodnikova, V. N Parmon,Kinet. Catal., 41 (2000) 332.

[65] S. Ito, T. Okuno, H. Matsushima, T. Tokii, Y. Nishida, J. Chem. Soc. Dalton Trans., (1996) 4479.

.....ꕥ.....

Chapter 7

OXIDATION OF BENZYL ALCOHOL

Selective oxidation of natural resource is a task of key importance for producing oxygenates to be employed as building blocks in chemical process that range from kilogram scale application in pharmaceuticals to thousand tone scale in industries. Both the gas phase oxidation of volatile substrates and liquid phase high boiling compound benefit from using catalysts able to lower the activation energy. The oxidation of alcohols and polyols is of interest owing to large array of biological hydroxyl derivatives obtained from natural and renewable sources in large amounts. In particular selective oxidation can transform alcohols and polyols in to corresponding cabonylic or carboxylic derivatives which both generally represent attractive chemicals for organic synthesis. This chapter deals with the selective oxidation of benzyl alcohol to benzaldehyde over transition metal modified pillared clays and porous clay heterostructures in liquid phase under mild reaction conditions using hydrogen peroxide as oxidant.

7.1 Introduction

The oxidation of alcohols to aldehydes or ketones is one of the fundamental and important functional group transformation in organic synthesis [1-3]. The desired aldehyde, ketone, ester and acid products are valuable intermediates for the fine chemical, agrochemical, and pharmaceutical sectors, with allylic aldehydes in particular high value components used in the perfume and flavourings industries [4]. For example, crotonaldehyde is an important agrochemical and valuable precursor to the food preservative sorbic acid, while citronellyl acetate and cinnamaldehyde confer fruity and cinnamon flavors respectively. The commercial synthesis of such compounds usually utilizes toxic or hazardous stoichiometric oxidants such as chromates, permanganates etc [5]. In addition to safety considerations, such current technologies are also atom inefficient due to poor selectivity and additional separation and treatment steps to isolate the product. Hence the development of effective heterogeneous catalytic routes using environmentally benign and inexpensive oxidants such as oxygen, hydrogen peroxide is an important challenge as water is the only main side product of these reactions.

Benzaldehyde is a very important organic intermediate in the industry of perfumery, pharmaceutical, dyestuff, flavoring and agrochemicals [6]. It is traditionally produced by hydrolysis of benzyl chloride and by oxidation of toluene [7,8]. However, benzaldehyde produced from hydrolysis of benzyl chloride often contains traces of chlorine impurities and is associated with copious evolution of waste products and the oxidation of toluene is usually carried out in organic solvents which are environmentally undesirable. Catalytic vapor phase oxidation of benzyl alcohol to benzaldehyde is a widely investigated alternative process as it provides chlorine-free benzaldehyde

required in perfumery and pharmaceutical industries. Selective aerobic oxidations of benzyl alcohol were reported over platinum group metals (Pt, Pd) and their nanoparticles supported materials [9-12]. Particle size dependent catalytic selective oxidation of benzyl alcohol to benzaldehyde has been reported for Pd cluster SiO_2-Al_2O_3[13] and NaX zeolite supports [14]. Palladium nanoparticles anchored on multi-walled (MWCNT) and single walled carbon nanotubes (SWCNT) show better selectivity and activity for aerobic selective oxidation of benzyl alcohol and cinnamyl alcohol compared with activated carbon [15-16]. Gold nanoparticles confined within SBA-15 [17] and GMS [18] mesoporous silicates are very selective for the aerobic oxidation of benzyl alcohol to benzaldehyde. Gold on amino-modified fumed silica can efficiently catalyze primary alcohol oxidation selectively to their esters in a single step [19]. While the use of molecular oxygen or air as an oxidant is particularly attractive, it raises a number of challenges in terms of activating the oxygen bond at low temperature (typically < 160 °C) in a three-phase system with the suppression of the decomposition and the combustion of reactant molecules [20]. Because of the formation of carbon-oxides which leads to appreciable carbon loss in the vapor phase reaction, it is preferable to produce benzaldehyde more selectively by catalytic liquid phase oxidation of benzyl alcohol.

Both homogeneous and heterogeneous catalysts have been successfully applied in liquid phase oxidation of alcohols. Efficient homogeneous catalysts based on cobalt [21-22] copper [23] palladium [24-25] and ruthenium [26-27] have been reported. Recently, monometallic and bimetallic gold based materials in the liquid phase alcohol oxidation are successfully explored [28]. The beneficial role of gold is related to an enhanced rate and selectivity of the

oxidation more over to an improved resistance to catalyst deactivation. Because of obvious advantage of heterogeneous catalysts in product isolation and catalyst recycling and facility for continuous processing via packed bed flow reactors with additional safety, economic and environmental benefits, liquid phase oxidation of alcohols using solid catalysts has attracted much attention in recent years.

In the past decade, many heterogeneous catalytic systems had been explored for selective-oxidation of benzyl alcohol with H_2O_2 such as Au/U_3O_8 [28], Cu, Ni and Co complexes encapsulated in zeolites [29], Fe-containing coordination polymers [30], hydrotalcites [31,32], layered-double hydroxides [33], Sn-MCM-48 [34] alkali treated ZSM-5 [35], Cu-SBA-15[36], transition metal incorporated SBA-15 [37], spinels and inverse spinels [38], V doped TiO_2 [46]. Wang et al. reported a MCM-41 immobilized Cr (salen) catalyst for the oxidation of benzyl alcohol and the catalytic performance was improved by surface-modification with hydrophobic methyl group [39]. Recently metalloporphyrin complex, [tetrakis(*o*-hlorophenyl)porphyrinato] Ni(II) in functionalized rice husk silica [40], phosphotungstic acid immobilized on graphene oxide [41] were employed for the title reaction. Chen et al. developed a mesoporous polyoxometalate based ionic hybrid $[TMGHA]_{2.4}$ $H_{0.6}PW$ for catalyzing water-mediated triphase oxidations of alcohols with H_2O_2 [42]. Zhan et al. proposed a Langmuir Hinshelwood model for the oxidation of benzyl alcohol over bio reduced Au/TS-1 catalysts [43].

Most of the catalysts reported in literature for the alcohol oxidation is based on noble metal supported catalysts and air oxidation under high pressure which is very expensive. Here in we report liquid phase oxidation of benzyl alcohol over transition metal incorporated pillared clays and porous clay

heterostructures under ambient conditions as the procedure described in section 2.4.2. Effect of different parameters such as effect of solvent, temperature, oxidants and catalyst amount were studied. Reaction mainly yielded benzaldehyde which further undergoes oxidation to form benzoic acid.

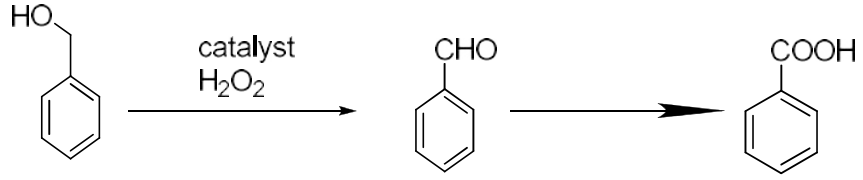

7.2 Effect of Reaction Parameters

7.2.1 Effect of solvents

It has been reported that the solvents and their polarity have profound influence on liquid phase oxidation of benzyl alcohol. Oxidation of benzyl alcohol was done in various solvents and results are given in Figure 7.1.

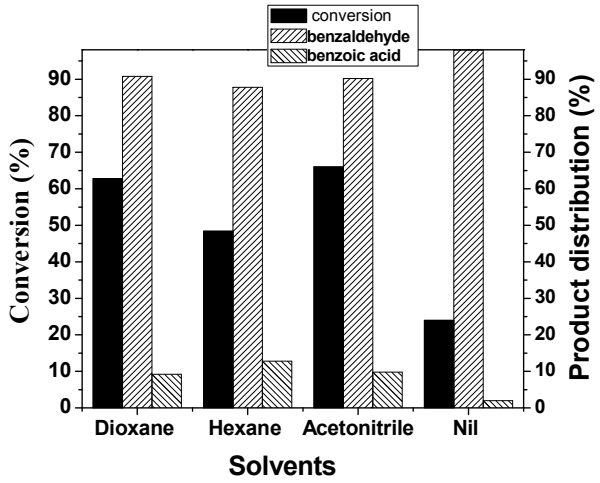

Figure 7.1 Effect of solvents, Reaction temperature- 70^{o}C, Catalyst amount- 100 mg, Benzyl alcohol-10 mmol, Benzyl alcohol to H_2O_2 ratio-1: 3, Time- 4 hour, Catalyst - V(5)ZrPC

The conversion of benzyl alcohol is very low when the reactions were done without solvents. Conversion is high in polar aprotic solvents such as acetonitrile and dioxane compared to nonpolar solvent hexane. In acetonitrile, the phase separation between benzyl alcohol and the aqueous oxidant was greatly decreased there by the easy transport of the active oxygen species for oxidation is permitted.

7.2.2 Effect of catalyst amount

The influence of catalyst amount on the oxidation of benzyl alcohol is depicted in Figure 7.2. The Conversion of benzyl alcohol increases with increase in catalyst amount due to the proportional increase of active sites with catalyst amount. The selectivity of benzoic acid increases with catalyst amount. Maximum conversion is obtained for 100 mg of catalyst but considering the selectivity factor, 80 mg was selected as optimum catalyst amount for further studies.

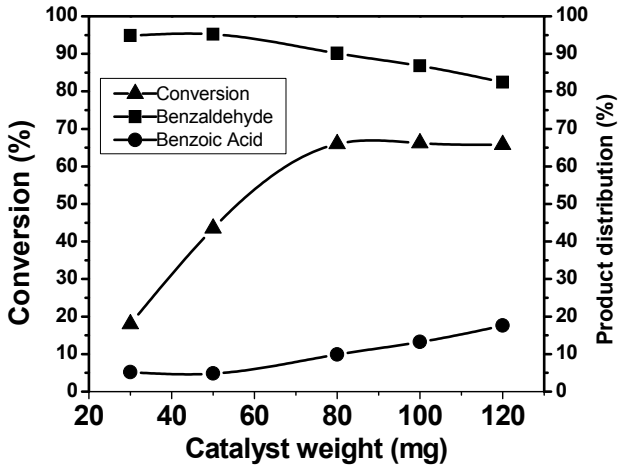

Figure 7.2 Effect of catalyst weight, Reaction temperature- 70°C, Benzyl alcohol-10 mmol, Benzyl alcohol to H_2O_2 ratio - 1: 3, Time- 4 hour, Solvent-acetonitrile, Catalyst-V(5)ZrPC

7.2.3 Effect of temperature

It has been reported that the temperature has strong influence on the progress of benzyl alcohol oxidation, which is believed as a very slow, kinetically controlled reaction with the catalyst and oxidant H_2O_2.The effect of reaction temperature on the reaction was studied in the temperature range 40^oC to 70^oC keeping all other parameters constant and the results are presented in the Figure 7.3. The results suggest that conversion of benzyl alcohol increases with increase in temperature and reaches maximum at 70^oC. This result is in accordance with earlier literature [44]. Further increase in temperature decreases the conversion. At higher temperature the self decomposition of H_2O_2 is prominent and it could not participate in the oxidation reaction. At higher temperature the evaporation of solvent is also high which may also result in the reduced conversion and hence 70^oC was taken as optimum temperature. A slight increase in benzoic acid selectivity is observed with increase in temperature.

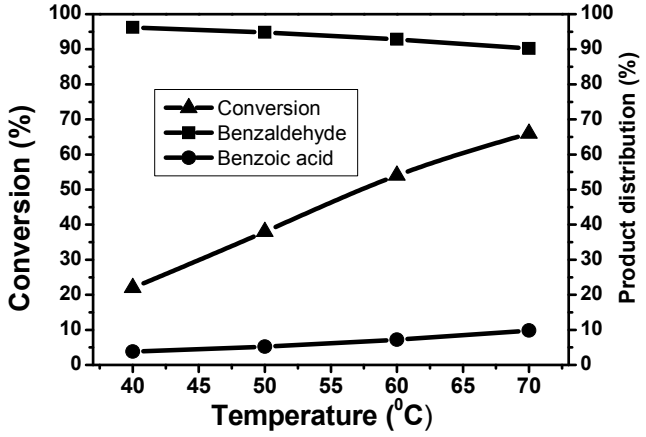

Figure 7.3 Effect of temperature, Benzyl alcohol-10 mmol, Benzyl alcohol to H_2O_2 ratio -1: 3,Time- 4 hour, Solvent-acetonitrile, Catalyst amount-80 mg, Catalyst-V(5)ZrPC

7.2.4 Effect of oxidants

Liquid phase oxidation of benzylalcohol was done with two oxidants 30% H_2O_2 and TBHP keeping all other constraints constant. Comparable results were obtained for both oxidants with a small increment for TBHP. But the selectivity of benzaldehyde was less for oxidant TBHP than that of H_2O_2. Hence H_2O_2 is taken as the oxidant for further studies.

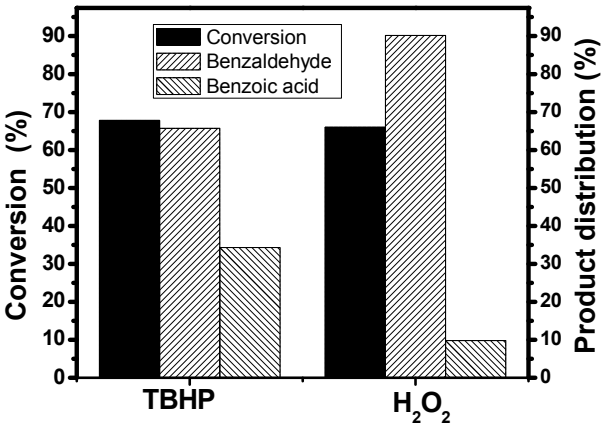

Figure 7.4 Effect of oxidants, Benzyl alcohol-10 mmol, Benzyl alcohol to oxidant ratio- 1:3, Time- 4 hour, Solvent-acetonitrile, Catalyst amount-80 mg, Temperature -70°C, Catalyst-V(5)ZrPC

7.2.5 Effect of oxidant ratio

The dosage of hydrogen peroxide is another important parameter that influence rate of the oxidation reaction. Effect of mole ratio of benzyl alcohol to hydrogen peroxide was investigated in the range of 1:1to1:5 and the results are given in Figure 7.5. A lower conversion is observed with 1:1 stochiometric ratio. Conversion increases with increase in oxidant ratio and conversion is maximum at benzyl alcohol to hydrogen peroxide ratio 1:3. Further increase in oxidant ratio results in decrease in conversion which may be due to the auto

decomposition of H_2O_2 at higher concentration. The presence of excess oxidant favors the further oxidation of initially formed product benzaldehyde to benzoic acid. This observation was also in accordance with earlier reports [41].

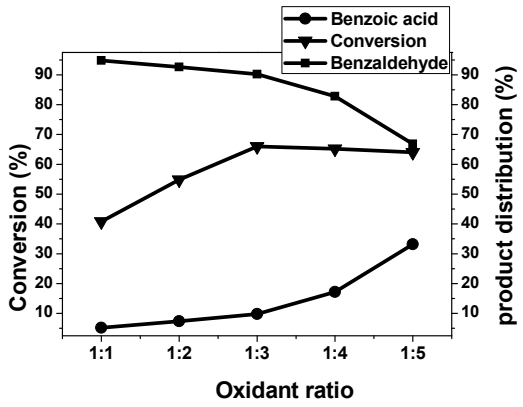

Figure 7.5 Effect of oxidant ratio, Temperature -70°C, Time- 4 hour, Solvent-acetonitrile, catalyst amount-80 mg, Benzyl alcohol-10 mmol, Oxidant-H_2O_2, Catalyst-V(5)ZrPC

7.2.6 Effect of time

The effect of time on the progress of benzyl alcohol oxidation and the selectivity to benzaldehyde at different reaction time is shown in Figure 7.6. Initial conversion of benzyl alcohol increase as reaction proceeds and maximum conversion is reached at fifth hour and then remained stable, which is due to the exhaustion of H_2O_2 by oxidation of benzyl alcohol and self-decomposition of H_2O_2. Not much increase in conversion was noted from fourth hour to fifth hour. However a prominent decrease in selectivity of benzaldehyde was noted. So the fourth hour is taken as optimum time for further studies. The selectivity of benzaldehyde decreases with time as benzaldehyde is further oxidized to benzoic acid.

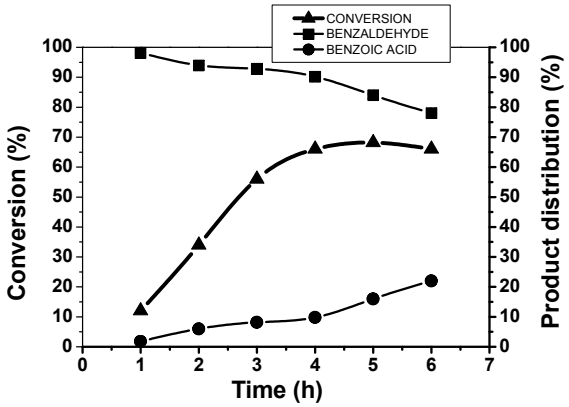

Figure 7.6 Effect of time, Temperature -70°C, Solvent-acetonitrile, Catalyst amount-80 mg, Benzyl alcohol-10mmol, Benzyl alcohol to H_2O_2 ratio - 1:3, Catalyst- V(5)ZrPC

7.2.7 Performance of different catalyst systems for the oxidation of benzyl alcohol

From the above observations it is clear that reaction conditions play a crucial role for the liquid phase oxidation of benzyl alcohol and its product distribution. Oxidation of benzyl alcohol was done over the prepared catalysts under optimized conditions described in the Table 7.1 as to obtain maximum conversion and selectivity.

Table 7.1 Optimised reaction conditions

Parameters	Optimized conditions
Temperature	70°C
Catalyst amount	80 mg
Benzyl alcohol	10 mmol
Oxidant (30% H_2O_2) ratio	1:3
Time	4 hour
Solvent	Acetonitrile

Table 7.2 Effect of different catalysts on benzyl alcohol oxidation

Catalysts	Conversion of benzyl alcohol (%)	Product distribution (%)	
		Benzaldehyde	Benzoic acid
ZrPC	21	95	5
Cu(1)ZrPC	33	92	8
Cu(3)ZrPC	48	90	10
Cu(5)ZrPC	58	92	8
Ni(1)ZrPC	29	93	7
Ni(3)ZrPC	32	91	9
Ni(5)ZrPC	45	88	12
V(1)ZrPC	33	97	3
V(3)ZrPC	49	93	7
V(5)ZrPC	66	91	9
Co(3)ZrPC	35	95	5
Co(5)ZrPC	47	92	8
FeAlPC	35	93	7
Ce(3)FeAlPC	43	95	5
CuZrSiPCH	49	96	4
NiZrSiPCH	47	97	3
CoZrSiPCH	56	93	7
VZrSiPCH	72	91	9
Nil	2	100	0

In all cases benzaldehyde was the major product and a small amount of benzoic acid was also detected. The long time paradox that why benzaldehyde readily undergoes autoxidation to form benzoic acid on exposure to air at room temperature and yet it can be formed in high yield from the oxidation of benzyl alcohol using a variety of procedures and catalysts have recently been resolved [45]. It is confirmed that benzyl alcohol (and a number of other

alcohols), even at low concentrations in benzaldehyde, inhibits the autoxidation of benzaldehyde to benzoic acid.

The bare ZrPC and ZrSiPCH have very low activity. Incorporation of transition metals improves the catalytic activity in both pillared clays and porous clay heterostructures. Among various metal loaded catalysts vanadium loaded pillared clays and porous clay heterostructures showed maximum activity. Vanadia and vanadium oxide supported catalysts have a prominent role in redox catalysis owing to easy oxidation, reduction and the existence of cation of different oxidation states as intermediates. The most important aspect of vanadia supported system is the selective oxidation activity towards partial oxidation products due to lattice oxygen mobility [47]. Very recently vanadium doped titania [46] and vanadium phosphorous oxides promoted by cobalt [48] were reported for benzyl alcohol oxidation with excellent activity and benzaldehyde selectivity. Copper loaded catalysts also showed remarkable activity owing to high redox and oxidation capabilities.

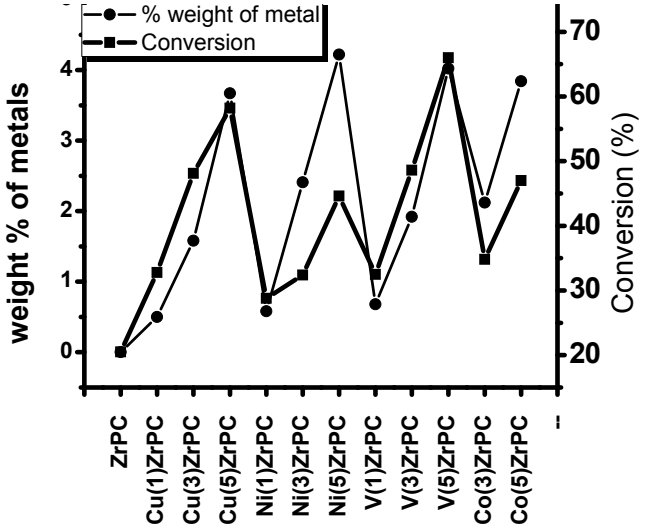

Figure 7.7 Correlation between activity and metal content

The conversion of benzyl alcohol increases with increase in metal content and the selectivity of benzaldehyde decrease with metal content. This may be due to further oxidation of benzaldehyde over the active metal species to benzoic acid. So attempt was made to correlate the activity of catalyst with metal content in metal loaded zirconium pillared clays (Figure 7.7) and a good correlation was obtained.

Porous clay heterostructures got higher conversion than pillared clays. For the same metal, the conversion of benzyl alcohol is higher in porous clay heterostructures than in pillared clays. This may be due to higher surface area and pore diameter of porous clay heterostructures which facilitate the easy diffusion of the products (benzaldehyde and benzoic acid). Lewis acid sites were believed as the active sites in catalytic oxidation of benzyl alcohol with H_2O_2 in polar solvents. In porous clay heterostructures the conversion of benzyl alcohol can be correlated with α-methyl styrene selectivity in cumene cracking reaction which corresponds to Lewis sites. Such correlation is not seen in metal loaded pillared clays.

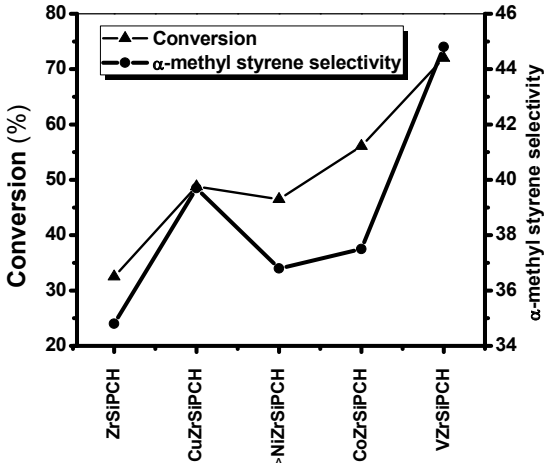

Figure 7.8 Correlation between activity and acidity

7.2.8 Leaching studies

A very important subject to be considered for the solid catalyst is the leaching phenomenon. Leaching can take place during a catalyzed reaction without an induction period and the nature of the reaction may gradually change from heterogeneous to homogeneous without any indication in the reaction profile. To prove the heterogeneous nature of the catalyst, the leaching studies of the two effective catalysts V(5)ZrPC, VZrSiPCH catalyst were carried out. The catalyst was removed by filtration after second hour from the reaction mixture and the mother liquor was again subjected for further reaction at the same conditions for an hour. The conversion remains more or less constant after the removal of the catalyst showing that metal ions were not leached from the catalyst surface during the oxidation process. The quantitative analysis of filtrate was also done which confirmed the absence of metal ions in the filtrate.

Table 7.3 Leaching studies

Catalyst	Time (h)	Conversion of benzyl alcohol (%)	Product distribution (%)	
			Benzaldehyde	Benzoic acid
V(5)ZrPC	2	32	96	4
	3	33	94	6
VZrSiPCH	2	36	94	6
	3	36	93	7

7.2.9 Reusability studies

The advantages of heterogeneous catalysis include the easy separation of catalysts from the final reaction mixture and subsequent reusage of the catalysts. The recycling of the catalyst for the same reaction is also a measure of catalyst structural stability. To study the reusability, the catalysts were removed

from the reaction mixture after the reaction by filtration. It was thoroughly washed with acetone and dried in an air oven and activated for 3 hours at 400^0C. The same catalyst was used again for carrying out another reaction under the same reaction conditions. The catalyst retained its activity even after fourth cycle. A slight decrese in selectivity of benzoic acid is observed after each cycle.

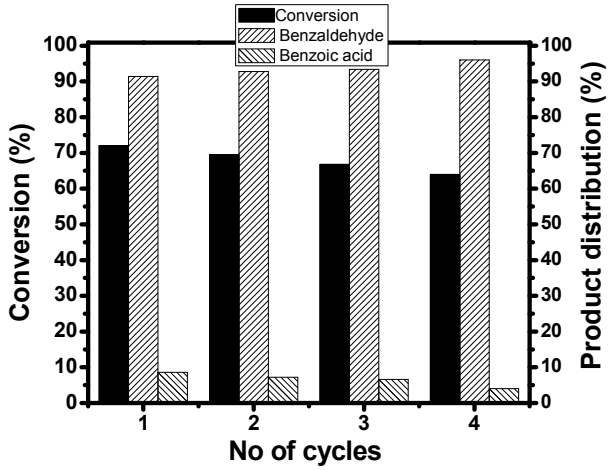

Figure 7.9 Reusability studies of VZrSiPCH for oxidation of benzyl alcohol.

7.3 Conclusions

- Various metal incorporated PILCs and PCHs were effectively utlilised for the oxidation of benzyl alcohol under milder reaction conditions with green oxidant hydrogen peroxide.
- The imperative roles played by the various reaction conditions were established and various reaction conditions are optimized to get maximum conversion.
- In metal Incorporated PILCs conversion increases with increase in metal content and good correlation is obtained with conversion and metal content.

- In metal incorporated PCHs a good correlation is obtained with conversion and methyl styrene selectivity in cumene cracking reaction.
- Vanadium incorporated PILCs and PCHs were found to be the effective catalyst for the oxidation of benzyl alcohol.
- Metal leaching studies revealed the true heterogeneous nature of the catalysts. The catalysts were found to be reusable and are resistant to rapid deactivation.

References

[1] R. Liu, X. Liang, C. Dong J. Am. Chem. Soc., 126 (2004) 4112.

[2] T. Hudlicky, J. D Price, F. Rulin, T. Tsunoda, J. Am. Chem. Soc., 112 (1990) 9439.

[3] A. Dijiksman, A. M. Gonzalez, A. M Payerra, J. Am. Chem. Soc., 123 (2001) 6826.

[4] Y. Uozumi, Y. M. A Yamada, Chem. Record, 9 (2009) 51.

[5] T. Mallat, A. Baiker, Chem. Rev., 104 (2004) 3037.

[6] C. P. Vinod, K.Wilson, A. F. Lee, J. Chem. Technol. Biotechnol., 86 (2011) 161.

[7] D. V. McGrath, R.H. Grubbs, J.W. Ziller, J. Am. Chem. Soc., 113 (1991) 3611.

[8] D. A. Knight, T. L. Schull, Synth. Commun., 33 (2003) 827.

[9] P. J. Miedziak, Q. He, J. K Edwards, S. H Taylor, D.W Knight, B. Tarbit, Catal. Today, 164 (2011) 315.

[10] N. Worz, A. Brandner, P. Claus, J. Phys. Chem. C, 114 (2010) 1164.

[11] U. R. Pillai, E. S. Demessie, Green Chem., 6 (2004) 161.

[12] S. E. J. Hackett, R. M. Brydson, M.H. Gass, I. Harvey, A. D. Newman, K. Wilson, Angew Chem. Int. Ed., 46 (2007) 8593.

[13] J. Chen, Q.H. Zhang, Y.Wang, H.L Wan, Adv Synth. Catal. 350 (2008) 453.

[14] F. Li, Q. H. Zhang, Y. Wang, Appl. Catal. A : Gen., 334 (2008) 217.

[15] A. Villa, D. Wang, N. Dimitratos, D.S. Su, V. Trevisan, L. Prati, Catal. Today.,150 (2010) 8.

[16] A. Corma, H. Garcia, A. Leyva, J. Mol. Catal. A: Chem., 230 (2005) 97.

[17] C.Y. Ma, B. J. Dou, J. J. Li, J. Cheng, Q. Hu, Z. P Hao, Appl. Catal. B: Environ., 92 (2009) 208.

[18] J. C. Hu, L. F Chen, K. K. Zhu, Catal. Today., 122 (2007) 277.

[19] R. L. Oliveira, P. K. Kiyohara, L. M. Rossi, Green Chem.,11 (2009) 1366.

[20] P. Vinod, K. Wilson, A. F. Lee, J. Chem. Technol. Biotechnol., 86(2011) 161.

[21] T. Iwahama S. Sakaguchi, Nishiyama, Tetrahed. letter., 36 (1995) 6923.

[22] T. Iwahama, Y. Yoshino, Y. Ishil, J. Org. Chem., 65 (2000) 6502.

[23] I. E. Marko, P. R. Giles, M. Tsukarazaki, J. Org. Chem., 64 (1999) 2433.

[24] N. S. Bijlani, S. B. Chandalia, Indian Chem. Eng., 23 (1981) 44.

[25] L. F. Liotta, A. M. Venezia, G. Deganello, A. Longo, A. Martorana, Catal. Today, 66 (2001) 271.

[26] I. E. Marko, P. R Giles. M. Tsukazaki, J. Am. Chem. Soc., 119 (1997) 12661.

[27] M. Hasan, M. Musawir, P.N. Davey, I.V Kozhevnikov, J. Mol.Catal. A, 180 (2002) 77.

[28] V. R. Choudhary, R. Jha, P. Jana, Green Chem., 9 (2007) 267.

[29] K. O Xavier, J. Chacko, K. K. M. Yusuff, Appl. Catal. A, 258 (2004) 251.

[30] H. Han, S. Zhang, H. Hou, Y. Fan, Y. Zhu, Eur. J. Inorg. Chem., 8 (2006) 1594.

[31] V. R. Choudhary, D. K. Dumbre, V. S. Narkhede, S. K. Jana, Catal. Lett., 86 (2003) 229.

[32] G. Wu, X. Wang, J. Li, N. Zhao, W. Wei, Y. Sun, Catal. Today., 131 (2008) 402.

[33] V. R. Choudhary, D. K. Dumbre, B. S. Uphade, V. S. Narkhede, J. Mol. Catal. A: Chem., 215 (2004) 129.

[34] S. Endud, K. L. Wong, Micropor. Mesopor. Mater., 101 (2007) 256.

[35] A. Z. Jia, L. L. Lou, C. Zhang, Y. Zhang, S. Liu, J. Mol. Catal. A: Chem., 306 (2009) 123.

[36] J. Du, D. Liu, J. Gui, X. Zhang, L. Song, Z. Sun, J. Petrochem. Univ., 19 (2006) 13.

[37] V. K Ambili, Studies on catalysis by ordered mesoporous SBA-15 Materials modified with transition metals, PhD thesis, CUSAT(2011).

[38] K. George, Studies on surface properties and catalytic activity of some chromites and related spinels, PhD thesis, CUSAT (2006).

[39] X. Wang, G. Wu, J. Li, N. Zhao, W. Wei, Y. Sun, Catal. Lett., 119 (2007) 87.

[40] F. Adam, O. W. Ting, J. Phys. Sci., 24 (2013) 1.

[41] K. Liu, T. Chen, Z. Hou, Y. Wang, L. Dai, Catal. Lett., 144 (2014) 314.

[42] G. Chen, Y. Zhou, Z. Long, X. Wang, J. Li, J.Wang, Appl. Mater. Interfaces., 6 (2014) 4438.

[43] G. Zhan, Y. Hong, F. Lu, A.R. Ibrahim, M. Du, D. Sun, J. Huang, Q. Li, J. Li, J. Mol. Catal. A: Chem., 366 (2013) 215.

[44] M. Ilyas, M. Sadiq, Chem. Eng. Technol., 30 (2007) 1391.

[45] M. Sankar, E. Nowicka, E. Carter, G.J. Hutchings**,** Nat. Commun.,5 (2014) 3332.

[46] M. Amini, H. Naslhajianb, S. Morteza, F. Farnia, New J. Chem., 38 (2014) 1581.

[47] C. Doornkamp, M. clement, X. Gao, G. Deo, I.E. Wachs, V. Ponec, J. Catal., 185 (1999) 415.

[48] V. Mahdavi, H. R. Hasheminasab, Appl. Catal. A: Gen.**,** 482 (2014) 189.

.....ꕥ.....

Chapter 8

PREPARATION, CHARACTERIZATION AND CATALYTIC ACTIVITY STUDIES OF TUNGSTOPOSPHORIC ACID SUPPORETED SILICON POROUS CLAY HETEROSTRUCTURES

Catalysis by heteropoly acids (HPAs) has attracted increasing attention in both academic and industrial fields because of their unique strong Bronsted acidity, multi functionality and structural alterabilility. The bulk heteropoly acids have some disadvantages like extremely small surface area and high solubility in polar solvents. Hence, to improve catalytic applications of HPAs, it has to be dispersed on high surface area of carriers such as silica, active carbon, molecular sieves Al_2O_3 and so on. Owing to relatively large pore size and surface area of PCHs, heteropoly acids can be successfully anchored on the mesoporous channels of silicon pillars of PCHs. This chapter includes brief introduction to heteropoly acids and its application in catalysis. Heteropoly acid dodeca tungstoposphoric acid is supported on PCHs by three methods, direct method, anchoring and impregnation methods. The prepared catalysts were characterized by various physico chemical methods and the catalytic activity was tested for acetalization of cyclohexanone.

8.1 Introduction

Heteropoly acids attracted the interest of scientific community due to their strong Bronsted acid sites [1-2], redox property, multi functionality [2-3], pseudo liquid behavior and structural mobility [4]. Solid HPAs possess a discrete ionic structure, comprising fairly mobile basic structural units heteropoly anions and counter cations (H^+, H_3O^+, $H_5O_2^+$ etc.) unlike the network structure of zeolites and metal oxides. This unique structure manifests itself to exhibit extremely high proton mobility called "pseudo liquid phase" [4]. In the last two decades, the broad utility of HPA as acid and oxidation catalysis has been demonstrated in a wide variety of synthetically useful selective transformations of organic substances [3-4]. Several new industrial processes based on HPA catalysis, such as hydration of olefins, oxidation of methacrolein, propene and butenes, polymerization of tetrahydrofuran etc., have been developed and commercialized [4-6].

Hetero polyacids (HPA) are poly oxometalates of general formula $[X_xM_mO_y]^{(q)}$ where X is the hetero atom such as B, Al, Si, Ge and P, located at the central of HPA, usually chosen from among a wide variety of group I to VII elements in the periodic table. M is the addenda atoms such as Mo, W, V, Ta, Nb, Os that are attached to hetero atoms through oxygen atoms and q is the charge usually varies from -3 to -28 [1].

Heteropoly acids have been known since the work of Berzelius [7] on the ammonium 12-molybdophosphate in 1826. However, the study of heteropoly anion chemistry did not accelerate until the discovery of the tungstosilicic acids and their salts in 1862 by Marignac [8]. He prepared and analyzed two isomers of 12-tungstosilicic acid viz. tungstosilicic acid and silicotungstic acid now known as α and β isomers. Thereafter, the field

developed rapidly, so that over 60 different types of heteropoly anions (giving rise to several hundred salts) had been described by the end of first decade of this century. The first step towards understanding the structure of heteropoly anions was taken by L. C. Pauling in 1929. Pauling [9] proposed a structure for 12:1 complexes based on an arrangement of twelve MO_6 octahedra surrounding a central XO_4 tetrahedron. After Pauling's proposal, in 1933 Keggin [10, 11] solved the structure of $[H_3PW_{12}O_{40}].5H_2O$ by powder X-ray diffraction and showed that the anion was indeed based on WO_6 octahedral units. As suggested by Pauling, these octahedra being linked by shared edges as well as corners. The application of X-ray crystallography for the determination of heteropoly structures accelerated the development of heteropoly acid chemistry and various types of structures were discovered.

8.1.1 Structure of heteropoly acids

Based on molecular formulae, type of sharing, building units and central units heteropoly acids are classified in to Keggin, Dawson, Waugh, Anderson, Silvertone etc [12-14]. The details are summarized in table 8.1.

Table 8.1 Structure of heteropoly acids

Types	Molecular Formulae	Building Units	Type of sharing	Central Groups
Keggin	$X^{n+}M_{12}O_{40}^{(8-n)-}$	M_3O_{13}	Edge	XO_4
Dawson	$X_2^{n+}M_{18}O_{62}^{(16-2n)-}$	M_3O_{13}	Edge	XO_4
Anderson	$X^{n+}M_6O_{24}^{(12-n)-}$	M_2O_{10}	Edge	XO_6
Waugh	$X^{n+}M_9O_{32}^{(10-n)-}$	M_3O_{13}	Edge	XO_6
Silvertone	$X^{n+}M_{12}O_{42}^{(12-n)-}$	M_2O_9	Face	XO_{12}

The ideal Keggin structure of $[PW_{12}O_{40}]^{3-}$ (dodeca phosphotungstate) is of α type withs Td symmetry consists of a central XO_4 tetrahedron

(X = heteroatom or central atom) surrounded by twelve MO_6 octahedra (M = addenda atom). The twelve MO_6 octahedra comprise four groups of three edge-shared octahedra, the M_3O_{13} triplet [7,8], which have a common oxygen vertex connected to the central heteroatom. The oxygen atoms in this structure fall into four classes of symmetry equivalent oxygens: $X\text{-}O_a\text{-}(M)_3$, M-Ob-M, connecting two M_3O_{13} units by comer sharing; $M\text{-}O_c\text{-}M$, connecting two M_3O_{13} units by edge sharing and O_d-M, The basic structure of heteropoly anion molecule itself is called a "primary structure" and is formed from the condensation of oxo anions.

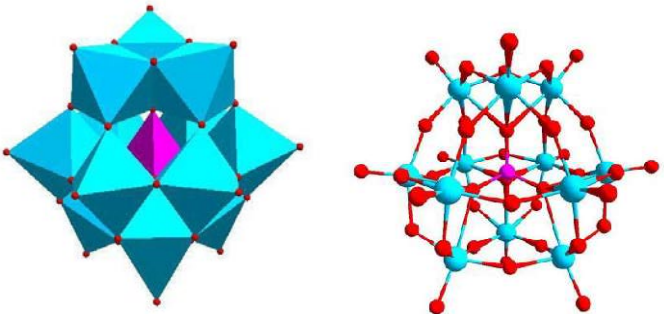

Figure 8.1 Keggin structure of heteropoly acids

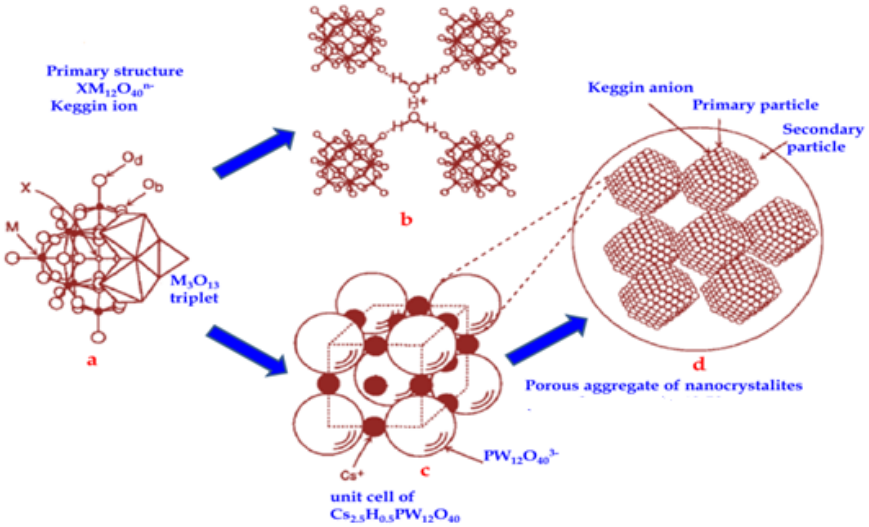

Figure 8.2 Primary, secondary and tertiary structure of heteropoly acids

The secondary structure of the solid HPAs is formed from the coordination of the heteropoly anion with acidic protons, other cations and/or water molecules of hydration. Solid HPAs assembled to form the tertiary structure.

Dodeca tungstophosphoric acid (DTP) is the most stable among all HPAs and is commonly used for acid catalysis since it possesses the highest Bronsted acidity. The acidity of these compounds are higher than that of well known solid acid catalysts such as silica-alumina, H_3PO_4/SiO_2, HX and HY zeolites [12]. Heteropoly acids are much stronger than the oxo acids of constituent elements and ordinary mineral acids. The central atom is the important factor in determining the acid strength and the acidity is related to the total charge on the anion than to the type of metal atom in the shell HPA. In solutions, the acid properties of HPAs are quite well documented in terms of dissociation constants and Hammett acidity function [13]. The determination of the acidity of HPAs by use of Hammett indicators found that the HPAs acidity ranged from +6 and -13. The acid strength of crystalline HPAs decreases in the series $H_3PW > H_4SiW > H_3PMo > H_4SiMo$ [2,13] which is identical to that in solutions. Usually, relative catalytic activities of HPAs are consistent with this order both in homogeneous and in heterogeneous systems. The strong acidity of HPAs is due to

i) Dispersion of the negative charge over many atoms of the polyanion

ii) The fact that the negative charge is less distributed over the outer surface of the polyanion owing to the double-bond character of the M=O bond, which polarizes the negative charge of O to M.

HPAs have a fairly high thermal stability. The Keggin-type PW, SiW, PMo, and SiMo decompose at 465, 445, 375 and 350°C respectively [2,11]. Heteropoly acids are extremely soluble in polar solvents such as water, lower alcohols, ethers, esters, ketones etc. Heteropoly acids are not readily soluble in non polar solvents like hydrocarbons.

In homogeneous liquid phase catalysis, the advantages of the HPAs are more distinctive due to their low volatility, low corrosiveness, high acidity, activity and flexibility. Depending on the reaction conditions, the activity per mole of protons in HPA may be higher by a factor of 3−100 times than sulphuric acid in Bronsted acid catalyzed liquid phase reactions [6]. But, the main disadvantages of HPAs as catalysts are their relatively low surface area (1–10 m^2/g) and the problem of separation from the reaction mixture. These disadvantages are mainly overcome by the following modification methods.

In one method, catalysts are prepared in the form of water insoluble alkali metal salts of HPA by partial substitution of acidic protons with Cs^+, K^+, NH_4^+ etc. [15,17]. These HPA salts have larger surface area than the pure acids and exhibit microporous or mesoporous behavior. Cesium salts of dodeca tungstophosphoric acid (DTP) have been reported to be better catalysts than DTP itself [6]. The partial substitution of protons of HPAs with Cs^+ renders them with higher surface area and improved thermal stability. $Cs_{2.5}H_{0.5}PW_{12}O_{40}$ was found to be the most active catalyst due to its insolubility in liquids as well as in polar solvent, however, its small particle size limits its catalytic applications in commercial fixed bed or slurry reactor and separation of the catalyst from the liquid remains a problem. Unfortunately, direct impregnation $Cs_{2.5}H_{0.5}PW_{12}O_{40}$ is not possible due to its insolubility in any kind of solvent and is quite challenging [15].

The second method is to support HPAs on acidic or neutral supports such as zeolite [5] SiO_2 [20], TiO_2 [21], ZrO_2 [22-23], acidic ion-exchange resins [24] and active carbon [25] by impregnation method. Impregnating HPAs on these supports significantly increases the specific surface area, which is very important for heterogeneous catalysis process. Apparently, besides the surface area, particle size, pore structure and distribution of the protons of HPAs, the nature of supports and interaction of HPAs with support is highly influential on catalytic activity. Acidity of the HPAs for certain catalytic reactions can be adjusted by choosing a suitable support. The acid strengths of HPA supported on some of the materials mentioned above were found to be lower than that of bulk HPA due to the interaction of HPA with surface functional groups of supports. It has been found that the basic solids like MgO [5,8] and Al_2O_3 [26] tend to decompose the HPAs, causing a significant decrease in their catalytic activities. Silica is the most often used support since it is relatively inert towards HPAs. However, further research showed that supported HPA was unstable with tendency to dissolve in polar solvents, which resulted in rapid activity loss after recycles.

Third method involve loading HPA in mesoporous materials utilizing the large pore size, high specific surface area, uniform mesoporous channels and high thermal stability of those materials. Mesoporous silica supported HPA may be easily obtained by the wet impregnation technique. After stirring the mixture of mesoporous silica and HPA in water/methanol, HPA molecules can be introduced in the channels through the interaction between Si-OH and terminal oxygen of heteropoly anions. The pore size is large enough to accommodate the HPAs in their mesoporous channels. The large pore size of mesoporous materials has high mass transfer efficiency, which benefits the

reactions involving large organic molecules. Furthermore, the supported HPAs can be transformed into metal oxides under controllable thermal treatment conditions [27]. With high loading of HPAs, nanowires and even three-dimensional nano-structured metal oxides of uniform morphology can be fabricated by reverse replication of the channels of mesoporous silica. There were large number of reports where heteropoly acids were supported on mesoporous materials such as MCM-41 [28-30], SBA-15 [2,31] or aluminophosphates [32]. This method also suffers from some drawbacks. The key issues to be addressed in supported heteropoly acid systems are

Firm fixing to the support
Maintaining the basic structure
Thermal stability

In this context, immobilization of HPAs by means of chemical bonding via functionalization appears to be a proper approach. In order to avoid leaching, the grafting method has been adopted to immobilize HPA on the supports. As reported by Vansant and coworkers [33], the silica surface may be modified with amino alkoxysilanes, which provides functional amino groups on the silica surface. Heteropoly acids and the basic amine groups form $\equiv Si(CH_2)_n\ NH_3 \cdot HPA$ salt which results the strong anchoring of HPAs and prevents the leaching of HPAs [34]. These types of heterogeneous catalysts are solvent-tolerant in the reactions involving polar reaction media. Even photo catalytic degradation of organic pollutants can be conducted with these catalysts in water. This approach has successfully been used by several researchers to immobilize $H_3PW_{12}O_{40}$, $H_4SiW_{12}O_{40}$ [34-36] and transition metal substituted polyoxometalates [37,38] on functionalized MCM-41 [39-40], SBA-15 [2,41] amorphous silica and silica-gel surface.

Introduction of HPA in to mesoporous channels of silica by direct method is also reported by several researchers [42-45]. HPAs can be incorporated into the silica matrix through sol-gel processes. These are simple routes to prepare silica-supported HPA materials in comparison with the grafting methods. HPA can be immobilized into the silica matrix strongly by electrostatic or complex interactions between the silica support and the HPA. The obtained HPA in silica materials are insoluble in polar solvents. They are thermally stable and readily separable. HPA in silica matrix exhibits resistance to leaching, even after hot water extraction at 373 K [10].

Clay as support for immobilization of heteropoly acids

Clays were also used as an effective support for immobilization of heteropoly acids. G.D Yadav et al. in their pioneering work supported Cesium exchanged heteropoly acid on Montmorillonite K10 by two step process in which cesium is first exchanged with interlayer cations of clay followed by impregnation of DTP and utilized the prepared catalyst for various organic transformations [6]. B.G Mishra et al. dispersed phosphomolibdic acid in to sulphated zirconium pillared clay and utilized the material for the synthesis of β-aminocarbonyl compounds in aqueous media. HPW loaded KSF is executed for the one pot synthesis of α-aminonitrile [46]. B. Li et al. immobilized tungstophosphoric acid on the mesoporous channels of silicon pillared clay by direct method [45].

Catalysis by supported heteropoly acids

Supported HPAs have been used in a variety of organic transformations such as acylation, akylation, esterification, isomerization, oxidation and hydrogenation. Enormous studies have been carried out on catalysis by supported HPAs by different groups and some of them are listed in the Table 8.2.

Table 8.2 Reactions of supported heteropoly acids

Catalyst	Reaction	Remarks /Reference
		Alkylation
$Cs_{2.5}H_{0.5}PW_{12}O_{40}$/ K10 clay	Alkylation of aniline with MTBE	47
	Tertiary butylation of phenol	6
	Isopropylation of benzene	48
	Isopropylation of phenol	49
	Alkylation of xylene	50
	Methylation of hydroquinone	51
	Disproportionation of ethyl benzene	52
		Alkylation
HPW/SBA-15	Tertiary butylation of phenol	31
HPW/MCM-41	Alkylation isobutene with 2 butene	53
$H_3PW_{12}O_{40}$/ TiO_2	Benzylation of phenol	54
$H_3PW_{12}O_{40}$/ TiO_2	Alkylation of para cresol	55
$H_3PW_{12}O_{40}$/ Ziconia or Titania	Alkylation of 2 Methyl naphthalene	56
60% PTA/ MCM-41	Alkylation of 1 dodecene with benzene	30
$H_3PW_{12}O_{40}$/ MCM41	Trans-de-te butylation of DBMP	29
$H3PW_{12}O_{40}$/ $H_4SiW_{12}O_{40}$/ $Cs_{2.5}$ $PW_{12}O_{40}$	Synthesis of bisphenol from phenol and acetone	57
$H_3PW_{12}O_{40}$ and $H_4SiW_{12}O_{40}$ supported on zirconia/ neutral alumina	Alkylation of phenol and cresols	58
		Acylation
$H_3PW_{12}O_{40}$ / Zeolites	Acylation of anisole with α, β unsaturated acid	59
$H_3PMO_{12}O_{40}$ or $H_3PW_{12}O_{40}$ promoted zirconia	Acylation of anisole	60
$H_3PW_{12}O_{40}$/ZrMCM-41	Veratrole acylation	61
Silicotungstic acid supported in Titania	Veratrole acylation	62
$Cs_{2.5}H_{0.5}PW_{12}O_{40}$/K10 clay	Benzoylation of para xylene	63
		Esterification
$H_3PW_{12}O_{40}$ or its Ce III salt	Esterificationof 2, 6-pyridinedicarboxylic acid with n-butanol	64
$H_3PW_{12}O_{40}$/SBA-15	Esterification of acetic acid with butanol	66

HPW/APTES-MCM41	Esterification acetic acid with butanol	67
Silica supported HPW heteropoly acid intercalated	Valorization of the essential oils	65
Zn/Al HTlc	Esterification of acetic acid and n-butanol	68
		Acetalization
CsDTP/K10	Ketal formation of cyclohexanone with glycerol	69
15% PTA/MCM-41	Reaction of Benzaldehyde with pentaerythritol	70
		Isomerization
$H_3PW_{12}O_{40}/SiO_2$ or ZrO_2 or Nb_2O_3	Isomerization of α-pinene and longifolene	71
Silica supported $H_3PW_{12}O_{40}$	Isomerization of styrene oxide to phenylacetaldehyde	72
		Electrophilic substitution
HPW supported on zirconia	Bromination of phenol	73
HPW supported on titanium phosphate	Bromination of phenol	74
$H_3PW_{12}O_{40}$ and $H_3PMo_{12}O_{40}$ intercalated zinc aluminium hydrotalcite	Nitration of phenol	75
$H_3PW_{12}O_{40}$ /Zirconia	Nitration of phenol	76
Molybdovanadophosphoric acid /zirconia	Hydroxylation of phenol	77
		Miscellaneous
Cs HPW	Dehydration of glycerol	78
HPA/KSF	One pot synthesis of α amino nitriles	46
HPW –APTES/SBA-15	One-pot tandem conversion of benzaldehydedimethylacetal to trans-1-nitro-2-phenylethylene	3
Grafted $K_{11}[Ce(PW_{11}O_{39})_2]$ on Functionalised SBA-15	Cyclohexene oxidation	80
PW_{12} /FSM-16	Electrocatalytic reduction for nitrite	81
PW_{12} on amine functionalized SiO_2	Tetrahydrofuran polymerization	82
HPW/SPC	DBT oxidation	45

8.2 Objectives of the present work

Dispersing of HPAs on solid supports with high surface area is important for catalytic applications. In general, HPAs strongly interact with supports at low loading levels, while the bulk property of HPAs prevails at high loading levels. Enhanced catalytic activity of HPAs was found when they were supported on to strongly acidic support. The higher activity was explained by the synergism due to the interaction of the heteropoly anion and protons of the support. In the present study silicon porous clay heterostructures (SPC) were selected for the immobilization of dodeca tungstophosphoric acid (DTP) due to the following reasons.

- SPC materials have high surface area and pore diameter.
- They have high thermal stability.
- Presence of surface Si-OH groups.
- Since they posses Bronsted acidity, substantial interaction between heteropoly anion and Bronsted acidic sites is expected.

8.3 Preparation of DTP incorporated silicon porous clay heterostrutures

DTP incorporated on porous clay heterostructures by three different methods

A) Direct method

B) Anchoring heteropoly acid in functionalized silicon porous clay heterostructures

C) Impregnation method.

8.3.1 Direct method

3g of NaM was refluxed with 100 mL of 0.2M Cetyltrimethyl ammonium bromide (CTAB) solution for 4 hour. Then, the pH of the gel was adjusted to 2 with dil.HCl solution. Subsequently, required amount of $H_3PW_{12}O_{40}\cdot 5H_2O$ was dissolved in ethanol, and added into the gel under vigorous stirring. After the mixture was stirred for 6 hours, tetraethyl orthosilicate (TEOS) along with hexa decylamine(HDA) was added, followed by stirring for 12 h at room temperature. The molar ratio of clay, CTAB: HDA: TEOS is maintained as 1:2:10. Then the mixture was transferred into an autoclave and heated for at 110^oC for 24 h. After wards, the autoclave was cooled, and the product was separated by filtration, thoroughly washed with deionized water, and dried in an oven at 110^oC. Finally, the dried sample was calcined at 400 ^oC for 6 h in a muffle furnace to get DTP incorporated SPC.

Fig 8.3 illustrates the proposed formation mechanism of the DTP-SPC by direct method. When NaM was exchanged with cationic surfactant CTAB, the surfactants form micelles in the interlayer region. Then pH was adjusted to 2. When DTP was introduced, $W_{12}O_{40}^{3-}$ can be attracted into the interlayer and substitute Br^- and Cl^- in the shell surrounding the micelle. Furthermore, the addition of HCl aqueous solution can keep the solution in a strong acidic environment to retain the Keggin-type heteropoly acid intact. When TEOS along with co- surfactant HDA was added into the gel mixture, it would intercalate into the clay interlayer region by solvation and rapidly hydrolyze in acidic condition to form the protonated $H_5SiO_4^+$ monomers. The silicate cations would interact with the anionic shell surrounding the surfactant micelle to trap both X^- (Cl^-, Br^-) and heteropoly anions, leading to the formation of a silica layer around the surfactant template [45]. Washing and drying steps did

not remove the heteropoly anions since they were trapped inside the clay interlayer. After the calcination step, the silica layer around template further condensed to yield the completely cross-linked framework of silica pillars with DTP molecules fixed into the pore walls while surfactant is removed from the pore system.

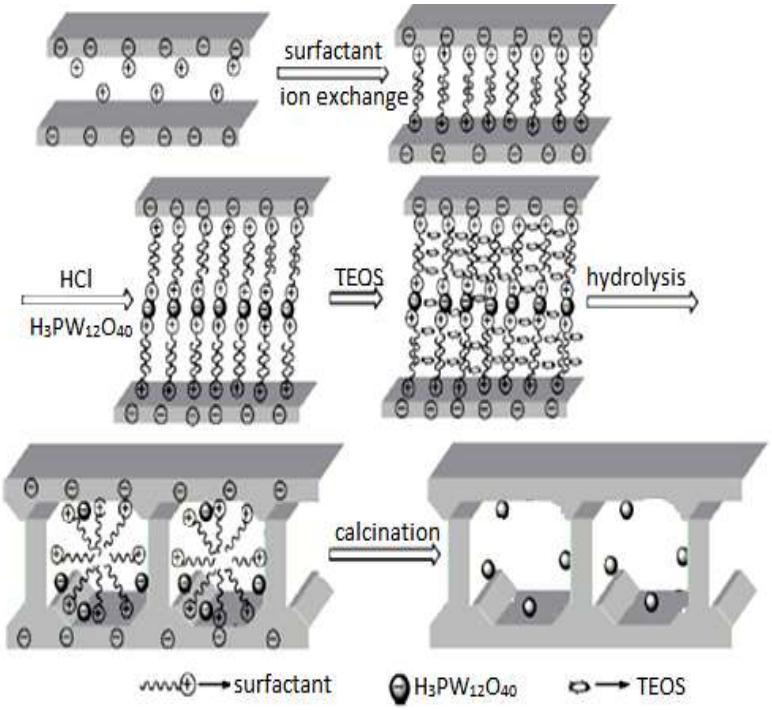

Figure 8.3 Formation mechanism of catalyst preparation by direct method.

8.3.2 Anchoring DTP into functionalized Porous clay heterostructures

Silicon porous clay heterostructure (SPC) was prepared by the procedure described in section 2.2.2. SPC was treated with a 10 % of 3-amino propyl triethoxy silane (APTES) in toluene for 6 hours at room temperature. It was filtered, washed several times with acetone and dried at 80^{o}C for 6 hours. This functionalized SPC is refluxed with required amount of DTP in ethanol and

stirred for overnight. It was then filtered washed and dried at 80° C for 6 hours to get DTP/SPC (F). Figure 8.4 shows schematic representation of the anchoring of tungstophosphate groups on functionalized SPC.

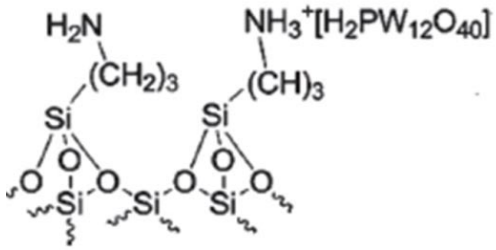

Figure 8.4 Anchoring of DTP molecules on functionalized SPC

8.3.3 Wet Impregnation

The required amount of DTP is dissolved in ethanol and is refluxed with SPC for 6 hours. It was filtered, dried at 80°C for 6 hours and calcined at 250°C to get DTP/SPC (IM).

The following catalysts were prepared and characterized.

Table 8.3 Catalyst Notation

Catalyst Notation	Description
SPC	Silicon porous clay heterostructure
DTP (10) /SPC	10 % DTP loaded SPC by direct method
DTP (20) /SPC	20 % DTP loaded SPC by direct method
DTP (30) /SPC	30 % DTP loaded SPC by direct method
DTP (30) /SPC (IM)	30 % DTP loaded SPC by impregnation method
DTP /SPC (F)	DTP anchored on functionalized SPC

8.4 Characterization of catalysts

8.4.1 Elemental Analysis

Since direct determination of the amount of tungstophosphoric acid in catalyst is not possible the amount of tungsten in the samples were estimated by ICP AES analysis. The figures in the bracket denote the theoretical weight % of tungsten loaded in the samples. In all cases the percentage weight of tungsten detected was less than that of theoretical one. In 30 % DTP loaded samples, catalyst prepared by impregnation method showed higher tungsten content and functionalized samples showed least tungsten content.

Table 8.3 Elemental analysis of catalysts

Catalyst	Wt. % of tungsten
DTP (10) /SPC	4.81 (7.65)
DTP (20) /SPC	11.78 (15.30)
DTP (30) /SPC	17.90 (22.95)
DTP (30) /SPC (IM)	20.80 (22.95)
DTP /SPC (F)	10.58 (22.95)

8.4.2 XRD analysis

Wide angle XRD pattern of pure DTP and DTP incorporated catalysts are given in Figure 8.4. Pure DTP shows peaks corresponding to the primary, secondary and tertiary arrangement of Keggins structure. The characteristic peaks of bulk DTP were observed at 2θ of 20.6°, 25.4° and 34.6° [82]. DTP can be supported as molecules or aggregates on the mesoporous material. If the DTP molecules were molecularly dispersed on the inner surface of the pores without forming a secondary structure, clear diffraction patterns of DTP

were not expected. In lower DTP loaded catalysts, peaks corresponds to DTP is absent as it is uniformly distributed on mesoporous channels of PCHs. The DTP diffraction peaks attributed to its secondary structure are considerably reduced due to high dispersion, but its molecular structure may be still maintained. Higher DTP loaded catalysts (30%) contain some characteristic peaks corresponding to DTP crystals with small shift or broadening. This is in agreement with the literature data that the DTP forms crystal phase on the silica surface above 20 % loading [82]. Peaks at 2θ value of 19.6^0 and 35.1^0 corresponds to the reflection from (110) and (130) planes of 2:1 phyllosilicate clay and are present in all catalysts indicating that the basic clay layer structure is preserved even after modification.

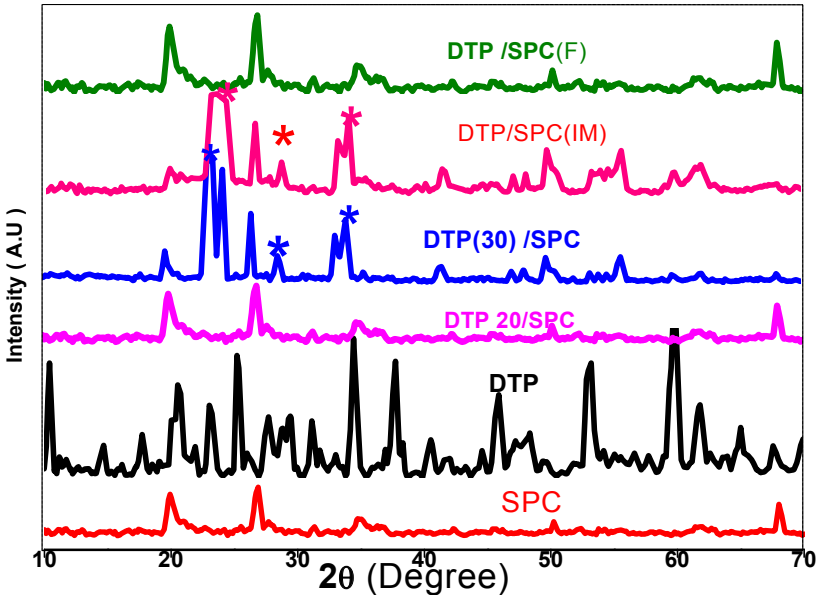

Figure 8.5 Wide angle XRD patterns of catalysts

Low angle XRD pattern of catalyst are given in Figure 8.6. The bare SPC shows peak at 2θ value 1.98^0. A small shift in this peak to lower angle is noted for

catalyst prepared by direct method. The presence of peaks in small angle region implies that the mesoscopic ordering is preserved even after modification. For catalysts prepared by anchoring method, the intensity of the peak is reduced. Absence of sharp peaks in higher DTP loaded catalysts prepared by impregnation method is an indication for loss of ordering. In higher DTP loading, there is a chance for agglomeration of DTP crystals which leads to partial loss of structural organization that eventually results delamination of clay layers and structure with irregular porosity may be obtained in that case.

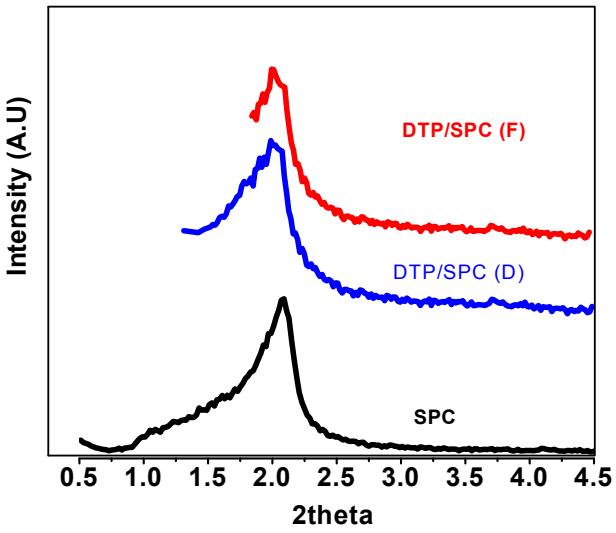

Figure 8.6 Low angle XRD patterns of catalysts

8.3.3 FT-IR Spectroscopy

FT-IR spectra of catalysts prepared by direct method and impregnation method in 600-1200 cm^{-1} region are shown in Figure 8.7. Bulk DTP showed the characteristic IR bands at 1080 cm^{-1} corresponds to asymmetric stretching of "P–O" in central tetrahedra, 980 cm^{-1} corresponds to asymmetric stretching of terminal "W=O", 890 and 801 cm^{-1} associated with the asymmetric vibrations

of the "W–O–W" in corner shared octahedra and edge shared octahedra respectively [31]. These characteristic bands are regarded as experimental evidences for the existence of Keggin type DTP molecules or molecular fractions in samples. The higher DTP loaded catalysts prepared by direct and impregnated method retained the characteristic peaks of DTP at 980 cm^{-1} and 890 cm^{-1}. However, their spectra are significantly different from each other, stronger characteristic peaks (W= O and W-O_c-W) at 980 cm^{-1} and 890 cm^{-1} indicate that the Keggin structure is more retained in impregnated sample than directly prepared one. Compared with the spectra of bulk DTP, red shifts in asymmetric stretching of "W= O" for the directly prepared and impregnated samples prove the intense chemical interaction between DTP and PCH materials. In all the catalysts the peak at 1080 cm^{-1} and 801cm^{-1} are obscured by presence of the asymmetric stretching peak of silica tetrahedra at 1050 cm^{-1} and asymmetric stretching frequency of alumina octahedral at 800cm^{-1} of PCHs materials respectively.

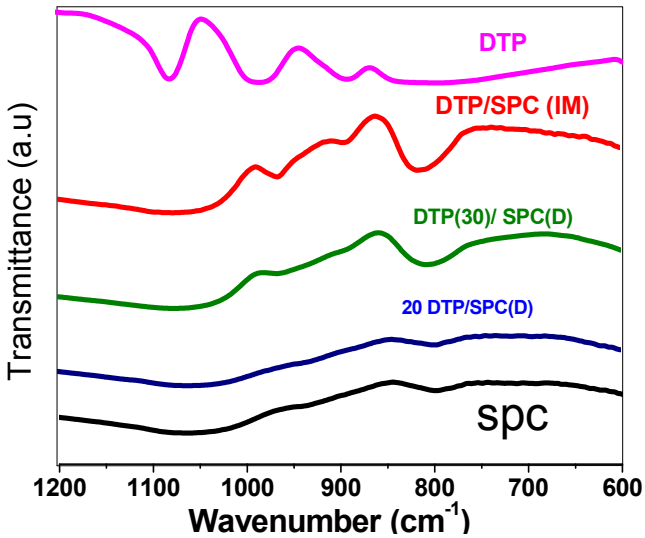

Figure 8.7 IR spectra of catalysts prepared by direct and impregnation method

IR spectrum of APTES functionalized SPC material and DTP anchored on functionalized SPC material are given Figure 8.8. In functionalized SPC a peak at 2950 cm^{-1} and 3470 cm^{-1} correspond to C-H stretching and N-H stretching vibration respectively. It confirms the functionalization of silanol groups with APTES in SPC. The intensity of OH stretching frequency decreases after functionalization. In DTP anchored functionalized SPC materials, the characteristic peaks of Keggin species is not visible as it may be obscured by the presence of other peaks in SPC or may be due to lower concentration of DTP.

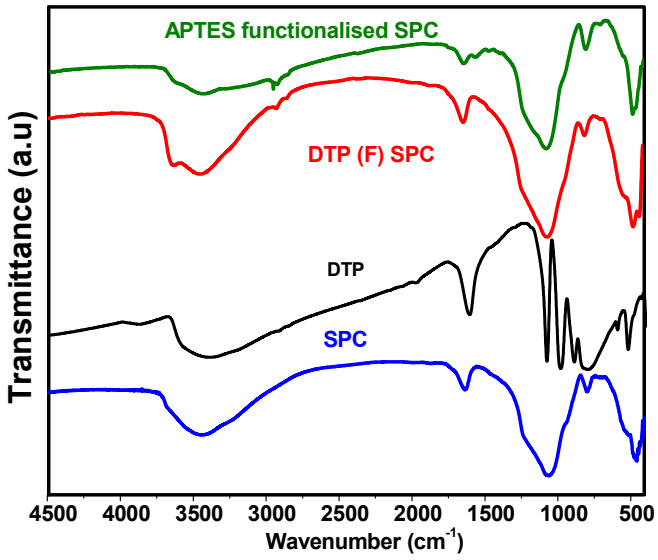

Figure 8.8 IR spectra of functionalized catalysts

8.4.4 Surface area and pore volume measurements.

The textural properties of catalysts are given in Table 8.5. The surface area, pore volume, average pore diameter etc decrease successively with increase in DTP content in direct prepared catalysts. This may be due to the occupancy of heteropoly anions inside the pore walls of the silica in between

the clay layers. The catalyst DTP/SPC (F) has lowest surface area, pore volume and pore diameter even though the DTP content is low. After the introduction of APTES and DTP, the surface area of SPC is reduced drastically. This may be attributed to the agglomeration of silica particles and/or occupation of pores after modification. More over most of the amino alkoxysilane group may be present near the pore opening which leads to partial pore blockage. A drastic reduction in surface area and pore volume due to pore filling is observed for catalysts prepared by impregnation method also. But 30 % DTP impregnated catalysts have higher pore diameter than direct prepared catalysts even though it contains higher DTP content. It may be due to partial delamination of clay layers after the incorporation of huge amount of DTP which may form complex structure with large pore diameter.

Table 8.5 Textural properties of catalysts

Catalysts	Surface area S_{BET} (m^2/g)	Pore volume cm^3/g	Pore diameter (Å)
SPC	441	0.7319	42.2
DTP (10) /SPC	334	0.6348	40.2
DTP (20) /SPC	293	0.4035	36.8
DTP (30) /SPC	236	0.3599	34.4
DTP (30) /SPC (IM)	183	0.3390	37.3
DTP /SPC (F)	158	0.2942	33.8

The adsorption isotherms of catalysts are shown in Figure 8.9. The adsorption isotherm of bare SPC is type IV with hysteresis loop H3 characteristics of the mesoporous materials with the cylindrical pores formed in gallery regions. The textural properties of porous clay heterostructures change up on DTP loading. The adsorption isotherm of directly prepared catalyst DTP (30) /SPC is of type IV with hysteris loop H2 corresponding to

ink bottle type pores. The catalyst DTP/SPC (IM) have adsorption isotherm of type IV corresponds to mesoporous material. The middle portion of hysteresis loop is similar to that of type H1 with steep increase in adsorption but towards the end it is like H4 /H3 hysteresis loop. This indicates a complex pore structure which probably formed due the delamination of clay layers due to high DTP loading.

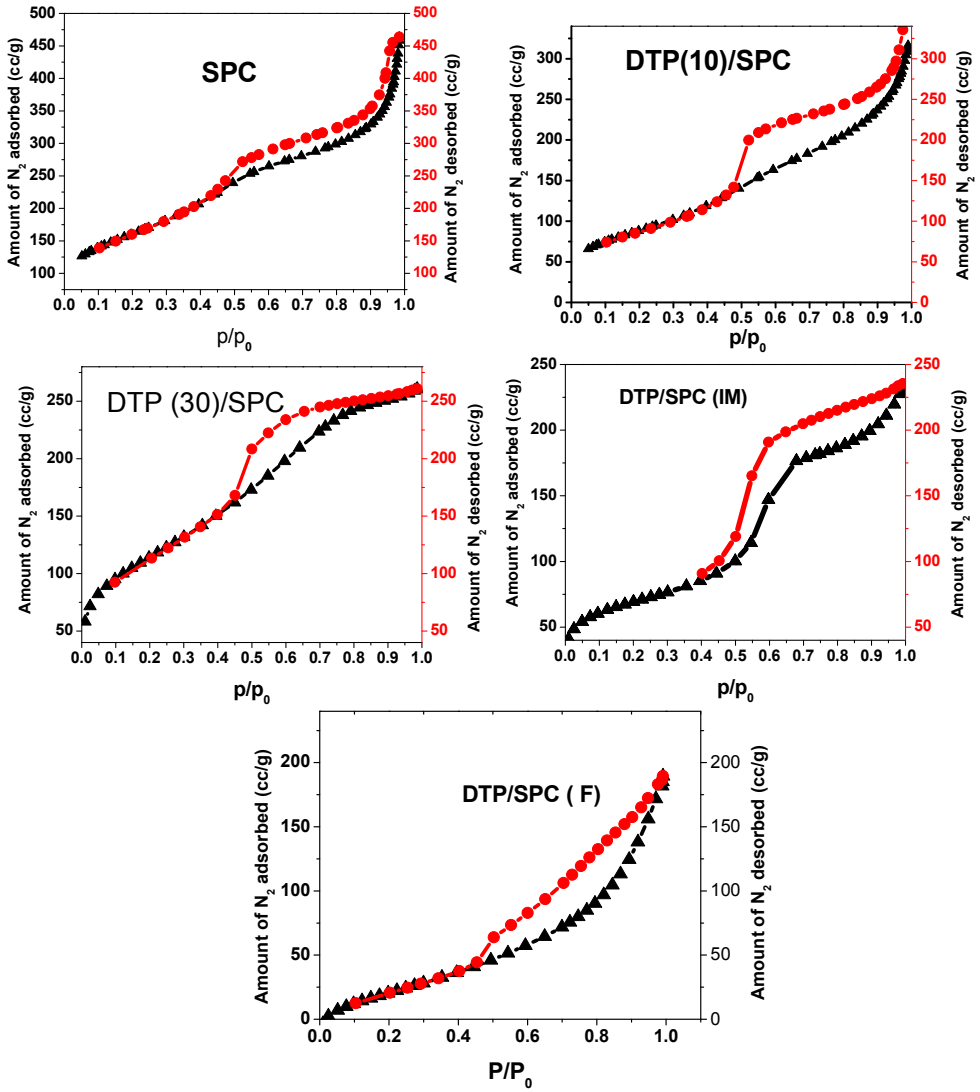

Figure 8.9 Adsorption isotherms of catalysts

8.4.5 Temperature Programmed Desorption of Ammonia (TPD of NH_3)

The cumulative acidity as well as acid site distribution of catalysts was determined by TPD of Ammonia. Bare SPC itself has reasonable acidity in weak and medium acidity region. Up on DTP incorporation, the weak and medium acidic sites increases and the increase in acidity is proportional to the amount of DTP incorporated. In DTP loaded catalysts, the catalyst DTP/SPC(F) have lowest acidity. In DTP/SPC(F) all the acidic sites may not be accessible to NH_3 molecules due to its smaller pore size and blocks in pores.

Table 8.6 Result of TPD of ammonia of catalysts

Catalyst	Weak (mmol/g) (35-200^{o}C)	Medium (mmol/g) (200-400^{o}C)	Strong (mmol/g) (400-600^{o}C)	Cumulative (mmol/g)
SPC	0.628	0.347	0.038	1.013
DTP (10) /SPC	0.742	0.463	0.041	1.246
DTP (20) /SPC	0.788	0.492	0.028	1.308
DTP (30) /SPC	0.884	0.517	0.043	1.444
DTP(30) /SPC (IM)	0.895	0.537	0.036	1.468
DTP /SPC (F)	0.658	0.463	0.018	1.139

8.4.6 X-ray Photoelectron Spectroscopy (XPS)

The nature of tungsten and its oxidation state in catalyst DTP (20)/SPC is studied using XPS. The survey scan of catalyst is given in Figure 8.10. The survey scan of catalyst is devoid of peak corresponding to phosphorous of Keggin species probably due to its low weight % and being surrounded by twelve W atom in the $PW_{12}O_{40}^{3-}$ anion.

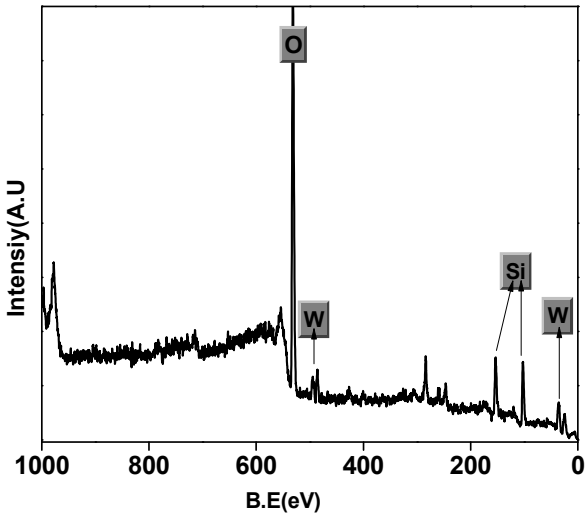

Figure 8.10 Survey scan of catalyst DTP (20)/SPC

The high resolution core level spectrum of catalyst is given in figure 8.11. The binding energy of tungsten $4f_{7/2}$ at 35.6 eV and $4f_{5/2}$ at 37.5 eV with gap of 2.1 eV corresponds to W^{6+} attached to oxygen atom [82-83]. The binding energy value is very close to that of pure DTP indicate that $PW_{12}O_{40}^{3-}$ anion is incorporated in porous clay heterostructures and the Keggin structure is more or less maintained.

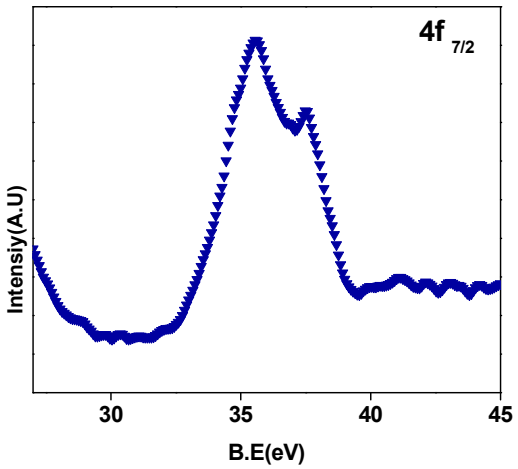

Figure 8.11 High resolution XPS spectra of catalyst

8.4.7 TEM

TEM image shows that particles consist of aggregated domains of several layers oriented in all directions. In SPC material wormhole like morphology is observed [84-85]. Catalysts prepared by direct method maintained wormhole like morphology with some dark patches corresponding to heteropoly anions. Large agglomerated crystals of DTP can be seen in the TEM image of catalyst prepared by impregnation method.

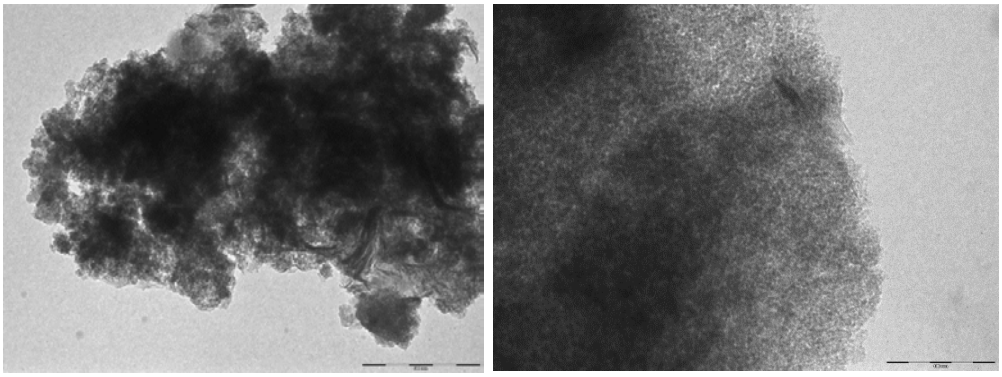

TEM image of DTP/SPC

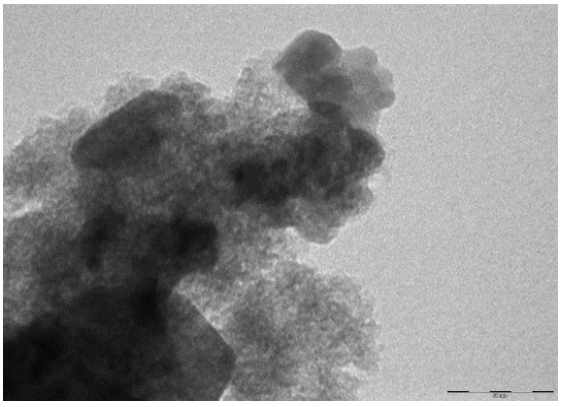

TEM image of DTP (30)/SPC (IM)

Fig 8.12: TEM image of catalysts

8.5 Activity studies: - Acetalization of cyclohexanone

The prepared catalysts were evaluated for the acetalization of cyclohexanone with methanol under milder reaction conditions. We have selected this reaction because the major acidic sites associated with present catalyst systems are Bronsted sites and acetalization reactions are usually catalysed by Bronsted acid sites. More over we are interested to explore the stability of immobilized heteropoly acid in polar reagents such as in methanol.

8.5.1 Acetalization of cyclohexanone

Acetalization is one of the most widely used protecting protocol for the protection of aldehydes and ketones in the field of synthetic organic chemistry as dialkyl acetals show great stability towards organic reagents, strong oxidants, strong bases and esterification reagents than corresponding carbonyl compounds [86]. Protection of the carbonyl group of aldehydes and ketones can be accomplished by alcohols [87], diols [88] or trioxanes or orthoester [89] in the presence of an acid catalyst. 1,2 diacetals are found to be efficient protecting group for vicinal 1,2 diol units in carbohydrates [90-91]. The synthetic routes for the preparation of commercially important large complex oligosaccharides involve unavoidable protecting group manipulation and activation protocols [91]. Tetra saccharides and penta saccharides can be prepared by the one pot sequential glycodization of four or five components. Grice and co-workers reported the preparation, structure, derivatization and NMR data of cyclohexane 1,2-diacetal protected carbohydrates [92].

In addition to the interest of acetals as protecting groups, many of them have direct application as fragrances [93-94] in cosmetics and as food additives [95-96]. Acetalization reaction is extensively used in the synthesis of

enantiomerically pure compounds [97], which find practical application in the fields of synthetic carbohydrates, food and beverage additives [98] steroids [99], pharmaceuticals, and fragrances [100]. Moreover, chiral acetals are efficient chiral auxiliary groups for enantioselective synthesis. The methyl and ethyl acetals of n-octanal and n-decanal, for example, find widespread applications in perfume and flavour industries [101]. The conversion of a carbonyl compound to its acetal alters its vapour pressure, solubility and aroma characteristics, and often results in flavour attenuation. For example, the propylene dioxy derivative of vanillin is commonly used as a vanilla flavour since it causes flavour attenuation [102]. Different formulations of several acetals named as potential fragrances are in the markets which, at the time of contact with the skin are hydrolyzed to give odorous compounds. Acetals can be used as additives that increase the cetane number of fuel and result in the efficient combustion of resulting mixture. Ketals of glycerol are often used as anti freezing agents.

The most general method for the synthesis of acetals is the reaction of carbonyl compounds with an alcohol or an ortho ester in the presence of acid catalysts. The commonly used acid catalysts include corrosive protic acids such as HCl, H_2SO_4 and Lewis acids such as $ZnCl_2$ and $FeCl_3$ [103-104]. Homogeneous acid catalysts ranging from $Mg(ClO_4)_2$ [105], p-toluene sulphonic acid [106], and series of cationic diphosphine. Lewis acidic complexes of Pt(II), Pd(II), and Rh(III) etc. have also been employed successfully for the generation of acetals [107]. Several Lewis acid complexes such as $[(dppe)M(H_2O)_2]$ where M is Pt or Pd, (dppe is 1,2 bis (diphenyl phosphino)ethane) have been successfully employed for acetalisation reaction in homogeneous medium [108-109]. However, acetalization procedures

mentioned above require tedious work-up, expensive reagents and neutralization of the strongly acidic media leading to the production of harmful wastes. Furthermore, the formation of dimethyl acetals in homogeneous phase is often carried out by using trimethyl ortho formate as the reagent. Methanol is more desirable for this reaction. Moreover in all these methods the catalysts and reagents are irreversibly lost leading to overall low atom economy and high E-factors. The solid acids are best alternatives for this reaction.

The solid acids reported for this reaction includes acidic zeolites [95,110], sulphated zirconia [111], sulphated titania [112], montmorillonite clays [113], mesoporous aluminosilicates [114-115], cation exchanged resins [116], modified MCM-41[117], metal loaded ceria [118], silica supported molybdenum trioxide [119], silica supported heteropoly acids [69] etc. Bejoy et al. compared the efficiency of different catalysts like metal exchanged clays (K10), zeolites, silica and alumina for the efficient protection of three ketones such as cyclohexanone, aceto phenone and benzophenone with methanol [120]. Velusamy et al. reported the chemo selective synthesis of acetals from aldehydes using Co (II) catalysts [121]. Recently Y. Jin et al. studied acetalization of benzaldehyde with alcohols over sulphonic acid bearing metal organic frame work (MOF)MIL-101 [122]. G.D. Yadav et al. studied the kinetics of acetalization of cyclohexanone with glycerol over cesium exchanged DTP supported on K10 [69]. Reaction between ethanol and acetaldehyde using solid acid resin Amberlyst-18 as a catalyst in a batch reactor was studied and found that experimental data verify Langmuir Hinshelwood model rate expression [123]. Yadav and Pujari observed that Eley Rideal mechanism prevails with the chemisorptions of aldehydes on active sites in the acetal formation reactions of n-octanal with methanol [124].

Here in DTP immobilized porous clay heterostructures were evaluated for the one pot acetalization of cyclohexanone under mild conditions. Various parameters were optimized to get maximum conversion. All the catalysts show exclusively 100% selectivity towards dimethylacetal.

8.5.2 Effect of temperature

In order to understand the effect of temperature on reaction, experiments were performed from 35^{o}C to 55^{o}C. Conversion increases with temperature and maximum conversion is obtained at 50^{o}C. After that a slight decrease in conversion is noted. This may be due to fact that energy may be required to reduce intermolecular association of cyclohexanone for dispersed adsorption and to avoid clustering around the Bronsted acid sites by hydrogen bonding. An increase in the temperature might force the reactant to get accessed to all the acid sites available in the catalysts particularly inside the pores for the formation of acetal [117].

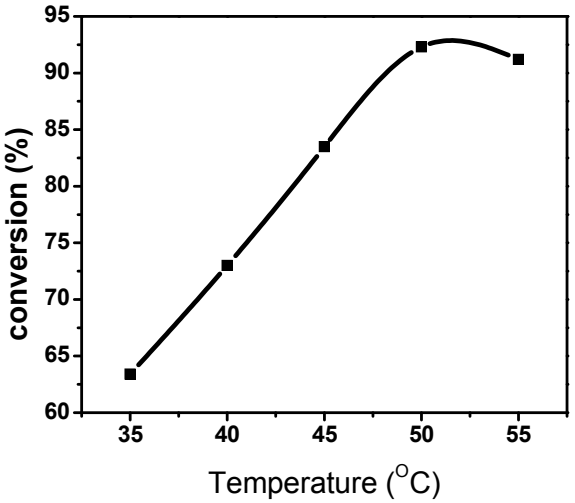

Figure 8.13 Effect of temperature, catalyst amount -125 mg, Cyclohexanone- 20mmol, cylohexanone to methanol ratio=1:10, Time -40minutes, Catalyst-DTP (30)/SPC

8.5.3 Effect of molar ratio

A set of experiments were conducted to study the effect of molar ratio of methanol on reaction rate and the result is given in Figure 8.14. Sharp increase in conversion is observed with increase in molar ratio of cyclohexanone to methanol from 1:5 to 1:10 and after that a slight decrease is noted. Hence 1:10 is taken as the optimum ratio. The formation of acetal with 100% selectivity for all the feed ratios is observed. The effect of mole ratio over the conversion can be attributed with the occupancy of ketone over the active sites and the availability of alcohol molecules for further acetalization. At low molar ratio, the ketone is chemisorbed on the active sites to form carbonium ion. The attack of these stable carbocations by the alcohol to form acetals has least effect at this molar ratio. Further, when the concentration of alcohol is increased, the approach of nucleophiles to the carbocation is enhanced. When the mole ratio is increased to 1:12, a decrease in conversion is observed due to the flooding of active sites with alcohol molecules which leads to the dilution of the reaction mixture and hindrance of protonation at the active sites.

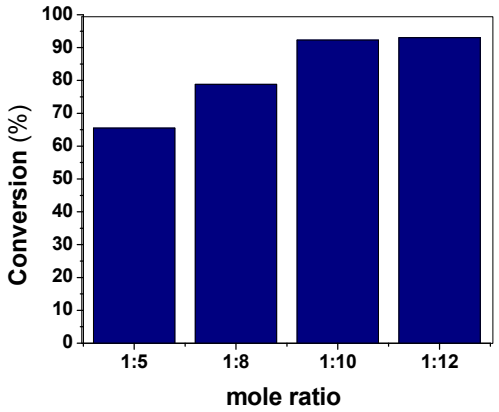

Figure 8.14 Effect of cyclohexanone to methanol mole ratio, Time -40 minutes, catalyst amount-125 mg, Temperature -50°C, Catalyst-DTP (30)/SPC

8.5.4 Effect of catalyst amount

Effect of catalyst amount was studied using catalyst amount of 50 mg to 150 mg. In the absence of external mass transfer resistance conversion is directly proportional to catalyst amount due to proportional increase in acidic sites. Maximum conversion was obtained for 125 mg catalyst. Further increase in catalyst amount leads to slight decrease in conversion.

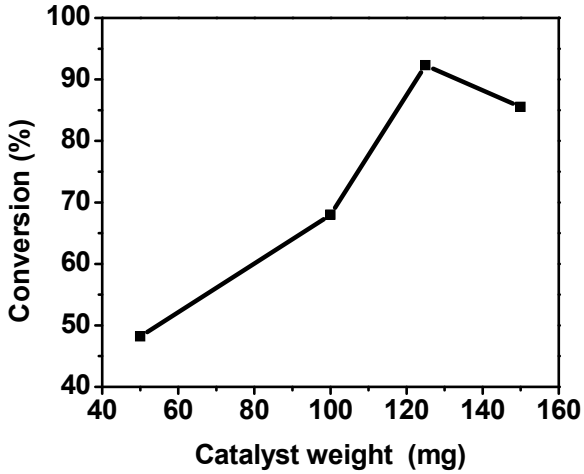

Figure 8.15 Effect of catalyst amount, temperature-50^{o}C, time-40 min,Cyclohexanone-20 mmol, Cylohexanone to methanol ratio- 1:10,Catalyst-DTP (30)/SPC

8.4.5 Effect of time

Conversion increases with progress of reaction time and maximum conversion is obtained at 40 minutes. After that conversion slightly decreases which may be due to adsorption of bulky reaction products with active sites which leads to the lower diffusion rate.

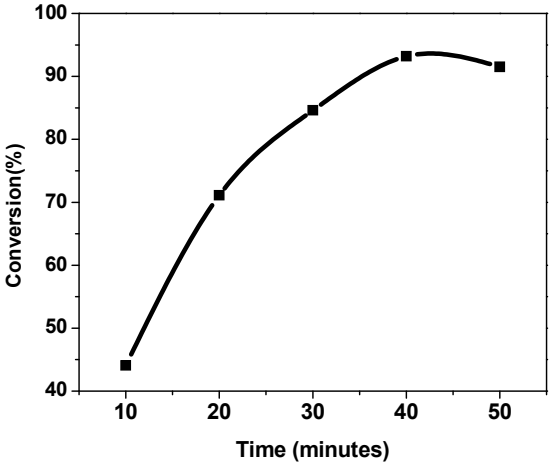

Figure 8.16 Effect of time, temperature-50^{o}C, Catalyst amount -125 mg, Cyclohexanone-20 mmol, cylohexanone to methanol ratio -1:10, Catalyst-DTP (30)/SPC

8.5.6 Effect of different catalysts

Acetalization of cyclohexanone was done over prepared catalyst under optimized reaction conditions and results are given in Table 8.7. From the reaction mechanism, it appears that the reaction proceeds with the formation of bulky intermediates and the mesoporous materials with high Bronsted acidity are expected to be highly active. The bare SPC shows reasonable activity due to the presence of substantial Bronsted acidity. Up on DTP incorporation the conversion increases and a steady increase in conversion is observed with increase in DTP loading. This may be due to the increase in acidity in weak as well as medium region after DTP incorporation. All the catalysts show exclusively 100% selectivity towards dimethylacetal. The catalyst prepared by impregnation method and direct method show comparable activity. The conversion of cyclohexanone can be correlated with total acidity obtained from TPD of ammonia.

Table 8.7 Acetalization of cyclohexanone over various catalysts Temperature-50°C, catalyst amount -125 mg, Cyclohexanone-20mmol, Time-40 min Cylohexanone to methanol ratio= 1:10

Catalyst	Conversion (%)	Rate constant ($min^{-1}m^{-2}$) (10^{-3})
SPC	68	0. 51
DTP (10) /SPC	79	0. 91
DTP (20) /SPC	85	1.28
DTP (30) /SPC	92	2.17
DTP (30) /SPC (IM)	94	3.07
DTP /SPC (F)	83	2.20

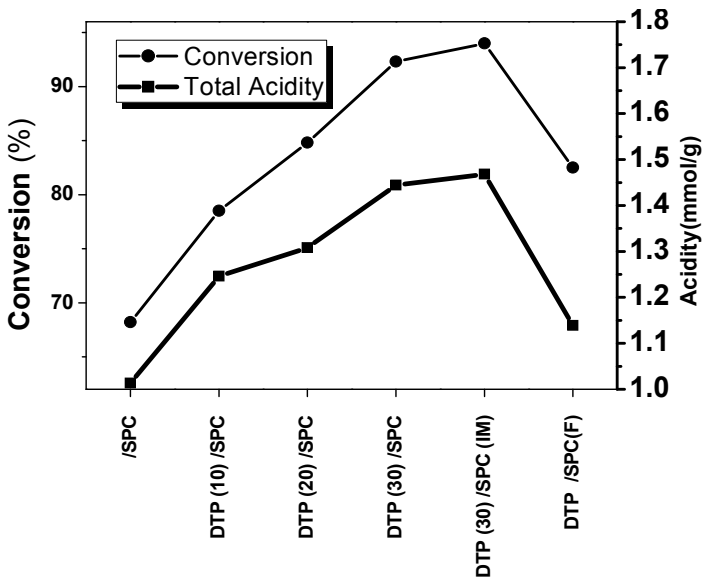

Figure 8.17 Correlation between acidity and activity

8.5.7 Effect of substrate

The acetalization reaction was also carried out with various carbonyl compounds using the catalyst DTP (30)/SPC under the specified reaction condition for comparative studies. The results are presented in Table 8.8. The activity of the catalyst in acetalization reaction of various substrates with methanol is in the order cylopentanone > cyclohexanone > benzaldehyde >

acetophenone > benzophenone. Corma et al. [126] pointed out that, diffusional properties of ketones are the deciding factor rather than electronic factors. It is seen from the molecular size calculation that the size follows the order cyclohexanone < acetophenone < benzophenone. Efficiency of acetalization of the three ketones follows the reverse order. The role of molecular size on reactivity cannot be overemphasized since it is known that cyclohexanone is more reactive towards nucleophiles than both acetophenone and benzophenone. This may also be due to the bulkiness of hemiacetals which prevent the attack of the methanol on the carbonyl carbon atom. The electron withdrawing power of phenyl group in acetophenone and benzophenone reduce the electron density on the carbonyl carbon during the reaction.

Table 8.8 Effect of substrate

Substrate		Conversion (%)
Cyclohexanone	Methanol	92
	Ethylene Glycol	97
Benzaldehyde	Methanol	91
	Ethylene glycol	94
Cyclopentanone	Methanol	94
Acetophenone	Methanol	53
Benzophenone	Methanol	36

The availability of acid sites and pore size of catalyst play a major role in acetalization reaction. M. Iwamoto et al. reported that smaller and larger pores were not suitable for the catalytic acetalization of cyclohexanone [126]. They found that MCM-41 materials with pore diameter greater than 40 A^0 have very little activity even though the exact reason for the low activity is not

known. Present catalyst systems have moderate pore diameter and high Bronsted acidity conducive for their better activity.

Acetal or ketal formation is a reversible reaction, which proceeds by a multi-step mechanism. Their formation is strongly affected by electronic and steric factors. The first step is the formation of hemiacetal, followed by the removal of a molecule of water. Formation of a cation from the protonated hemiacetal is the rate determining step of acetalization reactions [120]. The protonation of hemiacetal is also a slow step and the reaction medium has to be sufficiently acidic to promote efficient protonation of hemiacetal. The reaction medium must be polar enough to stabilize of the cation intermediate formed from hemiacetal.

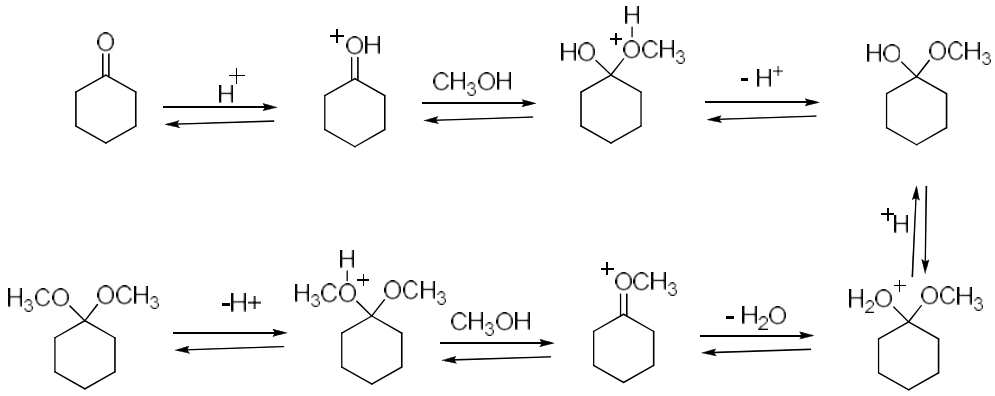

Figure 8.18 Mechanism of acetalization reaction.

8.5.8 Reusability studies

The stability as well as the true heterogeneity of catalysts was tested by conducting the experiments with regenerated catalysts. The catalyst was recovered by filtration after the reaction, washed several times with acetone, dried and calcined at 400^{o}C for 3h. Then the reaction was conducted with the recovered catalyst under the same reaction conditions. Table 8.9 shows

conversion obtained for regenerated catalysts. Catalysts prepared by direct method and functionalized methods retain their activity even after fourth cycle. The catalyst prepared by impregnation method lost its activity in consecutive runs due to the leaching of DTP in polar reagent methanol. Analysis of filtrate confirmed this fact. The leaching is negligible in directly prepared and functionalized samples as DTP is fixed firmly on the mesoporous channels of silica in the interlayer.

Table 8.9 Reusability studies

Catalyst	No. of cycles	Conversion (%)
DTP(30)/SPC	2	89
	3	87
	4	85
DTP(30)/SPC (IM)	2	87
	3	75
	4	70
DTP /SPC (F)	2	79
	3	76

8.6 Kinetic studies

Yadav et al. studied the kinetics of acetalization of cyclohexanone with glycerol based on a bimolecular surface reaction and formulated a pseudo first order kinetics [69]. The rate expression can be written as $-ln(1-X) = k.W.t$ where X is the conversion of cyclohexanone, k is the first order rate constant.

The rate equation can be validated by ploting –In (1-X) against time for different reaction temperatures. A straight line passing through the origin is obtained.

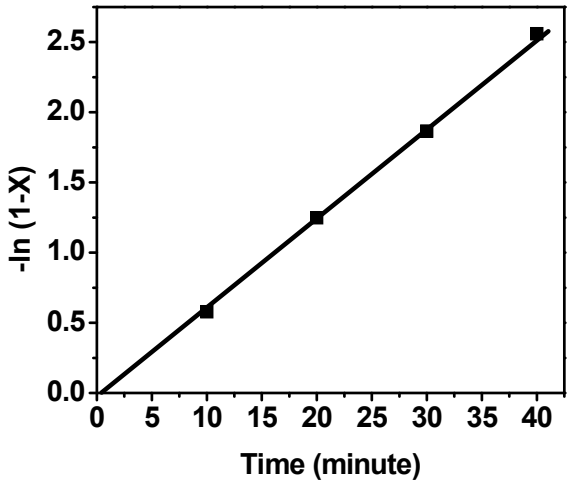

Figure 8.19 Validity of pseudo first order in acetalization of cyclohexanone over DTP(30)/SPC catalyst

The intrinsic rate constants were calculated by the equation

$$K\ (min^{-1}\ m^{-2}) = \frac{2.303}{t.W.A} log \frac{1}{1-X}$$

Where W is weight of catalyst, t is the time, A is surface area of the catalyst and X is the conversion.

The rate constant for the acetalization reaction with different catalysts were calculated and are given in Table 8.7. The Arrhenius plot of the reaction is given in Figure 8.20. The activation energy is calculated which shows that reaction is kinetically controlled. The kinetic parameters were also calculated and are given Table 8.10.

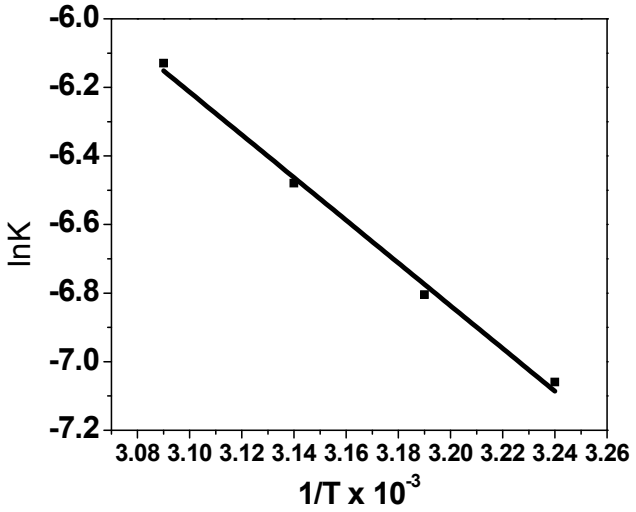

Figure 8.20 Arrhenius plot of acetalization reaction over DTP(30)/SPC catalyst

Table 8.10 Kinetic parameters of acetalization of cyclohexanone over DTP(30)/SPC catalyst

Kinetic parameters	
Activation energy E_a	51.796 kJ/mol
Frequency factor A	4.87x 10^8 (kg of catalyst)$^{-1}$ h^{-1}
Enthalpy of activation $\Delta H^{\dagger}$	46.84 kJ /mol
Entropy of activation $\Delta S^{\dagger}$	-152.64 J/Mol /K

8.7 Conclusions

- Dodeca tungstophosphoric acid is immobilized on PCH materials by three methods direct, anchoring and impregnation methods.
- The prepared catalysts were characterized by various physico-chemical methods.

- In lower DTP loading, DTP is uniformly distributed on catalyst support. Characteristic peaks of Keggin ions were visible in IR spectrum and XRD profiles of higher DTP loaded samples.
- The catalysts prepared by different methods have different textural properties as evident from the adsorption isotherm of catalysts.
- Acidic properties of catalysts were improved by the incorporation of DTP in PCH material as evidenced from TPD of ammonia.
- XPS spectrum of directly prepared catalyst showed that W is in $^{+}6$ oxidation state and Keggin structure is maintained.
- Prepared catalysts were evaluated for acetalization of cyclohexanone with methanol. All the catalysts showed excellent activity with 100% selectivity towards dimethyl ketal. The activity of the catalyst can be well correlated with total acidity obtained from TPD of ammonia.
- Recycle studies showed that catalyst prepared by the impregnation method lost its activity in consecutive runs.
- Catalysts prepared by direct and anchoring methods retain their activity in successive runs as they were stable against leaching since the heteropoly anion is firmly fixed on interlayer silica surface of clays.
- Kinetic studies reveal that reaction follows pseudo first order. Kinetic parameters were evaluated. The high value of activation energy indicates that reaction is kinetically controlled.

References

[1] T. Pope, Heteropoly and Isopoly Oxometalates, Springer-Verlag, Berlin (1993).

[2] I. V. Kozhevnikov, Chem. Rev., 98 (1998) 171.

[3] N. R. Shiju, A. H. Alberts, S. Khalid, D. R. Brown, G. Rothenberg. Angew. Chem. Int. Ed., 50 (2011) 9615.

[4] T. Okuhara, T. Nakato, Catal. Survey Jpn., 2 (1998) 31.

[5] Y. Izumi, K. Urabe, M. Onaka, Zeolite, Clay and Heteropoly acid in Organic Reactions; Kodansha/VCH: Tokyo (1992).

[6] Y. Izumi, K. Urabe, M. Onaka, Zeolite, Clay and Heteropoly acid in Organic Reactions; Kodansha/VCH: Tokyo (1992).

[7] J. J. Berzelius, Pogg. Ann. Phys. Chem., 6 (1826) 369.

[8] C. Marignac, Ann. Chim., 25 (1862) 362.

[9] L. C. Pauling, J. Am. Chem. Soc., 51 (1929) 2868.

[10] J. F. Keggin, Nature, 131 (1933) 908.

[11] J. F. Keggin, Proc. Roy. Soc. A, 144 (1934) 75.

[12] Y. Luo, Z. Hou, R. Li, X. Zheng, Micropor. Mesopor. Mater., 109 (2008) 585.

[13] J. B. Moffat, Metal-Oxygen Clusters: The Surface and Catalytic Properties of heteropolyoxometalates, Kluwer Academic / PlenumPublishers, New York (2001).

[14] M. Misono, Catal. Rev. Sci. Eng., 29 (1987) 269.

[15] M. Misono, In New Frontiers in Catalysis, Eds.; Elsevier: Amsterdam (1993).

[16] M. Misono, N. Nojiri, Appl. Catal., 64 (1990) 1.

[17] I. V. Kozhevnikov, S. Ts. Khankhasaeva, S. M. Kulikov, Chem. Rev., 62 (1993) 473.

[18] T. Okuhara, N. Mizuno, M. Misono, Adv. Cata., 41(1996)113.

[19] T. Okuhara, T. Nishimura, H. Watanabe, M. Misono, Stud. Surf. Sci. Catal., 90 (1994) 419.

[20] C. Rocchiccioli-Deltcheff, M. Amirouche, G. Herve, M. Fournier**,** M. Che**,** J.M. Tatibouet, J. Catal.,126 (1990) 591.

[21] J. C. Edwards, C. Y. Thiel, B. Benac, J. F. Knifton, Catal. Lett.,51 (1998) 77.

[22] E. Lopez-Salinas, J. G. Hernandez-Cortez, Schifter, Appl. Catal. A: Gen., 193 (2000**)** 215.

[23] B. M. Devassy, S. B. Halligudi, S. G. Hegde, Halgeri, A. B. Lefebvre, Chem. Commun., (2002**)** 1074.

[24] T. Baba, Y.Ono, Appl. Catal., 22 (1986) 321.

[25] Y. Izumi, K. Urabe, Chem. Lett., (1981) 663.

[26] L. R. Pizzio, C. V. Caceres, Blanco, Appl. Surf. Sci., 151 (**1999**) 91.

[27] R. Yuanhang, Y. Bin, G. Min and H. Heyong**,** Materials, 3 (2010) 764

[28] A. Ghanbari-Siahkali, A. Philippou, J. Dwyer, M. W Anderson, Appl. Catal. A: Gen., 192 (2000) 57.

[29] I. V. Kozhevnikov, K. R. Kloetstra, A. Sinnema, H. W. Zandbergen, H. van Bekkum, J. Mol. Catal. A: Chem., 114 (1996) 287.

[30] A. Llanos, L. Melo, F. Avendano, A. Montes, J. L. Brito, Catal. Today, 133 (2008) 20

[31] G. S. Kumar, M. Vishnuvarthan, M. Palanichamy, V. Murugesan, J. Mol. Catal. A: Chem., 260 (2006**)** 49.

[32] K. U. Nandhini, B. Arabindoo, M. Palanichamy, V. Murugesan, J. Mol. Catal. A: Chem., 223 (2004**)** 201.

[33] P. Van Der Voort, E. F. Vansant, J. Liq. Chrom. Related Technol., 19 (1996) 2723.

[34] H. L. Li, N. Perkas, Q. L. Li, Y. Gofer, Y. Koltypin, A. Gedanken, Langmuir 19 (2003) 10409.

[35] M. Kamada, H. Kominami, Y. Kera, J. Colloid Interface Sci.,182 (1996) 297.

[36] A. M. Khenkin, R. Neumann, A. B. Sorokin, A. Tuel, Catal. Lett., 63 (1999) 189.

[37] H. Jin, Q. Wu, P. Zhang, W. Pang, Solid State Sci., 7 (2005) 333.

[38] B. J. S. Johnson, A. Stein, Inorg. Chem ., 40 (2001) 801.

[39] S. S. Wu, P. Liu, Y. Leng, Wang, J. Catal. Lett ., 132 (2009) 500.

[40] T. Aliakbar, A. Mansour, N. Ali, K. Maryam, M. Mostafa, Amini, J. Colloid. Inter. Sci ., 303 (2006) 32.

[41] Y. Lina, Q. Yutai, Y. Xingdong, S. Jian, K. Jiman, J. Mol. Catal. A: Chem.,229 (2005) 199.

[42] A. Molnar, C. Keresszegi, B. Torok, Appl. Catal. A: Gen., 189 (1999) 217.

[43] L. Yang, Y.T. Qi, X.D. Yuan, H. Shen, J. Kim, J. Mol. Catal. A: Chem., 229 (2005) 199.

[44] C. F. Shi, R. W. Wang, G. S. Zhu, S. L. Qiu, Long, J. Eur. J. Inorg. Chem., (2006) 3054.

[45] B. Li, Z. Liu, C. Han, J. Liu, S. Zuo, Z. Zhou, X.Pang, J. Mol. Catal. A: Chem., 348 (2011) 106.

[46] S. Samantaray, S. K. Sahoo, G. Mishra, J. Porous Mater.,18(2010)570

[47] G. D. Yadav, N. S. Doshi, J. Mol. Catal. A: Chem ., 194, 195 (2003) 195.

[48] G. D. Yadav, S. S. Salgaonkar, N. S. Asthana. Appl. Catal. A: Gen., 265 (2004) 153

[49] G. D. Yadav, S. S. Salgaonkar, Ind. Eng. Chem. Res ., 44 (2005) 706.

[50] G. D. Yadav, S. B. Kamble, Ind Eng Chem. Res., 48 (2009) 9338.

[51] G. D. Yadav, S. A. R. K. Deshmukh, N. S. Asthana, Ind. Eng. Chem.Res., 44 (2005) 7969.

[52] G. D. Yadav, S. S. Salgaonkar, Ind. Eng. Chem. Res ., 44 (2005) 706.

[53] T. Blasco, A. Corma, A. Martínez, P. Martínez-Escolano, J. Catal .,177 (1998) 306.

[54] S. M. Kumbar, S. B. Halligudi, Catal. Comm ., 8 (2007) 800.

[55] S. M. Kumbar, G. V. Shanbhag, F. Lefebvre, S. B. Halligudi, J. Mol. Catal. A: Chem ., 256 (2006) 324.

[56] N. Lucas, A. Bordoloi, A. P. Amrute, P. Kasinathan, A. Vinu, W. Bohringer, J. C. Q. Fletcher, S. B. Halligud, Appl. Catal. A: Gen., 352, (2009) 74.

[57] K. Shimizu, S. Kontani, S. Yamada, G. Takahashi, T. Nihisyama, A. Satsuma, Saudi Arabia-Japan Joint Symposium (2008).

[58] N. Bhatt, A. Patel, J. Mol. Catal. A: Chem., 264 (2007) 214.

[59] C. De Castro, J. Primo, A. Corma, J. Mol. Catal. A: Chem., 134 (1998) 215.

[60] K. M. Parida, S. Mallick, G. C. Pradhan, J. Mol. Catal. A: Chem., 297 (2009) 93.

[61] D. P. Sawant, A. Vinu, F. Lefebvre, S. B. Halligudi. J. Mol. Catal. A: Chem., 262 (2007) 98.

[62] G. Sunita, B. M. Devassy, A. Vinu, D. P. Sawant, V. V. Balasubramanian, S. B. Halligudi, Catal. Comm., 9 (2008) 2026.

[63] G. D. Yadav, N. S. Asthana, V. S. Kamble. Appl. Catal. A: Gen., 240 (2003) 53.

[64] M. N. Timofeeva, R. I. Maksimovskaya, E. A. Paukshtis, I. V. Kozhevnikov. J. Mol. Catal. A., 102 (1995) 73.

[65] K. A. da Silva Rocha, N. V. S. Rodrigues, I. V. Kozhevnikov, E. V. Gusevskaya, Appl. Catal. A: Gen., 374 (2010) 87.

[66] S. S. Wu, J. Wang, W. H. Zhang, X. Q. Ren, Catal. Lett., 125 (2008) 308.

[67] S. S. Wu, P. Liu, Y. Leng, Wang, J. Catal. Lett. 132 (2009) 500.

[68] J. Das, K.M. Parida, J. Mol. Catal. A: Chem., 264 (2007) 248.

[69] G. D. Yadav, A. R. Yadav, Int. Rev. Chem. Eng., 4 (2012) 6.

[70] B. R. Jermy, Pandurangan, Appl. Catal. A: Gen., 295 (2005) 185.

[71] A. Alsalme, E. F. Kozhevnikova, I. V. Kozhevnikov, Appl. Catal. A: Gen., 349 (2008) 170.

[72] V. V. Costa, K.A. da Silva Rocha, I. V. Kozhevnikov, E. V. Gusevskaya, Appl. Catal. A: Gen., 383 (2010) 217.

[73] S. Mallik, K. M. Parida, S. S. Dash. J. Mol. Catal. A: Chem., 261 (2007) 172.

[74] D. P. Das, K. M. Parida, J. Mol. Catal. A: Chem., 253 (2006) 70.

[75] K. M. Parida, S. Parija, J. Das, P. S. Mukherjee. Catal. Comm., 7 (2006) 913.

[76] S. Mallick, K. M. Parida. Catal. Comm., 8 (2007) 1487.

[77] K. M. Parida, S. Mallick, J. Mol. Catal. A: Chem., 279 (2008) 104.

[78] A. Alhanash, E. F. Kozhevnikova, I. V. Kozhevnikov, Appl. Catal. A: Gen., 378 (2010) 11.

[79] Y. Zhou, B. Yue, R. L. Bao, M. Gu, H. Y. He, Catalyst. Stud. Surf. Sci.Catal., 165 (2007) 479.

[80] W. Li, L. Li, Z. Wang, A. Cui, C. Sun, J. Zhao, Mat. Lett., 49 (2001) 228.

[81] R. S. Ezzat, Rashidzadeh, E. Sara and J. Mohammad, Bull. Chem. Soc. Ethiop., 24(2) (2010) 209.

[82] Huming, Chuwei, L. X. dai Xiao, Chinese Sci Bull., 55 (2010) 24.

[83] N. Legaggneux, A. J. M. Basset, Dalton Trans., (2009) 2235.

[84] M. Polverejan, T. R. Pauly, T. J. Pinnavaia, Chem. Mater., 12 (2000) 2698.

[85] A. J. Tchinda, E. Ngameni, I. T. Kenfack, A. Walcarius, Chem. Mater., 21 (2009) 4111

[86] T. W. Greene, Protective Groups in Organic Synthesis, Wiley-Interscience, New York (1981) 178.

[87] P. Srivastava, R. Srivastava, Catal Commun., 9 (2008) 645.

[88] M. P. Sonal, U. V. Chudasama, A. G. Prallard, J. Mol. Catal. A, 194 (2003) 267.

[89] S. Chandan, H. Malik, Org Lett., 7 (2005) 5673.

[90] D. A. Entwistle, A. B. Hughes, S. V. Ley, G. Visentin,Tetrahedron Lett., 35 (1994) 777.

[91] P. Grice, S.V. Ley, J. Pietruszka, H. W. M. Priepke Angew, Chem. Int. Ed. Eng.,35 (1996) 197.

[92] P. Grice, S. V. Ley, J. Pietruszka, H. W. M. Priepke, E.P.E.Walther, Synlett., (1995) 781.

[93] M. J. Climent, A. Velty, A. Corma, Green Chem., 4 (2002) 565.

[94] K. Bauer, D. Garbe, H. O Surburg, Common fragrances and flavour materials, VCH, New York (1990).

[95] D. M. Clode, Chem. Rev., 79 (1979) 491.

[96] L. Nykanen, H. Suomalainen, Aroma of beer, wine and distilled alcoholic beverages, Kluwer Academic Publishers, Berlin, (1983) 73.

[97] M. K. Cheung, N. L. Douglas, B. Hinzen, S. V. X. Ley, Pannecoucke, Synlett., (1997) 257.

[98] S. V. Ley, H. W.M. Priepke, Angew. Chem. Int. Ed. Engl. 33 (1994) 2292.

[99] J. R. Bull, J. Floor, G. J. Kruger, J. Chem. Res. Synop., (1979) 224.

[100] M. J. Climent, A. Corma, S. Iborra, M. C. Navarro, J. Primo, J. Catal., 161 (1996) 783.

[101] S. Arctander, Perfumary and Flavour Chemicals, vols. I and II, Allured Publishing, New York (1969).

[102] G. A. BurdockFenarolis, Handbook of Flavour Ingradients, vol. 2, CRC, New York (1995).

[103] T. W. Greene, Protective groups in organic synthesis, Wiley-Interscience, New York (1981) 178.

[104] J. Bornstein, S. F. Bedell, P.E. Drummond, C. F. Kosoloki, J. Am. Chem. Soc.,78 (1956) 8.

[105] G. Strukul, Top. Catal., 19 (1) (2002) 33.

[106] C. A. McKinzie, J. H. Stocker, J. Org. Chem., 20 (1955) 1695.

[107] M. Cataldo, F. Neiddu, R. Gavagnin, F. Pinna, G. Strukul, J. Mol. Catal. A, 142 (1999) 305.

[108] E. Nieddu, M. Cataldo, F. Pinna, G. Strukul, Tetrahedron Lett., 40 (1999) 6987.

[109] G. Strukul, Top. Catal., 19 (1) (2002) 33.

[110] M. J. Climent, A. Velty, and A. Corma, Green Chem., 4 (2004) 565.

[111] C. H. Lin, S. D. Lin, Y. H. Yang, T. P. Lin, Catal. Lett., 75 (2–4) (2001) 121.

[112] J. I. Tateiwa, H. Horiochi, S. Uemora, J. Org. chem., 60 (1995) 4039.

[113] E. C. Taylor and C. S. Chiang, Synthesis, (1977) 467.

[114] N. S. Shaikh, S. S. Bhor, A. S. Gajare, V. H. Deshpande, and R. D. Wakharkar, Tetrahedron Lett., 45 (2004) 5395.

[115] M. J. Climent, A. Corma, S. Iborra, M. C. Navarro, J. Primo, J. Catal., 161(1996) 786.

[116] Y. Tanaka, N. Sawamara, M. Iwamoto, Tetrahedron Lett., 39 (1998) 9457.

[117] B. R. Jermy, A. Pandurangan, J. Mol. Catal. A: Chem., 256 (2006) 184.

[118] K. J. Rose Philo, S. Sugunan, IOSR J. Appli. Chem., 6 (2012) 24.

[119] S. B. Umbarker, B. Shubarangi, J. Mol. Catal. A, 310 (2009) 150.

[120] B. Thomas, S. Sugunan, J. Poro. Mater., 13 (2006) 99.

[121] S. Velusamy and T. Punniyamurthy, Tetrahedron Lett., 45 (2004) 4917.

[122] J. Yan, S. Jing, Z. Fumin, Z. Yijun, Z. Weidong, J. Mol. Catal. A: Chem., 383 (2014) 167.

[123] P. A. Parikh, N. Subramanyam, Y. S. Bhat, A. B. Halgeri, Appl. Catal. A, 90 (1992)1.

[124] G. D. Yadav, A. A. Pujari, Can. J. Chem. Eng., 77 (1999) 489.

[125] A. Corma, M. J. Climent, H. Garcia, J. Primo,J. Appl. Catal. A: Gen., 59 (1990) 333

[126] I. Masakazu, T. Yasuhiro, S. Naoki, N. Seitaro, J. Am. Chem. Soc., 125 (2003) 13033.

Chapter 9

SUMMARY AND CONCLUSIONS

The discovery of functional solid materials of high catalytic performance is crucial to most chemical processes by allowing the replacement of polluting homogeneous catalysts by reusable heterogeneous catalysts. Clay minerals are a class of inorganic layered silicate materials, which can be engineered into various functional solid catalysts due to their inherent features in composition and structure. The present work engrosses in the thrust area of heterogeneous catalysis which involve the development of clay based porous solid acids, their physico chemical characterization and evaluation of their activity in industrially important organic transformations. This chapter reviews the summary and conclusion of the work described in the preceding chapters. Finally, the scope for further work on the ever expanding field is also outlined.

The rational design and preparation of novel catalysts based on clay minerals has received many scholar's concern over the past four decades. Clay minerals provide distinct nanometer-scaled layers and interlayers for engineering them as active catalysts. The propping apart of natural clay layers by exchange with oligo or polymeric cationic complexes followed by calcination results in porous oxide pillars incorporated between the clay layers. The advantage of pillaring process include the increase in surface area, pore size, thermal stability and increase in acidity. Three decades passed since the first preparation of PILCs were reported. More than thousands of papers were published concerning the preparation and application of these materials. Wide varieties of single and mixed pillars were produced with different level of porosity, interlayer distance, surface area, acidity and redox properties. Eventhough the creation of regular porosity in pillared clays is a difficult task and the properties of pillared clays mainly based on empirical recipes, these materials continue to attract the attention of synthetic chemists especially in the era of strict environmental legislations.

Compared to pillared clays porous clay heterostructures are relatively new class of materials whose potential has not been explored completely yet. They are materials with mesoporous silica being incorporated between the clay layers. They transcend the pore size limitation of clays with high mass transfer efficiency and can be used in reactions involving large molecules. These materials possess the inherent acidic properties of clays along with the properties of silica (such as ability to be functionalized) which allow them to modify effectively for various potential applications.

Summary of the work

In this venture three distinct class of catalysts such as, pillared clays and transition metal loaded pillared clays , porous clay heterostructures and their transition metal loaded analogues and DTP supported on porous clay heterostructures etc. were prepared and characterized by various physico chemical methods. The catalytic activities of prepared catalysts were comparatively evaluated for the industrially important alkylation, acetalization and oxidation reactions. The thesis is divided in to nine chapters. The extracted essence of each chapter is presented below.

Chapter 1 involves brief introduction to clay minerals, structure of clays, different modification procedures such as pillaring, template assisted modifications like porous clay heterostructures etc. A brief review of modified clays and catalytic applications of modified clays for various organic transformations are presented. Scope and objectives of present work are also given in this chapter

Chapter 2- The methodology adopted for the preparations of catalysts and various experimental techniques adopted for the characterization of catalysts are briefly discussed. Pillared clays like zirconium pillared clay and mixed pillared clay like iron -aluminium pillared clays are prepared by ion exchange method and porous clay heterostructures like silicon and zirconium silicon PCHs are prepared by template assisted method. PILCs and PCHs are further modified by incorporating transition metals like copper, nickel, cobalt and vanadium by wet impregnation method. The prepared catalysts are characterized by various physicochemical methods. Brief descriptions about the methodology adopted for characterization are given in this chapter.

Chapter 3 contains the results and discussion of characterization of prepared catalysts. The success of pillaring process can be readily understood from XRD analysis. Drastic increase in surface area and pore volume was noted for both pillared clays and porous clay heterostructures after the modification. Porous clay heterostructures have higher surface area, average pore diameter and narrow pore size distribution than that of pillared clays. The IR spectra of PILCs and PCHs are in accordance with literature and not much variation in IR bands compared to parent montmorillonite which indicate that basic clay structure is retained even after modification. The thermal stability as well as heat changes accompanying in preparation stages were studied by TG analysis. Acid sites distribution and cumulative acidity were measured by Temperature Programmed Desorption of ammonia. The silicon NMR of PCHs materials confirm that mesoporous silica is incorporated between clay layers. Oxidation state of metals in metal loaded pillared clays and porous clay hetrostructures were understood from TPR, UV-Vis DRS and XPS analysis. The comparative account of results obtained from various characterization techniques for PILCs and PCHs are given in Table 9.1

Table.9.1 Comparative account of characterization results of PILCs and PCHs

Characterization technique		PILCs	PCHs
CEC		Reduction in residual CEC as a result of pillaring	Higher residual CEC than PILCs
d spacing (A^0)		~20 A^0	~ 40 A^0
BET Surface area (m^2/g)		90-150	250-450
Average pore diameter(A^0)		28-34	37-42
Pore volume (cm^3/g)		0.08 - 0.2	0.39-0.73
Adsorption isotherm		Blend of Type 1 and IV with hysteresis loop H4 which corresponds slit like pores	Type IV with hysteresis loop H3 characteristics of open cylindrical pores.
Thermal stability		Higher thermal stability than parent clay	Higher thermal stability than pillared clays
Silicon NMR		Q^3 peak is more intense than Q^4 peak. Q^3 peak broadens and shifts as a result of strain after pillaring	Q^4 peak is more intense than Q^3 peak confirm the incorporation of silica between clay layers
Metal linkage in metal loaded catalyst		Metal is preferentially linked to pillar -OH	Metal is preferentially linked to silanol groups
Acidity	TPD	Improvement in acidity in weak, medium and strong acidic sites region as a result of pillaring	Cumulative acidity is greater than Pillared clays .Major acid sites are in weak and medium region. Acidic sites in strong region improves up on metal loading
	Cumene cracking	Selectively for α-methyl styrene is higher than that of dealkylated products. Lewis sites are major acid site.	Selectively for dealkylated products is higher than that of α-methyl styrene. Major acid sites are Bronsted sites.
Morphology	SEM	Layer structure is preserved after the pillaring process.	
	TEM		Worm hole like morphology

Chapter 4-7 Elucidate the activity studies of the prepared catalysts for various organic reactions and efforts are made to correlate the activity with textural and acidic properties

The reactions selected are

Tertiary butylation of phenol.

Tertiary butylation of phenol was done in vapour phase. The porous clay heterostructures showed greater conversion and dialkylated product selectivity owing to its large pore size and acidity. The cobalt impregnated zirconium-silicon PCHs showed excellent activity. The reaction follows second order kinetics and kinetic parameters were evaluated. The high value of activation energy indicates that reaction is kinetically controlled.

Oxidation of phenol

Oxidation of phenol was done in aqueous media. Oxidation of Phenol mainly yielded catachol and hydroquinone which have great commercial importance. Catalytic activity improves with incorporation of transition metals in PILCs and PCHs. Cerium impregnated iron- aluminium pillared clays were found to be the better catalyst with more than 80% conversion owing to redox property and additional surface area provided by ceria mesopres. In iron pillared clays an induction period is noted suggesting a free radical type mechanism. In metal loaded zirconium pillared clays an electrophilic mechanism involving metalaxo-peroxide species is proposed. In metal loaded pillared clays activity can be correlated with total acidity obtained for TPD Of ammonia. In metal incorporated zirconium silicon porous clay heterostructures activity can be correlated with strong acidity obtained from TPD of ammonia.

Hydroxylation of benzene.

Direct hydroxylation of benzene to phenol was done over prepared catalysts in liquid phase. Superior activity is found for copper impregnated zirconium pillared clays. Nature and dispersion of copper species has tremendous effect on conversion and selectivity. Isolated Cu and vanadium oxide species were found to be active centres for hydroxylation of benzene. A plausible mechanism involving ionic intermediate and metaloxo hydroperoxide species was proposed.

Oxidation of benzyl alcohol

Oxidation of benzyl alcohol is performed over prepared catalysts with hydrogen peroxide as oxidant. Vanadium impregnated zirconium PILCs and ZrSiPCH showed promising activity due to their redox property and uniform dispersion over the support.

From the activity studies it was clear that for oxidation reactions in aqueous media (such as oxidation of phenol) the metal loaded pillared clays showed higher activity than porous clay heterostructures due to their higher hydrophilicity and Lewis acidity. The nature and dispersion of redox metal species are key factor in oxidation reactions. For hydroxylation of benzene, copper loaded zirconium pillared clays showed better activity than porous clay heterostructures due to the presence of more Lewis acid sites as benzene is strongly adsorbed over Lewis sites than on Bronsted sites. Vanadium loaded prous clay heterostructures showed better activity for the oxidation of benzyl alcohol than corresponding pillared clays due to their high surface area and larger pore size which is helpful for the easy diffusion of reactant and products. In alkylation reaction metal loaded porous clay heterostructures

obtained higher conversion and higher selectivity for dialkylated products than that of pillared clays by virtue of their higher surface area, large pore size and higher acidity.

Chapter 8 includes brief introduction in to heteropoly acids and their application in catalysis. Heteropoly acid dodeca tungstophosphoric acid is supported on PCHs by three methods, direct method, anchoring and impregnation methods. The prepared catalysts were characterized by various characterization methods. In lower DTP loading, DTP is uniformly distributed on catalyst support. Characteristic peaks of Keggin ions were seen in IR spectrum and XRD profiles of higher DTP loaded samples. The catalysts prepared by various methods have various textural properties as it is evident from surface area, pore volume measurements and adsorption isotherms. Acidic properties of the catalysts were improved by the incorporation of DTP in PCH material as evidenced from TPD of ammonia. XPS spectrum of directly prepared catalyst showed that W is in +6 oxidation state and Keggin structure is maintained. Heteropoly acids are fixed firmly on mesorepore channels of silica in direct prepared catalysts and catalyst prepared by anchoring method. The catalytic activity was tested for acetalization of cyclohexanone. and all the catalysts showed excellent activity. Catalysts prepared by impregnation method lost its activity in successive runs due to leaching. The catalysts prepared by direct method and anchoring methods retained its activity in consecutive runs.

Conclusions

The general conclusions drawn from the present investigation are

- Zirconium, iron - aluminium pillared clays were synthesized by ion exchange method and zirconium-silicon porous heterostructures were

prepared by intergallery template method. Transition metals were loaded in PILCs and PCHs by wet impregnation method.

- Textural and acidic properties of the clays were modified by pillaring and post pillaring modifications.
- The shift in 2θ value to lower range and increase in d (001) spacing indicate the success of pillaring process.
- Surface area, pore volume, average pore size etc. increased dramatically as a result of pillaring process.
- Porous clay heterostructures have higher surface area, pore volume, average pore diameter and narrow pore size distribution than that of pillared clays.
- The IR spectrum of PILCs and PCHs are in accordance with literature without much variation compared to parent montmorillonite which indicate that basic clay structure is retained even after modification.
- The silicon NMR of PCHs materials have intense peaks corresponding to Q^4 environment which indicate that mesoporous silica is incorporated between clay layers.
- Thermo gravimetric analysis showed that thermal stability is improved after the pillaring process. PCH materials have higher thermal stability than PILCs.
- In metal loaded pillared clays, up to 5% metal species were uniformly dispersed (with the exception of Ni) as evident from XRD and TPR analysis.

- Impregnation of transition metals in PILCs and PCHs enhanced acidity of catalysts as evident from TPD of ammonia and cumene cracking reactions.
- For porous clay heterostructures the acidic sites have major contribution from weak and medium acid sites which can be related to the Bronsted sites as evident from TPD of ammonia.
- Pillared clays got more Lewis acidity than PCHs as inferred from α-methyl styrene selectivity in cumene cracking reaction.
- SEM images show that layer structure is preserved even after modification. Worm hole like morphology is observed in TEM image of PCHs materials
- In ZrSiPCHS, Zr exists as Zr^{4+} and is incorporated to silica pillars in the intergallary of clay layers as evident from XPS analysis.
- In copper loaded zirconium pillared clays, copper exists as isolated species with +2 oxidation state at lower loading. At higher loading, Cu exists as clusters as evident from reduction peak at higher temperatures in TPR.
- In vanadium incorporated PILCs and PCHs, vanadium exist as isolated V^{5+} in tetrahedral coordination which is confirmed from TPR and UV-Vis DRS analysis.
- In cobalt loaded PCHs, cobalt exists as CoO with 2+ oxidation state as confirmed from XPS.
- Cerium incorporated iron aluminium pillared clay was found to be the best catalyst for the hydroxylation of phenol in aqueous media due to the additional surface area provided by ceria mesopores and its redox properties.

- Cobalt loaded zirconium porous clay heterostructures were found to be promising catalyst for the tertiary butylation of phenol due to higher surface area and acidic properties.
- Copper loaded pillared clays were found to be good catalyst for the direct hydroxylation of benzene to phenol.
- Vanadium loaded PCHs catalysts were found to be efficient catalysts for oxidation of benzyl alcohol.
- DTP was firmly fixed on the mesoporous channels of PCHs by Direct method and functionalization method.
- DTP supported PCHs catalyst were found to be good catalyst for acetalization of cyclohexanone with more than 90% conversion.

Future outlook

A wide variety of single or mixed oxide pillars can be inserted between clay layers. A rather extensive territory can be explored if one considers the great versatility originating from the different type of clay minerals and guest molecules. Incorporation of transition metals in pillared clays modifies acidity due to varying dispersion and interaction with oxide surface and contributes to over all conversion and selectivity. In the present work we have impregnated Ni, Cu, Co, V etc. in zirconium pillared clays and porous clay heterostructures. Other transition metals and rare earth metals can also be dispersed in those high surface area supports.

In the present work, zirconium was incorporated in to silica pillars in porous clay heterostructures by direct method. Other hetero atoms like Ti , Al or their mixed forms can be incorporated in to silica matrix. Acidic and

oxidation property of the catalyst have been exploited so far. Other properties of the catalyst such as reduction capability (In case of Ni loaded catalysts) or multifunctionality of catalyst could be explored. The intergallery silica can be functionalized for incorporating various active groups for various potential applications. Since the amino functionalized porous clay heterostructures possess basicity in addition to the inherent acidity of clays, they can be effectively utilized for reactions that require acidic and basic sites.

The prepared catalysts systems are effective for alkylation reaction. We have explored their activity only for tertiary butylation reaction of phenol. Alkylation reactions of large molecules can also be carried out over the prepared catalysts especially in porous clay heterostructures owing to their larger pore size and higher acidity. Since the pillared clays and porous clay heterostructures contain the acidity and pore size required for cracking and isomerisation reactions of large hydrocarbons, they can effectively compliment industrially used zeolites in these reactions. Oxidation of phenol and benzyl alcohol were carried out success fully over prepared catalysts and they can be used for other oxidation reactions also. Pillared clays are effective for the oxidation of phenol in aqueous media and it can be extended for the removal of phenolic compounds in water. Hydroxylation of benzene to phenol is effectively done over copper loaded zirconium pillared clays. Further extensive research is needed for the commercialization as it is regarded as one of the key reactions in future.

In the present work, DTP was immobilized on the intergallery frame work of silica in PCHs materials and their catalytic activity were evaluated for acetalization reaction. Other heteropoly acids can also be immobilized on

PCHs materials and catalytic reactions that require redox or multifunctionality nature can also be explored over those catalysts.

As the organic chemist is becoming more aware of the clay's efficacy, its uses in organic synthesis are bound to increase especially because it helps in developing eco-friendly chemical process. Besides the further expansion of their use in green catalytic process due to their environmentally friendly credentials, future developments of clay-based designer catalysts are worthwhile if the research is focused on the production of fuels and fine chemicals from renewable bio-resources and on solar-driven synthesis. In short the dark clays have a bright future.

.....ꕥ.....

PUBLICATIONS

List of Publications in National/International Journals

- Nissam Ellias and S. Sugunan, Wet peroxide oxidation of phenol over Cerium impregnated Aluminium and Iron- Aluminium Pillared Clays, IOSR Journal of Applied Chemistry 7,5 (2014) 80-85

List of papers in National or International seminars

- Nissam E and S.Sugunan, Wet peroxide green route oxidation of phenol over transition metal impregnated zirconium pillared clays, APT Chem -2009, March 2009, University of Calicut
- Nissam E and S.Sugunan, Direct Hydroxylation of benzene to phenol over transition metal impregnated pillared clays, Kerala Science Congress, KFRI Peechi, January 2010
- Nissam E and S.Sugunan, Synthesis, Characterization and catalytic activity studies of transition metal impregnated pillared clays for hydroxylation of phenol in aqueous media, MATCON 2010, CUSAT, Cochin
- Nissam E and S.Sugunan, Oxidation of benzyl alcohol over transition metal loaded pillared clays, CTric 2011, CUSAT, Cochin
- Nissam E and S.Sugunan, Synthesis, charactrisation and catalytic activity studies of transition metal impregnated porous clay heterosructures, AOP Chem, 2012, University of Calicut
- Nissam E and S.Sugunan, Tertiary butylation of phenol over transition metal impregnated zirconium silicon porous clay heterostructures, CTric 2012, CUSAT, Cochin
- Nissam E and S.Sugunan, Synthesis, characterization and catalytic activity studies of zirconium silicon porous clay heterostructures, National seminar on Nano Science and Technology, 2013, SNGCE Kolenchery

Work Shop Attended

- Orientation Programme in Catalysis Research held at NCCR, IIT Chennai, 17th November to 8th December 2008